Long-term neuroinflammation induced by influenza A virus infection and the impact on hippocampal neuron morphology and function

Von der Fakultät für Lebenswissenschaften

der Technischen Universität Carolo-Wilhelmina zu Braunschweig

zur Erlangung des Grades

einer Doktorin der Naturwissenschaften

(Dr. rer. nat.)

genehmigte

D i s s e r t a t i o n

von Shirin Hosseini

aus Khorramabad / Iran

1. Referent: Professor Dr. Martin Korte
2. Referent: Professor Dr. Reinhard Köster
eingereicht am: 11.10.2017
mündliche Prüfung (Disputation) am: 14.12.2017

Druckjahr 2017

Vorveröffentlichungen der Dissertation

Teilergebnisse aus dieser Arbeit wurden mit Genehmigung der Fakultät für Lebenswissenschaften, vertreten durch den Mentor der Arbeit, in den folgenden Beiträgen vorab veröffentlicht:

Publikationen eingereicht:

Shirin Hosseini, Esther Wilk, Kristin Michaelsen-Preusse, Ingo Gerhauser, Wolfgang Baumgärtner, Robert Geffers, Klaus Schughart, Martin Korte
‘ Long-term neuroinflammation induced by influenza A virus infection and the impact on hippocampal neuron morphology and function ’.
Under review

Tagungsbeiträge:

Hosseini S, Michaelsen-Preusse K, Wilk E, Schughart K, Korte M. The effect of neuroinflammation induced by influenza A virus infection on hippocampal neuron morphology. ***2nd N-RENNT Symposium on Neuroinfectiology, Hannover, Germany (2015)***.

Grigoryan G, **Hosseini S**, Chhatbar C, Arendt W, Michaelsen-Preusse K, Kalinke U, Korte M. Lack of type I IFN receptor affects synaptic plasticity in mouse hippocampus. ***2nd N-RENNT Symposium on Neuroinfectiology, Hannover, Germany (2015)***.

Hosseini S, Michaelsen-Preusse K, Wilk E, Schughart K, Korte M. The effect of neuroinflammation induced by influenza A virus infection on hippocampal neuron morphology. ***11th Göttingen Meeting of the German Neuroscience Society, Göttingen, Germany (2015)***.

Grigoryan G, **Hosseini S**, Chhatbar C, Arendt W, Michaelsen-Preusse K, Kalinke U, Korte M. Lack of type I IFN receptor affects synaptic plasticity in mouse hippocampus. ***11th Göttingen Meeting of the German Neuroscience Society, Göttingen, Germany (2015)***.

Hosseini S, Michaelsen-Preusse K, Wilk E, Schughart K, Korte M. The effect of neuroinflammation induced by influenza A virus infection on hippocampal neuron morphology and function. ***4th Venusberg Meeting on Neuroinflammation, Bonn, Germany (2015)***.

Hosseini S, Michaelsen-Preusse K, Wilk E, Schughart K, Korte M. Chronic neuroinflammation induced by influenza A virus infection and the impact on hippocampal neuron morphology and function. ***10th FENS Forum of Neuroscience, Copenhagen, Denmark (2016)***.

Grigoryan G, **Hosseini S**, Chhatbar C, Michaelsen-Preusse K, Kalinke U, Korte M. Ablation of interferon type I receptor impairs hippocampal synaptic plasticity and dendritic morphology. ***10th FENS Forum of Neuroscience, Copenhagen, Denmark (2016)***.

Hosseini S, Michaelsen-Preusse K, Wilk E, Schughart K, Korte M. Chronic neuroinflammation induced by influenza A virus infection and the role for hippocampal neuron morphology and function. ***12th Göttingen Meeting of the German Neuroscience Society, Göttingen, Germany (2017)***.

Hosseini S, Michaelsen-Preusse K, Wilk E, Schughart K, Korte M. Chronic neuroinflammation induced by influenza A virus infection and the role for hippocampal neuron morphology and function. ***5th Venusberg Meeting on Neuroinflammation, Bonn, Germany (2017)***.

Posterbeiträge:

Hosseini S, Michaelsen-Preusse K, Wilk E, Schughart K, Korte M. The effect of neuroinflammation induced by influenza A virus infection on hippocampal neuron morphology. ***7th International PhD Symposium, Braunschweig, Germany (2014)***.

Hosseini S, Michaelsen-Preusse K, Wilk E, Schughart K, Korte M. The effect of neuroinflammation induced by influenza A virus infection on hippocampal neuron morphology and function. ***6th Annual Public Retreat of the HZI Graduate School, Braunschweig, Germany (2015)***.

(3rd prize for the best presentations), oral presentation: Hosseini S, Michaelsen-Preusse K, Wilk E, Schughart K, Korte M. Neuroinflammation induced by viral infection and the role for hippocampal function. ***7th Annual Public Retreat of the HZI Graduate School, Goslar, Germany (2016)***.

Hosseini S, Michaelsen-Preusse K, Wilk E, Schughart K, Korte M. Chronic neuroinflammation induced by influenza A virus infection and the role for hippocampal neuron morphology and function. ***9th International PhD Symposium, Braunschweig, Germany (2016)***.

(2nd prize for the best presentations), oral presentation: Hosseini S, Michaelsen-Preusse K, Wilk E, Schughart K, Korte M. The effects of neuroinflammation induced by influenza A virus infection on hippocampal structure and learning in mice. ***8th Annual Public Retreat of the HZI Graduate School, Goslar, Germany (2017)***.

نابرده رنج گنج میسر نمی شود

مزد آن گرفت جان برادر که کار کرد

سعدی شیرازی (شاعر پارسی)

برای استاد همیشگی ام دکتر مسعود فریدونی که تمام هستی ام از اوست

You cannot achieve to treasure without working hard for it.

Saadi Shirazi (Persian poet)

For Professor Dr. Masoud Fereidoni

and

To all that this thesis information may help them someday

Table of contents

Table of figures

Zusammenfassung

Influenza Infektionen stellen auch heute noch ein beträchtliches gesundheitliches und wirtschaftliches Risiko dar, da in regelmäßigen Abständen mit Pandemien zu rechnen ist. Obwohl bei einer Infektion hauptsächlich obere Atemwege und Lunge betroffen sind, kann es zusätzlich zu neurologischen Symptomen kommen. Hierbei sind besonders die Langzeitfolgen einer Influenza Infektion für das zentrale Nervensystem noch weitgehend unbekannt.

Im ersten Teil dieser Arbeit sollte daher der Langzeiteffekt einer Infektion mit verschiedenen neurotropen (H7N7) und nicht-neurotropen (H1N1, H3N2) Influenza A Virus Subtypen auf die Struktur und Funktion des murinen Hippokampus untersucht werden. 30 Tage nach der Infektion mit H3N2 und H7N7 konnten zusätzlich zu einer Abnahme der *spine*-Dichte eine Beeinträchtigungen in der Langzeitpotenzierung wie auch im räumlichen Lernen festgestellt werden. Parallel hierzu war eine vermehrte Anzahl aktivierter Mirkogliazellen und Astrozyten festzustellen sowie auch erhöhte Level von Zytokinen. Obwohl H7N7 die stärksten Anzeichen einer Neuroinflammation hervorrief, zeigen diese Ergebnisse, dass selbst eine auf die Peripherie beschränkte Influenza Infektion weitreichende und lang andauernde Folgen für Funktion des Hippokampus haben kann.

Wie im ersten Teil dargestellt, kommt es während einer Influenza Infektion zu stark erhöhten Zytokin Leveln im Hippokampus, wie beispielsweise Interferon. Dies führt unter anderem zu einer Beeinträchtigung der hippokampalen Funktion. Es ist jedoch bisher wenig darüber bekannt, welche Rolle Interferon-Signalwege unter basalen Bedingungen im gesunden Gehirn spielen. Aus diesem Grund wurden im zweiten Teil dieser Arbeit *knockout* Mäuse für den Interferon Type I Rezeptor (IFNAR) untersucht, um dessen Rolle für die synaptische Plastizität und kognitive Funktion zu untersuchen. Es konnten hier eine Verringerung der *spine* Dichte im Hippokampus begleitet von einem Defekt in der Langzeitpotenzierung und Beeinträchtigung des räumlichen Lernens festgestellt werden. Weiterführende Untersuchungen an Zelltyp spezifischen konditionalen *knockout* Mäusen zeigten, dass sich dieser Phänotyp auf IFNAR Aktivierung in Astrozyten zurückführen lässt. Es bleibt nun zu klären, welche Signalwege und zellulären Mechanismen im Detail an der Interferon-vermittelten Interaktion von Astrozyten und Neuronen beteiligt sind.

Abstract

Influenza A viruses (IAV) as a major threat to human and animal health today are still a leading cause of worldwide severe pandemics. Although the primary target of these viruses in mammals is the lung, an influenza infection can be associated with neurological complications. However, the long-term consequences of an IAV infection for the central nervous system (CNS) remain largely elusive.

In the first part of this study, two months old female C57BL/6J mice were infected intranasally with non-neurotropic (H1N1 and H3N2) as well as neurotropic (H7N7) influenza A virus subtypes in order to investigate possible long-term effects on hippocampal structure and function. Dendritic spine loss detected at 30 days post infection was associated with an impairment in spatial learning, reduced Schaffer collateral long-term potentiation and an increase in the population of activated microglia and astrocyte density along with elevated levels of proinflammatory cytokines. While neuroinflammation induced by neurotropic H7N7 influenza A virus showed the strongest effect, systemic infection with the non-neurotropic H3N2 subtype resulted as well in long-term impairments in synapse number and hippocampal function. Taken together, these findings clearly show that even an influenza A virus infection restricted to the periphery can lead to long-term neuroinflammation and synapse loss with severe impact on hippocampal function in young adult animals in a virus subtype-specific manner.

As the findings of the first part of this study show, neuroinflammation induced by viral infection leads to high levels of proinflammatory cytokines such as interferons (IFNs) which can affect hippocampal function well beyond the acute disease phase. Little is known, however, about IFN signaling under physiological conditions in the healthy brain. Therefore, the second part of this study focused on the role of type I IFN signaling for synaptic plasticity and cognitive function. Experiments with healthy conventional type I interferon receptor (IFNAR) KO mice showed reduced hippocampal spine density together with deficits in synaptic plasticity and spatial learning. Analysis of different cell type specific conditional IFNAR KO animals indicated that IFN signaling in astrocytes is responsible for this phenotype. Further experiments are needed to identify the detailed signaling pathways and cellular mechanisms involved in the IFN mediated crosstalk between neurons and astrocytes discovered here, and the role for synaptic plasticity and cognitive function.

1. Introduction

Searching for the etiology of neuropsychiatric difficulties suggests that viral infection, as an environmental factor, can induce neuronal system dysfunction, resulting in a variety of behavioral abnormalities including cognitive and social deficits such as memory dysfunction, dementia and depression. It was shown that different viral infections can lead to deleterious complications in the central nervous system (CNS) by a direct entry of virus and/or indirect pathways without the entrance of virus into the brain. On the other hand, viral infection can cause a dysfunction of immune cells in the CNS (Tomonaga, 2004). The fact that neuropsychiatric abnormalities can be induced by viral infections became obvious during the deadly influenza pandemic, Spanish flu (1918/20), in which several psychiatric complications including schizophrenia, dementia or depression-like behavior were reported in many patients following influenza infection (Ravenholt and Foege, 1982). Furthermore, birth dates in winter are more likely correlated with the development of schizophrenia in early adulthood, therefore, pointing to viral infection and increased incidence of neurological disorders (Brown and Susser, 2002). Thus, investigations on viral infection induced complications in the CNS can potentially lead to novel insights into human mental illnesses and lead to possible prevention and treatment methods.

1.1. Influenza virus infection

Influenza or flu is an airborne contagious disease caused by influenza viruses. These viruses are negative sense, single-stranded segmented RNA (ssRNA) viruses with a protein envelope which belonging to the family of Orthomyxoviridae. Influenza viruses are classified into three main types including A, B and C. Influenza A viruses are the most virulent human pathogens among the three influenza types and cause the severest disease, furthermore this influenza type is responsible for the majority of yearly epidemics of seasonal flu and severe pandemics as well (Klenk et al., 2008). Influenza B viruses are only present among humans and cause some of the seasonal epidemics. Influenza C viruses can cause a mild infection in both humans and pigs and are very rare (Renegar, 1992). Therefore, influenza A viruses are considered as the most important influenza virus types. Influenza A viruses are categorized into several subtypes which are labeled according to the type of hemagglutinin (HA) and

neuraminidase (NA) which are the two large glycoproteins on the surface of the viral particles. HA is a lectin that mediates binding of the virus to the target cells to allow entry of the viral genome into the target cells. This protein is responsible for determining both which species, the strain can infect and where in the respiratory tract the strain will bind (Nicholls et al., 2008). Influenza strains that are easily transmitted between people have a type of hemagglutinin that can bind to receptors in the upper part of the respiratory tract, such as in the nose, throat and mouth. In contrast, the highly lethal influenza strains can bind to receptors that are mostly found deep in the lungs (van Riel et al., 2006). This difference in the site of infection may provide part of the reason why the highly pathogenic influenza strains cause severe viral pneumonia in the lungs but are not easily transmitted by people coughing and sneezing. On the other hand, neuraminidase is involved in the release of newly generated viruses from the infected cells, by cleaving sugars that bind the mature viral particles (Suzuki, 2005).

Many host species have their own influenza strains for example aquatic birds, pigs, dogs, bats and humans, although cross-species transmission occurs frequently (Tong et al., 2013). However, humans mostly can be infected with seasonal, pandemic and zoonotic influenza A viruses. Seasonal influenza A virus subtypes disseminate within the population causing yearly epidemics while pandemic influenza viruses are the result of cross-species transmission, after which they adapt to humans and spread worldwide (Ludlow et al., 2016).

There are several influenza A virus subtypes that have been found in humans, ordered by the number of known human pandemic deaths: H1N1, which caused the Spanish flu in 1918 and Swine flu in 2009, H2N2, which caused the Asian flu in 1957, H3N2, which caused the Hong Kong flu in 1968, H5N1, which caused the Bird flu in 2004 and H7N7, which has unusual zoonotic potential (Fouchier et al., 2004). Serious outcomes of flu infection can result in hospitalization or death. Some people, such as older people, young children, and people with certain health conditions, are at high risk for serious flu complications. The best way to prevent the flu is by getting vaccinated each year (Nichol and Treanor, 2006). Common symptoms of the flu such as fever, headaches, and fatigue are the result of high amounts of proinflammatory cytokines and chemokines (such as interferons or tumor necrosis factor) released from influenza-infected cells (Eccles, 2005; Schmitz et al., 2005). In contrast to the rhinovirus that causes the common cold, influenza does also cause tissue damage,

so symptoms are not entirely due to the inflammatory response (Winther et al., 1998). This massive immune response might produce a dangerous cytokine storm. This effect has been proposed to be the main cause of the unusual lethality of influenza infection pandemics around the world (Cheung et al., 2002).

1.1.1. Influenza A animal model

Influenza A virus infected mice are the most common model used to study the effects of influenza A virus strains infection on different body organs. After influenza A virus inoculation mice develop a lower respiratory infection and display different clinical symptoms such as decreased locomotor activity, diminished food and water intake and hypothermia (Klein et al., 1992). Moreover, highly pathogenic avian influenza A viruses can replicate efficiently in the mouse respiratory epithelium without any adaptation because there are fewer alpha 2,3-linked sialic acid residues which are necessary for attachment of the virus to the host cells. Therefore, infection with avian viruses can lead to morbidity, systemic spread of the virus, severe tissue pathology, and even death in mouse animal models (Maines et al., 2005). Furthermore, it has been shown that following influenza A virus infection, several proinflammatory and inflammatory cytokines such as tumor necrosis factor α (TNF-α) and interleukins (IL-6 and IL-1β) systemically increase in mice. Further evidence also suggest that in addition to the typical inflammatory cytokines associated with sickness behavior, interferons (type I IFNα/β and type II IFN-γ) also lead to fatigue syndrome and body weight loss as well as depressed locomotor activity and reduced food intake in infected mice (Cunningham et al., 2007; Majde et al., 2010). On the other hand, the ferret is also used as an influenza A virus infection model to investigate the effects on different body organs especially the brain. Similar to humans, upper respiratory epithelium mainly has alpha 2,6-linked sialic acid residues and infection of the epithelium with influenza A viruses produce fever and rhinorrhea in ferret, therefore, in this animal model the infection mimics more closely the reaction of the human body (Figure 1.1) (van Riel et al., 2006; Yamashita, 2016).

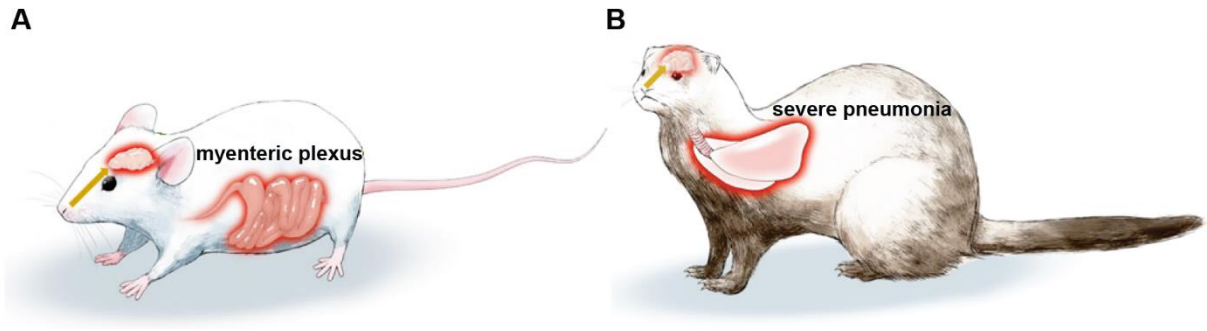

Figure 1.1 | Influenza A virus animal models (Yamashita, 2016). (A) Mouse influenza A virus infection animal model. In this model following intranasal infection with highly pathogenic strains, viruses can affect the CNS via the olfactory bulb or the mesenteric and myenteric (Auerbach's) plexus in the digestive tract and lead to neurological disorders. **(B)** Ferret influenza A virus animal model. After intranasal infection of ferrets with highly pathogenic influenza A viruses, the virus spreads from the olfactory system to the CNS, however, viruses can cause severe pneumonia in this model comparable to humans.

1.2. Influenza A virus strains

Following a different way of classification, influenza A virus subtypes categorize into the two groups due to their effects on the CNS depending on the type of HA and NA, the surface proteins. These groups include neurotropic and non-neurotropic influenza A virus strains (Fraser et al., 1959).

1.2.1. Neurotropic influenza A virus strains

It has been shown that the CNS is the important target site for several types of viral infections. Some of the influenza A virus strains are neuroinvasive which means that they can penetrate the CNS. Furthermore, they can infect neurons and glial cells in the CNS which is known as neurotropism. The neurotropic viruses are neuroinvasive and neurovirulent and have a potential capacity to cause neuronal dysfunction. Neurotropic influenza A virus strains are capable of accessing or entering the nervous system and causing disease within the nervous system (Atluri et al., 2015). These strains of influenza A virus can establish a persistent infection in the brain. For instance, the highly pathogenic avian influenza virus (H5N1) can indeed infect the CNS and subsequently lead to neuronal damage (Kristensson, 2006; Jang et al., 2012) which is induced by neuroinflammation through the activation of glial cells and

altered proinflammatory and inflammatory cytokine expression (Jang et al., 2009; Jang et al., 2012). It has been shown that neurotropic virus infections have a wide economic burden on society, and have a wide range of morbidity and mortality worldwide. Therefore, neurotropic virus infection is a major challenge to human and animal healthcare systems. This depends on the unique organization of the CNS with different cell types, very sophisticated structures and functions, reduced immune surveillance and limited regeneration capacity (Ludlow et al., 2016).

On the other hand, it is worth noting that humans and other vertebrates have highly complicated barrier systems to prevent the entry of potentially harmful substances and invasive pathogens into the CNS. These structures include the blood-brain barrier (BBB) and blood-cerebrospinal fluid barrier (BCSFB) of the choroid plexus in the ventricles of the brain. Despite these complex barriers, neurotropic viruses have evolved strategies to enter and infect the CNS, which can give rise to acute and chronic diseases such as meningitis, encephalitis, myelitis, paralysis, etc. Some of the neurotropic viruses are able to directly manipulate the BBB and BCSFB microvascular endothelial cells to enter the CNS via the so-called hematogenous route. Others can spread to the brain through the neural routes including entry via the olfactory bulb and peripheral facial nerves and the trigeminal ganglion (Ii and McGavern, 2015). Other neurotropic viruses hijack host immune cells and travel via infected peripheral immune cells to the brain (Tomonaga, 2004) (Figure 1.2). Most highly pathogenic avian influenza viruses are the neurotropic virus like the H5N1 subtype. Neurotropism of the H5N1 virus has been confirmed and studied in animal models, including mice, ferrets, cats and martens (Yamashita, 2016). Avian influenza A virus of the potentially polybasic and neurotropic subtypes H5 and H7 might be candidates for future pandemic outbreaks in humans, therefore, the investigations of the effects of these influenza A virus subtypes on the CNS are important. Recently, A number of avian viruses have crossed the species barrier and directly infected humans such as H7N7 influenza A virus, resulting in illness and in some cases, death and presenting a possible pandemic threat. Nevertheless, these viruses are not able to spread effectively from human to human (Cox et al., 2004).

In this study as a model for neurotropic influenza A virus infection, the polybasic rSC35M (recombinant A/Seal/Mass/1/80 mouse-adapted, H7N7) (Gabriel et al., 2005) was used. The effect of this virus on the CNS has not been analyzed before.

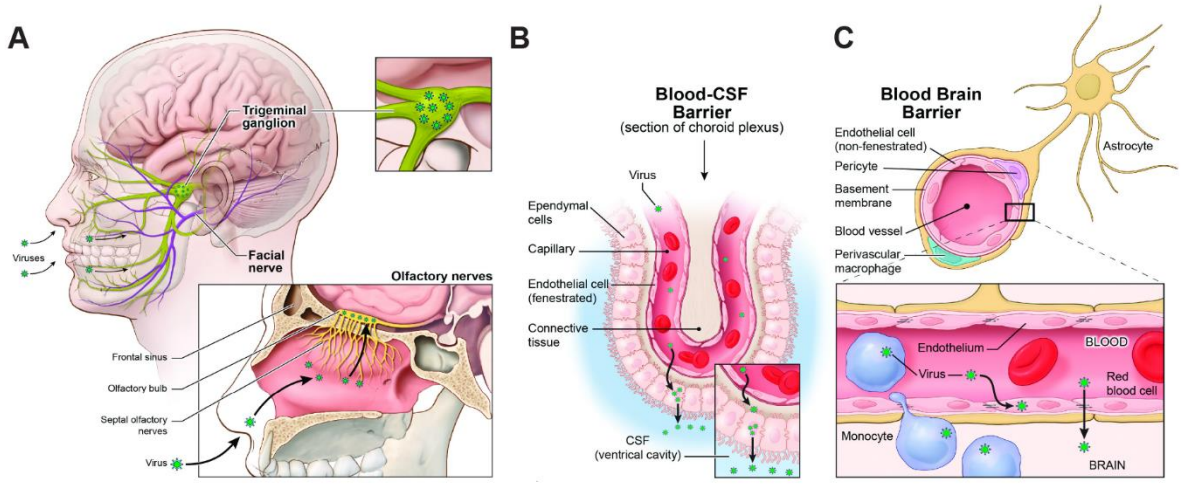

Figure 1.2 | Neurotropic viral entry routes to the central nervous system (CNS) (Ii and McGavern, 2015). (A) Viral entry through olfactory, facial nerve and trigeminal ganglion. (B) Viral entry through the blood-CSF barrier (BCSFB). (C) Viral entry through the blood-brain barrier (BBB).

1.2.2. Non-neurotropic influenza A virus strains

Most of the influenza A virus strains are non-neurotropic. Non-neurotropic influenza A viruses are not neuroinvasive and neurovirulent which means that they cannot penetrate the CNS. Therefore, infection associated alterations in the CNS might be due to the host immune response in the periphery (Atluri et al., 2015). In this respect, neuropsychiatric complications were reported especially in children after infection with non-neurotropic H1N1 influenza A virus (Surana et al., 2011). Moreover, children with neurodevelopmental problems were shown to be at increased risk for a severe outcome following influenza infection including death. Furthermore, several cognitive and neurological consequences related to non-neurotropic influenza A virus have been described for many decades after the 1918 “Spanish” flu (CDC, 2012; Ekstrand, 2012). In general non-neurotropic viral infection can change the CNS environment through the release of neurotoxins from macrophages in the periphery and subsequently from microglia and astrocytes within the brain. This indirect effects of non-neurotropic virus infection on the CNS exist as a dominant indirect pathway to affect both infected cells in the periphery and uninfected cells in the CNS (Tomonaga, 2004). Although the peripheral immune system cells can eliminate viruses efficiently without the destruction of neurons, in some cases it has been defined that the infiltrated peripheral immune system cells can actually induce neuronal damage (Irani

and Griffin, 2001). In addition, host autoimmune responses induced by non-neurotropic viral infections are also present as an indirect pathway of virus-induced neuropathogenesis. For example, it has been suggested that multiple sclerosis (MS), an autoimmune demyelinating disease, is initiated by persistent viral infection (Fazakerley and Walker, 2003). It is proposed that such indirect viral infection pathways might play a role in the development or aggravation of neurodegenerative disorders, such as Alzheimer's and Parkinson's diseases.

Most influenza strains are non-neurotropic, including the ones responsible for pandemics. This suggests that neurological symptoms do not occur only as a result of direct CNS viral infection but also because of a neuroinflammation induced by peripheral viral infection. In the present study, the impact of two different non-neurotropic influenza A virus variants on hippocampal neuron morphology and hippocampus-dependent behavior were investigated. First, the well-characterized and non-neurotropic PR8 (A/PuertoRico/8/34, H1N1) (Majde et al., 2007; Hodgson et al., 2012) and second, a non-neurotropic virus belonging to the H3N2 subtype, maHK68 (mouse-adapted A/Hong-Kong/1/68) (Haller et al., 1979).

1.3. The neuro-immune system

According to numerous clinical reports, neurotropic and non-neurotropic influenza A virus infection can lead to the development of several neurological complications (Ekstrand, 2012). It is believed that immune responses against pathogens are not limited to the periphery, as a systemic inflammation can also affect the CNS. Even an environmental insult can affect the interaction between neurons and peripheral immune responses. When an antigen such as virus enters the body, the immune system begins to produce and release cytokines. These cytokines can affect brain function and lead to release and activation of neurohormones, neuropeptides and neurotransmitters that influence the immune function (Chesnokova et al., 2016). Therefore, identification of the biochemical interactions between neurons and the immune system which is called the neuroimmune system is crucial.

The Neuroimmune system can also protect neurons from pathogens and other risk factors via the maintenance of the blood-brain barrier and blood-CSF barrier, moreover, it is triggering the wound healing processes in the damaged CNS (Rogers, 2012; Gimsa et al., 2013). The responses of the neuroimmune system can be

mediated by resident microglia and astrocytes which constitute the innate CNS immune cells without the direct association of their peripheral counterparts. Although the CNS immune reactions often take place in a different way than the common innate/adaptive immune system which characterizes peripheral immune responses, however, microglia and astrocytes are involved in a significant cross-talk with CNS-infiltrating T cells, monocytes, macrophages and other components of the peripheral innate immune system (Gimsa et al., 2013).

1.3.1. Microglia in physiology and pathology

Microglia are the resident immune cells in the brain and represent the major cellular components of the innate immune system of the brain. These cells monitor the cerebral microenvironment constantly to find pathogens or brain damage. Microglia can be found throughout the CNS, although some regions of the brain such as the gray matter contain more microglial cells than other regions (Soulet and Rivest, 2008). Microglia population cover around 10% to 20% of all glial cells in the CNS. They compose approximately 5% of glial cells in the white substance and around 18% in the gray matter. These cells are small and the size of their cell body does not exceed more than 5 to 10 µm (Kurpius et al., 2006).

According to their functions in different conditions, microglia obtain a ramified or amoeboid phenotype. The ramified phenotype under non-pathological conditions is characterized by a high number of processes which are very active and dynamic to facilitate the interaction of microglia with neighboring blood vessels, neurons and astrocytes (Heneka et al., 2014). There are numerous transporters, channels and receptors on the surface of microglial cells including the receptors for neurotransmitters, neurohormones, neuromodulators, cytokines and chemokines. Under non-pathological conditions and especially during development, microglia promote synapse formation by secreting growth hormones and thrombospondins. On the other hand, microglia utilize their processes to scan the environment for dysfunctional synapses, which they are able to eliminate by phagocytosis (Wake et al., 2009). Therefore, a cross-talk between neurons and microglia via cell-cell connections and secretion of neuronal factors such as chemokine (C-X_3-C motif) ligand (CX_3CL1, fractalkine) and the cluster of differentiation proteins such as CD47, CD200 and CD22 is needed. These factors can bind to the receptors CX_3CR1,

CD172, CD200R and CD45 on the surface of microglial cells and regulate microglial activation (Ransohoff, 2009). Furthermore, microglia are important for neuronal survival through their secretion of brain-derived neurotrophic factor (BDNF), a molecule which is crucial both during development and for learning-dependent synapse formation. Indeed, there is evidence that microglia under non-pathological conditions contribute to synaptic remodeling and adult neurogenesis in the brain (Parkhurst et al., 2013). Therefore, during the physiological state microglia are important for the maintenance of tissue homeostasis, neuronal integrity and network function in the brain (Heneka et al., 2014).

During an immune challenge, microglia that are found close to blood vessels lose their ramifications and become more amoeboid. It is not very clear whether amoeboid microglia form through phenotypic changes of the resident microglia or whether it is a step involved during the differentiation of blood-derived cells following an immune challenge. However, amoeboid microglia are also present during all stages of development of the CNS to eliminate dysfunctional synapses. Also, it is worth noting that microglia can proliferate in the presence of infectious agents or endogenously produced toxic proteins (Soulet and Rivest, 2008).

The direct interaction of microglia with pathogens and other types of immune cells is limited in the healthy brain as the intact BBB forms a physical barrier which isolates microglial cells in the brain parenchyma from the periphery (Pivneva, 2008). Ramified microglia in the healthy brain express many cell surface markers constitutively such as major histocompatibility complex (MHC) class II molecules which are important for immune regulation as well (Mittelbronn et al., 2001). However, in response to the presence of infectious agents, ramified microglia have the capacity to become activated not only through changes in their morphology but also via a rapid upregulation of a large number of receptors and surface molecules such as MHC class II. Activated microglia can also produce numerous secretory factors that contribute to the defense of neuronal cells on one hand and on the other hand, potentially, can damage the infected brain (Perlmutter et al., 1992; Nakamura, 2002). Activated microglia express several receptors and molecules for example members of the immunoglobulin superfamily, CD4 receptors, intercellular adhesion molecule 1 (ICAM-1), complement receptors (C1q and C5a), integrins such as CD11b, cytokine/chemokine receptors such as interferons (IFNs), interleukins (IL-1, IL-6, IL-10, IL-12, IL-16), TNF-α, macrophage colony-stimulating factor (M-CSF), chemokine

receptor (CCR), CXC chemokine receptors (CXCR), CX3C chemokine receptor (CX3CR), CD14 receptors, mannose receptors, purinergic receptors and Toll-like receptors (TLRs) particularly to recognize pathogen-associated molecular patterns (PAMPs) produced by different pathogens such as bacteria and viruses. Toll-like receptors 3, 7, 8 and 9 are engaged in viral PAMPs recognition and at least TLR 3, 7 and 9 are expressed in activated microglia. Microglia can respond to TLR ligands and produce many types of proinflammatory and inflammatory cytokines, for instance, TNF-α, IL-6, IL-1β and IFNs (Rock et al., 2004).

Following CNS neurotropic viral infection, cytokines play a dual role. Whereas mild innate immune factors mediate a protective response which leads to viral clearance and tissue recovery in the brain, uncontrolled production of proinflammatory and inflammatory cytokines can induce immunopathogenesis and neuroinflammation (Ramesh et al., 2013). It has been shown that microglia in the presence of influenza virus infection produce several cytokines including pro-inflammatory/inflammatory (TNF-α, IL-6 and IL-1β) and anti-inflammatory, chemokines, and antiviral cytokines (IFNs) (Teijaro, 2014). Anti-inflammatory cytokines such as IL-10 and transforming growth factor beta (TGF-β) produced by activated microglia play an important role in the maintenance of the balance between protective immunity and the development of an immune pathology in the context of an infectious disease. For instance, neuraminidase glycoproteins of most influenza A viruses can convert latent TGF-β to overt (active) TGF-β, which plays a critical role in protecting the host from influenza pathogenesis (Wang et al., 2016). Furthermore, during infectious and inflammatory conditions, a population of microglia, which present characterizations similar to dendritic cells in the peripheral immune system may present antigens to CNS infiltrating T helper 1 (Th1) lymphocytes that secrete IFN-γ and thereby participate in chronic neuroinflammation of the nervous system. Although microglia contribute to immune responses through their interactions with CD4+ and CD8+ lymphocytes which enter the nervous system during infection or inflammation conditions, they are the only key cells in the innate immunity of the nervous system (Rock et al., 2004). Therefore, although microglial activation is necessary for host defense and neuroprotection, increased or prolonged activation can have detrimental and neurotoxic effects (Block et al., 2007).

1.3.2. Astrocytes in physiology and pathology

Astrocytes are stellar-shaped glial cells in the CNS. The astrocyte proportion can vary in different brain regions, also depending on the counting technique, they cover between 20% and 40% of glial cells (Verkhratsky and Butt, 2013). Under physiological conditions, astrocytes contribute to different brain functions. For instance, they are involved in the integration of signals and maintenance of homeostasis between neurons, immune cells and the vascular system. Astrocytes processes are in close contact with neuronal synapses, moreover, they are an important internal part of the BBB. This allows these cells to react rapidly to local changes in neuronal activity and at the same time monitor environmental properties and respond to peripheral disturbances. For this purpose, they also form connections with each other and neuronal cells via gap junctions (Barres, 2008; Cekanaviciute and Buckwalter, 2016). Astrocytes protect neurons controling the levels of glucose, neurotrophic factors, and neurotransmitters such as glutamate. Glutamate transporter (GLT-1) and glutamate aspartate transporter (GLAST) expression by astrocytes act to clear excessive glutamate from the synaptic cleft thereby protecting neurons from excitotoxicity (Anderson and Swanson, 2000). Astrocytes are crucial for the formation and function of synapses during the CNS development and in adulthood. In addition, astrocytes regulate the permeability of the BBB and microglial activation states by producing anti-inflammatory cytokine such as TGF-β (Griffin, 2003; Cekanaviciute and Buckwalter, 2016).

Under pathological conditions such as viral infection, astrocytes can detect changes in their extracellular environment and transform into reactive astrocytes, a process termed astrogliosis. The development of astrogliosis depends on the severity of the insult which includes progressive alterations in the molecular expression patterns as well as cellular hypertrophy. In severe cases, proliferation and scar formation can occur (Sofroniew and Vinters, 2010). In addition, the strong glial fibrillary acidic protein (GFAP) expression is a major hallmark of reactive astrocytes which is essentially needed for alteration in their morphology and gene expression. During viral infection, reactive astrocytes can be triggered via direct viral infection, released viral particles, viral proteins, viral RNA, viral replication and neuronal cell damage, as well as other immune challenges (Chen et al., 2010). In addition, microglial activation following viral infection can induce reactive astrogliosis. Yet, resting astrocytes can

also regulate and terminate microglial activation (Bender et al., 2012). Toll-like receptors 3, 7 and 9 are expressed in reactive astrocytes as well as microglia, and are crucial for reactive astrocyte formation and the induction of immune responses within the CNS to protect neuronal cells from virus invasion. Furthermore, reactive astrocytes exhibit high expression levels of ion channels such as K^+ and Ca^{2+}, the glutamate transporters GLT-1 and GLAST and the glucose transporter GLUT1 (Chen et al., 2010). Reactive astrocytes produce and release many proinflammatory and inflammatory cytokines such as IL-1, IL-6, TNF-α, IFN-γ and type I IFNs which are critical to inhibit viral spread in the CNS. Moreover, astrocytes produce anti-inflammatory cytokines such as IL-10 which help to attenuate their activity extension and decrease the expression of molecules like MHCII, adhesion molecules and matrix metalloproteinases that modulate antigen presentation and trafficking of peripheral inflammatory immune cells into the CNS, respectively (Yong, 1996; Bender et al., 2012). In addition to activated microglia, reactive astrocytes play critical roles in both the inflammatory and neuroprotective responses following viral infection.

1.4. Acute and chronic neuroinflammation

Neuroinflammation or reactive gliosis is an endogenous central nervous system reaction to insults (Streit et al., 2004). During the immune responses in the CNS activated glial cells produce and release proinflammatory and inflammatory mediators analogous to the responses of the peripheral activated immune cells (Pivneva, 2008). In case of a compromised BBB, activation of peripheral immune cells leads to the entrance of leukocytes into the brain tissue, which can produce mirror inflammatory responses very similar to those in the periphery (Takeshita and Ransohoff, 2012). However, in most of the cases of acute neuroinflammation without an alternation in BBB permeability, the pure brain immune system responses are composed of the rapid activation of glial cells without leukocyte infiltration (Sroga et al., 2003).

In general, the term neuroinflammation is used more often to describe a chronic and prolonged state caused by gliosis in the brain in which the sustained activation of microglia and astrocytes can be observed (Streit et al., 2004). Chronic neuroinflammation can lead to neurodegeneration which is involved in the expansion, maintenance and worsening of the pathological processes and disease side effects (Kraft and Harry, 2011). It can be induced by many types of viral infections which lead

to the activation of microglia and astrocytes accompanied by peripheral leukocytes, meningeal and perivascular infiltration into the brain parenchyma (Jang et al., 2009; Li et al., 2015). One important example of a chronic neuroinflammation induced by viruses is the human immunodeficiency virus (HIV) infection (Garden, 2002).
It becomes more and more clear that neuroinflammation induced neurodegeneration could be a cause for dementia (Streit et al., 2004).

1.5. Immune-brain communication

Innate immune cells produce and release many soluble proinflammatory and inflammatory cytokines such as TNF-α, IL-1β, IFNα/β and IFN-γ which can affect the CNS and cause sickness behavior. The peripheral immune responses are critical for the body to protect itself against the destructive effects of pathogens. However, a prolonged activation of the peripheral immune responses, for instance in cancer or autoimmune diseases, immune signaling to the brain can contribute to or even be the main cause for neuropsychiatric disorders. This fact might be the reason for an increased rate of depression in physically ill individuals (Dantzer et al., 2008). However, it is important to know how inflammatory cytokine signals from the periphery can affect the brain. It is known that cytokines are large molecules which cannot pass through the BBB freely. Nevertheless, several investigations reveal that cytokine signals can reach the brain via three different pathways including humoral, neural and cellular pathways (Figure 1.3).
In the humoral pathway, the cytokines and peripherally produced pathogen-associated molecular patterns (PAMPs) can reach the brain through a leaky area of the BBB including the choroid plexus and circumventricular organs (CVOs) (Capuron and Miller, 2011; Khandaker, 2016). The choroid plexus is responsible for removing metabolic wastes and other destructive materials from the cerebrospinal fluid. Therefore, it has to monitor the extracellular environment through the called blood-cerebrospinal fluid barrier (Laterra et al., 1999). On the other hand, CVOs which contain both sensory and secretory organs in the brain are part of the neuroendocrine system and in order to perform their different function and connecting the brain with the peripheral blood flow, they do not have a normal BBB (Fry and Ferguson, 2007). Therefore, circulating cytokines in the blood flow might reach the brain freely through the choroid plexus and CVOs by volume diffusion, moreover, the choroid plexus and

CVOs can provide a direct access for PAMPs to the brain tissue which in turn can cause the local production of proinflammatory cytokines by microglial cells (Vitkovic et al., 2000b; Khandaker, 2016). In addition, circulating cytokines in the blood flow can activate the endothelial cells and subsequently these cells release prostaglandins (PGE2) and nitric oxide (NO) within the brain parenchyma.

In the neural pathway, PAMPs and circulating cytokines in the periphery can stimulate the primary afferent nerves, such as the vagus nerve (Dantzer et al., 2000) which is the pneumogastric nerve and involved in parasympathetic control of the lungs, heart and digestive tract (Berthoud and Neuhuber, 2000). Following stimulation of the vagus nerve, the signals stimulate the primary and secondary projections of the neural pathway and reach the nucleus tractus solitaries (NTS) at first and different hypothalamic brain nuclei subsequently. Therefore, the cytokines or PAMPs stimulating signals might affect other brain regions as well (Dantzer et al., 2000).

Finally, in the cellular pathway, proinflammatory cytokines such as TNF-α which reaches the brain via the two other pathways or is produced locally can trigger microglial cells to produce and release monocyte chemoattractant protein-1 (MCP-1), which allows the entry of peripheral activated monocytes into the brain. Later on, these monocytes are able to produce inflammatory markers and affect the brain cells (D'Mello et al., 2009).

Many investigations have revealed that differential activation of each of these pathways can mediate the effect of cytokines on the brain. For example, subdiaphragmatic vagotomy can inhibit sickness behavior in rats following intraperitoneally lipopolysaccharide (LPS) administration, while it did not diminish the production and release of proinflammatory cytokines at the periphery (Bluthe et al., 1994). Therefore, when circulating cytokines in the periphery enter or send stimulatory signals to the brain, the resident immune cells including microglia and astrocytes start to locally secrete proinflammatory cytokines, chemokines and proteases within the brain. Following the increase of inflammatory mediators, elevated levels of oxidative stress elevation and activation of the hypothalamic-pituitary-adrenal (HPA) axis can be observed. These processes can lead to mood and cognitive impairment and might contribute to psychiatric disorders (Dantzer et al., 2008; Capuron and Miller, 2011). Overall, several findings reveal that a diffuse system of cytokine-brain interaction can affect neuronal circuits and neurotransmitters that are responsible for physiological and pathological behavior.

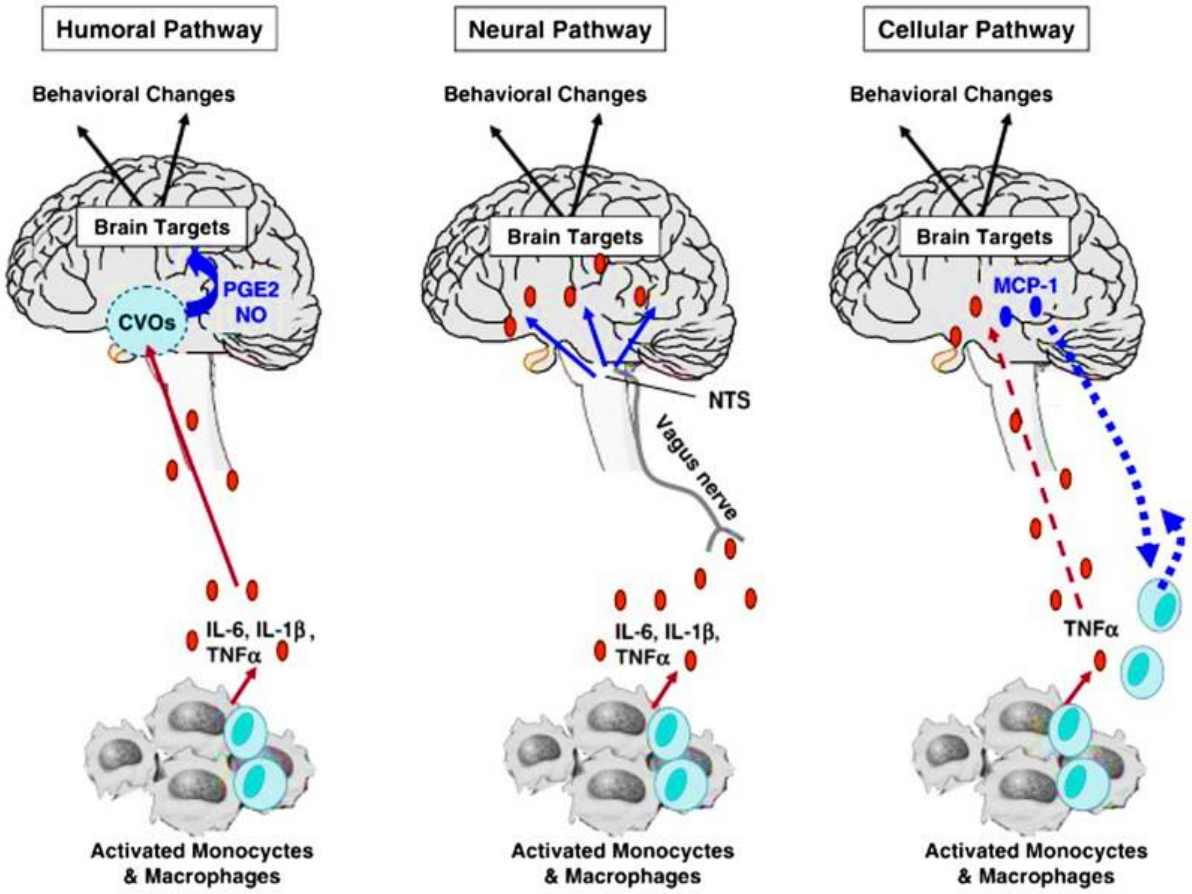

Figure 1.3 | Peripheral immune system and brain communication routes (Capuron and Miller, 2011; Khandaker, 2016). CVOs: Circumventricular organs, PGE2: Prostaglandins, NO: Nitric oxide, NTS: Nucleus tractus solitaries, MCP-1: Monocyte chemoattractant protein-1, IL-6: Interleukin-6, IL-1β: Interleukin-1β, TNFα: Tumor-necrosis factor alpha.

1.6. Neuroinflammation and cognitive function

Under conditions such as infection or brain injury in which the immune system is strongly activated, a prolonged activation of microglia and astrocytes in the brain can lead to elevated production and secretion of proinflammatory and inflammatory cytokines such as TNF-α, IL-6, IL-1β, IFNs and prostaglandins (Block et al., 2007; Yirmiya and Goshen, 2011). It has been shown that these inflammatory mediators in addition to induction of some disease symptoms such as fever, can cause a number of sickness behavior which include anhedonia, fatigue syndrome, decreased food uptake, concentration problems and many cognitive function disorders (Dantzer et al., 2000). It is worth noting that the tight balance in neurophysiological function which

is critical for the maintenance of cognitive functions can be interrupted by secretion of inflammatory mediators. Therefore, disrupting this balance might lead to adverse effects on learning and memory, neuronal plasticity and neurogenesis (Yirmiya and Goshen, 2011). These noxious effects which are mediated by neuroinflammation induced neurotoxicity and adrenocortical stimulation (Miller et al., 2009), subsequently followed by diminished production of neurotrophic factors such as BDNF, nerve growth factor (NGF), neurotrophins and other molecules which are involved in plasticity (Calabrese et al., 2014). These changes might underlie many neuropsychiatric disorders such as learning and memory impairment and aging-induced neuropathology as well as neurodegenerative diseases (Yirmiya and Goshen, 2011).

1.7. Synaptic plasticity and neuroinflammation

Alternations in the number of excitatory glutamatergic postsynaptic sites as dendritic spines density affect synaptic plasticity which is in turn considered as the cellular mechanism underlying the learning and memory processes (Moser et al., 1994; Segal, 2005; Korte and Schmitz, 2016). Several findings reveal that many neuropsychiatric deficits are the results of impaired synaptic plasticity mechanisms (Citri and Malenka, 2008; Richter and Klann, 2009). Synaptic plasticity can be achieved at least through two physiological events including short-term and long-term potentiation (Citri and Malenka, 2008). Short-term synaptic plasticity happens as a result of synaptic terminals releasing neurotransmitters in response to a presynaptic action potential which depends on a transient elevation of Ca^{2+} ion concentration inside the presynaptic terminals that causes the exocytosis of synaptic vesicles (Stevens and Wesseling, 1999; Emptage et al., 2001). On the other hand, in long-term synaptic plasticity or long-term potentiation (LTP), a repetitive stimulation of excitatory synapses, at a determined range of frequency, in the hippocampus leads to a strong synaptic potentiation which lasts from hours to even years (Bliss and Lømo, 1973). LTP characterize by stages including induction, expression and maintenance (Figure 1.4). At the induction phase of LTP, prior to the potentiation, N-methyl-D-aspartate (NMDA) glutamate receptors are channels which are blocked by Mg^{2+} ion inside the channel conduit, but after postsynaptic membrane depolarization by glutamate stimulation through the α-amino-3-hydroxy-5-methyl-4-

isoxazolepropionic acid (AMPA) receptors, Mg^{2+} is pushing out from the conduit and the NMDA channel now is ready to be opened in response to glutamate. Then, Na^{+} and Ca^{2+} ions enter to the postsynaptic neuron. This increased Ca^{2+} influx leads to the activation of calcium-dependent cascades and the activation of protein kinases like Ca^{2+}/calmodulin-dependent protein kinase (CaMKII) and protein kinase C (PKC) (Malenka and Bear, 2004). Afterward, in the expression stage of LTP, synaptic elevation of cell signaling cascades trigger the insertion of the internal AMPA receptors to the postsynaptic membrane. Hereafter the cooperation of both AMPA receptors with an excessive postsynaptic membrane population and NMDA receptors augment the postsynaptic activity (Collingridge et al., 2004). The maintenance stage of LTP as mRNA and protein synthesis-dependent stage leads to either structural alternations such as increase of the size of the pre-existing dendritic spines or formation the new ones to potentiate synapses (Sweatt, 1999).

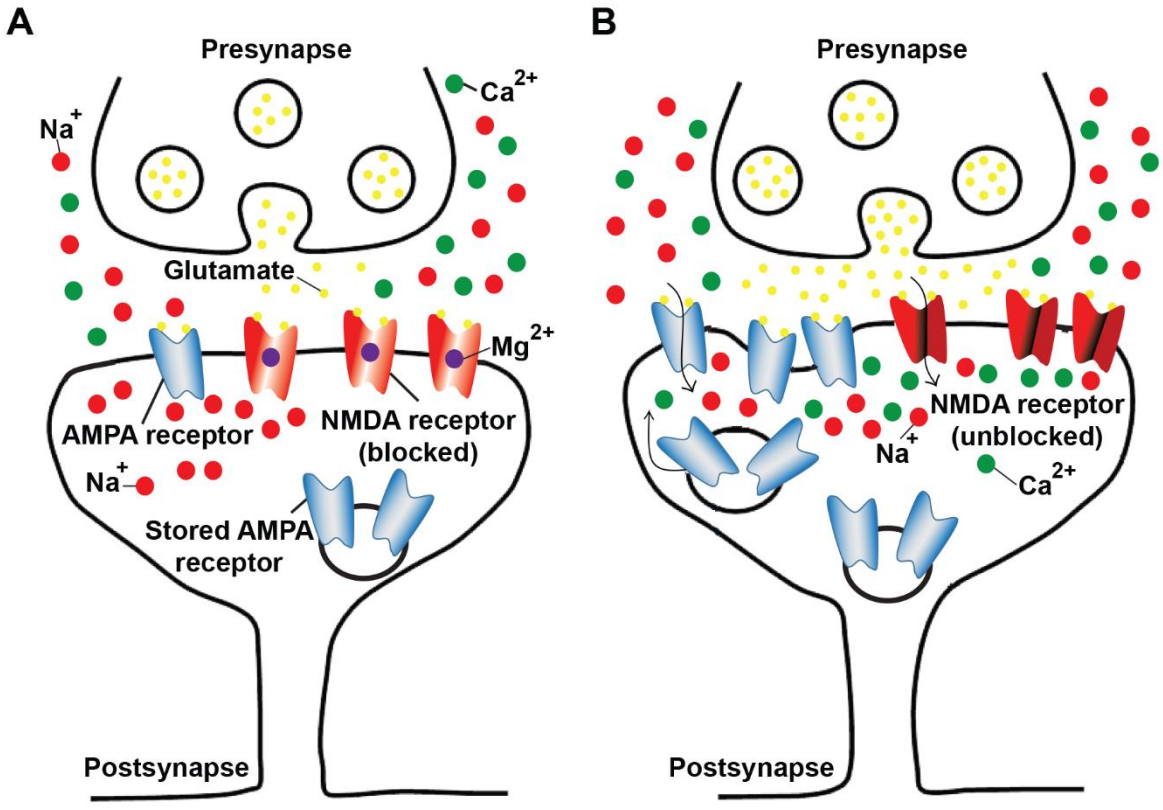

Figure 1.4 | Schematic illustration of long-term potentiation (LTP) at the level of the single dendritic spine. (A) Following basal synaptic transmission, the released glutamate binds to both NMDA and AMPA receptors. As NMDA receptors are blocked by Mg^{2+}, just AMPA receptor move the Na^{+} ions into the postsynaptic neuron and lead to the postsynaptic response. **(B)** Following LTP event,

NMDA receptors active in the results of the tetanic stimulation and elevation of the presynaptic release of glutamate and depolarization of postsynaptic neuron following the AMPA receptors function. Subsequently, NMDA receptors become unblocked which in turn leads to an increase of Ca^{2+} influx and then, activation of protein kinases-dependent pathways and insertion of new AMPA receptors in the plasma membrane.

Hippocampus is a highly plastic region in the brain and LTP was recognized in the hippocampus first time. It is believed that LTP is one of the critical mechanisms underlying the learning and memory processes (Bliss and Lømo, 1973).

Since the hippocampus is especially vulnerable to neuroinflammation (Vitkovic et al., 2000b; Lynch, 2002), hippocampal neuronal morphology changes which are induced by inflammation can lead to a hippocampal function impairment in association with learning and memory (Atluri et al., 2015). It has been demonstrated that some of the inflammatory cytokines can impair LTP (Pickering and O'Connor, 2007; Riazi et al., 2015). Moreover, they can inhibit the signaling of neurotrophic factors including NGF, BDNF and neurotrophins which are essential for neuronal function and survival, thereby negatively influencing synaptic plasticity and memory formation (Tong et al., 2008; Tong et al., 2012). For instance, intrahippocampal IL-1β administration led to BDNF mRNA expression reduction in the CA1 and dentate gyrus subregions of rat hippocampus and caused learning and memory deficits subsequently (Barrientos et al., 2004). Furthermore, neurite outgrowth was inhibited by the supernatant of LPS-stimulated microglia treatment which contains high levels of inflammatory cytokines (Münch et al., 2003). A retraction of dendrites was induced by TNF-α elevation (Neumann et al., 2002). In addition, earlier findings showed that a decrease in hippocampal dendritic spine density and an impairment in synaptic plasticity could be observed following activation of peripheral as well as central immune responses following viral infections or LPS stimulation (Milatovic et al., 2003; Jurgens et al., 2012; Vasek et al., 2016). It is believed that cell death and a subsequent reduction in the neuronal population do not occur even for very severe inflammatory challenges such as West-Nile virus infection although an impairment in cognitive function could be observed after recovery (Vasek et al., 2016). This suggests that indeed alterations in neuronal structure and function are causative for behavioral and cognitive function deficits. For example, dendritic retraction and growth inhibition were revealed following IFN-γ administration without any significant cell death and axonal

morphology changes (Kim et al., 2002). In confirmation of these findings, influenza A/PR8/34 (H1N1) virus infected mice showed cognitive impairment and hippocampal neuroinflammation along with considerable changes in CA1 and dentate gyrus neuronal morphology as well as neurotrophic factors reduction at 7 days post infection (Jurgens et al., 2012). Indeed, it is now well-established that inflammatory cytokines secreted by activated microglia following central and peripheral immune stimulation can affect neuronal function and morphology (Riazi et al., 2015). Microglia perform housekeeping functions within the healthy CNS including roles in synapse turnover and synaptic plasticity whereas long-term microglia activation might interfere with these processes (Nimmerjahn et al., 2005; Yirmiya and Goshen, 2011; Hristovska and Pascual, 2015). Moreover, elevation in the phagocytic characterization of reactive microglia can induce synaptic loss along with learning and memory deficits following peripheral and central inflammation (Vasek et al., 2016; Bialas et al., 2017). As it is believed that local induction or peripheral entrance of type I IFNs can stimulate microglial engulfment of synaptic components resulting in synapse loss and impaired synaptic plasticity and cognitive function (Bialas et al., 2017). On the other hand, activation of astrocytes in the hippocampus can affect synaptic functions as well. During neuroinflammation reactive astrocyte release inflammatory cytokines which are detrimental for synaptic plasticity (Sofroniew and Vinters, 2010). In addition, following central or peripheral inflammation, the expression level of aquaporin 4 (AQP4) which is a water channel and involved in calcium signal transduction as well as the regulation of neurotransmission and synaptic plasticity is reported to be downregulated (Xiao and Hu, 2014). In reactive astrocytes following the reduction in the expression level of AQP4, the expression of high affinity glutamate transporter (GLT-1) which is coexisted with AQP4 is also decreased, therefore, a reduction of glutamate uptake by astrocytes could happen which leads to LTP and cognitive function impairment (Zeng et al., 2007; Singh and Abraham, 2017) (Figure 1.5).

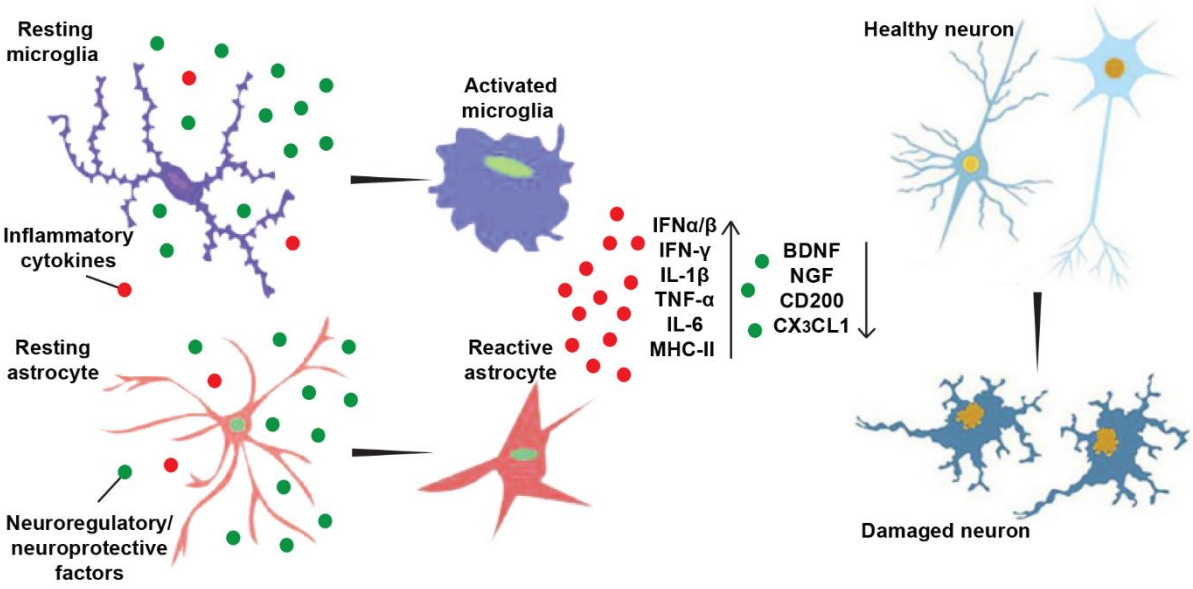

Figure 1.5 | Prolonged microglial and astrocytes activation lead to neuronal structure and function impairment. Activated microglia and astrocyte by increased inflammatory cytokines including IFNs, IL-1β, TNF-α, IL-6 and MHC-II production and decreased neuroregulatory/neuroprotective factors expression such as BDNF, NGF, CD200 and CX_3CL1 contribute in neuronal damage and cause neurobehavioral complications (Jurgens et al., 2012).

1.8. Cytokines and neurophysiology

Cytokines can induce a dose-dependent neuronal damage and neuronal function deficits. Under pathological conditions, it is believed that cytokine dysregulation leads to cognitive functions impairment (Wilson et al., 2002). Interestingly, it is worth noting that the functions of cytokines are not limited only to their destructive effects. As at the physiological state, networks of cytokines and their soluble receptors participate and regulate physiological function in neurons and glial cells. For instance, physiological levels of both peripheral and central cytokines can modulate neurotransmission such as the regulation of noradrenergic, dopaminergic, and serotonergic metabolism in the hippocampus, hypothalamus and nucleus accumbens (Shintani et al., 1993; Linthorst et al., 1995; Vitkovic et al., 2000a). The importance of a constitutive expression of different cytokines and their receptors under physiological conditions in the brain is becoming more and clearer. Constitutive levels of cytokine differ between neurons, microglia and astrocytes as well as in brain different regions. For example, it has been shown that the hippocampus and hypothalamus show the highest levels of IL-1, -2 and -6 and TNF-α in the absence of inflammation (Vitkovic

et al., 2000a). Cytokines have neuromodulatory effects in the brain during development and repair following neuronal damage. It could be even shown that IL-1, -6 and TNF-α can act as neurotrophic factors during development for neurons and glial cells in the brain (Wilson et al., 2002). Constitutive levels of IL-6 promote the survival of catecholaminergic neurons in the brain, whereas under pathological conditions such as accumulations of amyloid beta or oxidative stress elevated levels of this cytokine are involved in neurodegeneration (Toulmond et al., 1992). Furthermore, it has been revealed that constitutive levels of for instance IL1 are important for synaptic plasticity and subsequently learning and memory processes (Zhao and Schwartz, 1998). Moreover, recently it was shown that TNF-α might act as a synaptic modulator in the healthy CNS, and that the release from glial cells contributes to the homeostatic regulation of activity-dependent synaptic plasticity (Stellwagen and Malenka, 2006).

A different group of cytokines also produced by all cell types of the CNS under physiological conditions are interferons which have been shown to promote neuronal differentiation in the developing brain (Jonakait, 1996). In addition, physiological concentrations of type I interferons are used as a therapeutic agent in patients suffering from multiple sclerosis (Group, 1993). Therefore it can be concluded that while a high level of cytokines can be found during periods of neuroinflammation, physiologic levels might indeed be needed for proper signal transduction at the synapse and neuronal function.

1.8.1. Interferons (IFNs) and their classification

Interferons (IFNs) are implicated as an important component of the innate immune system, inflammation, and immune surveillance. They build a group of pleiotropic cytokines which mostly are produced by virus-infected cells. However, endotoxins such as LPS and antigenic and mitogenic stimuli as well can trigger the production of IFNs. On the other hand, interferons are able to bind to neighbouring cells during an infection and promote antiviral effects (Ignatowski and Spengler, 2008). Protection against viral infections by immune surveillance is crucial for the CNS and here IFNs constitute the important cytokines. Under inflammatory conditions, high expression level of IFNs can however also induce detrimental neuronal damage and behavioral disturbances as neuronal cells express IFNs receptors and respond to them (Owens et al., 2014). Several types of IFNs have been discovered till now. Although all of them are involved in antiviral functions frequently, the details of their roles are different. IFNs are classified into three main groups including types I, II, and III. The most important interferons subtypes are IFN-α and IFN-β which belong to type I interferons and IFN-γ is a type II interferon. IFN-γ is crucially involved in antiviral protection in the periphery whereas IFN-α and IFN-β are the predominant interferons in the CNS which can be produced by all CNS cell types. However, the highest levels are produced by glial cells including microglia and astrocytes.

In addition to the protective role of type I IFNs against viral infection, IFNs act as neuromodulators in the CNS as well and play important roles for synaptic transmission and function (Ignatowski and Spengler, 2008). Moreover, recent investigations have indicated obvious roles for type I interferons in the recruitment of immune cells to the CNS and highlighted the necessity of this process for brain maintenance, protection and repair (Deczkowska et al., 2016).

1.8.1.1. Type I IFN receptor (IFNAR)

It is believed that all CNS cell types can produce type I IFNs, by expression of the respective receptor. Both IFN-α and -β bind to the same heterodimeric type I IFN receptor (IFNAR) (Borden et al., 2007).

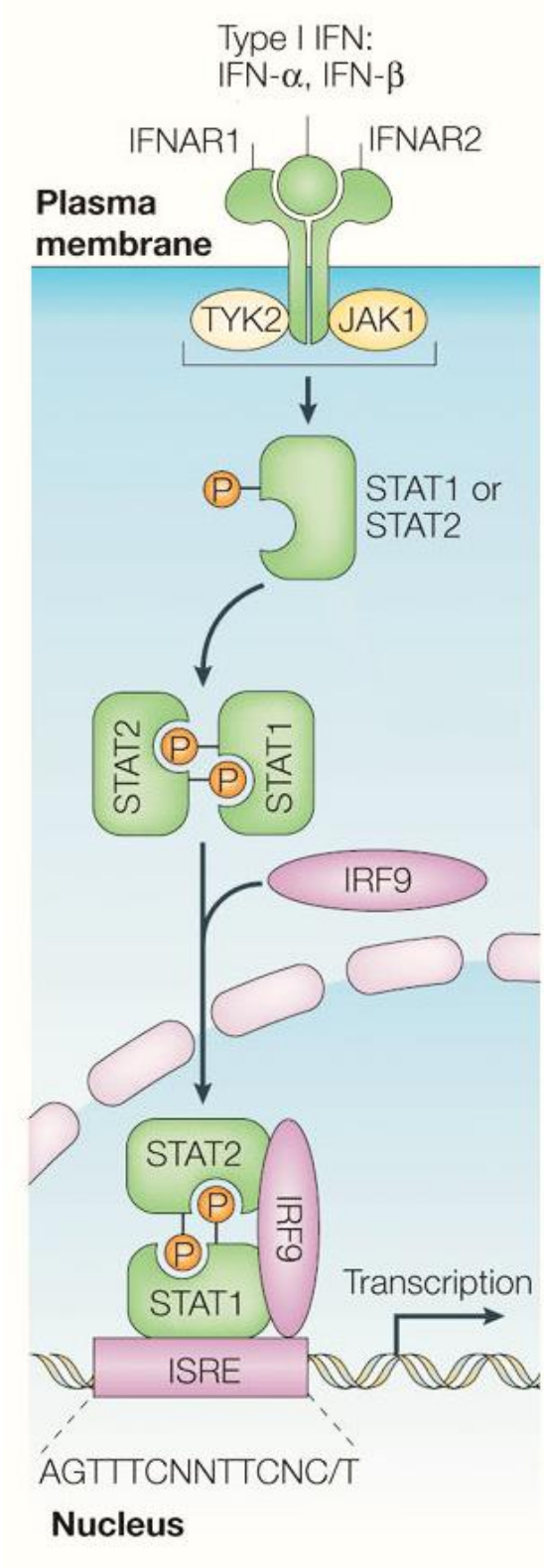

The heterodimeric IFNAR consists of two membrane spanning polypeptide chains including IFNAR1 and IFNAR2. IFNAR1 subunits are associated with the tyrosine kinase 2 (Tyk2), whereas the IFNAR2 subunit is associated with the Janus kinase (JAK1) (Figure 1.6). The affinity of IFNAR for different type I interferons differs. It is believed that IFNAR has a higher affinity for IFN-β compared to the IFN-α. Both IFNAR subunits can bind to the respective ligands and are involved in signal transduction (Thomas et al., 2011). Initially, IFN-α or IFN-β bind to the IFNAR1 subunit initiating the formation of the heterodimeric receptor complex which leads to activation of Ty2 and JAK1 subsequently.

Phosphorylation of the cytosolic domains of IFNAR subunits can be triggered by Ty2 and JAK1 activation and leads to activation of STAT1 and STAT2 transcription factors (signal transducer and activator of transcription 1, 2) downstream.

Figure 1.6 | Interferon receptors and activation of classical JAK-STAT pathways by type I interferons (Platanias, 2005).

Phosphorylation of STAT1 and STAT2 transcription factors triggers the formation of a STAT1-STAT2 heterodimer. Together with the IFN-regulatory factor 9 (IRF9) it forms the STAT1-STAT2-IRF9 transcription factor complex which is also known as the IFN-stimulated gene (ISG) factor 3 (ISGF3). This complex translocates to the nucleus and can bind to IFN-stimulated response elements (ISREs) in DNA to start gene transcription (Platanias, 2005; Owens et al., 2014). The type I IFNs signal transduction can be regulated by many factors such as suppressors of cytokine signaling (SOCS) (Hofer and Campbell, 2013).

Despite the fact that type I IFNs have the ability to bind the IFNAR2 subunit of the IFNAR receptor, the findings of Müller and colleagues defined that, mice lacking the IFNAR1 subunit of the type I IFNs receptor were as well completely unresponsive to both types I IFNs. This suggests that the existence of this receptor polypeptide chain (IFNAR1) is likewise essential for type I IFNs to mediate signal transduction. Mice lacking type I IFN signaling did not show any overt anomalies, however, they were unable to cope with viral infections efficiently nevertheless of otherwise normal immune responses (Muller et al., 1994).

1.8.1.2. Type I IFNs in the CNS

The major cellular source of IFN-α and IFN-β are dendritic cells which are able to produce type I IFNs approximately 1000 fold more than the other cells. Although these cells are normally not present in the brain parenchyma, their number in the CSF increases during inflammatory pathological conditions. Nevertheless, in the CNS almost all cell types are able to produce type I IFNs in response to viral infections or other stimuli (Pestka et al., 2004). Microglial cells which express all types of TLRs are the first line of defense against the detrimental effects of pathogens, and they are one of the main sources of type I IFNs in the CNS (Costello and Lynch, 2013). Depending on the type of pathological condition, microglia can be the main responder to type I IFNs. For instance, it has been shown that during neurodegenerative disease the immunostaining intensity of human brain tissue using an anti-IFNAR antibody was increased (Yamada et al., 1994). In addition, type I IFNs help to maintain the phagocytic properties of microglia, as the phagocytosis of dead infected cells debris is essential during infection. This phagocytic function of microglia provides a more permissive environment for axonal outgrowth as well (Hosmane et al., 2012). On the

other hand, microglia are also able to produce type I IFNs under physiological conditions of the brain (Owens et al., 2014).

Another source of type I IFNs in the CNS are astrocytes (Carpentier et al., 2005). Similar to microglia, astrocytes express TLRs, with TLR3 being the predominant isoform (Bsibsi et al., 2002). It has been defined that during many types of viral infections astrocytes produce both IFN-α and IFN-β. For instance, histological experiments revealed that astrocytes were able to produce IFN-α in brains of patients who died of Aicardi–Goutieres syndrome (AGS) and viral encephalitis (Van Heteren et al., 2008). Furthermore, it was shown that in La Crosse virus infected mice which developed La Crosse encephalitis, IFN-β was produced and released by astrocytes prominently. On the other hand, synaptic degeneration due to injury in the murine entorhinal cortex led to the induction of interferon regulatory factor 7 (IRF7) expression in microglia, but not in astrocytes, therefore microglia produce type I IFNs. In this injury-induced type I IFNs signaling, astrocytes contributed to the phosphorylation and activation of STAT1 and STAT2 proteins. Therefore, in this proposed scenario, astrocytes are indeed the major responder to type I IFNs produced by microglia (Khorooshi and Owens, 2010) (Owens et al., 2014).

Oligodendrocytes are the other CNS cell types which have the capacity to produce and respond to type I IFNs. However, oligodendrocytes express the IFNAR receptor only sparsely in comparison to astrocyte and microglia. Furthermore, information about oligodendrocytes as a source of type I IFN are controversial (Hanke and Kielian, 2011).

Neurons are another CNS cells types which produce and respond to type I IFNs under both physiological and pathological conditions. For example, under pathological conditions following neurotropic rabies virus infection an IFN-β response was detected in neurons to control the infection in the brain (Owens et al., 2014), whereas the expression of IFNAR by Nestin positive neuroectodermal cells including neurons and astrocytes in the olfactory bulb was identified as a way of controlling vesicular stomatitis virus infection in the brain (Detje et al., 2009). It is believed that non-neuronal sources of type I IFNs seem to participate in the virus entrance to the brain after infection by neurotropic viruses but neuron can response to type I IFNs following these kinds of infections (Owens et al., 2014).

1.8.1.3. IFNs and neuronal function

IFNs as immune molecules are also involved in modulating processes in neurons such as synaptic transmission. Therefore, they act as neuromodulators which can directly affect synaptic function, however, the detailed neurophysiological mechanisms remain elusive (Ignatowski and Spengler, 2008). As a matter of fact, neurons express IFN receptor on both pre- and postsynaptic membranes (Vikman et al., 1998). Earlier investigations revealed that both IFN-α and IFN-β were able to elevate the excitability of CA3 pyramidal neurons in the hippocampus (Mu et al., 1993). In addition, 30 minutes after IFN-α administration in neuronal culture, the excitability and spontaneous activity of cerebellar neurons were increased for several hours (Calvet and Gresser, 1979).

On the other hand, it was shown that treatment of rat hippocampal acute slices with IFNs led to a reduction of short-term potentiation and impaired LTP investigated by extracellular field recordings (D'Arcangelo et al., 1991). Moreover, the activity of dopaminergic neurons in the mouse brain was inhibited after repeated IFN-α application (Capuron and Miller, 2004). Therefore, it is believed that the effects of IFNs can differ depending on the exposure time in neurons. In addition, it was shown that acute application of IFN-γ for 48 hours in primary embryonic neuronal culture led to an elevation of the frequency of AMPA receptor-mediated spontaneous excitatory postsynaptic currents without any alteration in AMPA receptor clustering. In contrast to this, a prolonged administration of IFN-γ for 2 weeks reduced AMPA receptor clustering and trafficking without any changes in spontaneous excitatory postsynaptic currents (Vikman et al., 2001). Trafficking of AMPA receptors is thought to be crucial, at least in part, for both the rapid forms of synaptic plasticity (changes in AMPA receptors sensitivity and conductivity) and slower homeostatic changes (alterations of postsynaptic membrane AMPA receptor trafficking and population). In addition, the postsynaptic membrane expression of AMPARs appears to be tightly regulated in neurons (Stellwagen et al., 2005). Therefore, it seems that prolonged IFN exposure might lead to alterations in the homeostasis of synaptic transmission. It has been shown that dendritic spine density of hippocampal neurons, as well as the formation of the new spines, were decreased following prolonged IFN-γ administration (Kim et al., 2002).

It has been shown that physiological levels of IFNs have distinct roles during the development of the CNS and synaptogenesis. Therefore, elevation of IFN levels during inflammation and immune system responses might lead to neuronal structure and function alternations in the CNS and potentially underlie many neurological complications (Ignatowski and Spengler, 2008).

in addition to the IFNs concentration and exposure time to the neurons which determine the protective or pathologic effects of IFNs, because IFN-β has a faster kinetic action on IFNAR than IFN-α (Shepardson et al., 2016), therefore, the type of IFNs which activate its receptor could be also considered as a determinant of the outcome of the IFN effects (Owens et al., 2014).

Taken together the outcome of IFNs signaling in the brain is based on concentration and exposure time and whether it happens under physiological or pathological conditions IFN may act as a double-edged sword which could be either detrimental or neuroprotective.

1.9. Aim of study

1.9.1. Part I: Long-term effects of influenza A virus infection on the CNS

Influenza A virus infection generally manifests as a respiratory disease. However, it is occasionally associated with neurological complications ranging from mild cognitive deficits to encephalopathy, parkinsonism and seizures. The recent outbreaks of H1N1 (“Swine Flu”), H5N1, H5N8 and H7N9 underlined the role of influenza A virus infection as a serious threat to human and animal health worldwide with a considerable economic burden. It was shown that in the acute phase of non-neurotropic influenza A virus infection, neuroinflammation processes can lead to alterations in hippocampal neuronal morphology as well as cognitive deficits. Nevertheless, long-term effects of non-neurotropic and neurotropic influenza A virus strains on the brain remained so far elusive.

This study was therefore aimed to investigate the long-term effects of neuroinflammation induced by a neurotropic (H7N7) and two non-neurotropic (H1N1 and H3N2) influenza A virus subtypes on cognitive function. Spatial learning and memory formation in the Morris water maze, as well as Schaffer collateral long-term potentiation, were analyzed together with dendritic spine and glial density in different hippocampal subregions.

1.9.2. Part II: Type I IFN signaling in the healthy CNS

Neuroinflammation characterized by high cytokines level can lead to cognitive deficits. Cytokines such as interferons (IFNs) are pleiotropic molecules, affecting many cell types even under basal conditions in the healthy state. Type I IFNs and their receptor (IFNAR) are of particular interest mediating the communication between cells either in the absence or the presence of viral infection. IFNs can be released by glial and neuronal cells and their role as neuromodulatory factors is just beginning to become clear. Therefore, this study was aimed at investigating the cell-type specific importance of IFNAR signaling under physiological conditions in healthy individuals for cognitive function, hippocampal synaptic plasticity and dendritic spine density.

2. Materials and Methods

2.1. Materials

2.1.1. Chemicals and reagents

All used chemicals and reagents in the experiments of this thesis were distributed by AppliChem, Invitrogen, Roth, Merck or Sigma. Exceptions were specified respectively.

2.1.2. Influenza A virus strains

Virus	Provider	Dose
A/PuertoRico/8/34 PR8M (H1N1)	Stefan Ludwig University of Münster	2×10^3 FFU
A/Hong-Kong/1/68 maHK68 (H3N2)	Georg Kochs University of Freiburg	10 FFU
A/Seal/Mass/1/80 rSC35M (H7N7)	Gülsah Gabriel Heinrich-Pette Institute, Hamburg	10 FFU

FFU = Focus forming units

*(Results of the Focus Forming Assay (FFA) for counting the number of viruses in a defined volume are expressed as FFU/ml)

2.1.3. Buffers and solutions

Phosphate Buffered Saline (PBS), pH 7.3		
Ingredient	10X	Working solution 1X
NaCl	1370 mM	137 mM
KCl	27 mM	2.7 mM
Na_2HPO_4	80 mM	8 mM
KH_2PO_4	20 mM	2 mM

Sodium Phosphate Buffer (PB), pH 7.4		
Ingredient	1 M	Working solution 0.1 M
$NaH_2PO_4•H_2O$	138 g/l (42.3%)	13.8 g
$Na_2HPO_4•H_2O$	142 g/l (57.7%)	14.2 g

Fixative: 4% Paraformaldehyde (PFA) in 0.1 M Phosphate Buffer, pH 7.4	
PFA	40 g
0.1 M PB	1000 ml

Blocking Solution for Immunohistochemistry in PBS 1X	
Triton X-100	0.2%
Goat serum	10%
Bovine serum albumin (BSA)	1%

Artificial Cerebrospinal Fluid (ACSF), pH 7.4	
NaCl	124 mM
KCl	4.9 mM
KH_2PO_4	1.2 mM
$MgSO_4$	2 mM
$CaCl_2$	2 mM
$NaHCO_3$	24.6 mM
D-glucose	10 mM

Tissue Protein Extraction Reagent	
STKM Buffer (4 ºC) + Proteases Inhibitor	
Sucrose	250 mM
Tris-HCl pH 7.5	50 mM
KCl	25 mM
$MgCl_2$	5 mM
cOmplete™ Protease Inhibitor Cocktail Tablets (1 tablets per 10 ml STKM buffer)	

2.1.4. Antibodies

Primary antibody	Antigen	Dilution	Manufacturer
Mouse Monoclonal Anti-GFAP	Glial fibrillary acidic protein (GFAP)	1:1000	Sigma-Aldrich Catalog No.: G3893
Rabbit Polyclonal Anti-IBA1 / AIF 1: affinity purified	Ionized calcium-binding adaptor molecule 1 (IBA-1)	1:1000	Synaptic Systems Catalog No.: 234003

Secondary antibody	Conjugate	Dilution	Manufacturer
Goat Anti-Mouse IgG (H+L) Code: 115-165-166	Cyanine Cy™3	1:500	Jackson Immuno Research Laboratories
Goat Anti-Rabbit IgG (H+L) Code: 111-165-144	Cyanine Cy™3	1:500	Jackson Immuno Research Laboratories

2.1.5. Kits

Product name	Catalog No.	Manufacturer	Consumption
FD Rapid GolgiStain™	PK401	FD NeuroTechnologies	Neuronal staining
Mouse IFN-γ DuoSet ELISA	DY485-05	R&D Systems	ELISA assay
Mouse IL-1β/IL-1F2 DuoSet ELISA	DY401-05	R&D Systems	ELISA assay
Mouse TNF-α DuoSet ELISA	DY410-05	R&D Systems	ELISA assay

2.1.6. Mouse lines

2.1.6.1. C57BL/6J mice

In the first part of this thesis, female inbred mice of the strain C57BL/6J were obtained from Janvier, France, and maintained under specific-pathogen-free conditions in the central mouse facility of the Helmholtz Centre for Infection Research, Braunschweig, according to the German animal welfare law. Adult mice were kept on a 12 h light/dark cycle with *ad libitum* access to water and food, 5 animals per cage.

2.1.6.2. Type I interferon receptor (IFNAR) knockout mice

In the second part of this thesis, female and male C57BL/6J mice, also referred to as wild-type (WT), were originally purchased from Harlan-Winkelmann, Germany, or Janvier, France, and breeding from these animals were carried. To elucidate the physiological role of the type I interferon (IFN) system in the hippocampal function, the mice with a deficient type I IFN system were utilized. For this purpose, as the inactivation of entire type I IFN gene family is impossible, the gene encoding the known receptor subunit (IFNAR1) was chosen as a target. Inactivation of the IFNAR1 gene in embryonic stem cells was achieved by homologous recombination (Muller et al., 1994). IFNAR-deficient mice ($IFNAR^{-/-}$) were backcrossed to the C57BL/6J background. In order to enable selective depletion of IFNAR on different CNS cell types, conditional IFNAR mice ($IFNAR^{flox/flox}$) (Kamphuis et al., 2006) were intercrossed with transgenic mice that express Cre recombinase in neuroectodermal cells including neurons, astrocytes and oligodendrocytes ($NesCre^{+/-}IFNAR^{flox/flox}$) (Tronche et al., 1999), neurons ($Syn1Cre^{+/-}IFNAR^{flox/flox}$) (Zhu et al., 2001) and astrocytes ($GFAPCre^{+/-}IFNAR^{flox/flox}$) (Bajenaru et al., 2002) respectively and were back bred into C57BL/6J mice. Mice were kept under specific-pathogen-free conditions in the central mouse facility of the Twincore, Centre for Experimental and Clinical Infection Research, Hannover, and at the Helmholtz Centre for Infection Research, Braunschweig. Mice were transported at least 1 week prior to the experiments to the animal facility of the TU-Braunschweig. In all experiment sets of this part, both male and female mice within the all experimental groups exhibited

similar characteristics without any significant differences that allowed us to pool and present the data which obtained from the animals of both genders together.

2.1.6.3. Ethics statement

The experiments performed with mice were approved according to the animal welfare law in Germany. All protocols used in this thesis have been reviewed and approved by the local committees at the Helmholtz Centre for Infection Research and TU Braunschweig and the authorities (LAVES, Oldenburg, Germany; permit number: 3392 42502-04-13/1234) according to the national guidelines of the animal welfare law in Germany ('Tierschutzgesetz in der Fassung der Bekanntmachung vom 18. Mai 2006 (BGBl. I S. 1206, 1313), das zuletzt durch Artikel 20 des Gesetzes vom 9. Dezember 2010 (BGBl. I S. 1934) geändert worden ist.').

2.2. Methods

2.2.1. Virus preparation

All virus strains preparation and mouse infections (except for ELISA experiment) were performed by Dr. Esther Wilk and Prof. Dr. Klaus Schughart, Department of Infection Genetics, Helmholtz Centre for Infection Research, Braunschweig. Stocks of viruses were obtained from Stefan Ludwig, University of Münster (H1N1), Münster variant (Blazejewska et al., 2011), Georg Kochs, University of Freiburg (mouse-adapted H3N2) (Haller et al., 1979), and from Gülsah Gabriel, Heinrich Pette Institute, Hamburg (mouse-adapted H7N7) (Gabriel et al., 2005). Virus stocks were propagated by infection of 10 days old embryonated chicken eggs (H1N1, H3N2) obtained from a commercial vendor (Charles River, Germany) or in MDCK (Madin-Darby Canine Kidney) cell culture (H7N7) as described previously (Wilk and Schughart, 2012).

2.2.2. Mouse infection

Earlier studies in mice have demonstrated sex differences in the immune responses during influenza virus infection. Female mice are reported to be more susceptible and produce more neutralizing antibodies and higher levels of chemokines and cytokines

than males during infection with influenza viruses (Geurs et al., 2012). Therefore, only female mice were used in this study. Mice between 8 to 10 weeks of age were anesthetized by intraperitoneal injection of 0.9% (w/v) NaCl ketamine-xylazine solution (85% NaCl (0.9%), 10% ketamine (100 mg/ml), 5% xylazine (20 mg/ml); 10 ml per 1 kg body weight) and then infected intranasally with a dose of 10 (H3N2 and H7N7) or $2x10^3$ (H1N1) FFU of the respective virus in 20 µl sterile phosphate-buffered saline (PBS 1X). Afterward, the body weight of all mice was monitored for two weeks to confirm the successful infection with influenza A virus strains and subsequent recovery of all infected mice. Percent body weight was calculated compared to body weight at the time of infection. Mice showing more than 30% of body weight loss were euthanized. Control (non-infected) mice received sterile PBS 1X intranasally.

2.2.3. Behavioral assays

In general, the behavioral assays use to investigate the relationship of different behaviors to the environmental or an experimental condition. In this thesis, all behavioral experiments in control and experimental groups were operated during the light period under a dim light illumination between 9:00 to 16:00. The repeated tests were performed almost at the same time of day.

2.2.3.1. Open field test

The open field test is a widely used tool in the behavioral research. Open field locomotion behavior has been examined in a variety of species ranging from invertebrates and birds to mammals (Choleris et al., 2001). In this study, spontaneous locomotor activity and willingness to explore of the mice were assessed using open field test as previously described (Walsh and Cummins, 1976). Mice were placed along the one side of a white PVC open field apparatus (50 cm × 50 cm × 50 cm) for 5 min. The central area of the arena was specified as the center part (30 cm × 30 cm). Between each session of experiments, the apparatus was completely cleaned with Bacillol® to reduce the odor cues. Movement data including total distance traveled, average speed and percentage of mice activity in the periphery and center parts of the arena were collected by ANY-maze (Stoelting, Dublin, Ireland) or Video Mot 2 (TSE Systems GmbH, Bad Homburg, Germany) behavioral tracking software.

2.2.3.2. Elevated plus maze test

Recent research employing the elevated plus maze to assess anxiety in rodents. In this study as well, the elevated plus maze test was performed as previously described in order to investigate anxiety-like behavior (Hogg, 1996). The apparatus comprised a cross with two opposed open arms (25 cm × 5 cm) and two opposed closed arms (25 cm × 5 cm) surrounded by 20 cm high walls. The arena was made of white PVC and was elevated 50 cm above the floor. Mice were placed in the central part of the arena (5 cm × 5 cm) facing toward an open arm and permitted to move freely in the arena for 5 min. Locomotion data including the percentage of time spent in open and closed arms were collected by ANY-maze behavioral tracking software (Stoelting, Dublin, Ireland).

2.2.3.3. Morris water maze test (MWM)

In order to investigate the cognitive behavior of the mice, spatial learning and memory formation was assessed by normal and reversal learning tasks of Morris water maze test. Spatial learning in the Morris water maze is a hippocampus-dependent task where the animals have to locate a hidden platform using visual cues surrounding the pool (Morris, 1984; Vorhees and Williams, 2006). The maze was comprised of a circular pool 150 cm in diameter which was filled with water at 19-20 ^{o}C colored opaque with non-toxic white paint (Titaandioxide, Euro OTC Pharma). The transparent platform was 10 cm in diameter and hidden 1 cm underneath the surface of the opaque water in the target quadrant of the maze with around 35 cm distance to the pool wall. Different black and white visual cues (circle, triangle, 4 vertical stripes) were adjusted an average distance of 30 cm to the maze (Figure 2.1A). Prior to the training a visible platform task was performed as a pre-training and was used to ensure that swimming ability and visual acuity were intact in control and experimental groups, moreover, this phase was important for the animals to get accustomed to the test situation. During this phase, the animals had two trials (maximum of 60 s each) per day for three consecutive days to reach the visible platform, the position was alternated during the trials (Figure 2.1B).

Subsequently, training in the Morris water maze test was performed for 8 days with the invisible platform located in the northeast (NE) quadrant. Each day, animals were

placed in the water for four trials, with different starting points (SE, S, W, and NW) randomly at a 5 min intertrial interval. The animals were permitted to swim freely for 60 seconds or until the platform was reached. Otherwise, they were guided to the platform and allowed to sit on it for 20 seconds. The mice were traced with a camera in the ceiling at the top of the pool.

For qualitative aspects of spatial memory formation during the 8 days of acquisition training, the pathway map to find the platform was analyzed as the searching strategy. Over time, mice switch from egocentric hippocampus-independent strategies including scanning characterized by <60% and >10% surface coverage, chaining characterized by >80% time in a doughnut-shaped annulus zone and random swimming characterized by >60% surface coverage to allocentric directed search strategies characterized by >80% time in Wishaw's corridors (40° goal corridor) which depend on the hippocampus (Whishaw, 2004; Garthe et al., 2009; Garthe and Kempermann, 2013) (Figure 2.1C-E).

For evaluation of reference memory, three probe trial tests were performed at the third and at the sixth day of the acquisition training, prior to starting the four trials of training at that day. Another reference memory test was performed 24 h after the last day of acquisition training (day 9). During the probe trial, the platform was removed and the animals were allowed to swim freely for 45 seconds.

After the third probe trial test, the platform was moved to the opposite quadrant of the pool to test the ability of the animals to form a new memory which then competes with the memory for the old platform position in the reversal Morris water maze task. The task consisted of three training days with maximum 60 seconds time for freely swimming. Afterward, on the fourth day, one single probe trial was performed. This test required plasticity and flexibility of behavior (D'Hooge and De Deyn, 2001). All data including the escape latency (time to reach the platform), percentage of searching time spent in the four quadrants of the pool, percentage time spent in the border (thigmotaxis), annulus (chaining), central circle (scanning) zones and Whishaw's corridors (direct search) of the pool, and occupancy plot of the presence in the quadrants for the animals groups were collected by ANY-maze (Stoelting, Dublin, Ireland) or Video Mot 2 (TSE Systems GmbH, Bad Homburg, Germany) behavioral tracking software.

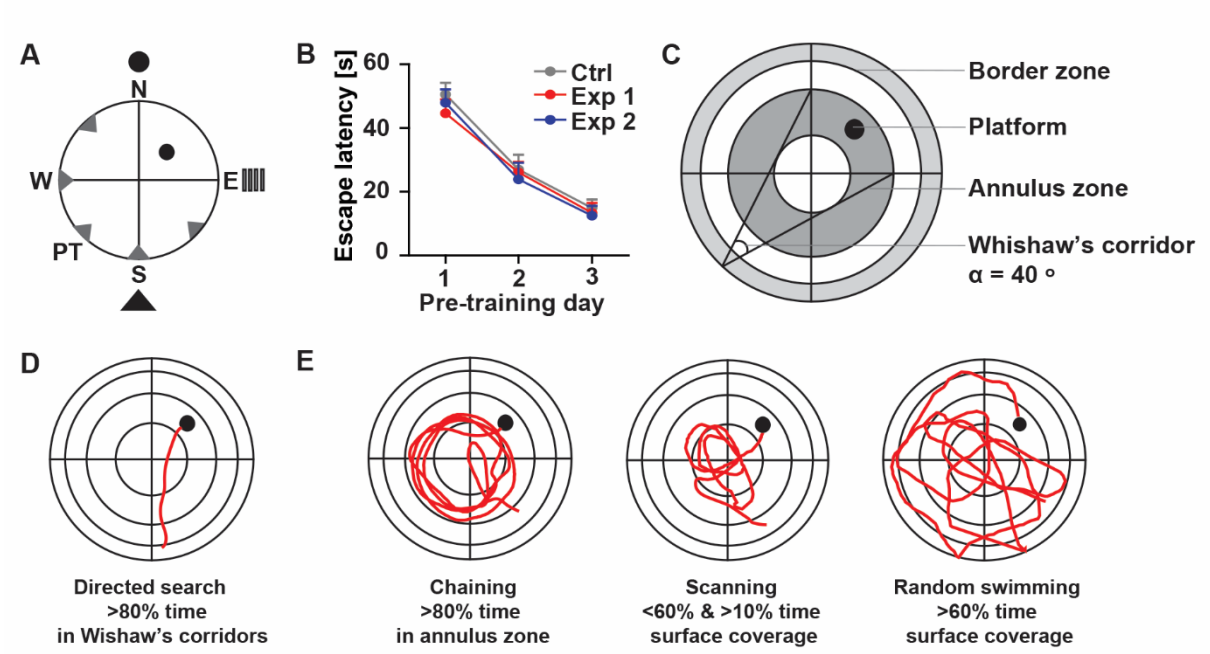

Figure 2.1 | Indicative illustration of the Morris water maze (MWM) used for the assessment of spatial learning and memory. (A) Hidden platform was located in the northeast quadrant of the maze. Black symbols were placed in the north, east and south as the visual cues for the animals. Starting points of the mice swimming during the training and probe trial (PT) were assigned as the gray arrows. **(B)** Representative reduced escape latency example of control and two experimental groups over 3 days of pre-training. **(C)** MWM divided into the four quadrants, the border zone, the donate-shaped annulus zone and Wishaw's corridor. **(D)** Hippocampus-dependent strategy (directed search) and **(E)** hippocampus-independent strategies (chaining, scanning and random swimming) were assessed conforming to the time spent in the different zones of the MWM arena.

2.2.4. Electrophysiological experiment

To investigate the activity of CA1 hippocampal neurons to determine possible compromised hippocampal function, the extracellular electrophysiological recording experiments were performed in control and experimental groups.

2.2.4.1. Preparation of hippocampal acute slices

Mice were deeply anesthetized with 100% CO_2 then sacrificed and the skull was opened. The brain was quickly removed and transferred into the ice-cold carbogenated (95% O_2 and 5% CO_2) artificial cerebrospinal fluid (ACSF). Then, the cerebellum as well as the olfactory bulb, prefrontal cortex and striatum were cut with a scalpel. The hemispheres were separated and one was immediately put back into

the cold ACSF. Afterward, the hippocampus was dissected with two spatulas by gently removing the midbrain and thalamus. Transverse hippocampal slices with 400 µm thickness were obtained by using a manual tissue chopper (whole procedure was done in 2 to 3 min). The interface chamber was washed in advanced with MilliQ-H_2O (de-ionized water) for 30 min and with ASCF for another 20 min with a flow rate of 0.5 ml per min and heated to 32°C by a proportional temperature controller (PTC) (Scientific System Design). The hippocampal slices were transferred to an interface recording chamber (Scientific System Design) on a nylon net where they were incubated at 32°C with constant flow rate (0.5 ml/min) of carbogenated ACSF for 2 hours prior to the start of recordings to ensure the recovery of cell metabolism.

2.2.4.2. Electrophysiological recording experiments

Field excitatory postsynaptic potentials (fEPSPs) were recorded in stratum radiatum of CA1 subregion in hippocampal acute slices. Responses were evoked by stimulation of the Schaffer collateral pathway using two monopolar, lacquer coated stainless-steel electrodes (5 MΩ; AM Systems; S1 and S2). These electrodes were positioned equidistantly on both sides of the recording electrode and by this means two independent stimulation pathways could be used for the same CA1 recordings region (Figure 2.2A). For recording fEPSP (measured as its first slope function), the recording electrode (5 MΩ; AM Systems) was placed at 100 µm depth in the CA1 apical dendritic layer (at least 20 µm far from the soma) (Figure 2.2B) and signals were amplified by a differential amplifier (Model 1700, AM Systems). The signals were digitized using a CED 1401 analog-to-digital converter (Cambridge Electronic Design). Later, only one stimulating electrode was used to evoke long-term potentiation (LTP), the other one considered as a control pathway. When the initial fEPSP acquired with both stimulating electrodes, the slices were incubated for another 20 minutes in the previously mentioned conditions.

2.2.4.3. Input-output curve and paired pulse facilitation

An input–output curve (afferent stimulation vs. fEPSP slope) for assessment the basal synaptic transmission was generated after the pre-incubation period. The given stimulus intensity in µA was associated with the evoked fEPSP slope as a scale for

the synaptic output of a specified population of CA1 neurons. The fEPSPs were recorded at 100 to 600 µA stimulus intensity. The final test stimulation intensity was modified to be adjusted to extract fEPSP slope as 40% of the maximal fEPSP response for both synaptic inputs S1 (stimulus 1) and S2 (stimulus 2) for further electrophysiological experiments.

Then to investigate the short-term plasticity, the paired-pulse stimulation protocol was used with two consecutive stimuli with equal intensity from one of the stimulating electrodes in each hippocampal slice. Paired-pulse facilitation (PPF), is a phenomenon in which EPSP evoked by an impulse is elevated when that impulse closely follows a prior impulse. Therefore, PPF is a form of short-term synaptic plasticity. PPF occurs due to the elevated presynaptic Ca^{2+} concentration upon the first stimulus leading to a greater release of neurotransmitter-containing synaptic vesicles after the second stimulus (Zucker and Regehr, 2002). In this study, PPF extracted from the fEPSP slopes as a response to the second stimulation over the first one at different interpulse intervals (IPIs) included 10, 20, 40, 60, 80, and 100 ms. Analysis of the PPF data was done by calculating the slopes ratio as the second fEPSP slope divided by the first, multiplied by 100.

2.2.4.4. Long-term potentiation (LTP)

In long-term potentiation (LTP), the high-frequency stimulation of hippocampal excitatory synapses produced a rapid and long-lasting elevation in the strength of these synapses that could persist for many days (Bliss and Gardner-Medwin, 1973). LTP which has been demonstrated at synapses throughout the brain remains till now one of the most attractive cellular models for learning and memory (Nicoll, 2017).

Therefore, in the first part of this study, LTP as long-term synaptic plasticity was measured following the assessment of the basal synaptic transmission and the PPF as short-term plasticity experiments in each hippocampal acute slice. To investigate the LTP, after 20 minutes of baseline recording at 40% of the maximal fEPSP slope and with four 0.2 Hz biphasic, constant-current pulses (0.1 ms/polarity) per input channel at 0.003 Hz, LTP was induced by theta-burst stimulation (TBS) including four bursts at 100 Hz repeated 10 times by a 200 ms interval. This stimulation was repeated three times as time distance between one stimulation start to initiation of the next stimulation was 10 seconds (Figure 2.2C). Only the healthy sections with

stable baseline during the baseline recording were induced LTP and included in the electrophysiological data analysis. The slope of fEPSPs was measured over time and normalized to baseline. Data acquisition and offline analysis were performed using IntraCell software (Version 1.5, Institute für Neurobiologie Magdeburg, 2000).

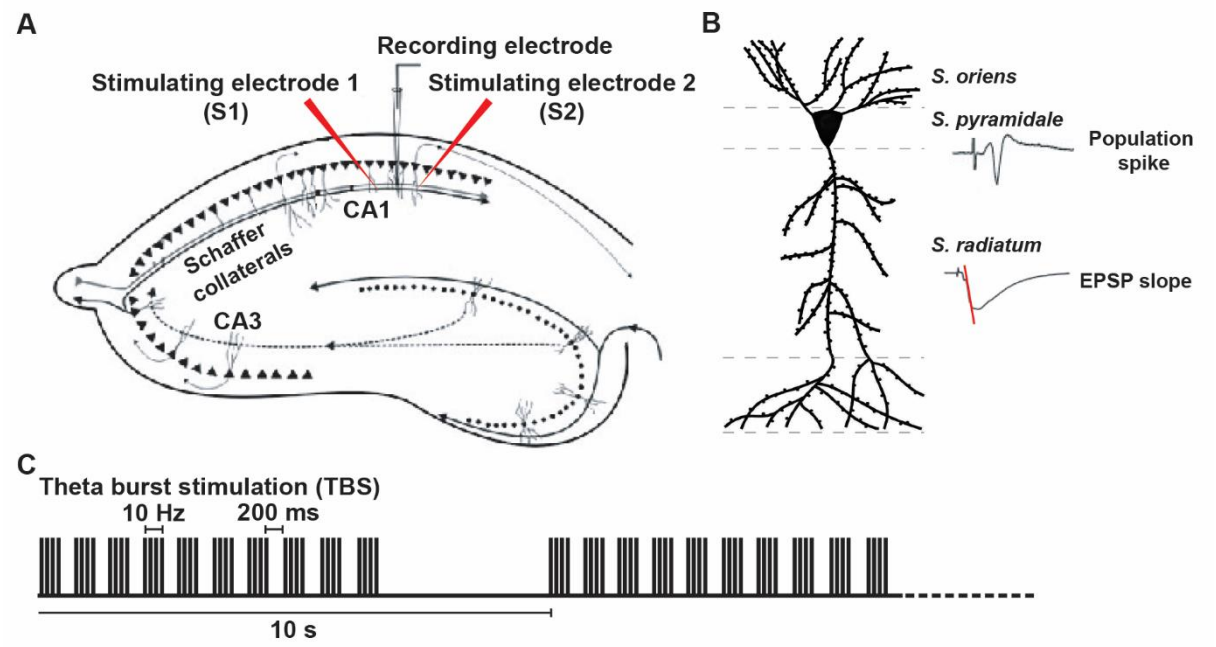

Figure 2.2 | Schematic illustration of the field excitatory postsynaptic potential (fEPSP) recording in the CA1 subregion of a hippocampal acute slice. (A) Transversal hippocampal acute slice with the positioning of two stimulating electrodes and one recording electrode in the stratum radiatum of CA1 hippocampal subregion. **(B)** An indicative example of the fEPSP signal and slope measurement when recording electrode was located in the CA1 stratum radiatum and population spike as the criterion of exclusion when the electrode was located in the wrong areas. **(C)** Theta burst stimulation (TBS) protocol.

2.2.5. Morphological analysis of hippocampal neurons: Golgi-Cox staining

For morphological quantification of hippocampal neurons of control and experimental groups, Golgi-Cox staining was performed. For this purpose, mice were deeply anesthetized with CO_2 and sacrificed via decapitation at the right time point. The whole brain was removed rapidly. The left hemisphere was prepared for further immunohistochemical experiments whereas the right one was incubated in FD rapid Golgi stain kit according to the manufacturer's protocol. Briefly, each hemisphere was immersed in 2 ml impregnation Golgi solution, a mixture of solutions A (potassium dichromate and mercuric chloride) and B (potassium chromate) for at least 14 days

to 1 month at room temperature in the dark followed by one week in tissue-protectant solution C at 4 ºC. Both impregnation and solution C were replaced with fresh solutions on the second day. Metal instruments must be avoided during the impregnation steps. Subsequently, hemispheres were blocked in 2% agar and 200 µm thick coronal sections were cut using a vibratome (Leica VT 1000 S) while chamber filled with 6% sucrose solution in PBS 1X. The slices were collected on gelatin-coated glass slides. Afterward, the sections were processed with solutions D and E for signal development for 10 minutes before being dehydrated through graded alcohols and mounted using Permount (Thermo Fisher Scientific). After finishing the mounting of all samples, the slides are sealed with nail polish. The slides are then kept in a horizontal position for drying in the dark for at least 48 h before imaging. The sections can be subsequently stored in slide boxes in the dark at 4 ºC for long time usage.

2.2.5.1. Agar solution for brain tissue embedding

A solution mixture of 0.15% NaH_2PO_4 (Monosodium dihydrogen phosphate), 0.68% Na_2HPO_4 (Disodium hydrogen phosphate) and 2% Agar in MilliQ-H_2O (de-ionized water) was prepared. The mixture was boiled for some minutes and stirred constantly while heating until melting agar. The temperature should fall to approximately 37-40 ºC before using.

2.2.5.2. Gelatin-Coating Slides

Fifty plain microscopic slides (Thermoscientific) are first placed in five staining racks, washed thoroughly with Mucasol (1:3 in MilliQ-H_2O) overnight, then at least 1 h with running water from the tab and afterward 10 minutes with MilliQ-H_2O. The slides kept for drying in a dust-free area (under a chemical hood) for 2-3 hours. In the meantime, 1% gelatin solution was prepared by dissolving 5 g gelatin (Merck) in 500 ml MilliQ-H_2O with constant stirring and heating to 50-60 °C. After cooling down to 37 °C, 0.5 g Chromium (III) potassium sulfate ($KCr(SO_4)_2$) was added to the solution. The solution was then filtered with filter paper into a clean histological staining jar. A rack with the cleaned slides was immersed into the gelatin solution for 2 times (each time 1 min), subsequently placed on plenty tissue papers and kept at room temperature in

a dust-free area overnight. The slides are usable for 200 µm thick-brain sections. These gelatin-coated slides were stored in closed histological staining boxes and were used within a month of preparation.

2.2.5.3. Imaging and analysis of Golgi-Cox stained neurons

To survey the hippocampal neuron morphology (Figure 2.3), second- or third-order branches of both apical and basal dendrites within the pyramidal shaped CA1 and CA3 neurons as well as both superior and inferior dendrites within dentate gyrus (DG) layers (10 cells in each subregion per animal, 40-50 dendrites per group) were imaged in three-dimensions (z-stack thickness of 0.5 µm) using an Axioplan 2 imaging microscope (Zeiss) equipped with an ApoTome module (Zeiss) with a 63x (N.A. 1) oil objective accompanied with a digital camera (AxioCam MRm, Zeiss). In all selected neurons, spine density per each micrometer of dendrites was calculated using Fiji software (BioVoxxel) on the segments of dendritic branches with a length of more than 60-70 µm which were located at least 40-50 µm away from the cell soma. The total number of spines along the segments of dendritic branches was counted manually. All slides were coded and analyses were performed blindly.

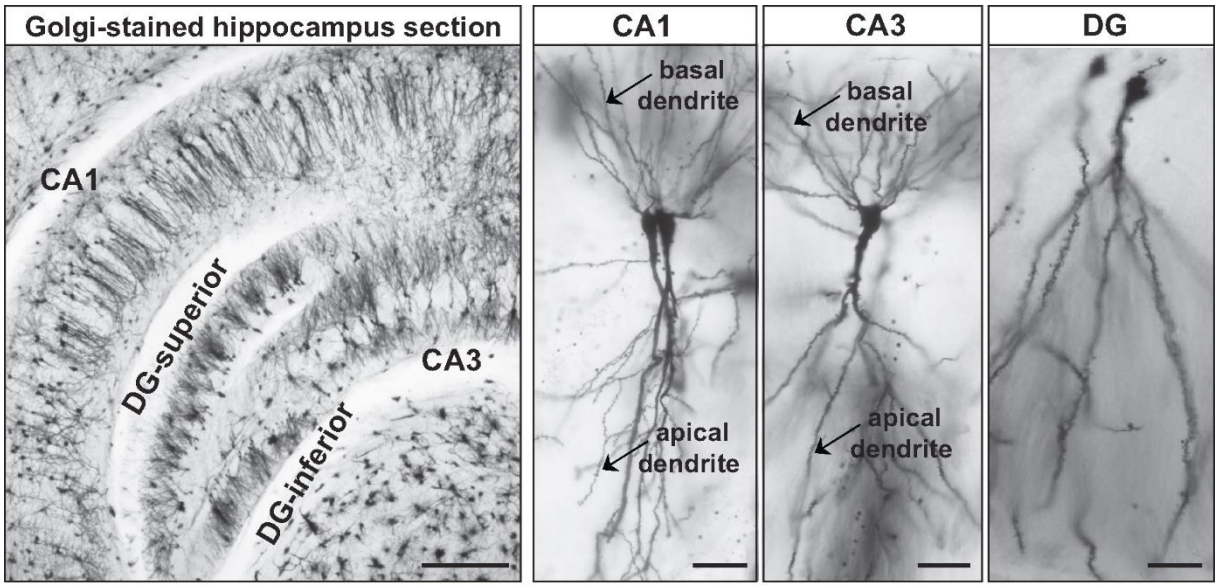

Figure 2.3 | Representative examples of Golgi-stained hippocampal sections and neurons. CA1, CA3 pyramidal neurons and dentate granule cells being located in the superior and inferior blade of the granule cell layer (dentate gyrus, DG) in the hippocampus. Arrows indicated the basal and apical dendrites. Magnification for hippocampal section = 2.5X, scale bar = 200 µm and for hippocampal neurons = 20X, scale bar = 20 µm.

2.2.6. Immunohistochemical experiments

To determine the density and activity of the involved cells in the brain innate immunity, microglia and astrocytes were stained using the immunohistochemical method. For this purpose, the left hemisphere of the mouse brain was isolated and fixed in 4% PFA for 24 hours and then cryoprotected in 30% sucrose solution in 0.1 M PB for another 24 hours. When brain hemispheres were sunk to the ground, they were frozen and stored in Tissue-Tek® O.C.T.™ compound (A.Hartenstein Laborversand) at -70 ºC. For fluorescence immunostaining, 30 µm sections were cut using a freezing microtome (Frigomobil, R.jung Heidelberg, Germany). Afterward, the ten successive sections (five for IBA-1 staining and five for GFAP staining) were washed with PBS 1X and blocked in PBS 1X solution containing 0.2% Triton X-100, 10% goat serum and 1% BSA for 1 hour at room temperature. Sections were incubated overnight at 4ºC with the primary antibodies including IBA-1 (1:1000; rabbit polyclonal) and GFAP (1:1000; mouse monoclonal) diluted in PBS 1X, 0.2% Triton X-100 and 10% goat serum. After three times washing with PBS 1X (each 30 min), the sections were incubated with respective secondary antibodies which were diluted in PBS 1X (1:500; Cy^{TM}3) for 2 hours at room temperature in the dark. Sections were washed by PBS 1X thoroughly (30 min) twice and stained with 4′,6-diamidino-2-phenylindole (DAPI, Sigma-Aldrich) 1:1000 for 3 minutes in order to visualize the nucleus of the cells. After washing, the procedure followed by cover-slipping the slides with Fluoro-gel mounting medium (Electron Microscopy Sciences, Hatfield, PA).

2.2.6.1. Imaging and quantification of glial cells

The IBA-1- and GFAP-stained images from hippocampal subregions including CA1, CA3, superior and inferior blade of DG (5 frames of each subregion per animal, 15-25 frame per each group) were taken in three-dimensions (z-stack thickness of 1 µm) using an Axioplan 2 imaging microscope (Zeiss) equipped with a 20x objective (N.A. 0.8) and a digital camera (AxioCam MRm, Zeiss) under appropriate frequency of ultraviolet light. To quantify the density of microglia and astrocytes, a region of interest (ROI) was drawn in each frame of the hippocampal subregions and the total number of IBA-1 and GFAP positive cells with clearly visible nuclei by DAPI were counted manually by Fiji software (BioVoxxel) and the sampled volume was calculated as the

product of partition area through the section thickness (30 µm). Results are expressed as the number of cells per mm^3 tissues volume. For morphometric analysis of IBA-1 positive cells, 30 microglial cells were randomly selected per hippocampal subregions of IBA-1 stained images from each animal (6 microglia per frame, 90-150 microglial cells per each group). The total primary microglial cell processes were counted using Fiji software (BioVoxxel). For the immunohistochemical experiments as well, all slides were coded and analyses were performed blindly.

2.2.7. Evaluation of blood-brain barrier (BBB) permeability

To determine the blood-brain barrier (BBB) integrity following influenza A virus infection, spectrophotometry was used. Eight weeks old female C57BL/6J mice were infected by H3N2 and H7N7 influenza A virus, then at 4, 8 and 10 days post infection they were injected with a 2% Evans blue solution (Sigma-Aldrich) in normal saline (4 ml/kg of body weight) intraperitoneally. The dye was allowed to distribute by the circulatory system for 5 hours (4 and 8 days post infection) to 20 hours (10 days post infection). Afterwards, the mice were sacrificed and the brain was isolated and frozen in liquid nitrogen and stored at -70°C.

For assessment the presence of the Evans blue dye in the brain tissue as an indicator of a compromised BBB, the brain sample was homogenized in 1100 µl of PBS 1X, sonicated and centrifuged (30 min, 15000 g, 4°C) and the supernatant was collected in aliquots. To each 500 µl aliquot, an equal amount of 50% trichloroacetic acid (TCA) was added, incubated overnight at 4°C and centrifuged (30 min, 15000 g, 4 °C) again. Evans blue absorbance was detected at 610 nm using a spectrophotometer (Denovix DS-11 fx, USA). Finally, to determine the presence of the Evans blue dye in the brain tissue the measured absorbance of the supernatant prepared from brain was calculated according to the absorbance of the standard Evans blue samples (Figure 2.4).

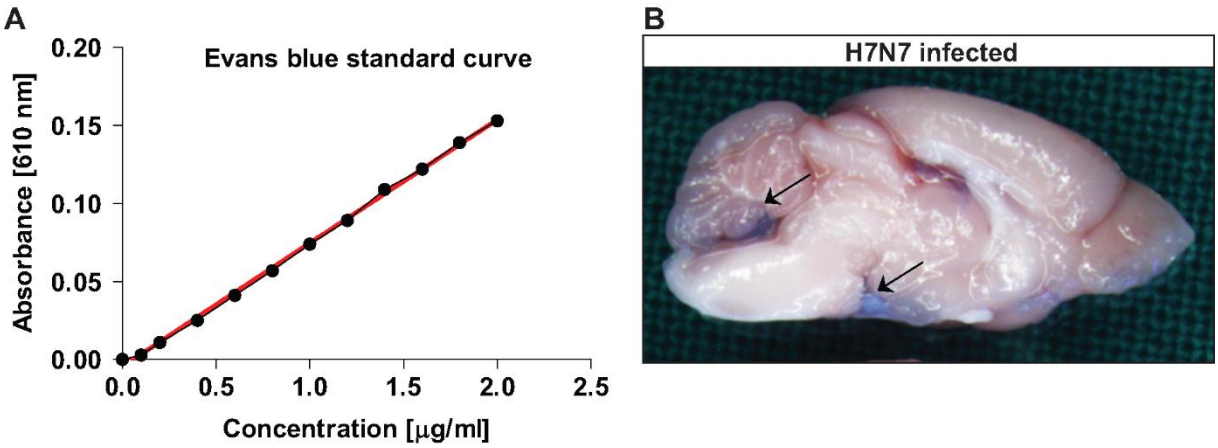

Figure 2.4 | Evaluation of BBB permeability. (A) A standard curve: Evans blue dye concentration (µg/ml) versus light absorbance was plotted. The best equation of the tangent to the curve was Y = 0.07899 X - 0.004486, R = 0.9986. **(B)** Representative examples of the brain of H7N7 infected mouse (10 days post infection) 20 hours after Evans blue injection. Arrows indicate the Evans blue dye.

2.2.8. Enzyme-linked immune sorbent assay (ELISA)

Enzyme-linked immunosorbent assay (ELISA) is a biochemical technique to detect the presence of an antibody or an antigen in a sample using color changes. In this study, to quantify the presence of proinflammatory cytokines including interferon gamma (IFN-γ), interleukin 1 beta (IL-1β) and tumor necrosis factor alpha (TNF-α) in the blood serum and the supernatant of homogenized hippocampi or brain hemispheres of influenza A virus infected mice, ELISA experiment was performed. This method allows detection of secreted cytokines at the protein level.

2.2.8.1. Samples collection

Eight weeks old female C57BL/6J mice were inoculated with influenza A virus strains and PBS as a control. Body weight was monitored and the samples were collected at 8 days post infection (before, the maximum body weight loss was observed at this time). Briefly, mice were deeply anesthetized with CO_2 and sacrificed via decapitation. Blood was taken using a pipette and collected in 1.5 ml Eppendorf tubes. The samples were incubated for at least 30 minutes at room temperature. To separate the serum from the cellular blood components, the samples were centrifuged at 2000 g for 20 minutes at room temperature. The supernatant (blood serum) was immediately transferred to a fresh tube and frozen in liquid nitrogen. The

whole brain was removed rapidly. The right hemisphere was frozen in liquid nitrogen. The hippocampus from left hemisphere was dissected and frozen as well. All samples were stored at -70°C until further use.

2.2.8.2. Tissue protein isolation

The samples were weighed at first. Tissues were homogenized smoothly using an Eppendorf-fitting pestle in 400 µl STKM lysis buffer containing protease inhibitor cocktail. During the entire protein isolation method, the samples were kept on ice as much as possible. Afterwards, the samples were centrifuged for 10 min at 4 °C at 13000 g. The supernatant was collected into a fresh pre-cold Eppendorf tubes and stored at -70 °C before starting the test. The repeated freeze-thaw cycles were avoided.

2.2.8.3. Cytokine assay

To determine cytokines level, a mouse IFN-γ, IL-1β and TNF-α ELISA kits were used according to the manufacturer's recommendations. Briefly, for each cytokine, the standard solution was prepared. 100 µl of samples or standards in Reagent diluent (assay buffer) were added to IFN-γ, IL-1β and TNF-α antibody-coated wells on the 96 well ELISA plate and incubated at room temperature for 2 h. Wells were washed three times before the addition of 100 µl of the detection antibody and incubated for another 2 hours at room temperature. After a second washing cycle (3 times), 100 µl of Streptavidin-horseradish peroxidase was added to the wells and incubated for 20 min at room temperature in the dark. After washing (3 times), 100 µl of hydrogen peroxide/tetramethylbenzidine (TMB) substrate solution was added per well, and the plate was incubated for 30 min at room temperature in the dark. The reaction was stopped by addition of 50 µl of the hydrochloric acid solution provided in the kit. Absorbance at 450 nm was measured with a Tecan Sunrise™ microplate reader with a wavelength correction at 680 nm connected to Magellan software. Finally, the measured optical density of the reaction was compared with the optical density of the known standard samples to determine protein concentration in the samples (Figure 2.5). The intensity of the color is proportional to the amount of cytokine bound to the capture antibody.

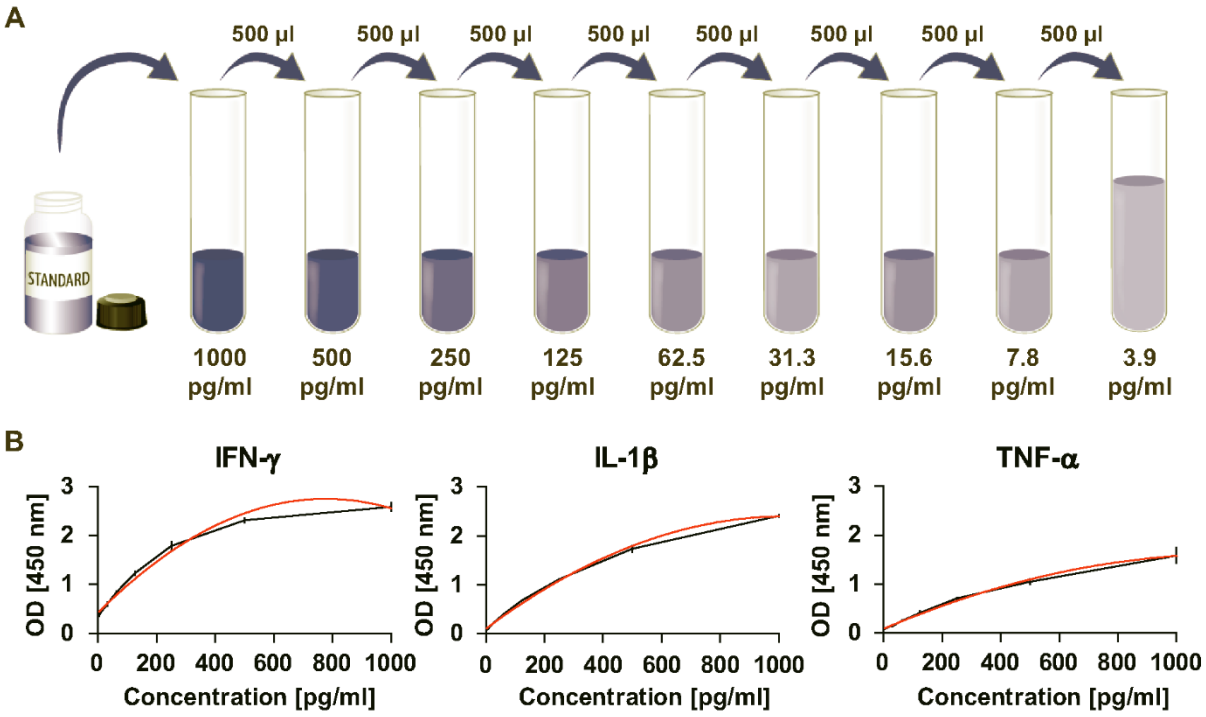

Figure 2.5 | The ELISA standards of mouse IFN-γ, IL-1β and TNF-α. (A) The standard solutions for determining the cytokines in the samples were prepared according to the manufacturer's instruction. **(B)** The standard curves for mouse IFN-γ, IL-1β and TNF-α with error bars based on two replicates for each concentration versus optical density (OD) were plotted. The best equation of the tangent to the IFN-γ curve was $Y = -0.000007696\ X^2 + 0.007753\ X + 0.3609$, $R = 0.9859$; to the IL-1β curve was $Y = -0.000002181\ X^2 + 0.004485\ X + 0.09719$, $R = 0.9968$ and to the TNF-α curve was $Y = -0.0000005496\ X^2 + 0.002098\ X + 0.1103$, $R = 0.9845$.

2.2.9. RNA isolation and gene expression analysis by microarray

This experiment was performed by Prof. Dr. Klaus Schughart, Department of Infection Genetics, Helmholtz Centre for Infection Research, Braunschweig. Briefly, on days 18 and 30 post infection mice were euthanized by CO_2 asphyxiation and the hippocampus was dissected out. Immediately after dissection, the tissue was placed into RNAlater solution (Qiagen), incubated overnight at 4°C and stored at -20°C. For each group, at least three mice were prepared as independent biological replicates. Tissues were homogenized with FastPrep®-24 instrument placing them in a 2 ml lysing matrix tube (MP Biomedicals) containing 1 ml QIAzol Lysis Reagent. Homogenization was performed with 6.0 M/S speed for 1 min. Isolation of RNA was performed with the Rneasy Lipid Tissue Mini Kit (Qiagen). The quality and integrity of the RNA were controlled on the 2100 Bioanalyzer (Agilent Technologies). For DNA

microarray hybridization, 100 ng of total RNA was applied for the Cy3-labelling reaction using the one color Quick Amp Labeling protocol (Agilent Technologies). Labeled cRNA was hybridized to Agilent´s mouse 4x44k microarrays for 16 h at 68°C and scanned using the Agilent DNA Microarray Scanner. The software package Feature Extraction 10.5.1.1 (Agilent Technologies) was used to calculate the respective expression values. Microarray data were analyzed using the R software package (Team, 2013). Pre-processing steps included background correction, quantile normalization and annotation using the MmAgilentDesign026655.db (Carlson, 2014), LIMMA (Smyth, 2004), and Agi4x44PreProcess (Gentleman et al., 2004) packages.

Multi-group comparisons and identification of differentially expressed probe sets (DEPs) were performed with the LIMMA package (Smyth, 2004) using BH correction for multiple testing (Benjamini and Hochberg, 1995). DEPs in the hippocampus were identified based on an adjusted *p*-value of < 0.1 and exhibiting more than a $\log_2$ of 0.5 (1.4 fold) absolute difference in expression levels. Also, KEGG pathway enrichment analysis and cluster profiling were performed (Kanehisa and Goto, 2000). The raw data has been deposited in the GEO expression database (http://www.ncbi.nlm.nih.gov/geo/).

2.2.10. Statistical analysis

Data were analyzed and plotted by GraphPad Prism 6 / 7 (GraphPad Software, Inc. USA) and presented as mean±SEM. Differences in dendritic spine density, IBA-1 and GFAP immunohistochemistry data and cytokines level were subjected to a one-way ANOVA whereas repeated measures ANOVA was used for behavioral and electrophysiological experiments. Bonferroni's correction was used as a post hoc test. The minimum significance value was considered as $p < 0.05$. All experiments were analyzed in a strictly blind fashion.

3. Results

3.1. Long-term neuroinflammation induced by influenza A virus infection and the impact on hippocampal neuron morphology and function

Influenza infection caused by non-neurotropic and neurotropic virus types is one of the important causes of illness and death throughout the world, making it a serious threat for public health (Jurgens et al., 2012). The neurotropic highly pathogenic influenza A virus infection is a zoonosis that results in high mortality in both animals and humans. While influenza virus primarily targets the respiratory system, it is also capable of infecting the CNS (Yu et al., 2014). Many clinical cases with neurological symptoms in the human population have been reported during the swine flu pandemic in 2009 which caused by non-neurotropic H1N1 influenza A virus (Surana et al., 2011). An earlier study provided the first evidence that also a peripheral influenza infection can induce neuroinflammation, altered hippocampal neuron morphology and impaired cognition in adult mice, during the acute phase of the disease (Jurgens et al., 2012). Although most of the people can fully recover from influenza infection, especially the long-term consequences on the CNS function remain elusive. Therefore, to investigate the long-term consequences of non-neurotropic and neurotropic influenza A virus infection on hippocampal neuron morphology and function, an influenza infection mouse model which was generated by Dr. Esther Wilk and Prof. Dr. Klaus Schughart, Department of Infection Genetics, Helmholtz Centre for Infection Research, Braunschweig (Wilk and Schughart, 2012) for investigation on the CNS, was utilized.

3.1.1. Infection of C57BL/6J mice with different influenza A virus subtypes - a mouse model to study the long-term effects on hippocampal function

In this study, female C57BL/6J mice at the age of 8 to 10 weeks were infected with influenza A viruses by intranasal inoculation under anesthesia with ketamine/xylazine. Three different influenza A virus subtypes were chosen. First, the well-studied mouse-adapted human PR8 (H1N1) virus (Blazejewska et al., 2011) was selected. This specific non-neurotropic influenza A virus variant was also used by Jurgens et al. demonstrating altered hippocampal neuron morphology and impaired cognition during the acute phase of the infection (Jurgens et al., 2012). In addition,

another non-neurotropic mouse-adapted human influenza A virus strain, the maHK68 (H3N2) (Haller et al., 1979) was chosen that recently was investigated frequently (Leist et al., 2016). To include also a neurotropic virus of avian origin, which was isolated from seals and adapted to the mouse, rSC35M (H7N7) (Gabriel et al., 2005) as a model virus for high pathogenic avian derived viruses, was used. The advantage of this virus is that a substantial amount of mice are able to survive the infection, whereas mice infected with neurotropic H5N1 influenza virus could not survive. Similar to H5N1, the avian H7N7 virus also caused disease in mammals in the past including humans and represent a potential pandemic threat if interspecies transmission occurs (Lang et al., 1981; Banks et al., 1998; Fouchier et al., 2004; Shinya et al., 2005). In summary, two non-neurotropic human variants (H1N1 and H3N2) and a neurotropic mouse-adapted variant (H7N7) of high pathogenic avian origin that successfully crossed the species barrier were selected in this study. The appropriate doses to sub-lethal concentrations which allow us to study long-term effects of three different mouse-adapted influenza A viruses were adjusted. First, 2×10^3 FFU (Focus forming assay) of low-virulent mouse-adapted A/PuertoRico/8/34 (H1N1), Münster variant (PR8M) (Blazejewska et al., 2011), second, 10 FFU of maHK68, mouse-adapted A/Hong-Kong/1/68 (H3N2) (Haller et al., 1979) and third 10 FFU of the avian, polybasic virus with known neurotropism rSC35M, A/Seal/Mass/1/80 mouse (H7N7) (Gabriel et al., 2005) were used. Control mice inoculated intranasally with an equal volume (20 µl) of sterile PBS 1X (vehicle). Following infection with 2×10^3 FFU of H1N1, 100%, 10 FFU of H3N2, 84% and 10 FFU of H7N7 76% of infected mice survived (Control: 100 ± 0 %, H1N1: 100 ± 0 %, H3N2: 84.12 ± 4.60 % and H7N7: 76.34 ± 4.40 %) (Figure 3.1.1A).

The body weight of all animals was controlled over 14 days after infection to confirm the successful infection and subsequent recovery of all tested infected mice. Body weight loss of rodents can be associated with pathogen burden and cytokine release for many infectious diseases (van Heeckeren et al., 2000). After infection with influenza A viruses, no change in the general appearance of the mice was observed during the first 2 days after inoculation. However, after the third day, infected mice with all three used viruses showed reduced activity and ruffled fur accompanied by reduced food and water intake and obvious and comparable body weight loss (Figure 3.1.1B). While the maximum percentage of body weight loss related to the initial body weight in H3N2 (79.16 ± 2.21 % of the initial body weight) and H7N7 (78.92 ± 1.89

%) infected mice occurred at day 9 post infection, this was one day later than in H1N1 (79.54 ± 2.95 %) infected animals. Subsequently, all surviving infected mice recovered. Control animals showed no change in body weight over the whole period of measurement (Figure 3.1.1B). Next, the positive staining for viral nuclear protein (NP) in the brain of influenza A virus infected mice was performed by Dr. Esther Wilk. NP positive cells in the brains of H1N1 and H3N2 non-neurotropic influenza A virus infected mice were not detectable which in turn confirms that these variants are not able to infect the brain directly (Figure 3.1.1C), whereas this was indeed the case in H7N7 infected animals. NP positive cells in H7N7 infected mice could be observed in various regions of the brain (e.g. mesencephalon, thalamus, medulla oblongata, cerebellum, cortex, olfactory bulb and hippocampus) indicating that there are no specific target areas (Figure 3.1.1D).

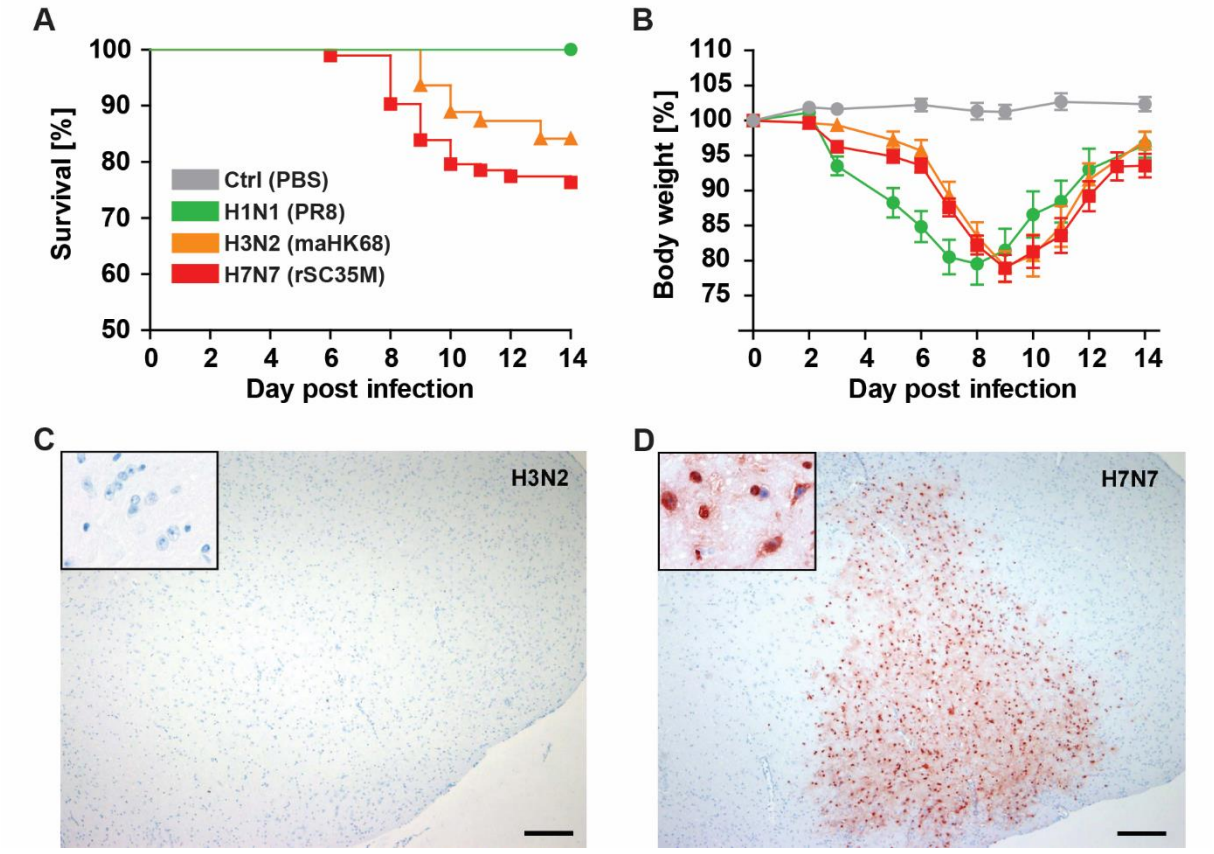

Figure 3.1.1 | Influenza A virus infection with 2×10^3 FFU H1N1 (PR8), 10 FFU H3N2 (maHK68) and 10 FFU H7N7 (rSC35M) in young female C57BL/6J mice. Control mice received the vehicle, PBS 1X solution. (A) The survival rate of control and infected mice is presented. 100% of control and H1N1 infected mice (n=37) survived while 84% of H3N2 (n=63) and 76% of H7N7 infected mice (n=93) survived from infection. **(B)** A representative experiment of body weight loss depicted as percentage

of the starting weight of C57BL/6J mice during the acute phase of influenza A virus infection is shown; Body weight loss of infected mice as a cause of the immune stimulation due to the infection started from day 3 post infection, and subsequent recovery during the first 14 days, while the recovery phase of H1N1 infected mice was started one day (day 8) before H3N2 and H7N7 infected mice (day 9) (n=10-18). **(C)**, **(D)** Immunohistochemistry using Mayer's hematoxylin as counterstaining did not reveal influenza nucleoprotein (NP) in the CNS (medulla oblongata) of mice 7 days after infection with H3N2 whereas the high numbers of virus infected cells in the medulla oblongata of H7N7 infected mice was observed (Bar=80 µm). **These results were provided by Dr. Esther Wilk and Prof. Dr. Klaus Schughart, Department of Infection Genetics, Helmholtz Centre for Infection Research, Braunschweig.**

3.1.2. Long-term effects of influenza A virus infection on locomotor activity, exploration and anxiety-like behavior of C57BL/6J mice

It is speculated that viral infection in the acute phase could be responsible for a wide range of behavioral abnormalities, including cognitive, motor and social behavioral impairments (Brown and Susser, 2002). Locomotor activity, exploration and anxiety-like behavior using the open field and the elevated plus maze test are frequently applied in the assessment of behavioral effects of viral infection in animals. Therefore, in this study to evaluate whether infection with different influenza A virus subtypes could alter spontaneous activity or anxiety-like behavior in mice, the open field and elevated plus maze tests were performed (Figure 3.1.2 and 3.1.3). First, mice were tested 30 and 120 days post infection (pi) for 5 minutes in the open field arena, total distance traveled, average speed and the activity percentage of mice in the different zones of the arena were analyzed. In both time points, 30 and 120 days pi, total distance traveled based on meter as unit (30 days pi - Control: 1.62 ± 0.11, H1N1: 1.13 ± 0.09, H3N2: 1.41 ± 0.17 and H7N7: 1.38 ± 0.19) (120 days pi - Control: 1.53 ± 0.17, H3N2: 1.68 ± 0.15 and H7N7: 1.06 ± 0.07) and average speed based on meter per second as unit (30 days pi - Control: 0.0055 ± 0.0004, H1N1: 0.0037 ± 0.0003, H3N2: 0.0048 ± 0.0005 and H7N7: 0.0046 ± 0.0005) (120 days pi - Control: 0.0050 ± 0.0005, H3N2: 0.0057 ± 0.0005 and H7N7: 0.0035 ± 0.0002) in control and influenza A virus infected mice did not reveal any considerable sickness behavior and locomotor deficiency (Figure 3.1.2A,B). To evaluate anxiety-like behavior, the percentage of time spent in the periphery and the center zones of the open field arena was assessed. Since control and infected mice at 30 (Periphery, control: 72.16 ± 2.99 %, H1N1: 79.53 ± 4.15 %, H3N2: 74.02 ± 6.82 % and H7N7: 87.08 ± 3.68 % - Center,

control: 27.83 ± 2.99 %, H1N1: 18.97 ± 3.87 %, H3N2: 25.97 ± 6.82 % and H7N7: 12.92 ± 3.68 %) and 120 days pi (Periphery, control: 68.20 ± 7.52 %, H3N2: 81.55 ± 1.81 % and H7N7: 82.30 ± 3.34 % - Center, control: 31.80 ± 7.52 %, H3N2: 18.44 ± 1.81 % and H7N7: 17.70 ± 3.34 %) spent comparable time in the periphery and the center zones of the open field arena, they did not show any differences in exploratory and anxiety-like behavior (Figure 3.1.2C).

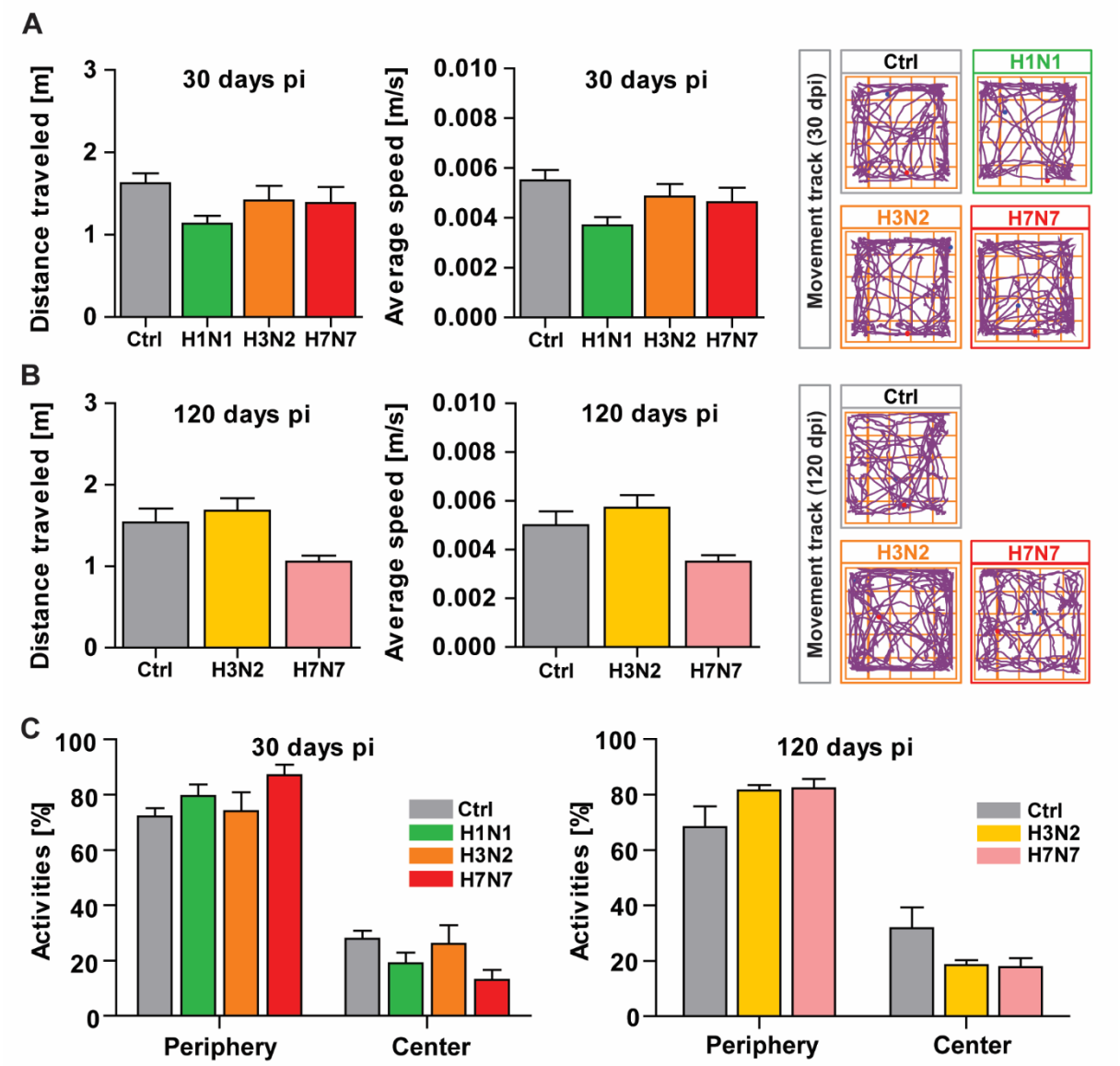

Figure 3.1.2 | Long-term effects of influenza A virus infection on general locomotion, willingness to explore and anxiety-like behavior in the open field test. (A), **(B)** At 30 and 120 days post infection (pi) a total distance traveled, average speed and representative tracks of movement patterns of mice in an open field box are presented. There was no significant difference between all tested groups. **(C)** Activity percentage of mice in the periphery and center part of open field arena as

well did not show any significant changes. Therefore no sickness behavior, locomotors deficiency or anxiety-like behavior was detectable in infected mice. Data are presented as mean ± SEM, (n=7-10).

Next, anxiety-like behavior was tested specifically using the elevated plus maze test. For this purpose, 30 and 120 days pi mice were tested for 5 minutes in the elevated plus maze and the tracks on open and closed arms were analyzed. Naturally, rodents are neophobic and averse to bright light, the animals tend to avoid open spaces and stay close to the walls or closed arms when they are placed in a novel, well-lit open field or elevated plus maze arena (Tomonaga, 2004), therefore, the tested mice spent most of the time in closed arms. Again, the percentage of time spent in open and closed arms was similar in all groups tested 30 days (Closed arms, control: 67.06 ± 5.35 %, H1N1: 81.03 ± 6.43 %, H3N2: 77.90 ± 4.72 % and H7N7: 81.61 ± 2.95 % - Open arms, control: 15.86 ± 4.00 % , H1N1: 4.74 ± 0.58 %, H3N2: 9.45 ± 2.56 % and H7N7: 9.32 ± 1.85 %) and 120 days pi (Closed arms, control: 81.73 ± 8.50 %, H3N2: 79.16 ± 5.68 % and H7N7: 83.03 ± 4.77 % - Open arms, control: 8.50 ± 2.19 %, H3N2: 6.26 ± 1.37 % and H7N7: 5.23 ± 1.40 %) (Figure 3.1.3). Thus, control, as well as infected mice, did not reveal any significantly elevated anxiety levels.

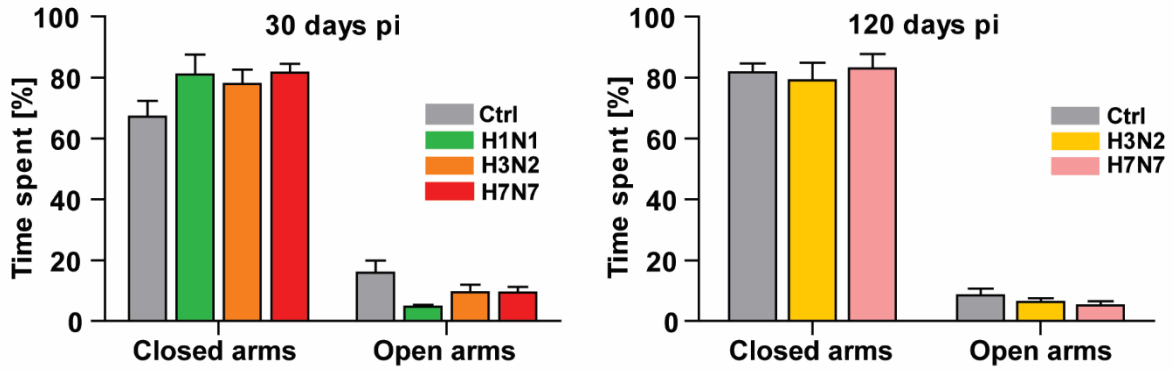

Figure 3.1.3 | Long-term effects of influenza A virus infection on anxiety-like behavior. The percentage of time spent in the open and closed arms of the elevated plus maze were similar in all groups tested at 30 and 120 days post infection (pi). Therefore, the mice did not indicate elevated anxiety levels. Data are presented as mean ± SEM, (n=7-10).

3.1.3. Long-term effects of influenza A virus infection on cognitive function of C57BL/6J mice

Cognition is a parameter that shows an integrated function of the neuronal system, because cognitive abilities involve many tasks, including learning, memory, motivational, and/or motor activities. Assessment using the Morris water maze is often performed to investigate dysfunctions or neuroanatomical abnormalities in specific brain regions, particularly in the hippocampus. Several viruses, including Borna disease virus (BDV), herpes simplex virus (HSV), Simian immunodeficiency virus (SIV), lymphocytic choriomeningitis virus (LCMV) and murine leukemia virus (MLV), induce learning and memory impairment in rodent or non-human primate models (Weed and Gold, 2001; Tomonaga, 2004). On the other hand, earlier studies indicate that influenza infection can be associated with neurological symptoms as cognitive and emotional impairment (Beraki et al., 2005; Asp et al., 2009; Jurgens et al., 2012). Therefore, in this study, it was investigated whether infection with different influenza virus strains would affect mouse behavior in a virus-specific manner.

The hippocampus is a brain region crucially involved in cognitive functions which is moreover especially vulnerable to neuroinflammation (Heneka et al., 2014; Korte and Schmitz, 2016). In addition, the H7N7 variant could also be detected in the hippocampus of infected animals. Therefore, the well-established normal and reversal Morris water maze task as a paradigm to study the long-term consequences of an influenza A virus infection on learning and memory formation 30 and 120 days post infection was chosen (Morris, 1984; Vorhees and Williams, 2006). First, mice were trained to locate the hidden platform in the northeast quadrant of the maze for 8 consecutive days. A reference memory test without platform was performed on day 3 and 6 prior to the training session and on day 9 after the entire training period. It has to be emphasized again that the behavioral assays were performed at a time where the animals were fully recovered from the acute infection. Therefore, the physical weakness caused by acute infection could not affect the outcome of behavioral tests. The Morris water maze task reveals hippocampus-dependent spatial learning and memory formation as the animals have to navigate to a hidden platform using distal cues. Swimming time (escape latency) and path length can be used as a measure for memory formation over consecutive days (Morris, 1984; Vorhees and Williams, 2006). After 8 days of acquisition training in both time points

(30 and 120 days pi), the escape latency was reduced significantly in control as well as in infected mice (Figure 3.1.4A,B), thereby indicating that all groups showed hippocampus-dependent spatial learning and memory formation (repeated measures ANOVA: $F_{CONT\text{-}30dpi}$ (7, 49) = 11.2199, $p < 0.001$, $F_{H1N1\text{-}30dpi}$ (7, 63) = 12.9900, $p < 0.001$, $F_{H3N2\text{-}30dpi}$ (7, 42) = 9.5023, $p < 0.001$, $F_{H7N7\text{-}30dapi}$ (7, 49) = 7.1953, $p < 0.001$, $F_{CONT\text{-}120dpi}$ (7, 42) = 18.1155, $p < 0.001$, $F_{H3N2\text{-}120dpi}$ (7, 42) = 5.6197, $p < 0.001$ and $F_{H7N7\text{-}120dpi}$ (7, 49) = 10.1193, $p < 0.001$). Yet, The escape latency in H7N7 infected mice 30 days post infection was significantly higher than control, non-neurotropic H1N1 and H3N2 influenza A virus infected mice (Day 5: Control: 9.90 ± 1.34 s, H1N1: 8.50 ± 1.78 s, H3N2: 12.82 ± 2.24 s and H7N7: 28.79 ± 3.63 s – Day 7: Control: 5.27 ± 0.91 s, H1N1: 7.56 ± 0.88 s, H3N2: 8.76 ± 1.23 s and H7N7: 22.76 ± 3.11 s) (Figure 3.1.4A), pointing out an impairment in spatial learning and memory formation following infection with this neurotropic virus ($F_{treatment}$ (3, 1024) = 57.85, $p < 0.0001$). Three months later, at day 120 post infection analysis of the escape latency in control as well as influenza A virus infected mice did not reveal any significant differences ($F_{treatment}$ (2, 680) = 0.3500, $p = 0.7048$) (Figure 3.1.4B). While the escape latency provides a read out for memory acquisition, the reference memory test (probe trial) provides a quantification for the retrieval of the specific memory. During the probe trials, the platform is removed and animals are allowed to freely explore the pool. The test was performed on day 3 and 6 prior to the training session and on day 9 before the actual training began (Figure 3.1.4C,D). The results of the probe trial tests revealed that the time spent in the target quadrant by H1N1 and H3N2 influenza A virus infected mice at day 30 post infection increased over the training time similar to control mice. Again, as was the case for the learning H7N7 infected mice showed a significantly reduced preference for the target quadrant on day 6 and 9 compared to the other groups tested (Day 6: Control: 43.94 ± 3.18 %, H1N1: 52.55 ± 4.61 %, H3N2: 48.73 ± 4.87 % and H7N7: 29.22 ± 4.06 % - Day 9: Control: 50.25 ± 2.32 %, H1N1: 65.13 ± 4.13 %, H3N2: 62.06 ± 6.39 % and H7N7: 44.25 ± 6.70 %) (Figure 3.1.4C) indicating an impairment in memory retrieval. The quadrant preference was tested again during and after the training, at 120 days post infection and the analysis revealed comparable results in all groups irrespective of the previous infection (Figure 3.1.4D).

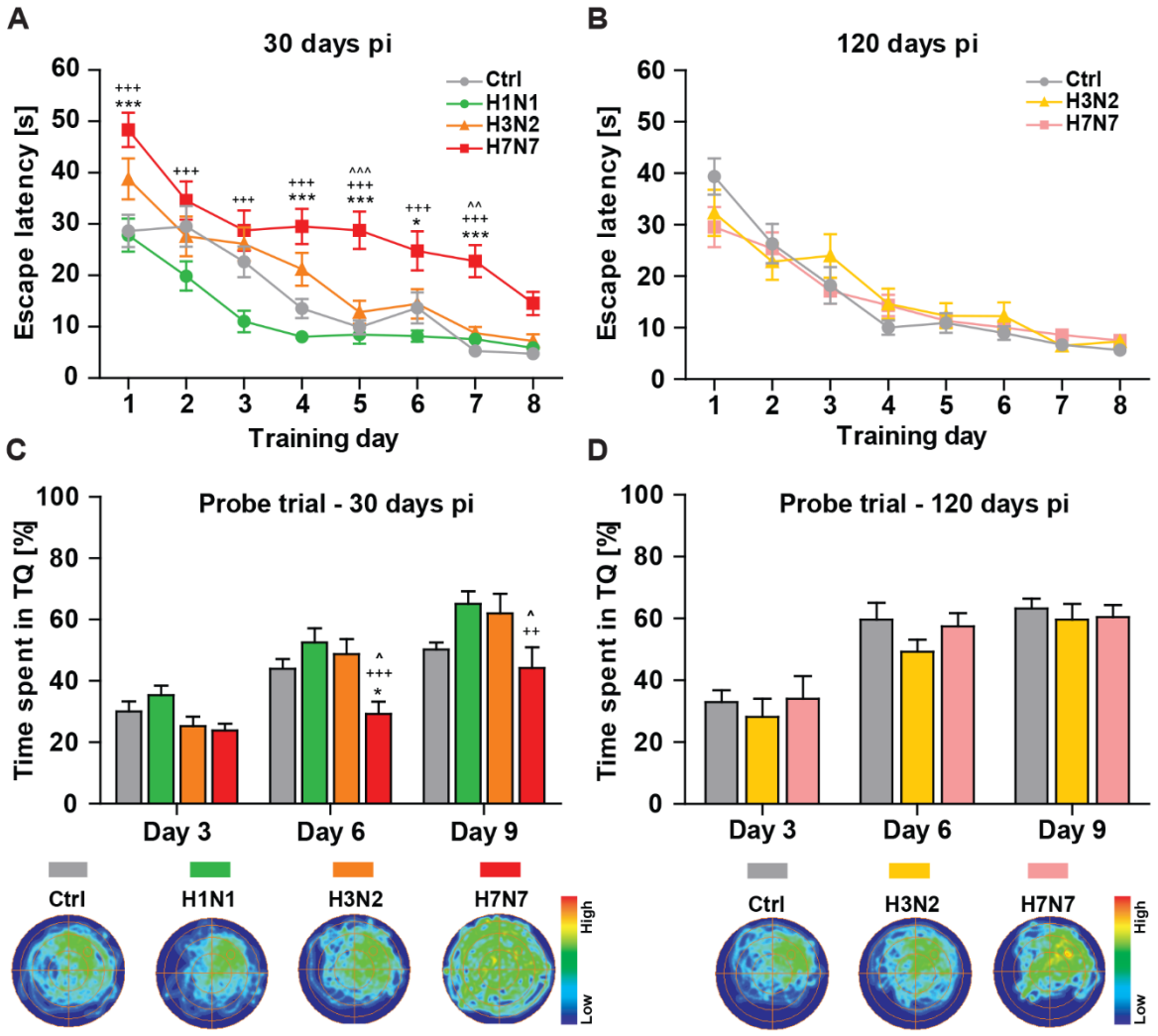

Figure 3.1.4 | Long-term effects of influenza A virus infection on cognitive function. During 8 days of acquisition training, the escape latency reduced significantly in each group of control and infected mice but **(A)** at 30 days post infection (pi) the escape latency in H7N7 infected mice was significantly increased compared to control and non-neurotropic H1N1 and H3N2 influenza A virus infected mice. **(B)** At 120 days pi the escape latency in all control as well as influenza A virus infected mice did not reveal any significant differences. One single probe trial was performed after day 3, 6 and 9 of the training period. **(C)** The time percentage spent in the target quadrant (TQ, northeast) by H1N1 and H3N2 influenza A virus infected mice at day 30 pi was increased like the control mice, though H7N7 infected mice had a significant target quadrant preference reduction on day 6 (as the occupancy plot showed) and 9 compared to the other groups. **(D)** The quadrants preference during the probe trials were tested again 120 days pi and it was similar in all groups as the occupancy plot of probe trial of day 6 showed. Data are presented as mean ± SEM, (n=7-10). * $p < 0.05$ and *** $p < 0.001$ compared to control. ++ $p < 0.01$ and +++ $p < 0.001$ compared to H1N1. ^ $p < 0.05$, ^^ $p < 0.01$ and ^^^ $p < 0.001$ compared to H3N2.

To investigate the quality of spatial learning during the acquisition training days between control and infected groups, the search strategies were analyzed. This detailed analysis of the swimming path allows for a qualitative assessment of learning in mice during the acquisition training days. Progressively over time, healthy animals switch from egocentric to allocentric strategies to navigate to the hidden platform while a spatial map of the maze is formed (Garthe et al., 2009; Garthe and Kempermann, 2013). The quantification of the time spent in the middle of the pool, the outer regions, an annulus doughnut-shaped zone or the Wishaw's corridor allows to differentiate the searching strategies used by the mice into hippocampus-dependent (spatial learning) allocentric search strategy including directed search with increasing accuracy and hippocampus-independent (non-spatial learning) egocentric strategies like chaining, scanning and random swimming (Figure 3.1.5 and 3.1.6). The results indicated that all groups showed an augmentation of hippocampus-dependent search during the 8 days of training (repeated measures ANOVA: F_{30dpi} (7, 232) = 16.60, $p < 0.001$ and F_{120dpi} (7, 152) = 8.22, $p < 0.001$). However, this progression was clearly decreased for H3N2 and H7N7 influenza A virus infected animals 30 days post infection (repeated measures ANOVA: $F_{treatment\text{-}30dpi}$ (3, 232) = 11.29, $p < 0.001$) as these mice utilized significantly more hippocampus-independent searching strategies (repeated measures ANOVA: $F_{treatment\text{-}30dpi}$ (3, 232) = 24.43, $p < 0.001$) (Figure 3.1.5A). Differences in the distribution of search strategies including directed search and random swimming were significantly different between control, H7N7 and even H3N2 influenza infected mice (Directed search, Day 4: Control: 40.62 ± 8.09 %, H1N1: 42.50 ± 8.40 %, H3N2: 21.42 ± 6.52 % and H7N7: 18.75 ± 4.09 % - Random swimming, Day 4: Control: 0.00 ± 0.00 %, H1N1: 5.00 ± 3.30 %, H3N2: 32.14 ± 11.85 % and H7N7: 53.12 ± 11.99 %) (Figure 3.1.5B). However, 120 days post infection no significant differences in the percentage of hippocampus-dependent and -independent strategies used between influenza A virus infected and control mice were observed during the acquisition training days (Figure 3.1.6A). Also, the detailed analysis of directed search and random swimming strategies during the 8 days of training did not reveal any significant differences between control and influenza A virus infected mice (repeated measures ANOVA: directed search $F_{treatment\text{-}120dpi}$ (2, 152) = 1.32, $p = 0.26$ and random swimming $F_{treatment\text{-}120dpi}$ (2, 152) = 0.92, $p = 0.39$) (Figure 3.1.6B).

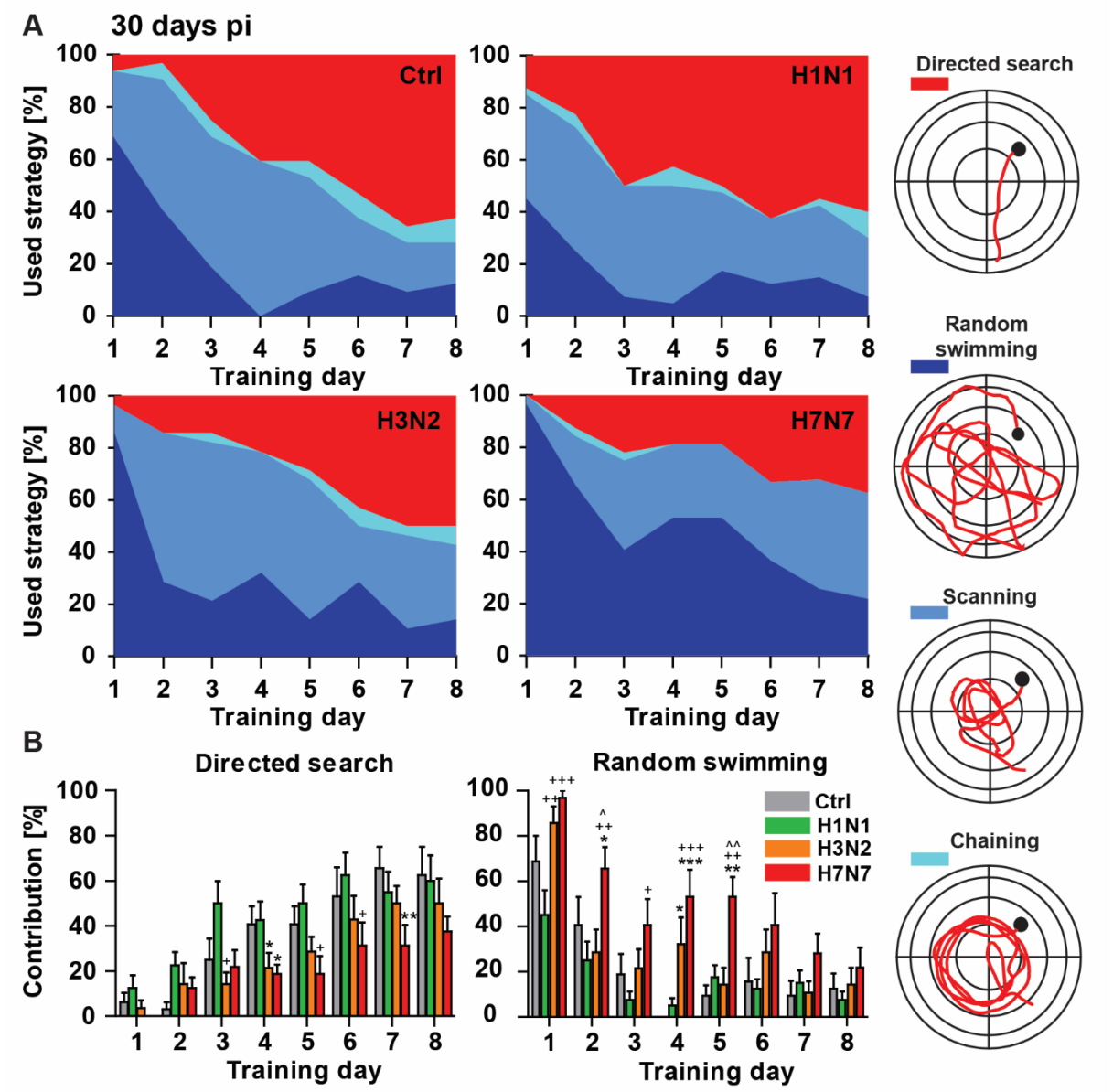

Figure 3.1.5 | Long-term effects of influenza A virus infection on qualitative analysis of spatial learning in mice (30 days post infection). With regard to the different searching strategies to locate the hidden platform during the acquisition phase of the Morris water maze experiment, hippocampus-independent searching strategies including random swimming, scanning and chaining decreased over time whereas hippocampus-dependent searching strategy such as direct search increased. The searching strategies (directed search, chaining, scanning and random swimming) were color-coded and the contribution of the respective strategy in percent was presented for each day of the Morris water maze task. **(A)**, **(B)** The hippocampus-dependent strategy was decreased following H7N7 infection compared to other groups, also H3N2 infected mice showed the reduced usage of hippocampus-dependent strategy at 30 days pi. Data are presented as mean ± SEM, (n=7-10). * $p < 0.05$, ** $p < 0.01$ and *** $p < 0.001$ compared to control. + $p < 0.05$, ++ $p < 0.01$ and +++ $p < 0.001$ compared to H1N1. ^ $p < 0.05$ and ^^ $p < 0.01$ compared to H3N2.

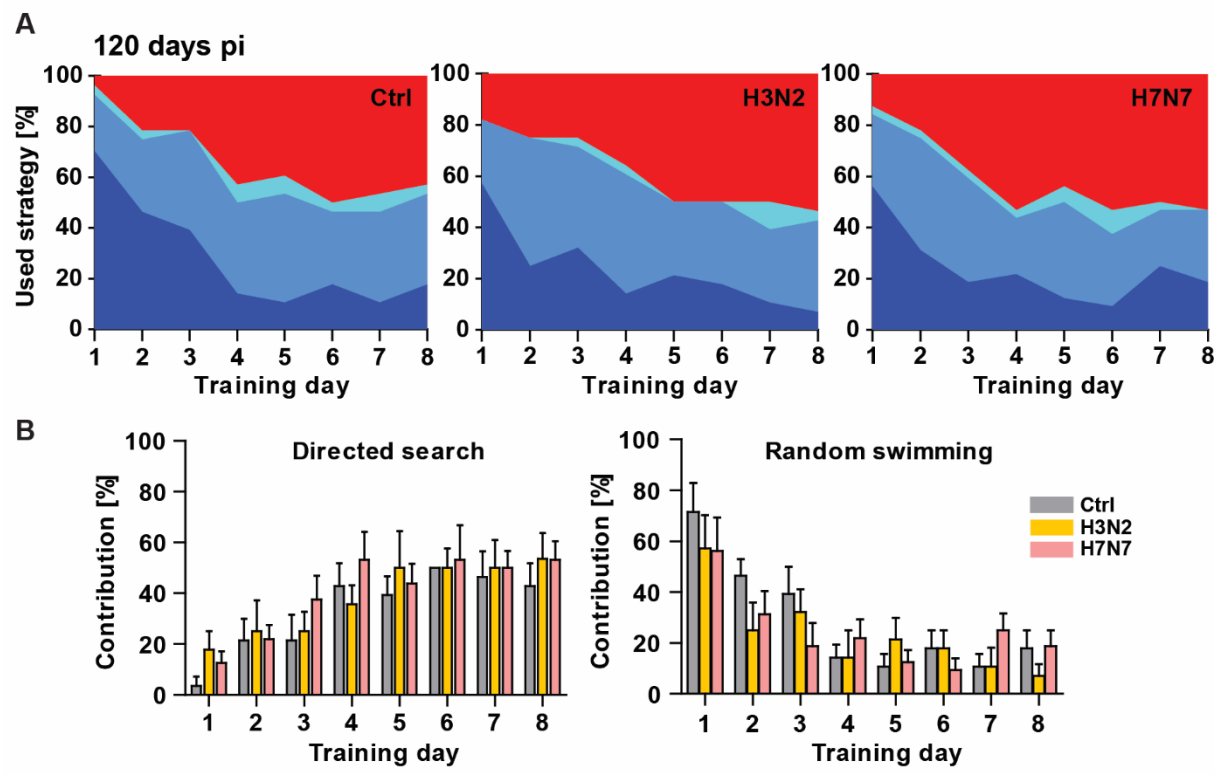

Figure 3.1.6 | Long-term effects of influenza A virus infection on qualitative analysis of spatial learning in mice (120 days post infection). (A), **(B)** No significant differences in searching strategies between influenza A virus infected and control mice were observed 120 days pi. Data are presented as mean ± SEM, (n=7-10).

While H7N7 influenza A infected mice showed a cognitive impairment at 30 days post infection, H3N2 infected mice only showed a mild impairment in the initial formation of the memory indicated by a reduction in hippocampus-dependent searching strategies compared to control mice (Figure 3.1.5). However, cognitive deficits became apparent during the reversal phase of the Morris water maze task (Figure 3.1.7). In the reversal water maze paradigm, the hidden platform was moved to the opposite quadrant of the pool but all distal visual cues remained constant. Once a spatial map including the distal cues is formed, a new platform position only needs to be updated in the already existing cognitive map and can, therefore, be memorized faster. However, depending on the flexibility of the animal the two memories can also compete with each other which can be seen especially during the probe trial test. During 3 days of reversal training, the escape latency to the new platform position decreased significantly in control (repeated measures ANOVA: $F_{CONT\text{-}30dpi\text{-}R}$ (2, 14) = 16.1558, $p < 0.001$), H1N1 ($F_{H1N1\text{-}30dpi\text{-}R}$ (2, 18) = 42.2855, $p < 0.001$) and H7N7 ($F_{H7N7\text{-}}$

$_{30dpi\text{-}R}$ (2, 14) = 8.7589, p = 0.003) but not in H3N2 ($F_{H3N2\text{-}30dpi\text{-}R}$ (2, 12) = 2.593, p = 0.0810) influenza A virus infected mice at 30 days post infection (Figure 3.1.7A). In addition, H7N7 influenza A virus infected mice showed a significantly higher escape latency than control and H1N1 infected mice. Therefore, both H3N2 and H7N7 viruses led to a reduced ability to memorize the new location of the hidden platform 30 days post infection (Figure 3.1.7A). However, influenza A virus infected mice tested 120 days post infection revealed no significant differences in escape latency compared to the control animals (Figure 3.1.7B).

Subsequently, a single probe trial test 24 hours after the last day of reversal training was performed. 30 days post infection, both control and H1N1 infected mice spent significantly more time in the new target quadrant (T) (Control: 41.17 ± 2.62 % and H1N1: 44.07 ± 2.92 %) in comparison to the average time spent in non-target quadrants (NT) (Control: 19.60 ± 1.58 % and H1N1: 18.62 ± 1.75 %) whereas in H3N2 and H7N7 infected animals no preference for the new target quadrant could be observed (T: H3N2: 33.37 ± 4.78 % and H7N7: 23.72 ± 3.72 %, NT: H3N2: 22.21 ± 2.90 % and H7N7: 25.43 ± 3.47 %) (Figure 3.1.7C). Again, no differences were detected 120 days post infection between the groups tested. All groups spent more time in the new target quadrant compared to the average time spent in non-target quadrants (Figure 3.1.7D).

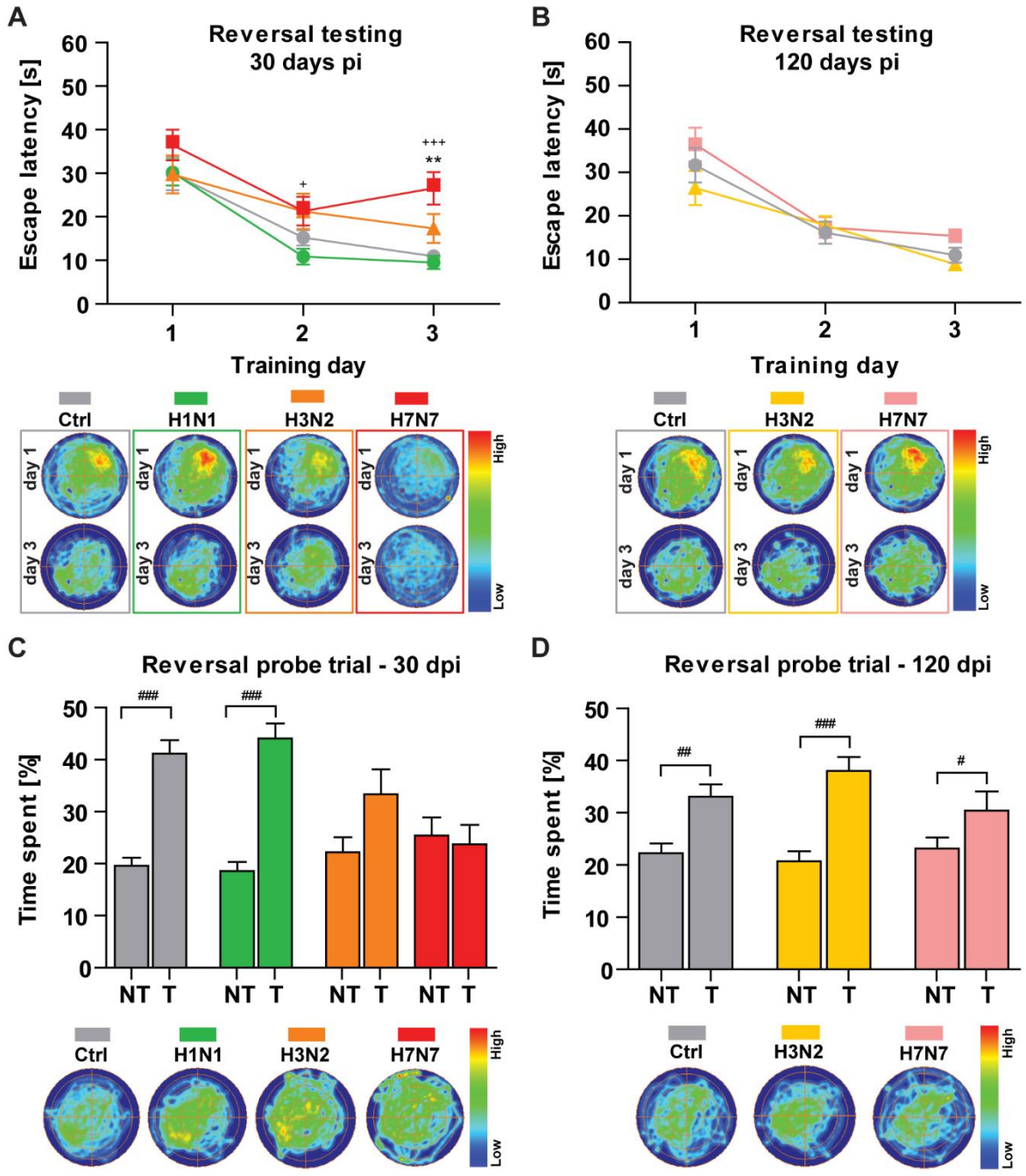

Figure 3.1.7 | Long-term effects of influenza A virus infection on cognitive function during reversal Morris water maze task in mice. (A) At 30 days post infection (pi), during 3 days of training, the escape latency to a new place of the hidden platform at southwest quadrant decreased significantly in all the control, H1N1 and H7N7 influenza infected mice over testing days but not in H3N2 influenza infected mice (as the occupancy plots showed as well). H7N7 infected mice had a significantly higher escape latency than control and H1N1 infected mice. **(B)** At 120 days pi, the influenza A virus infected group did not reveal any significant differences in escape latency compared to the control (as the occupancy plots showed). A single probe trial test 24 hours after the last day of reversal training was performed. **(C)** Control and H1N1 infected mice spent more time in the new target quadrant (T) than

the average time spent in non-target quadrants (NT) at 30 days pi (as occupancy plot showed). **(D)** All tested groups spent more time in T compared to NT at 120 days pi. Data are presented as mean ± SEM, (n=7-10). ** $p < 0.01$ compared to control. + $p < 0.05$ and +++ $p < 0.001$ compared to H1N1. # $p < 0.05$, ## $p < 0.01$ and ### $p < 0.001$ compared to the time spent in NT.

3.1.4. Long-term effects of influenza A virus infection on synaptic plasticity in the hippocampus of C57BL/6J mice

It has been shown that alterations in synaptic plasticity, may underlie many learning and memory processes (Cajal, 1894). Therefore, given the observed impairment in cognitive function following H3N2 and H7N7 influenza infection, it was investigated whether hippocampal network function could be compromised during a long-term timescale by the influenza A virus infection. For this purpose, synaptic plasticity using electrophysiological experiments at the Schaffer collateral pathway connecting the CA3 with the CA1 subfield, one of the most extensively studied synapses in the CNS, was analyzed. First, the dependence of the field excitatory postsynaptic potential (fEPSP) slope on stimulation intensity was assessed from input/output curves to acquire appropriate intensity to use in the rest of experiments. Similar input/output relations in the CA1 neurons in all hippocampal slices from control and influenza A virus infected mice were found for both time points of 30 and 120 days following infection ($p_{30dpi} = 0.8950$, $p_{120dpi} = 0.8644$) (Figure 3.1.8A). This results indicated that there were no initial differences between groups in the response to stimuli of a given intensity and population of presynaptic neurons firing action potentials. In addition, the potential effects of influenza A virus infection on short-term synaptic plasticity at the Schaffer collateral-CA1 synapses were investigated 30 and 120 days pi (Figure 3.1.8B) using paired-pulse facilitation (PPF). PPF is a presynaptic form of short-term plasticity in which the synaptic response to the second of a pair of closely spaced stimuli is increased due to residual Ca^{2+} in the presynaptic nerve terminal from the first stimulus adding to the influx of Ca^{2+} from the second stimulus (Patterson et al., 1996). Influenza A virus infection did not alter PPF as fEPSP2/fEPSP1 in hippocampal slices at 30 and 120 days post infection ($p_{30dpi} = 0.9994$, $p_{120dpi} = 0.9699$) (Figure 3.1.8B). Taken together these results showed that basal synaptic transmission, as well as short-term synaptic plasticity in the hippocampal CA1 region, were not affected by influenza A virus infection (Figure 3.1.8).

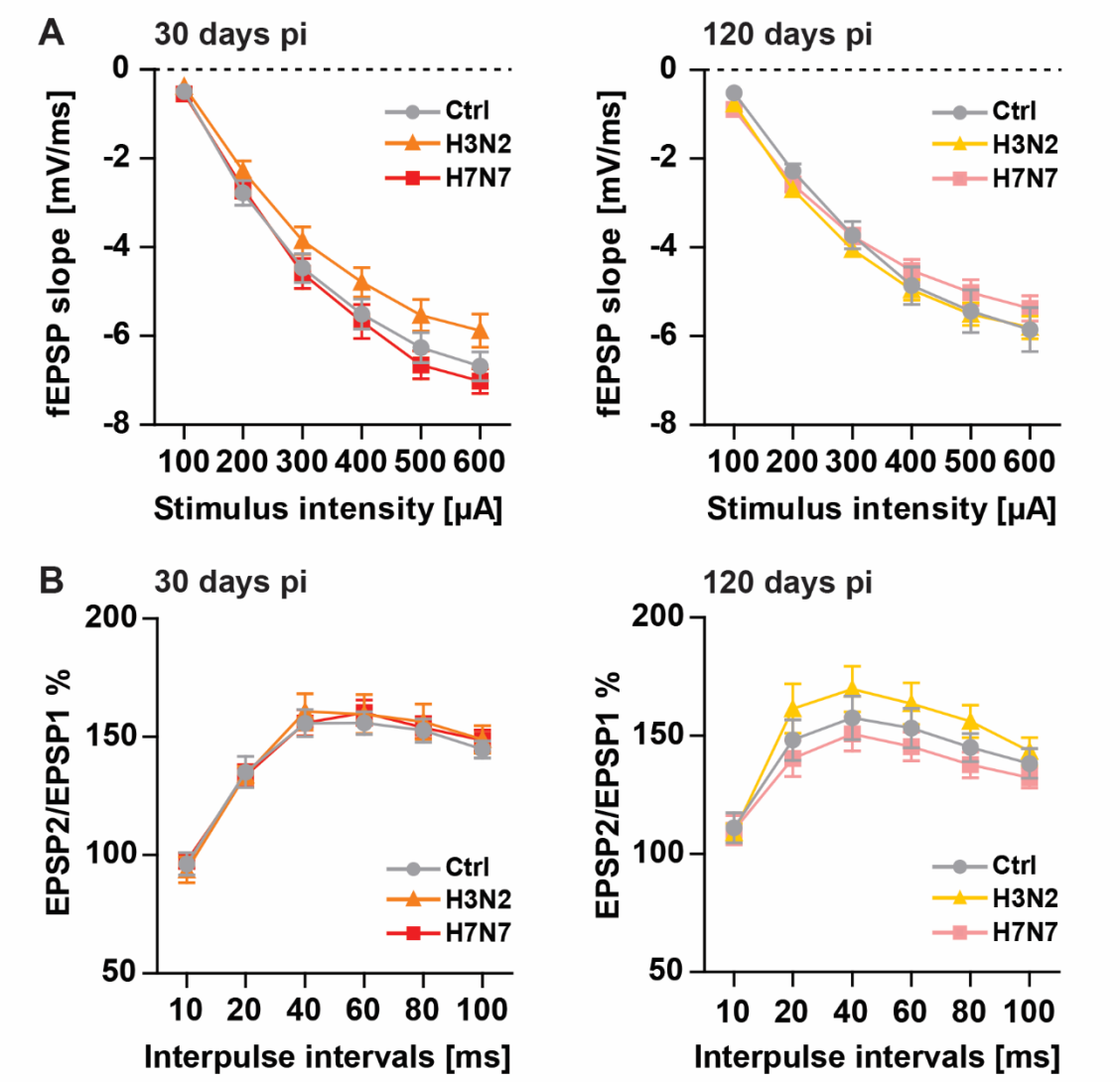

Figure 3.1.8 | Long-term effect of influenza A virus infection on basal synaptic transmission and short-term plasticity. (A) Input-output curves of field excitatory postsynaptic potential (fEPSP) slopes in hippocampal slices of control and infected mice at 30 and 120 days post infection (pi) did not show any significant differences between groups. **(B)** The paired-pulse facilitation (PPF) of the fEPSP slopes distinct as a response to the second stimulation over the first one at different interpulse intervals (10, 20, 40, 60, 80, and 100 ms) in hippocampal slices did not show any differences between the groups at 30 and 120 days pi. Data are presented as mean ± SEM, (n (number of animals) in each group=4-5, m (number of slices)=10-11 in each group).

As a next step, long-term synaptic plasticity, the capability of synapses to change their strength which is considered a cellular correlate of the ability to form new memories, (Bliss and Collingridge, 1993) was investigated. Long-term potentiation (LTP) at the Schaffer collateral CA3 to CA1 pathway was induced by theta-burst stimulation (TBS) after 20 min of baseline recording (refer to 2.2.4.4) (Figure 3.1.9).

30 days post infection, the induction phase of LTP (time 0 to 5 min after TBS) was significantly reduced only in hippocampal slices derived from H7N7 infected mice (p = 0.01). However, the stable phase of LTP (time 55 to 60 min after TBS) was significantly decreased in slices obtained from both H3N2 and H7N7 influenza virus infected mice (p = 0.004) thereby revealing a significant impairment in synaptic plasticity compared to control hippocampal slices ($F_{treatment}$ = 2.33, p = 0.004) (Figure 3.1.9A,B). 120 days post infection the induction (p = 0.74) and maintenance (p = 0.43) phase of LTP in both H3N2 and H7N7 were comparable to control slices ($F_{treatment}$ = 0.85, p = 0.43) (Figure 3.1.9C,D).

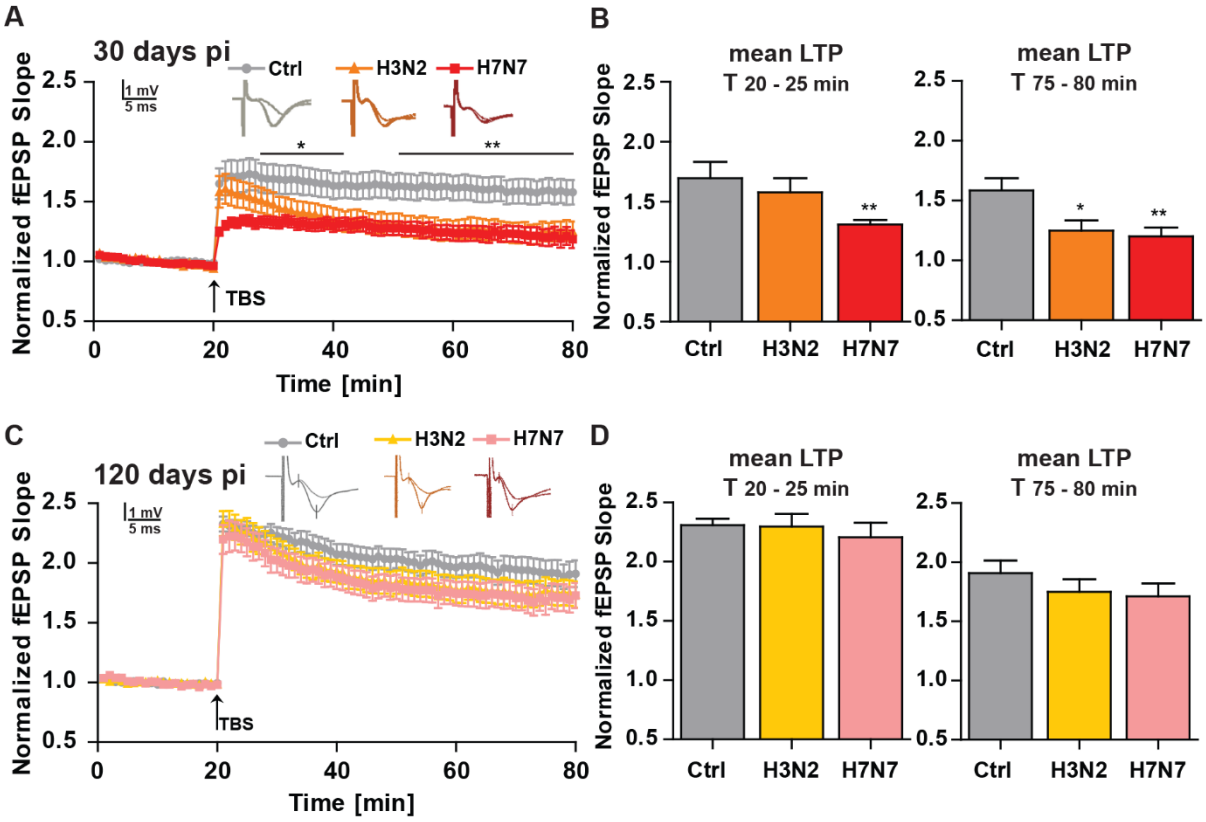

Figure 3.1.9 | Long-term effect of influenza A virus infection on long-term potentiation (LTP). **(A)** In the hippocampal slices from control and infected mice, LTP was induced by theta-burst stimulation (TBS) = four bursts at 100 Hz repeated 10 times in a 200 ms interval. This stimulation was repeated three times in a 10 s interval. The hippocampal slices from H7N7 infected mice exhibited significantly lower induction and maintenance of LTP compared to control, whereas H3N2 infected mice showed a reduced maintenance of LTP compared to control at 30 days post infection (pi). **(B)** At the induction phase of LTP (T_{20-25}), only hippocampal slices from H7N7 infected mice had a significant reduced LTP but at the stable phase of LTP (T_{75-80}) both groups of slices from H3N2 and H7N7 influenza virus infected mice revealed a significant reduction in LTP compared to control hippocampal

slices. **(C)**, **(D)** At 120 days pi, the induction and maintenance phases of LTP did not show any differences between control and infected groups. Data are presented as mean ± SEM, (n (number of animals) in each group=4-5, m (number of slices)=11-17 in each group). * $p < 0.05$ and ** $p < 0.01$ compared to control.

3.1.5. Long-term effects of influenza A virus infection on hippocampal neurons morphology of C57BL/6J mice

Excitatory synapses on hippocampal neurons are located mostly at dendritic spines which are tiny protrusions, therefore, the density of these structures could be taken as an index of synaptic changes underlying the LTP defects and the deficiency to form memories (Moser et al., 1994). Hippocampal neuronal morphology was quantified 30, 60 and 120 days post infection (Figure 3.1.10). Therefore, dendritic spines were counted separately on apical and basal dendrites of CA1 and CA3 pyramidal neurons as well as on dentate granule cells being located in the superior and inferior blade of the granule cell layer in the hippocampus (Figure 3.1.10). A significant reduction in spine density of apical and basal dendrites of CA1 and CA3 pyramidal neurons was observed in H3N2 (apical dendrite - CA1: Δ 17.08%, CA3: Δ 19.24% and basal dendrite - CA1: Δ 20.93%, CA3: Δ 24.96%) and H7N7 (apical dendrite - CA1: Δ 22.13%, CA3: Δ 15.02% and basal dendrite - CA1: Δ 15.70%, CA3: Δ 22.57%) infected mice at 30 days post infection ($p < 0.001$), whereas H1N1 infection showed no effect compared to control ($p = 0.5337$) (Figure 3.1.10A,B). The extent of the phenotype differed between the hippocampal subregions as in both the superior and inferior dentate gyrus (DG) blade, only infection with H7N7 influenza A virus led to a significant reduction in dendritic spine density (DG-superior: Δ 17.08% and DG-inferior: Δ 21.95%) ($p < 0.001$) (Figure 3.1.10C). Further assessment of H3N2 and H7N7 infected animals showed at day 60 post infection a partial recovery of the reduced spine density predominantly for the dentate gyrus and CA3 subregions and more pronounced for H3N2 infected animals (Figure 3.1.10A-C). 120 days post infection, spine density in H7N7 and H3N2 infected mice was indistinguishable from control animals in all subregions of the hippocampus ($p < 0.001$ compared to 30 days pi) (Figure 3.1.10A-C).

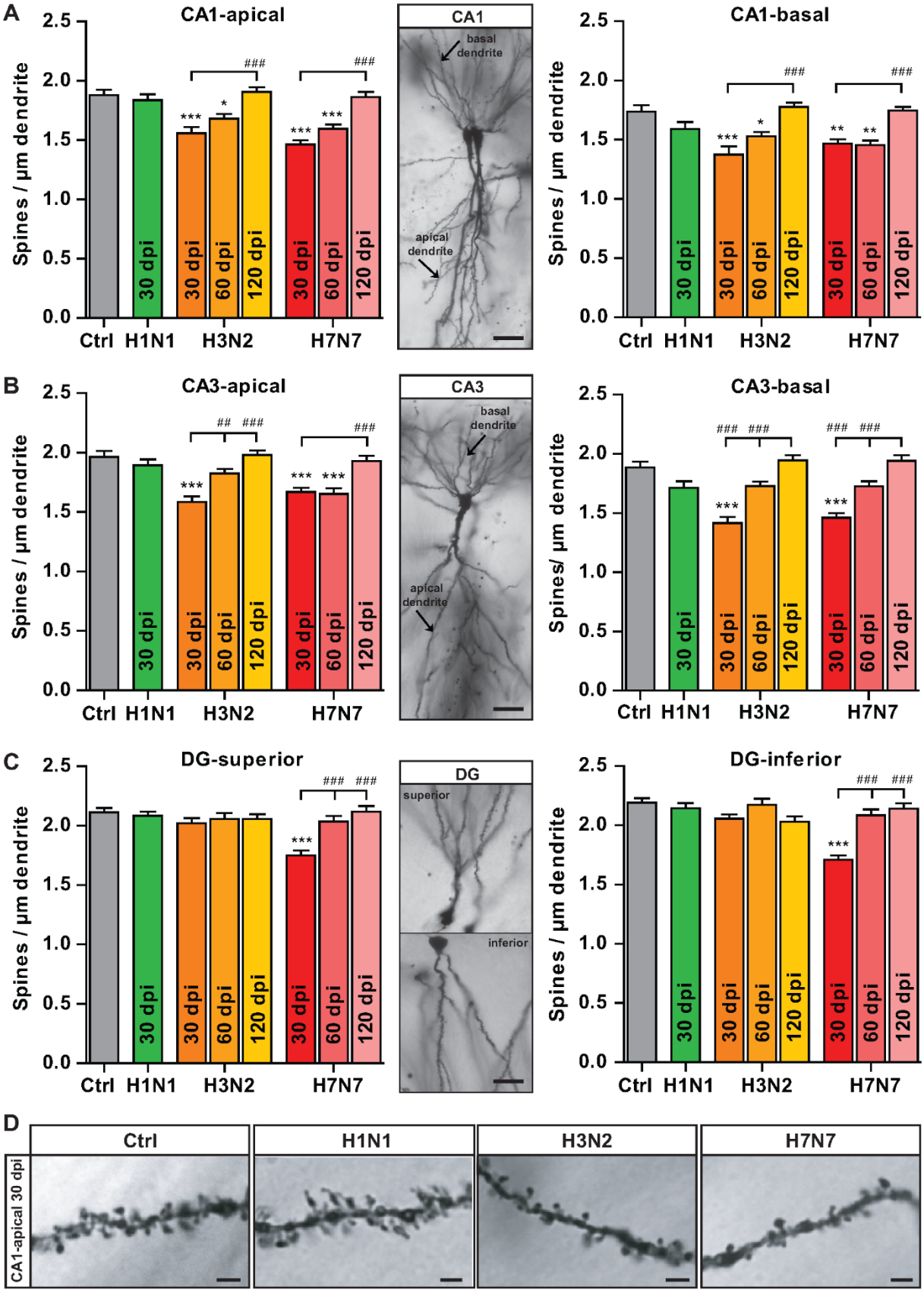

Figure 3.1.10 | Long-term effects of influenza A virus infection on dendritic spine density of hippocampal neurons. (A), **(B)** Following infection with H3N2 and H7N7 Influenza A virus, the spine

density of apical and basal dendrites of CA1 and CA3 hippocampal neurons (Bar=20 µm, 20X) decreased at 30 days post infection (dpi), **(C)** but only H7N7 influenza A virus infection reduced dendritic spine density of dentate granule cells located in the superior and inferior blade of the granule cell layer (Bar=20 µm, 20X). **(A-C)** Notably, 60 dpi a partial recovery occurred in the DG and CA3 hippocampal subregions of infected animals, and 120 dpi the dendritic spine density fully recovered in all regions of the hippocampus. **(D)** Representative images of dendritic spines in hippocampal CA1-apical neurons 30 days following infection with influenza A viruses (Bar=2 µm, 63X). Data are presented as mean ± SEM, (n (number of animals) in each group=4-5, m (number of dendrites)=40-50 in each group). * $p < 0.05$, ** $p < 0.01$ and *** $p < 0.001$ compared to control. ## $p < 0.01$ and ### $p < 0.001$ compared to 30 dpi time point.

3.1.6. Long-term effects of influenza A virus infection on microglial cell density and activation status within the hippocampus of C57BL/6J mice

Microglia represent the immune cells in the CNS which can react directly to the presence of a pathogen but also to a peripheral infection (Riazi et al., 2015; Vasek et al., 2016). The delicately balanced cross-talk between microglia, astrocytes and neurons in the brain is important for proper brain function even in the absence of infection. A local parenchymal brain inflammatory reaction (neuroinflammation) is characterized by an increase in the population and activation status of microglia and astrocytes in the CNS (Vesce et al., 2007). As processes of prolonged neuroinflammation following influenza A virus infection might be the underlying cause for the alterations observed in this study, ranging from single synapses to neuronal plasticity and eventually affecting mouse behavior, the effect of influenza A viruses on microglial density and activation status in the hippocampus was analyzed.

For this purpose, IBA-1 staining was performed (Figure 3.1.11). IBA-1 positive cells were counted and analyzed separately in the CA1, CA3 region and DG superior and inferior blade of the granule cell layer in the hippocampus. The results revealed that whereas microglia density was not affected 30 days post infection with H1N1 (although this virus infection led to elevation of microglia density in the CA1 subregion at 18 days post infection (see Figure 3.1.12)), microglia density in the CA3 subregion (Δ 31.3%) and inferior blade of the dentate gyrus (Δ 27.4%) was increased significantly after H3N2 infection ($p < 0.001$) (Figure 3.1.11B). The neurotropic H7N7 influenza A virus infection induced a robust increase in microglia density for all hippocampal subfields analyzed (CA1: Δ 24.7%, CA3: 32.1%, DG-superior: 49.2%, DG-inferior: 56.0%) ($p < 0.001$) (Figure 3.1.11B). Afterwards, a partial recovery of

microglial density could be observed in the dentate gyrus and CA3 subregions 60 days post infection, especially in H3N2 infected animals. At day 120 post infection, microglia cell density in all influenza A viruses infected mice was comparable to control levels (Figure 3.1.11B).

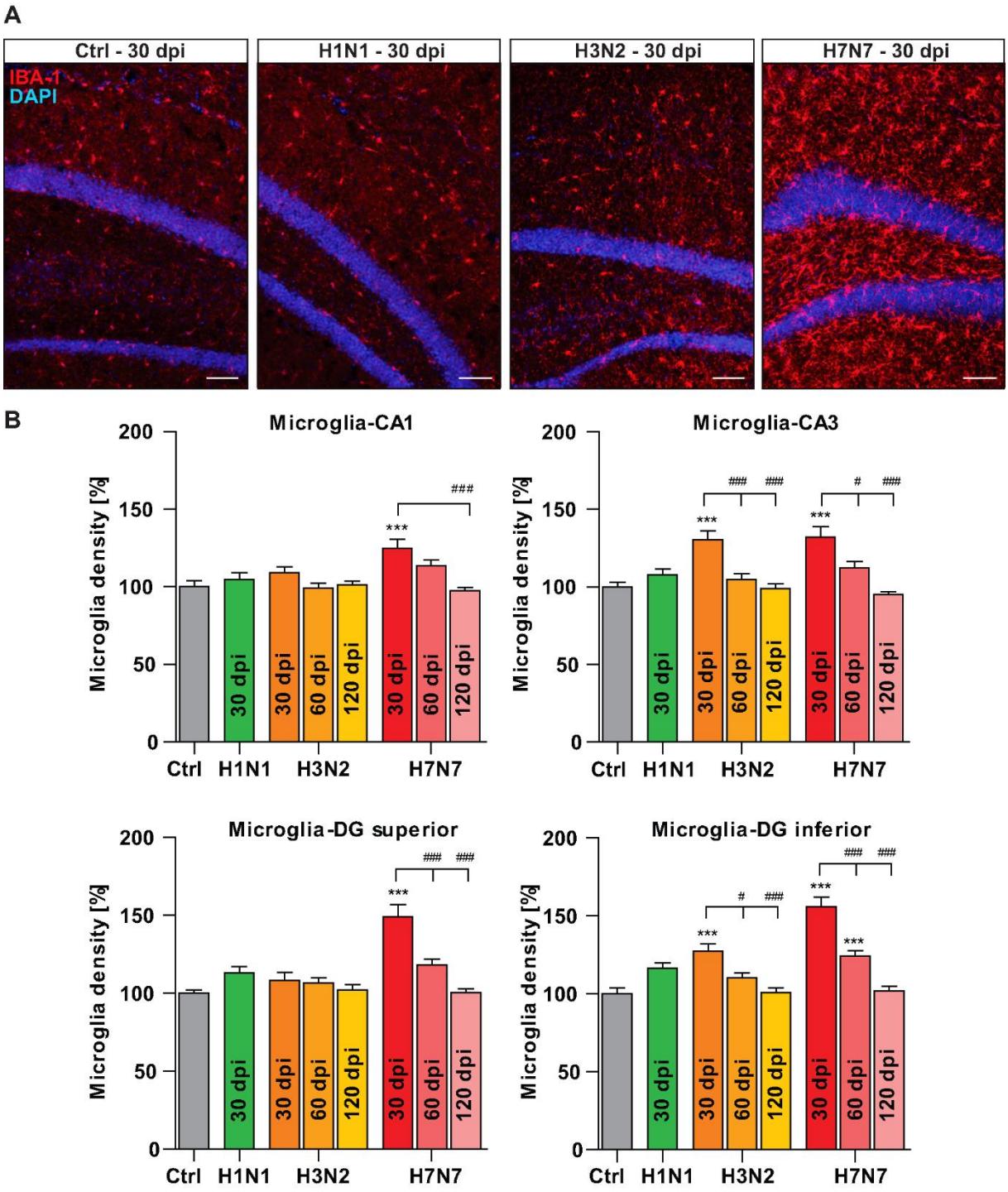

Figure 3.1.11 | Long-term effects of influenza A virus infection on microglia density within the hippocampal subregions. (A) Representative examples of IBA-1 immunostained hippocampal

sections of influenza A virus infected mice at 30 dpi (Bar=100 µm, 10X). **(B)** Following infection with H3N2 influenza A virus, microglia density in the CA3 region and inferior blade of the dentate gyrus was increased significantly; whereas the neurotropic H7N7 influenza A virus infection induced an increased microglia density in all hippocampal subregions at 30 days post infection (dpi). Notably, at 60 dpi a partial recovery occurred in the CA3 and DG regions of infected mice especially with H3N2 and 120 dpi the microglia density was fully recovered in all subregions of the hippocampus. Data are presented as mean ± SEM, (n (number of animals) in each group=4-5, m (number of a region of interest (ROI))=20-25 in each group). *** $p < 0.001$ compared to control. # $p < 0.05$ and ### $p < 0.001$ compared to 30 dpi time point.

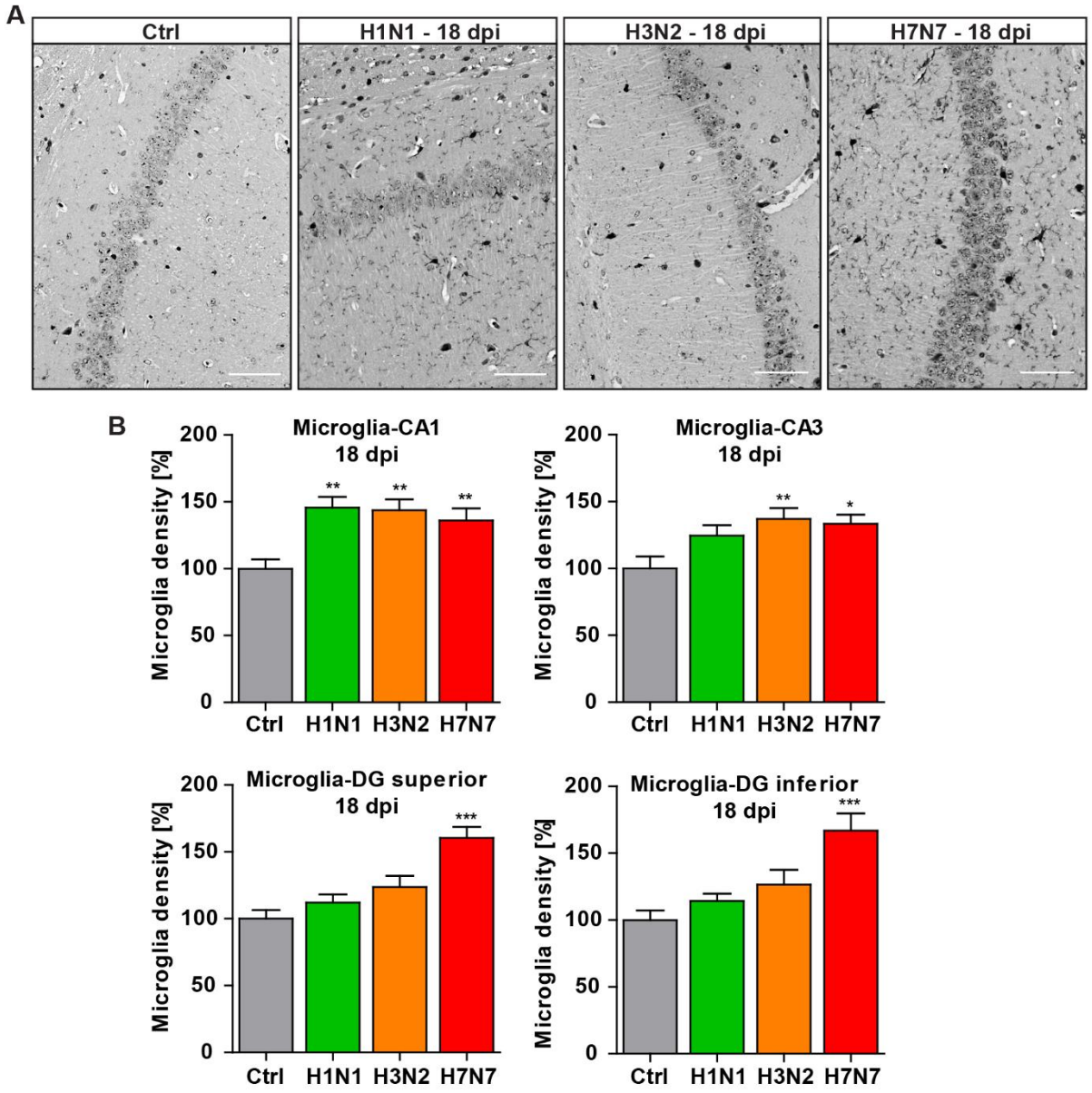

Figure 3.1.12 | Effects of influenza A virus infection on microglia density within the hippocampal subregions at 18 days post infection (dpi). (A) Representative examples of IBA-1

immunostaining at 18 dpi (Black dots are IBA-1 positive cells, Bar=50 µm, 20X). **(B)** 18 days following infection with H1N1 and H3N2 non-neurotropic influenza A virus strains, microglia density in CA1 subregion of the hippocampus was increased significantly but only H3N2 infection could elevate the microglia density in the CA3 hippocampal subregion. The neurotropic H7N7 influenza A virus infection induced an increased microglial density in all hippocampal subregions at 18 dpi. Data are presented as mean ± SEM, (n (number of animals) in each group=3-4, m (number of regions of interest (ROI)=15-20 in each group). * $p < 0.05$, ** $p < 0.01$ and *** $p < 0.001$ compared to control.

In the healthy state, microglial cells show an elaborate cell architecture with numerous fine processes constantly scanning the microenvironment. These 'resting' microglia can transform into an activated status during the infection state to act as macrophages thereby displaying a more and more round cell shape (Papageorgiou et al., 2015). Therefore, in order to determine the activation status of microglia cells in influenza A virus infected individuals compared to control animals the number of primary processes per cell was quantified (refer to 2.2.6.1) (Figure 3.1.13A). For both H3N2 and H7N7 influenza A virus subtypes, the number of primary processes per cell was diminished in all subregions of the hippocampus 30 days post infection (CA1, H3N2: Δ 27.70% and H7N7: Δ 27.79% - CA3, H3N2: Δ 28.31% and H7N7: 31.54%) ($p < 0.001$) (Figure 3.1.13B). Interestingly, the strongest reduction was found in the superior and inferior blade of the dentate gyrus upon H7N7 infection (DG superior, H3N2: 18.04% and H7N7: 29.81% - DG inferior, H3N2: 20.88% and H7N7: 34.78%) ($p < 0.001$ compared to control and H3N2 influenza A infected mice) (Figure 3.1.13B). a partial recovery of the activation status of microglia was observed in the DG and CA3 subregions 60 days post infection which was more pronounced for H3N2 infected animals. At day 120 post infection microglia activation status in infected mice was comparable to control levels (Figure 3.1.13B).

Taken together, in the hippocampus of H3N2 and H7N7 influenza A virus infected mice the microglia revealed an inflammatory activation status even 60 days post infection, however, this inflammation was recovered 120 days post infection.

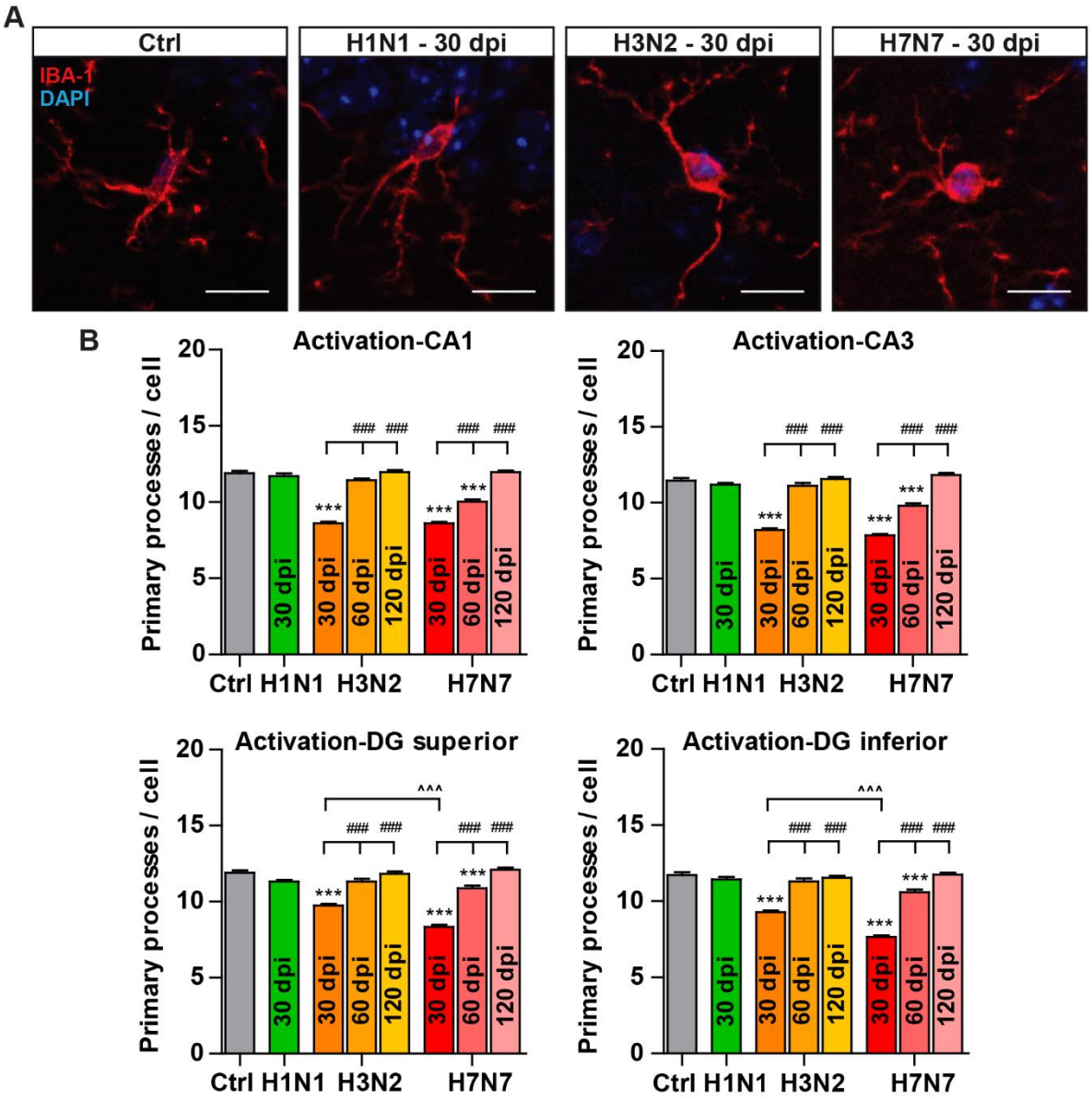

Figure 3.1.13 | Long-term effects of influenza A virus infection on microglia activation status within the hippocampal subregions. (A) Representative examples of IBA-1 positive cells in control and infected groups at 30 days post infection (dpi) (Bar=10 µm, 20X). **(B)** Following infection with H3N2 and H7N7 influenza A virus, the number of primary processes of microglia in all subregions of the hippocampus decreased at 30 days post infection (dpi), however, upon H7N7 infection, the strongest reduction became visible in the superior and inferior blade of the granule cell layer. Notably, at 60 dpi a partial recovery occurred in the CA3 and DG regions of infected samples, and by 120 dpi the microglia activation status was fully recovered in all subregions of the hippocampus. Data are presented as mean ± SEM, (n (number of animals) in each group=4-5 (5 regions of interest (ROI) per each animal), m (number of counted microglia=120-150 in each group (6 cells per each ROI). *** $p < 0.001$ compared to control. ### $p < 0.001$ compared to 30 dpi time point. ^^^ $p < 0.001$ compared to H3N2.

3.1.7. Long-term effects of influenza A virus infection on astrocyte density within the hippocampus of C57BL/6J mice

In addition to the effect of influenza A virus infection on microglia, the density of astrocytes in all hippocampal subregions was investigated using GFAP staining (Figure 3.1.14A,B). Astrocytes have been traditionally viewed as supportive partners of neurons. However, today it is known that synaptic function can be supported and even modulated by astrocytes through various mechanisms which mostly rely on diffusion of ions or metabolites and signaling molecules into the extracellular space (Vesce et al., 2007). Interestingly, studies within the last years demonstrated that astrocytes can be responders as well as targets for infectious agents, especially viruses (Sofroniew and Vinters, 2010). Several observations indicate the putative protective barrier function of reactive astrocytes which is known as astrogliosis. (Sofroniew, 2009). An increase in the number and activation status of astrocytes is therefore also considered as a neuroinflammatory marker. However, the exact role of reactive astrocytes during the responses to infection remains largely elusive. Therefore, to determine whether influenza A virus infection would induce astrogliosis, astrocyte density in all regions of the hippocampus was quantified 30, 60 and 120 days post infection. The results revealed that the astrocyte density was increased 30 days post infection independently of the subregion with H7N7 influenza A virus (CA1: Δ 44.9%, CA3: Δ 45.8%, DG-superior: Δ 14.9%, DG-inferior: Δ 22.6%) ($p < 0.05$), whereas only the CA1 (Δ 29.5%) and CA3 (Δ 29.3%) subregions were affected by infection with H3N2 ($p < 0.001$) (Figure 3.1.14C). As was the case for spine density and microglia, H1N1 did not affect astrocyte number in the hippocampus (Figure 3.1.14C). On the level of astrocytes, a full recovery comparable to control numbers could be observed already 60 days post infection ($p < 0.01$ compared to 30 days post infection).

In summary, 30 days post infection astrogliosis was detectable within the hippocampus following both non-neurotropic H3N2 and neurotropic H7N7 influenza A virus infection which was completely recovered at 60 days post infection, notably earlier than microglia number and activation status (refer to 3.1.6).

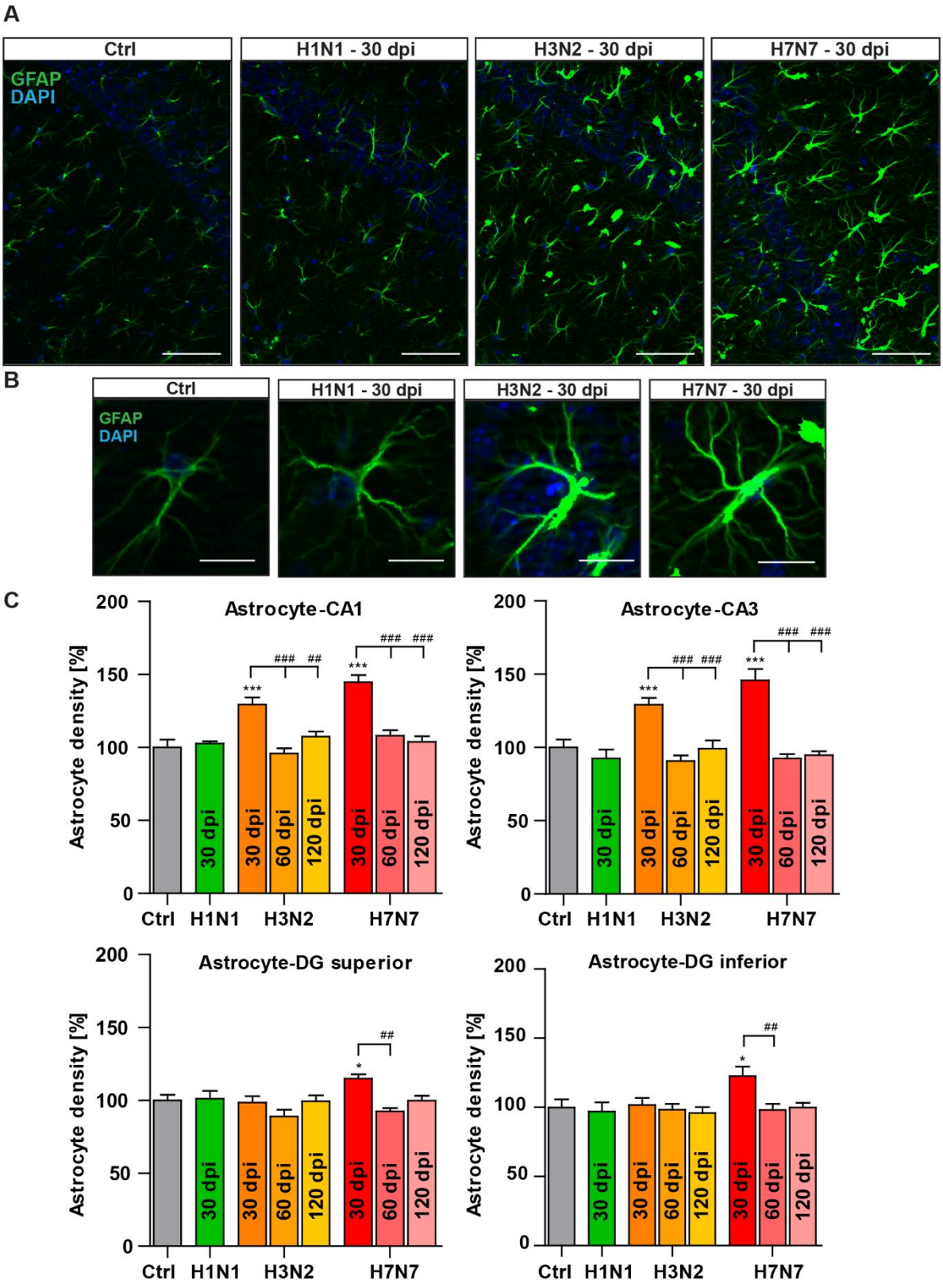

Figure 3.1.14 | Long-term effects of influenza A virus infection on astrocyte density within the hippocampal subregions. (A) Representative examples of GFAP immunostained CA1 hippocampal subregion at 30 days post infection (dpi) (Bar=50 µm, 20X). **(B)** Representative examples of GFAP

positive cells in control and infected groups at 30 dpi (Bar=10 µm, 20X). **(C)** The astrocyte density in all hippocampal subregions was increased at 30 dpi with H7N7 influenza A virus, whereas CA1 and CA3 subregions were affected after H3N2 influenza A virus infection. Interestingly at 60 dpi a reduction of GFAP positive cells to the level of control was observed already. Data are presented as mean ± SEM, (n (number of animals) in each group=3-4, m (number of regions of interest (ROI))=15-20 in each group). * $p < 0.05$ and *** $p < 0.001$ compared to control. ## $p < 0.01$ and ### $p < 0.001$ compared to 30 dpi time point.

3.1.8. Effects of influenza A virus infection on blood-brain barrier permeability in C57BL/6J mice

As a next step, given the elevated microglia and astrocyte density and activation status in the hippocampus of influenza A virus infected mice even following non-neurotropic H3N2 infection (refer to 3.1.6 and 3.1.7), it can be hypothesized that increased peripheral inflammatory signals during infection might be responsible for the activation of microglia within the hippocampus as its underlying mechanisms. The integrity of the blood-brain barrier (BBB) is crucial for regulating the flow of nutrients from the blood to the brain and restricting access of toxins, pathogens, and other substances that are harmful to the CNS. Moreover, the BBB also restricts the access of inflammatory cells and cytokines to the CNS, which protects irreplaceable cells such as neurons from damage (Růžek et al., 2011). Therefore, the integrity of the BBB following H3N2 and H7N7 influenza A virus infection was examined as peripheral cytokines might be able to cross a leaky BBB (Růžek et al., 2011).

For this purpose, the animals were injected with 2% (w/v) Evans blue intraperitoneally at day 4, 8 and 10 post infection to determine an increased Evans blue absorbance in brain tissue in the case of a compromised BBB (Figure 3.1.15). Evans blue dye absorbance was measured using spectrophotometer at 610 nm and the amount of Evans blue in the brain was calculated according to the absorbance of the standard Evans blue samples. Upon infection with H3N2 and H7N7 influenza A virus, an increased Evans blue absorbance in the brain tissue and therefore a compromised BBB was observed at 8 days post infection ($p < 0.05$) (Figure 3.1.15A). On day 10 post infection, only H7N7 infected mice showed an increased Evans blue absorbance ($p < 0.001$) in the brain compared to control and H3N2 infected mice (Figure 3.1.15A). Evans blue staining was well visible macroscopically in the brain of H7N7 infected

mice at 10 days post infection, whereas in the brain of H3N2 infected mice it was only slightly visible around the ventricles (Figure 3.1.15B).

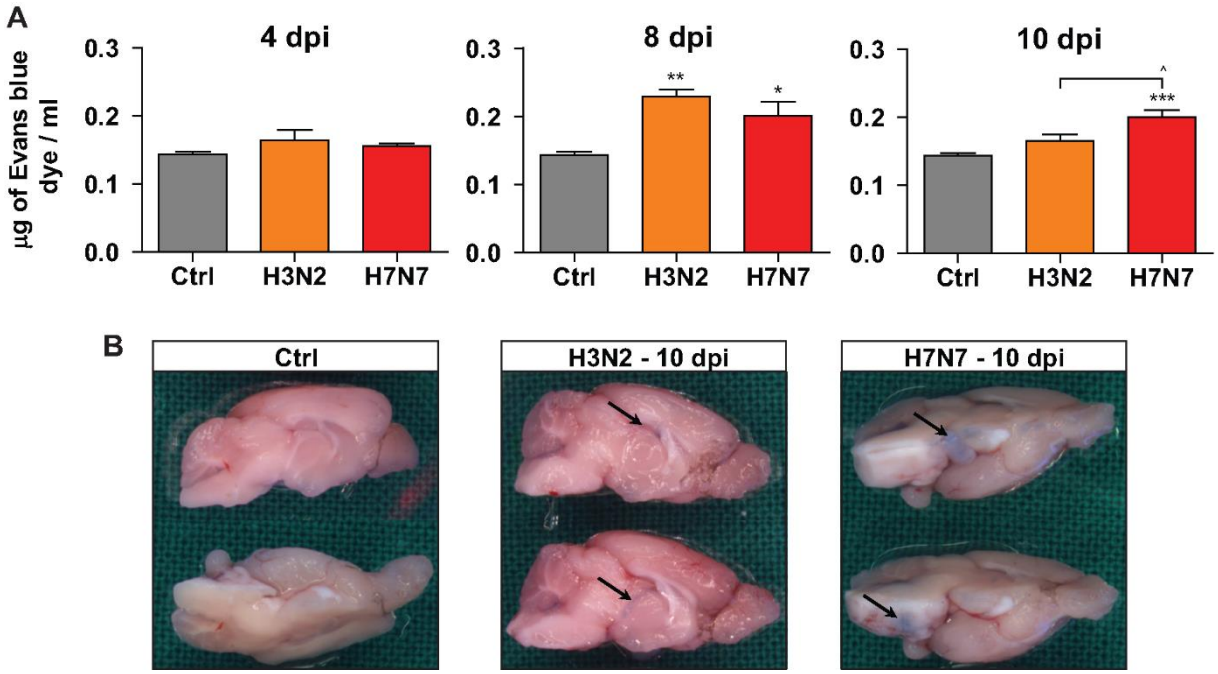

Figure 3.1.15 | Effects of influenza A virus infection on blood-brain barrier (BBB) permeability. **(A)** The injection of Evans Blue dye for assessment of the BBB integrity upon infection with H3N2 and H7N7 influenza A virus did not exhibit an increased Evans blue presence in the brain on day 4 post infection (dpi) in both H3N2 and H7N7 infected mice. On day 8 post H3N2 and H7N7 influenza A virus infection, the Evans blue dye in the brain was elevated. The increased Evans blue dye in the brain of H7N7 infected mice was detected at the 10 dpi. **(B)** At 10 dpi, Evans blue dye was macroscopically well-visible only in H7N7 infected mice, whereas in H3N2 infected mice it was slightly visible around the ventricles (black arrow). Data are presented as mean ± SEM, (n=3-5). * $p < 0.05$, ** $p < 0.01$ and *** $p < 0.001$ compared to control. ^ $p < 0.05$ compared to H3N2 infected group.

3.1.9. Effects of influenza A virus infection on cytokines level in blood plasma and brain of C57BL/6J mice

It is known that the cytokines produced during an infection can affect the brain as well (Guyon et al., 2008). In addition, there is abundant evidence that inflammatory mechanisms within the CNS contribute to the cognitive impairment via cytokine-mediated interactions between neurons and glial cells (Wilson et al., 2002). As an increased permeability of the BBB following H3N2 and H7N7 influenza A viruses at 8 days post infection (Figure 3.1.15) could be detected, it is interesting to investigate if cytokines level would be increased as well in the periphery and especially also in the CNS after influenza A virus infection. An earlier study suggested that interferons (IFNs) and tumor necrosis alpha (TNF-α) have a significant role in priming cells for higher cytokine and chemokine production during influenza A virus infection (Veckman et al., 2006). Furthermore, Interleukin-1 (IL-1) is a potent activator of the host defense responses to infection in the periphery and the CNS (Tong et al., 2008). Therefore, IFN-γ, TNF-α and IL-1β levels were assessed in the periphery and the CNS via the enzyme-linked immunosorbent assay (ELISA) at 8 days post infection as the compromised BBB was observed at this time in both infected groups (Figure 3.1.15). Cytokines levels were quantified in the blood serum, in the CNS as a whole and in the hippocampus of influenza A viruses infected mice (Figure 3.1.16). The data revealed that the levels of IFN-γ and TNF-α were significantly elevated in the blood serum, CNS and hippocampus of H7N7 influenza A virus infected mice ($p < 0.05$) (Figure 3.1.16A,B). Infection with the other two non-neurotropic influenza virus subtypes H1N1 and H3N2 led to significantly increased levels of TNF-α in the hippocampus of infected mice compared to control ($p < 0.01$) (Figure 3.1.16B) but not in the serum. Moreover, at 8 days post infection, the level of IL-1β was significantly enhanced only in the CNS independently of the influenza A virus subtypes ($p <0.001$) but not in the blood serum and hippocampus (Figure 3.1.16C).

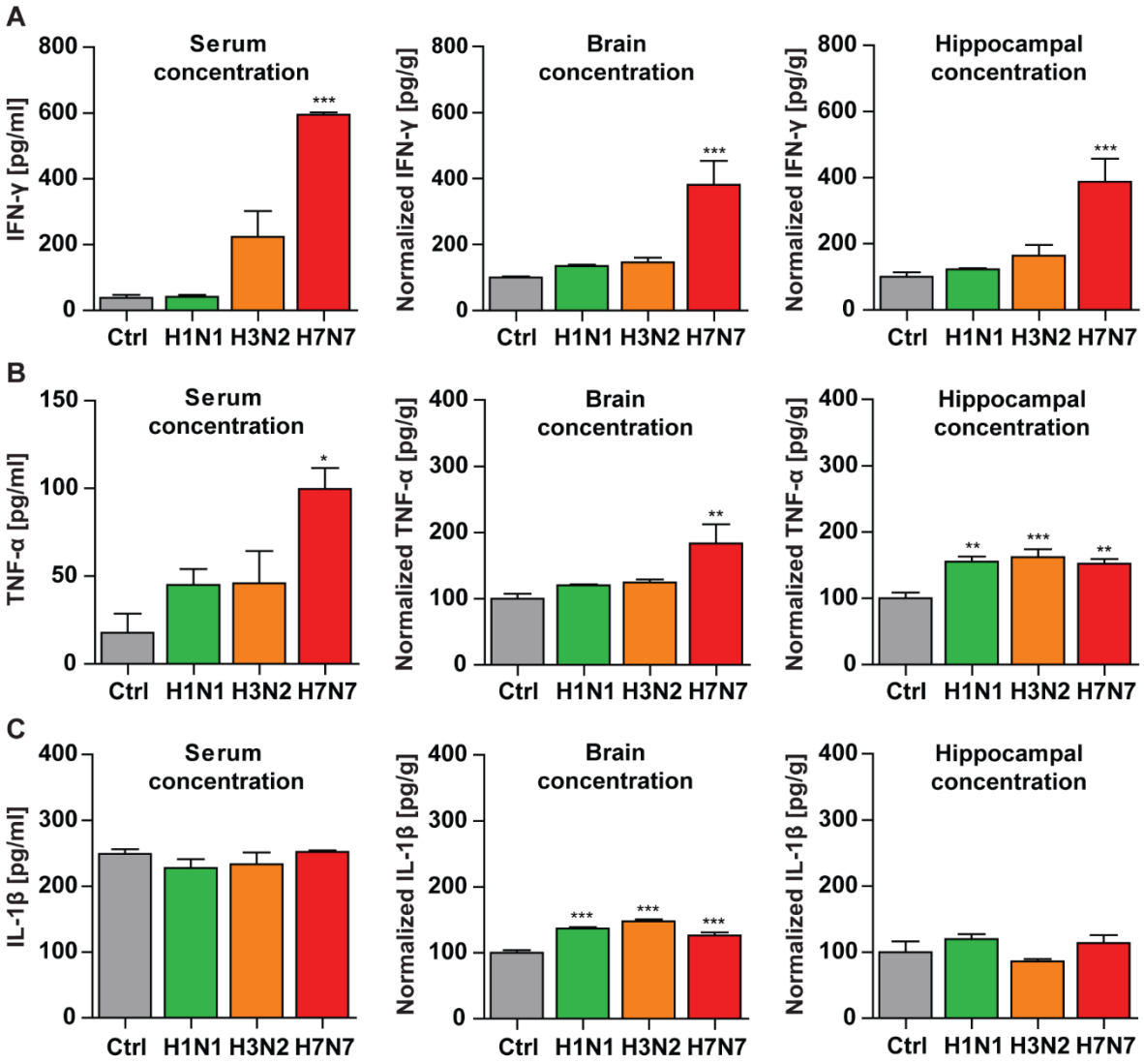

Figure 3.1.16 | Effects of influenza A virus infection on cytokines level in the blood serum and CNS. (A), **(B)** The levels of IFN-γ and TNF-α were significantly elevated in the blood serum, brain and hippocampus of mice 8 days post H7N7 influenza A virus infection. H1N1 and H3N2 non-neurotropic influenza virus infection led to significantly increased TNF-α levels within the hippocampus of infected mice. **(C)** The level of IL-1β was enhanced in the brain of all influenza A virus subtypes infected mice significantly. Data are presented as mean ± SEM, (n=3-4). * $p < 0.05$, ** $p < 0.01$ and *** $p < 0.001$ compared to control.

3.1.9. Effects of influenza A virus infection on gene expression in the hippocampus of C57BL/6J mice

To follow influenza A virus induced gene expression changes in the hippocampus possibly responsible for the differences observed in the long-term effects mediated by infection with the respective variant, transcriptome analysis was performed by Prof. Dr. Klaus Schughart, Department of Infection Genetics, Helmholtz Centre for Infection Research, Braunschweig. First, 18 days post infection was chosen as the first time point to isolate RNA as it was shown previously that following infection with a neuro-adapted influenza A virus strain (WSN/33), the virus was cleared from the brain within 12 days (Beraki et al., 2005), and that the largest number of gene regulations emerged 18 days post Rabies virus infection which in turn, is a neurotropic virus (Zhang et al., 2016). Therefore, in present study, hippocampi of mice infected with the respective influenza A virus subtypes were prepared for genetic assessment at 18 and 30 days post infection. By these time points, the neurotropic virus should not be present in the brain any longer and the mice fully recovered from the acute phase of influenza A virus infection. As in this study, long-term cognitive function impairment was not observed following H1N1 influenza A virus infection, therefore, gene analysis and comparisons are presented only for H3N2 and H7N7 influenza A virus infected groups.

First, probesets were identified that differentially expressed (DEPs, defined based on an adjusted *p*-value of < 0.1 and exhibiting more than a $\log_2$ of 0.5 (1.4 fold) absolute difference in expression levels) in pair-wise comparisons between control and each of the two virus-infected mouse groups. The findings revealed that although at 18 days post H3N2 infection 487 differentially expressed genes (DEGs) were detected, at 30 days post infection no significant DEGs were found in this group. However, 18 and 30 days post H7N7 infection, 174 and 250 DEGs were observed respectively (Figure 3.1.17A). In addition, Venn diagram showed that there was a limited overlap of DEGs between the two infected groups indicating indeed a virus-specific induction of gene expression (Figure 3.1.17B). KEGG pathway analysis of DEGs revealed a significant induction of immune responses and inflammatory processes related genes and pathways exclusively 18 days after H7N7 influenza A virus infection which continued until day 30 post infection, however, for H3N2 influenza A virus infection in contrast, theses pathways were induced significantly only 18 days post infection

(Figure 3.1.18). Especially, B and T cell specific genes (e.g. *Ighg*, *Ighm*, *CD3d*) and the genes that are involved in antigen processing and presentation were found among the most strongly upregulated genes following H7N7 influenza A virus infection demonstrating the presence of peripheral immune cells and pathogen in the CNS which is in line with the observation of a compromised BBB even until 10 days pi. Furthermore, KEGG analysis (Figure 3.1.18) of DEGs in both H3N2 and H7N7 influenza A virus infected mice compared to control revealed top pathway of cell adhesion molecules (CAMs) which play a critical role in a wide array of biological processes that include hemostasis, the immune response, inflammation and development of neuronal tissue (Joseph-Silverstein and Silverstein, 1998). Moreover, cell-cell adhesions are important for brain morphology and highly important cognitive functions such as learning and memory (Bailey et al., 2015).

In addition, a number of candidate genes are displayed in table 1-5 separately. The analysis of CNS cell-related genes revealed a significant adverse regulation in neuron-, microglia- and astrocyte-specific genes following influenza A virus infection. For instance, *Rbfox3* (NeuN), *Nrcam* (neuronal cell adhesion molecule) and Cacna1c (calcium channel voltage-dependent) which expresses in neurons were diminished similarly in both H3N2 and H7N7 infected groups 18 days post infection (Table 1). Dysfunction of these genes has been identified in several neurodevelopmental and neuropsychiatric disorders such as autism, schizophrenia and cognitive impairments (Demyanenko et al., 2014; Lee et al., 2016; Lin et al., 2016). In addition, *Rbfox3* knockout mice showed a defective hippocampal gene expression as well as deficits in synaptic transmission and plasticity in the dentate gyrus (Wang et al., 2015).

An increased expression of *Olfml3* (microglia) (Table 2) and *Gfap* (astrocytes) (Table 4) was observed in the hippocampus of H3N2 and H7N7 influenza A virus infected mice. However, some microglia specific genes such as *Tmem119* and *Trem2* were elevated significantly only following H7N7 influenza A virus infection (Table 2). The analysis of genes reflecting microglia activation in particular MHC class II family, microglial-mediated phagocytosis (*Fcgr4*, *Dap12* and *Ctsz*) and the complement system genes (*C1qa*, *C1qb*, *C1qc* and *Vwf*) revealed a significant upregulation especially in the group of H7N7 infected animals (Table 3).

Moreover, down-regulation of the neurotrophic factors *Bdnf* and *Ntf3* as well as neuron-glia cross-talk gene (*Cx3cr1*), a number of important solute carriers such as *Slc4a7* (bicarbonate cotransporter), *Slc30a5* (zinc transporter), *Slc2a1* (glucose

transporter, GLUT-1) and *Slc1a2* (glutamate transporter), and synapse associated genes including *Grm5* (glutamate receptor) and *Dlg3* (SAP102) were observed irrespective of the virus subtype (Table 1-4). Previously, SAP102 knockout mice exhibited impaired spatial learning and search strategies along with defect synaptic plasticity (Cuthbert, 2007).

It is worth noting that following both H3N2 and H7N7 influenza A virus infection, upregulation of some of the interferon-response related genes including *Psmb9*, *Lgals3bp*, *Oas2* and *CCL5* which could promotes cognitive decline (Laurent et al., 2017) were observed (Table 5). However, in between those interferon-response upregulated genes, *Ifit3* was observed only following H7N7 influenza A virus infection which is basally expressed in granule cell neurons (Cho et al., 2013) and is associated with cognitive decline in aging mice (Bordner et al., 2011). This specific innate immune response programs even in the different neuronal subtypes possibly can determine susceptibility to infection in the brain by influenza virus subtypes.

Furthermore, interestingly these microarray analysis showed that 30 days post H7N7 infection dopamine neurotransmitter transporter gene (*Slc6a3*) was upregulated significantly which it can be considered as a possible mechanism underling the depression and other related psychiatric disorders, which were reported (Uddin et al., 2011), could be induced by such viral infections (Sinanan and Hillary, 1981).

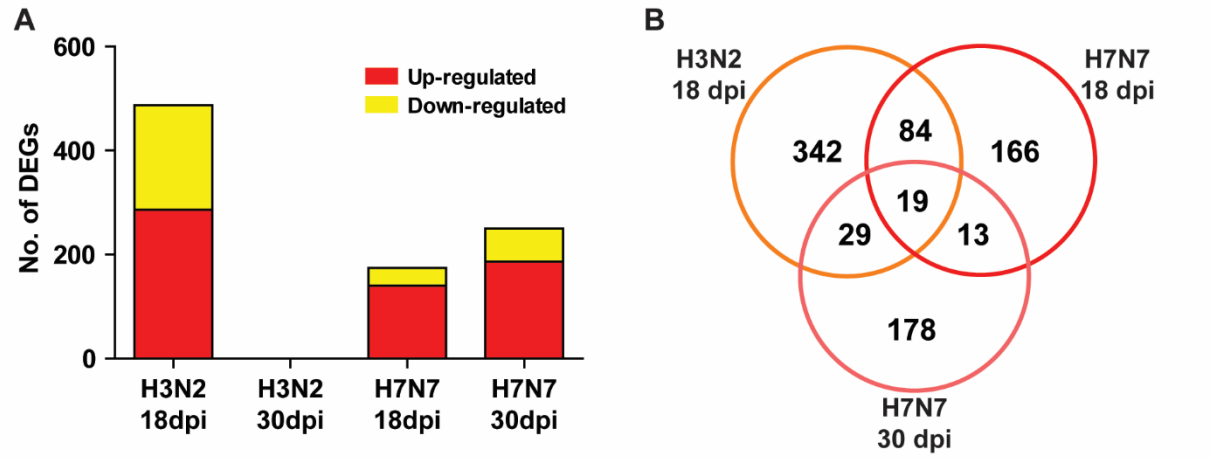

Figure 3.1.17 | Whole genome microarray analysis from the hippocampus of influenza infected mice at 18 and 30 days post infection (dpi). DEPs (differentially expressed probe sets) were identified based on an adjusted *p* value of < 0.1 and exhibiting more than a $\log_2$ of 0.5 (1.4 fold) absolute difference in expression levels. **(A)** 18 days post infection 487 and 174 differentially expressed genes (DEGs) were detected in the hippocampus of H3N2 and H7N7 infected mice

respectively, however, at 30 days post infection 250 DEGs just were found following H7N7 influenza A virus infection. **(B)** Overlap of DEPs is presented as Venn diagram. (n=3-4).

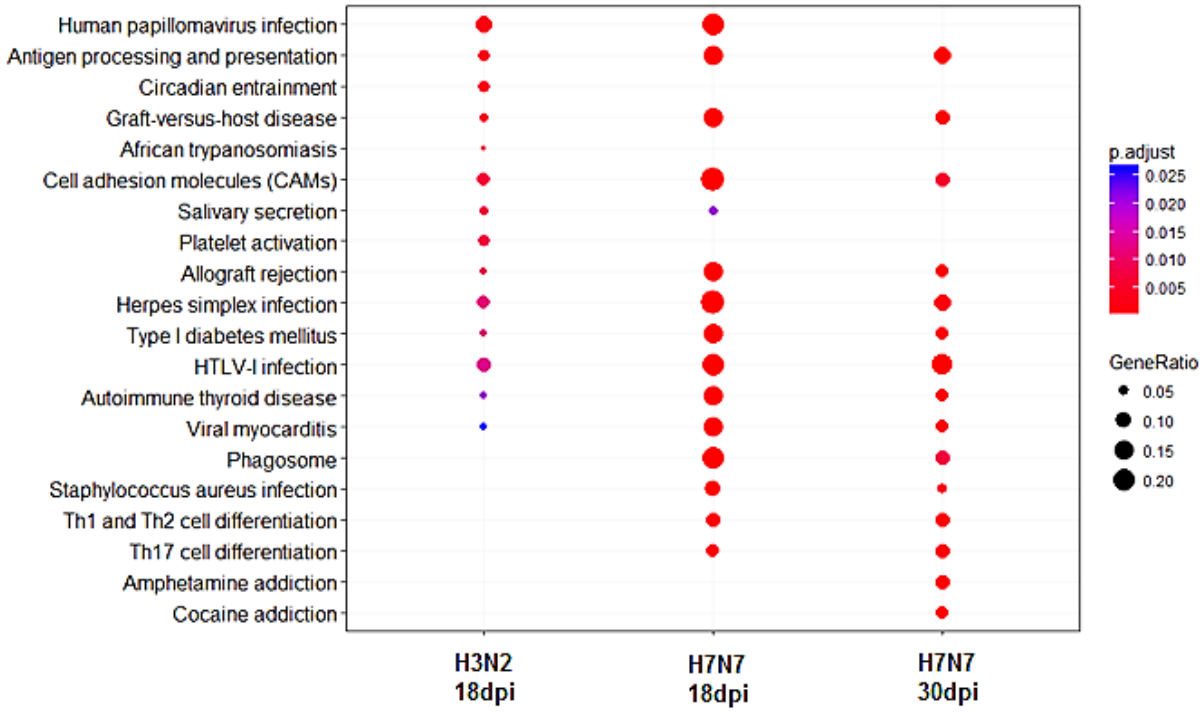

Figure 3.1.18 | KEGG pathway analysis of upregulated genes following H3N2 and H7N7 influenza A virus infection. KEGG pathway analysis was performed revealing significant pathways involved in local immune responses in the hippocampus of H3N2 and H7N7 infected mice at 18 days post infection which is more pronounced and continued until 30 days post infection for H7N7 influenza A virus. The diameter of the dots indicates the gene ratio - range of 0.05 (smallest dot) to 0.20 (biggest dot), (n=3-4). **These results were provided by Prof. Dr. Klaus Schughart, Department of Infection Genetics, Helmholtz Centre for Infection Research, Braunschweig.**

Table 1 | Relative expression level changes of neuron-related genes and neurotrophic factors in the hippocampus of influenza A virus infected mice

	Symbol	Description	Function	Fold change [log_2]			Studies
				H3N2 18 dpi	H7N7 18 dpi	H7N7 30 dpi	
Neuron-related genes	***Rbfox3***	RNA binding protein, fox-1 homolog (C. elegans) 3 (NeuN)	Marker of mature neurons, required for hippocampal circuit balance and function	**-0.46 * p=0.03**	**-0.50 * p=0.07**	**-0.22 * p=0.05**	(Wang et al., 2015)
	Nrcam	neuronal cell adhesion molecule	Regulator of axon growth, schizophrenia and autism candidate gene	**-0.47 * p=0.01**	**-0.43 * p=0.04**	**-0.35 * p=0.01**	(Demyanenko et al., 2014)
	Cacna1c	calcium channel, voltage-dependent, L type, alpha 1C subunit	Neuropsychiatric disease-associated gene, mediates survival of young hippocampal neurons	**-0.22 * p=0.04**	**-0.38 * p=0.03**	**-0.10 p=0.2**	(Lee et al., 2016)
	Dlg3	discs, large homolog 3 (Drosophila)	Synapse-associated protein 102, involved in spatial learning strategy and synaptic plasticity	**-0.35 * p=0.02**	**-0.33 * p=0.08**	**-0.20 * p=0.04**	(Cuthbert, 2007)
	Grm5	glutamate receptor, metabotropic 5	Encodes mGluR5, decreased following viral infection	**-0.46 * p=0.03**	**-0.31 p=0.1**	**0.09 p=0.2**	(Vasek et al., 2016)
	***Slc4a7* (NBCn1)**	solute carrier family 4, sodium bicarbonate cotransporter, member 7	Expressed in hippocampal neurons, associated with a Na^+ conductance, some NBCn1 colocalizes with the postsynaptic density marker PSD-95	**-0.49 * p=0.02**	**-0.53 * p=0.04**	**+0.12 p=0.3**	(Cooper et al., 2005; Majumdar and Bevensee, 2010)
	***Slc24a3* (NCKX3)**	solute carrier family 24 sodium/potassium/calcium exchanger, member 3	Responsible for regulating the dynamics of sodium, potassium, and calcium ions in neurons undergoing changes in polarization	**-0.18 p=0.2**	**-0.27 * p=0.06**	**-0.33 * p=0.04**	(Benes, 2010)
	Slc6a3	solute carrier family 6 (neurotransmitter transporter, dopamine), member 3	Increased in depression and other psychiatric disorders	**+1.46 p=0.4**	**+3.15 p=0.2**	**+5.09 * p=0.007**	(Uddin et al., 2011)
Neurotrophic factors	***Bdnf***	brain derived neurotrophic factor	Required for support the survival of existing neurons, and encourage the growth and differentiation of new neurons and synapses	**-0.43 * p=0.05**	**-0.51 * p=0.08**	**-0.11 p=0.2**	(Huang and Reichardt, 2001)
	Ntf3	neurotrophin 3		**-0.58 * p=0.009**	**-0.45 * p=0.07**	**-0.11 p=0.1**	

Significant regulation (* $p < 0.1$, ANOVA adjusted) is marked with an asterisk. A partial recovery in the altered genes expression was observed 30 days post H7N7 infection.

Table 2 | Relative expression level changes of microglia-related genes in the hippocampus of influenza A virus infected mice

	Symbol	Description	Function	Fold change [log_2]			Studies
				H3N2 18 dpi	H7N7 18 dpi	H7N7 30 dpi	
Microglia-specific genes	***Olfml3***	olfactomedin-like 3	Increased in resident microglia during neurodegeneration	**+0.31 * p=0.04**	**+0.37 * p=0.03**	**+0.01 p=0.8**	(Chiu et al., 2013; Bennett et al., 2016)
	Tmem119	transmembrane protein 119		**+0.13 p=0.1**	**+0.28 * p=0.09**	**-0.07 p=0.4**	
	Trem2	triggering receptor expressed on myeloid cells 2	Increased in the preclinical stages of Alzheimer's disease, stimulates the production of inflammatory cytokines	**+0.04 p=0.7**	**+0.45 * p=0.05**	**+0.23 * p=0.02**	(Zhong et al., 2017)
	Crybb1	crystallin, beta B1	Mediating fear-induced anxiety-like behavior	**+0.23 p=0.1**	**+0.34 * p=0.07**	**+0.15 p=0.2**	(Spadaro et al., 2015)
	Adora3	adenosine A3 receptor	Increased in neuronal injury, promoting inflammatory processes	**+0.23 * p=0.02**	**+0.49 * p=0.06**	**+0.35 * p=0.02**	(Haskó et al., 2005)
	Slc30a5	solute carrier family 30 (zinc transporter), member 5	Zinc deficiencies lead to dementia, downregulated during aging and Alzheimer's disease	**-0.33 * p=0.02**	**-0.23 * p=0.09**	**+0.03 p=0.5**	(Lovell, 2009; Nuttall and Oteiza, 2014; Crotti and Ransohoff, 2016)
	Hexb	hexosaminidase B	Decreased following microglial activation and several upregulated inflammation-related genes, Increased during autophagy and lysosomal biogenesis	**-0.20 * p=0.05**	**-0.01 p=0.9**	**+0.26 * p=0.01**	(Kyrkanides et al., 2008; Landel et al., 2014)
	Cx3cr1	chemokine (C-X3-C motif) receptor 1	Neuron-glia crosstalk associated gene, decreased following immune challenges	**-0.48 * p=0.02**	**-0.30 p=0.2**	**+0.04 p=0.7**	(Wolf et al., 2013)

Significant regulation (* $p < 0.1$, ANOVA adjusted) is marked with an asterisk. A partial recovery in the altered genes expression was observed 30 days post H7N7 infection.

Table 3 | Relative expression level changes of microglial activation markers in the hippocampus of influenza A virus infected mice

		Symbol	Description	Function	Fold change [log_2]			Studies
					H3N2 18 dpi	H7N7 18 dpi	H7N7 30 dpi	
Microglia activation markers	Major histocompatibility complex family related	***H2-Aa***	histocompatibility 2, class II antigen A, alpha	Genes involved in antigen presentation pathways, increased in demyelination processes in neurodegenerative disease, elevated following CNS infection by mouse neurotropic viruses and *Toxoplasma gondii*, markers of activated microglia with phagocytic activity	**+0.52 * p=0.04**	**+1.44 * p=0.08**	**+0.82 * p=0.007**	(Elliott et al., 2013; Tanaka et al., 2013; Fu et al., 2014; Crotti and Ransohoff, 2016)
		H2-Ab1	histocompatibility 2, class II antigen A, beta 1		**+0.70 * p=0.1**	**+1.85 * p=0.09**	**+1.43 * p=0.007**	
		H2-D1	histocompatibility 2, D region locus 1		**+0.45 * p=0.03**	**+1.39 * p=0.04**	**+0.43 * p=0.007**	
		H2-DMb1	histocompatibility 2, class II, locus Mb1		**+0.27 * p=0.03**	**+0.63 * p=0.06**	**+0.73 * p=0.006**	
		H2-Eb1	histocompatibility 2, class II antigen E beta		**+0.73 * p=0.03**	**+1.81 * p=0.06**	**+1.19 * p=0.007**	
		H2-K1	histocompatibility 2, K1, K region		**+0.50 * p=0.01**	**+1.10 * p=0.04**	**+0.20 * p=0.04**	
		H2-Q7	histocompatibility 2, Q region locus 7		**+0.51 * p=0.01**	**+1.36 * p=0.04**	**+0.65 * p=0.006**	
		Cd74	Cluster of Differentiation 74	A transporter associated with antigen processing binding protein, increased in Alzheimer's disease and viral infection	**+1.13 * p=0.01**	**2.37 * p=0.05**	**+1.25 * p=0.01**	(Bryan et al., 2008; Elliott et al., 2013)
	Phagocytic activity	***Fcgr2b***	Fc receptor, IgG, low affinity IIb	Genes associated with microglia/macrophage -mediated phagocytosis within the brain during inflammatory processes	**+0.06 p=0.4**	**+0.45 p=0.1**	**+0.25 * p=0.02**	(Hickman et al., 2013; Vasek et al., 2016)
		Fcgr3	Fc receptor, IgG, low affinity III		**+0.03 p=0.7**	**+0.51 * p=0.06**	**+0.20 * p=0.01**	
		Fcgr4	Fc receptor, IgG, low affinity IV		**+0.20 * p=0.02**	**+0.77 * p=0.05**	**+0.41 * p=0.01**	
		Vav1	vav 1 oncogene		**-0.05 p=0.6**	**+0.44 * p=0.04**	**+0.08 p=0.2**	
		Tyrobp (Dap12)	TYRO protein tyrosine kinase binding protein		**+0.22 * p=0.07**	**+0.55 * p=0.05**	**+ 0.36 * p=0.008**	
		Cd14	Cluster of Differentiation 14		**+0.04 p=0.6**	**+0.35 * p=0.05**	**+0.11 p=0.3**	
		Cd48	Cluster of Differentiation 48		**-0.01 p=0.8**	**+0.52 * p=0.09**	**+0.09 p=0.2**	
		Ctsz	cathepsin Z	A lysosomal cysteine protease potentially involved in the degradation of viral antigens	**+0.22 * p=0.04**	**+0.29 * p=0.04**	**-0.05 p=0.5**	(Elliott et al., 2013)
	Complement pathway	***C1qa***	complement component 1, q subcomponent, alpha polypeptide	Mediates synaptic pruning by microglia during early postnatal development, involved in microglia-mediated synapse loss during viral infection	**+0.14 p=0.2**	**+0.48 * p=0.03**	**+0.25 * p=0.01**	(Stevens et al., 2007; Vasek et al., 2016)
		C1qb	complement component 1, q subcomponent, beta polypeptide		**+0.10 p=0.2**	**+0.37 * p=0.04**	**-0.02 p=0.8**	
		C1qc	complement component 1, q subcomponent, C chain		**+0.15 p=0.2**	**+0.29 * p=0.1**	**+0.32 * p=0.01**	
		Vwf	Von Willebrand factor		**+0.65 * p=0.02**	**+0.66 * p=0.06**	**-0.13 p=0.8**	

Significant regulation (* $p < 0.1$, ANOVA adjusted) is marked with an asterisk. A partial recovery in the altered genes expression was observed 30 days post H7N7 infection.

Table 4 | Relative expression level changes of astrocyte-related genes in the hippocampus of influenza A virus infected mice

	Symbol	Description	Function	Fold change [log_2]			Studies
				H3N2 18 dpi	H7N7 18 dpi	H7N7 30 dpi	
Astrocyte-related genes	***Gfap***	glial fibrillary acidic protein	An intermediate filament protein in the cytoskeleton of astrocyte, elevated level represents astroglial activation and gliosis during neurodegeneration	**+0.37 * p=0.08**	**+0.47 p=0.1**	**-0.02 p=0.7**	(Brahmachari et al., 2006)
	Lcn2	lipocalin 2	Secreted by reactive astrocytes to promote neuronal death	**+0.34 * p=0.009**	**+0.17 p=0.1**	**-0.36 p=0.6**	(Bi et al., 2013)
	H2-T23	histocompatibility 2, T region locus 23	Expressed by reactive astrogliosis	**+0.52 * p=0.01**	**+1.09 * p=0.04**	**+0.001 p=0.9**	(Liddelow et al., 2017)
	Psmb8	proteasome (prosome, macropain) subunit, beta type 8 (large multifunctional peptidase 7)	Astrocytic immunoproteasome related gene, increased in Alzheimer's disease	**+0.20 * p=0.04**	**+0.81 * p=0.05**	**+0.38 * p=0.02**	(Orre et al., 2013)
	Gjb6	gap junction protein beta 6 (Connexin 30)	Involved in direct intercellular conduits between astrocytes and neurons	**+0.37 * p=0.06**	**+0.30 p=0.1**	**+0.16 p=0.1**	(Pannasch et al., 2011; Chung et al., 2015)
	Aqp4	aquaporin-4 (Water channel in astrocytes)	A key molecule for maintaining water and ion homeostasis, required for K^+ reuptake by astrocytes	**-0.11 p=0.3**	**-0.30 * p=0.08**	**+0.02 p=0.8**	(Scharfman and Binder, 2013)
	Slc1a2	solute carrier family 1 (glial high affinity glutamate transporter), member 2 (EAAT2/GLT-1)	Associated gene with glutamate transport and metabolism, required for proper synaptic activity	**-0.33 * p=0.02**	**-0.18 p=0.2**	**-0.18 * p=0.05**	(David et al., 2009)
	***Slc25a18* (GC2)**	solute carrier family 25 (mitochondrial carrier), member 18	Mitochondrial glutamate carrier, downregulation of GC1 in astrocytes leads to intracellular glutamate accumulation	**+0.22 * p=0.08**	**+0.35 * p=0.04**	**-0.18 * p=0.02**	(Goubert et al., 2017)
	Slc2a1	solute carrier family 2 (facilitated glucose transporter), member 1 (GLUT-1)	Responsible for glucose uptake into astrocytes and neurons, decreased in Alzheimer's disease	**-0.21 * p=0.06**	**-0.31 * p=0.08**	**+0.53 * p=0.01**	(Liu et al., 2008)

Significant regulation (* $p < 0.1$, ANOVA adjusted) is marked with an asterisk. A partial recovery in the altered genes expression was observed 30 days post H7N7 infection.

Table 5 | Relative expression level changes of interferon-response genes in the hippocampus influenza A virus infected mice

	Symbol	Description	Function	Fold change [log_2]			Studies
				H3N2 18 dpi	H7N7 18 dpi	H7N7 30 dpi	
Interferon-response gene	***Psme1***	proteasome (prosome, macropain) activator subunit 1 (PA28 alpha)	IFN-γ induced proteasome, immune-inflammatory gene, increased in aging	**+0.06 p=0.4**	**+0.26 * p=0.05**	**+0.15 * p=0.04**	(Porter et al., 2012)
	***Psmb9* (LMP2)**	proteasome (prosome, macropain) subunit, beta type 9 (large multifunctional peptidase 2)	IFN-α-inducible gene, depression-associated gene	**+0.22 * p=0.08**	**+0.79 * p=0.05**	**+0.51 * p=0.007**	(Hoyo-Becerra et al., 2015)
	Tap1	transporter 1, ATP-binding cassette, sub-family B (MDR/TAP)	IFN-γ induced gene, required for transport of MHC I molecules	**+0.07 p=0.4**	**+0.45 * p=0.06**	**+0.15 p=0.2**	(Neumann et al., 1997)
	Lgals3bp	lectin, galactoside-binding, soluble, 3 binding protein	Type I IFN-induced gene, modulation activity of immune cells	**+0.41 * p=0.04**	**+0.67 * p=0.05**	**+0.44 * p=0.01**	(Goffinet, 2016)
	Gbp2	guanylate binding protein 2	IFN-induced GTPase, expressed in immune cells	**+0.11 p=0.6**	**+0.61 * p=0.09**	**+0.32 * p=0.04**	(Mastrondardi et al., 2015)
	Oas2	2'-5' oligoadenylate synthetase 2	Defense and innate immune response to virus	**+0.43 * p=0.01**	**+0.75 * p=0.04**	**+0.49 * p=0.008**	(Bao et al., 2017)
	CCL5	chemokine (C-C motif) ligand 5	Type I IFN-induced chemokine, associated with hippocampal T-cell infiltration, promotes cognitive decline	**+0.40 * p=0.02**	**+2.15 * p=0.07**	**+1.52 * p=0.006**	(Laurent et al., 2017)
	Ifit3	interferon-induced protein with tetratricopeptide repeats 3	Stat1 and IFN signaling-dependent gene, expression higher in granule cell neurons	**+0.08 p=0.6**	**+0.68 * p=0.07**	**+0.20 p=0.3**	(Cho et al., 2013)
	Mx1	MX dynamin-like GTPase 1	Type I IFN-induced gene, induction of microglial activation	**+0.11 p=0.2**	**+0.46 * p=0.08**	**+0.15 p=0.2**	(Bialas et al., 2017)

Significant regulation (* $p < 0.1$, ANOVA adjusted) is marked with an asterisk. A partial recovery in the altered genes expression was observed 30 days post H7N7 infection.

3.2. Type I interferon (IFN) signaling ablation alters hippocampal synaptic plasticity and cognitive function

In the healthy state of the CNS, the regulation of the synapse, and therefore the ability of a neuron to conduct its signal, involves several interactions between neurons and glial cells. These interactions are modulated by many mediators, including short-acting soluble factors which are called cytokines. Interferons (IFNs) are glycoproteins also known as cytokines which can affect synapse function (Ignatowski and Spengler, 2008). In general, type I interferon proteins and their receptor (IFNAR) are part of a pathway that has a fundamental role in the immune response against viral infection, therefore, individuals who have an impaired type I interferon response can be prone to infections (McGlasson and Hunt, 2017). Ablation of type I IFN signaling in the brain could, however, not only impair host defense mechanisms but basal levels of interferon signaling might indeed be needed to maintain neuronal health and function. Therefore, as the main focus of this study, the fundamental role of type I IFNs and their receptor in the healthy CNS was investigated.

3.2.1. IFNAR$^{-/-}$ mice

In order to study the importance of physiological levels of type I IFNs for the CNS, cognitive function and synaptic plasticity were investigated in type I alpha/beta interferons receptor deficient mice (IFNAR$^{-/-}$). These mice are unresponsive to type I IFNs (IFN-α and IFN-β), suggesting that this receptor is pivotal for type I IFN-mediated signal transduction. Earlier studies indicated that IFNAR$^{-/-}$ mice did not show obvious anomalies but were unable to cope with viral infections, despite normal immune responses (Muller et al., 1994; Detje et al., 2015). In this part of the study, 6 to 8 weeks old mice lacking the IFNAR1 subunit (IFNAR$^{-/-}$) were used. As this is a conventional knockout (KO) mouse model, the receptor was absent from all cell types including those of the CNS.

3.2.1.1. IFNAR$^{-/-}$ mice show hyperactivity

Type I IFN signal transduction is crucial for maintaining neuronal health and brain function (Ignatowski and Spengler, 2008). Therefore, to investigate general behavior in IFNAR$^{-/-}$ mice, the open field test was performed. This test provides an opportunity

to assess novel environment exploration, general locomotor activity, and can be also used as an initial screen for anxiety-related behavior in rodents (Buccafusco, 2000). For this purpose, wild-type (WT) and IFNAR$^{-/-}$ mice were tested for 5 min in the open field arena and total distance traveled, average speed and the activity percentage of mice in the different zones of the arena including periphery and center were analyzed (Figure 3.2.1). IFNAR$^{-/-}$ mice traveled a significantly longer distance (WT: 2.77 ± 0.16 m, IFNAR$^{-/-}$: 3.97 ± 0.21 m) (Figure 3.2.1A) with higher average speed (WT: 0.009 ± 0.0005 m/s, IFNAR$^{-/-}$: 0.013 ± 0.0007 m/s) (Figure 3.2.1B) compared to WT mice ($p < 0.001$). To evaluate anxiety-like behavior in IFNAR$^{-/-}$ mice, the time spent in different zones of the open field apparatus was measured. WT and IFNAR$^{-/-}$ mice spent comparable times in the periphery and center zones of the open field arena (Periphery, WT: 84.62 ± 1.67 %, IFNAR$^{-/-}$: 89.35 ± 1.41 % - Center, WT: 15.38 ± 1.68 %, IFNAR$^{-/-}$: 10.65 ± 1.41 %) (Figure 3.2.1C). These observations, therefore, revealed hyperactive behavior in IFNAR$^{-/-}$ mice.

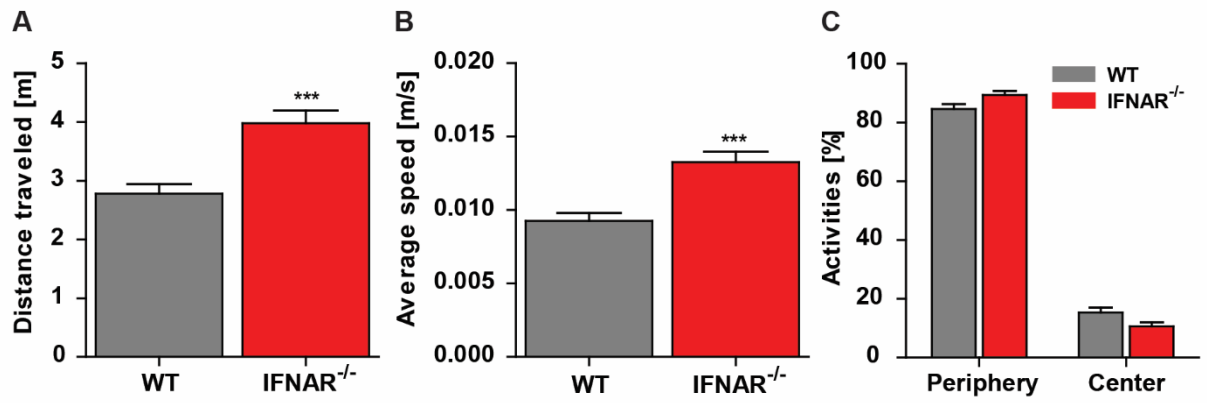

Figure 3.2.1 | General behavioral phenotype in IFNAR$^{-/-}$ mice. IFNAR$^{-/-}$ mice exhibited **(A)** a longer distance traveled with **(B)** higher average speed in comparison to WT mice. **(C)** Time of both tested groups spent in the periphery versus the center part of the open field arena did not differ between genotypes. Data are presented as mean ± SEM, (n=9). *** $p < 0.001$ compared to WT.

3.2.1.2. Impaired spatial learning and memory formation in IFNAR$^{-/-}$ mice

As a next step to identify the putative role of type I IFN receptor signaling for cognitive function, IFNAR$^{-/-}$ and WT mice were trained for 8 days in the Morris water maze test. In this test both escape latency and swim distance were analyzed as performance representation of memory formation over consecutive days. As shown in figure 3.2.2, the swim distance and duration (escape latency) to reach the platform progressively decreased over 8 days during the acquisition training in WT animals but not in IFNAR$^{-/-}$ mice (Swim distance - repeated measure ANOVA: F_{WT} (7, 56) = 10.17, $p < 0.001$ and $F_{IFNAR^{-/-}}$ (7, 64) = 0.70, $p = 0.67$, Escape latency - F_{WT} (7, 56) = 10.67, $p < 0.001$ and $F_{IFNAR^{-/-}}$ (7, 64) = 0.8120, $p = 0.5806$). A Comparison of the data between both tested groups as well showed that swim distance (Figure 3.2.2A) and escape latency (Figure 3.2.2B) during the acquisition time were significantly higher in IFNAR$^{-/-}$ compared to WT mice (Swim distance - Two-way ANOVA: $F_{Treatment}$ (1, 120) = 15.50, $p < 0.001$, Escape latency – $F_{Treatment}$ (1, 120) = 10.46, $p < 0.01$). Both groups were submitted to reference memory tests (probe trials without the platform) on day 3 and 6, prior to the training session and on day 9. On day 6 and 9 in both groups, the time spent in the target quadrant (TQ) was significantly higher than the time spent in the other quadrants (OQs). On day 9, IFNAR$^{-/-}$ mice (39.42 ± 4.31 %) spent slightly less time in the TQ compared to WT animals (49.56 ± 2.07 %) although this difference was not statistically significant (Figure 3.2.2C).

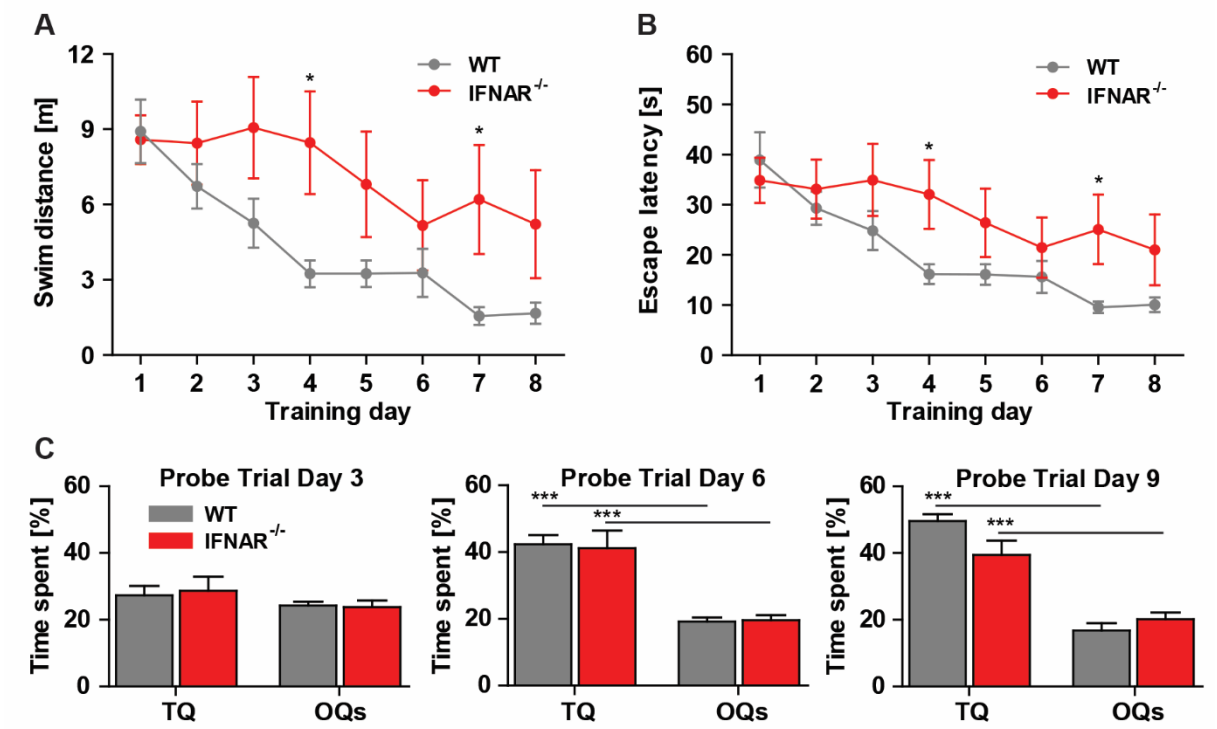

Figure 3.2.2 | Spatial learning and memory assessment in IFNAR$^{-/-}$ mice. IFNAR$^{-/-}$ mice showed **(A)** longer swim distance and **(B)** higher escape latency and therefore, impaired spatial learning and memory compared to WT animals. **(C)** Percent time spent in the target quadrant (TQ) in comparison to the mean time spent in other quadrants (OQs) without the platform on days 3, 6 and 9. Data are presented as mean ± SEM, (n=8-9). * $p < 0.05$ compared to WT and *** $p < 0.001$ compared to OQs.

Furthermore, to analyze differences in the quality of spatial learning even further, searching strategies were analyzed (Figure 3.2.3). For this purpose, the swim path of each animal and trial were reviewed. This detailed analysis of the swimming path allows for a qualitative assessment of learning in mice during the training days. The time spent in the different zones of the pool including the center zone, the outer zone, the doughnut-shaped annulus zone and the Wishaw's corridor allows to differentiate searching strategies used by mice into hippocampus-dependent (spatial learning) allocentric search strategies (directed search) and hippocampus-independent (non-spatial learning) egocentric strategies including chaining, scanning and random swimming. Over time, mice learn to use more allocentric strategies compared to egocentric strategies to navigate the hidden platform (Garthe et al., 2009; Garthe and Kempermann, 2013). The results revealed that both WT and IFNAR$^{-/-}$ mice used more hippocampus-dependent searching with increasing training time. However, this progression was clearly decreased for IFNAR$^{-/-}$ mice compared to WT animals

(Figure 3.2.3A) as hippocampus-independent search strategies were significantly increased (Day 7: WT: 28.13 ± 5.66 % and IFNAR$^{-/-}$: 61.11 ± 11.87, Day 8: WT: 25.00 ± 4.72 % and IFNAR$^{-/-}$: 66.67 ± 8.33 %) and hippocampus-dependent search strategy was significantly decreased (Day 7: WT: 71.88 ± 5.66 % and IFNAR$^{-/-}$: 38.89 ± 11.87, Day 8: WT: 75.00 ± 4.72 % and IFNAR$^{-/-}$: 33.33 ± 8.33 %) on day 7 and 8 of the acquisition training in IFNAR$^{-/-}$ animals compared to WT mice ($p < 0.05$) (Figure 3.2.3B).

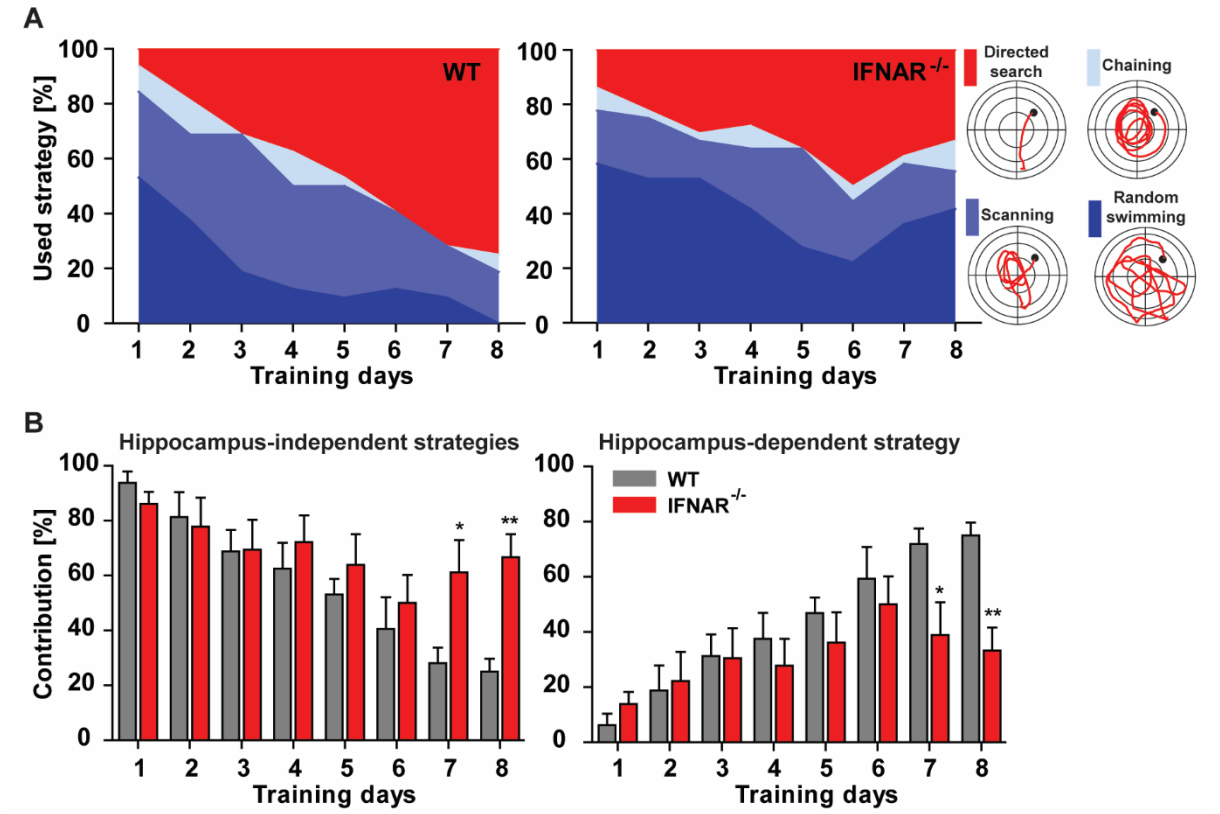

Figure 3.2.3 | Learning strategies used during the Water maze training. (A), **(B)** The hippocampus-dependent strategy was decreased and hippocampus-independent strategies were increased in IFNAR$^{-/-}$ mice compared to WT. Data are presented as mean ± SEM, (n=8-9). * $p < 0.05$ and ** $p < 0.01$ compared to WT.

3.2.1.3. IFNAR$^{-/-}$ mice exhibit impaired hippocampal synaptic plasticity

Results of the Morris water maze indicated a learning impairment in IFNAR$^{-/-}$ mice. Therefore, as a next step, synaptic plasticity was investigated to reveal potential cellular mechanisms responsible for this deficit. For this purpose, field excitatory postsynaptic potentials (fEPSP) in stratum radiatum of the hippocampal CA1 area in response to stimulation of the Schafer collaterals were recorded and fEPSP slopes were analyzed and compared between WT and IFNAR$^{-/-}$ mice. Electrophysiological experiments for this part of the study were performed by Dr. Gayane Grigoryan, in the cellular neurobiology department of the TU-Braunschweig. The fEPSPs were recorded from hippocampal slices of 6-8 weeks old animals. The input-output curve of the EPSP slope dependence to the stimulation intensity did not reveal any significant difference between IFNAR$^{-/-}$ and WT mice (Figure 3.2.4A). Thus, the basal synaptic transmission was not affected by the alpha/beta interferon receptor deficiency. Paired-pulse facilitation of the fEPSP to afferent stimulation, a form of short-term synaptic plasticity, was examined in hippocampal slices taken from mice of both groups by using the paired-pulse stimulation protocol. In brief, two consecutive stimuli with equal intensity (conditioning and test stimuli, respectively) were delivered at varying (10, 20, 40, 60, 80 and 100 ms) interpulse intervals. The facilitation of the second response was calculated as a percent ratio of the fEPSP slope of the second response to the first response (EPSP2/EPSP1%). Paired-pulse facilitation of the fEPSP was not affected in hippocampal slices taken from IFNAR$^{-/-}$ mice compared to control (Figure 3.2.4B). To study the role of type I IFN receptor in processes of long-term synaptic plasticity, long-term potentiation (LTP) was analyzed. LTP was induced by theta-burst stimulation (TBS, refer to 2.2.4.4). Before LTP induction, evoked fEPSPs were recorded for a stable baseline period, at least for 20 minutes. The results revealed that slices taken from IFNAR$^{-/-}$ mice show a significant impairment in LTP compared to WT animals (Figure 3.2.4C). Also, the mean value of the maintenance phase of LTP (last 5 minutes of recording) was significantly diminished in IFNAR$^{-/-}$ mice (1.10 ± 0.04) thereby revealing an impairment in synaptic plasticity compared to WT animals (1.40 ± 0.08) ($p < 0.001$) (Figure 3.2.4D).

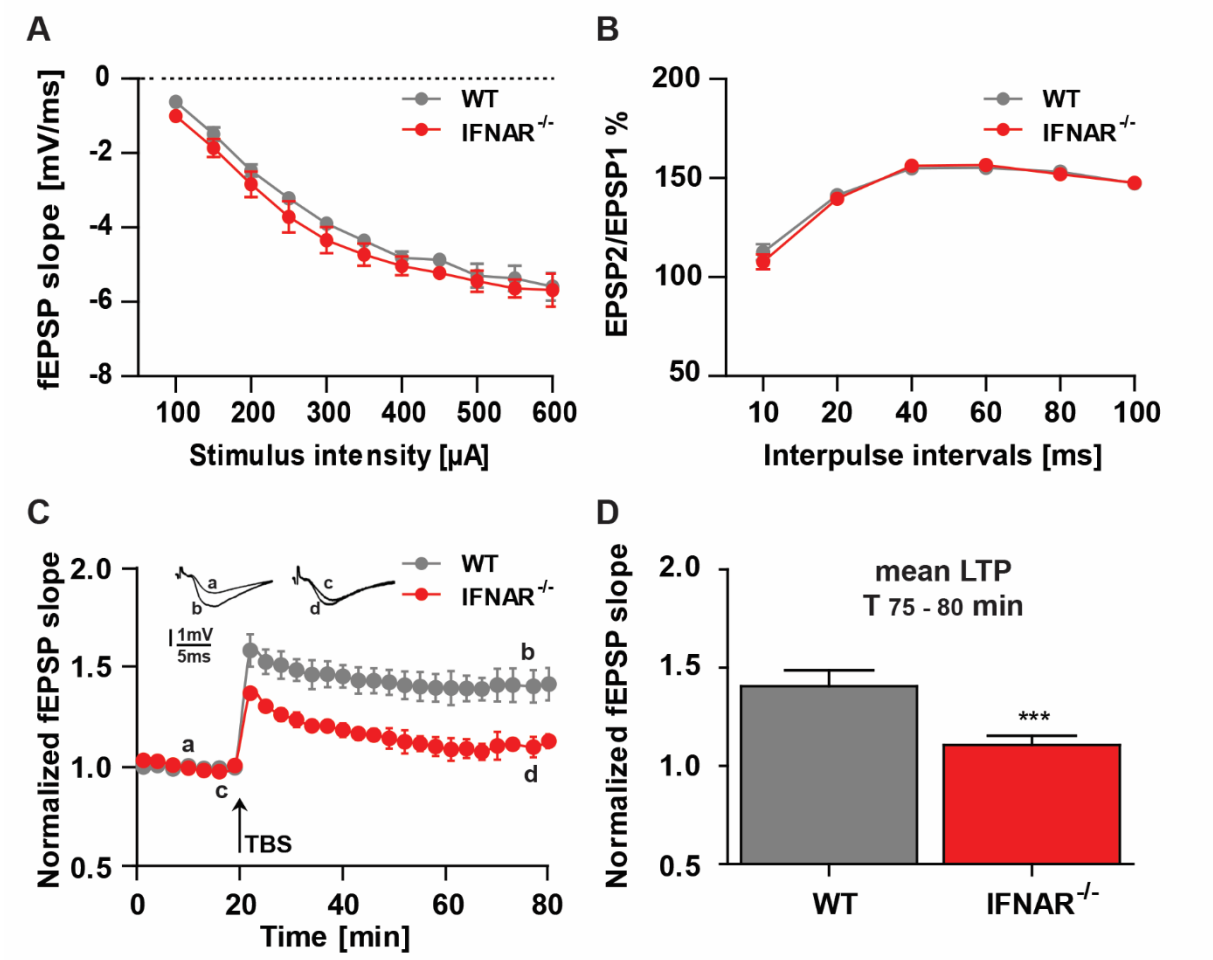

Figure 3.2.4 | Long-term potentiation (LTP) assessment in the hippocampal CA1 subregion of IFNAR$^{-/-}$ mice. (A) Input-output curves representing the dependence of the EPSP slope on stimulation intensity showed no difference in basal synaptic transmission between WT and IFNAR$^{-/-}$ mice. **(B)** No alteration was found in paired-pulse facilitation at different (10, 20, 40, 60, 80 and 100 ms) interpulse intervals between WT and IFNAR$^{-/-}$ mice. **(C)** IFNAR$^{-/-}$ mice showed a significant impairment in LTP induced by theta-burst stimulation (TBS, four bursts at 100 Hz repeated 10 times in a 200 ms interval, repeated three times in a 10 seconds interval; denoted with an arrow). **(D)** The mean LTP magnitude (average of last 5 minutes of recording) was significantly lower in IFNAR$^{-/-}$ animals than the WT. Data are presented as mean ± SEM, (n (number of slices)=21-28 in each group). *** $p < 0.001$ compared to WT. Dr. Gayane Grigoryan did this experiment.

3.2.1.4. Type I IFN receptor deficiency alters hippocampal neuron morphology

Spines are tiny dendritic protrusions that receive most of the postsynaptic excitatory synaptic input in the hippocampus and neocortex. In addition, alterations in dendritic spine density and morphology have been shown to correlate with defects in synaptic plasticity and cognitive function in general (Moser et al., 1994). Therefore, to

investigate the potential cellular mechanism underlying the observed impairment in spatial learning and LTP in IFNAR$^{-/-}$ mice, hippocampal neuron morphology was analyzed. For this purpose, dendritic spines were counted separately on apical and basal dendrites of CA1 and CA3 pyramidal neurons as well as dentate granular cells being located in the superior and inferior blades of the granule cell layer in the hippocampus of both IFNAR$^{-/-}$ and WT mice (Figure 3.2.5). A significant reduction in spine density of apical (CA1: Δ 19.44%, CA3: 9.36%) and basal (CA1: Δ 22.01%, CA3: Δ 14.32%) dendrites of CA1 and CA3 pyramidal neurons in IFNAR$^{-/-}$ mice compared to WT could be observed ($p < 0.001$) (Figure 3.2.5A,B). Furthermore, type I IFN receptor deficiency led to a reduction in dendritic spine density in granule cells of the inferior blade in the dentate gyrus (Δ 8.77%) ($p < 0.01$) while granule cells in the superior dentate gyrus blade (Δ 0.08%) were not affected (Figure 3.2.5C).

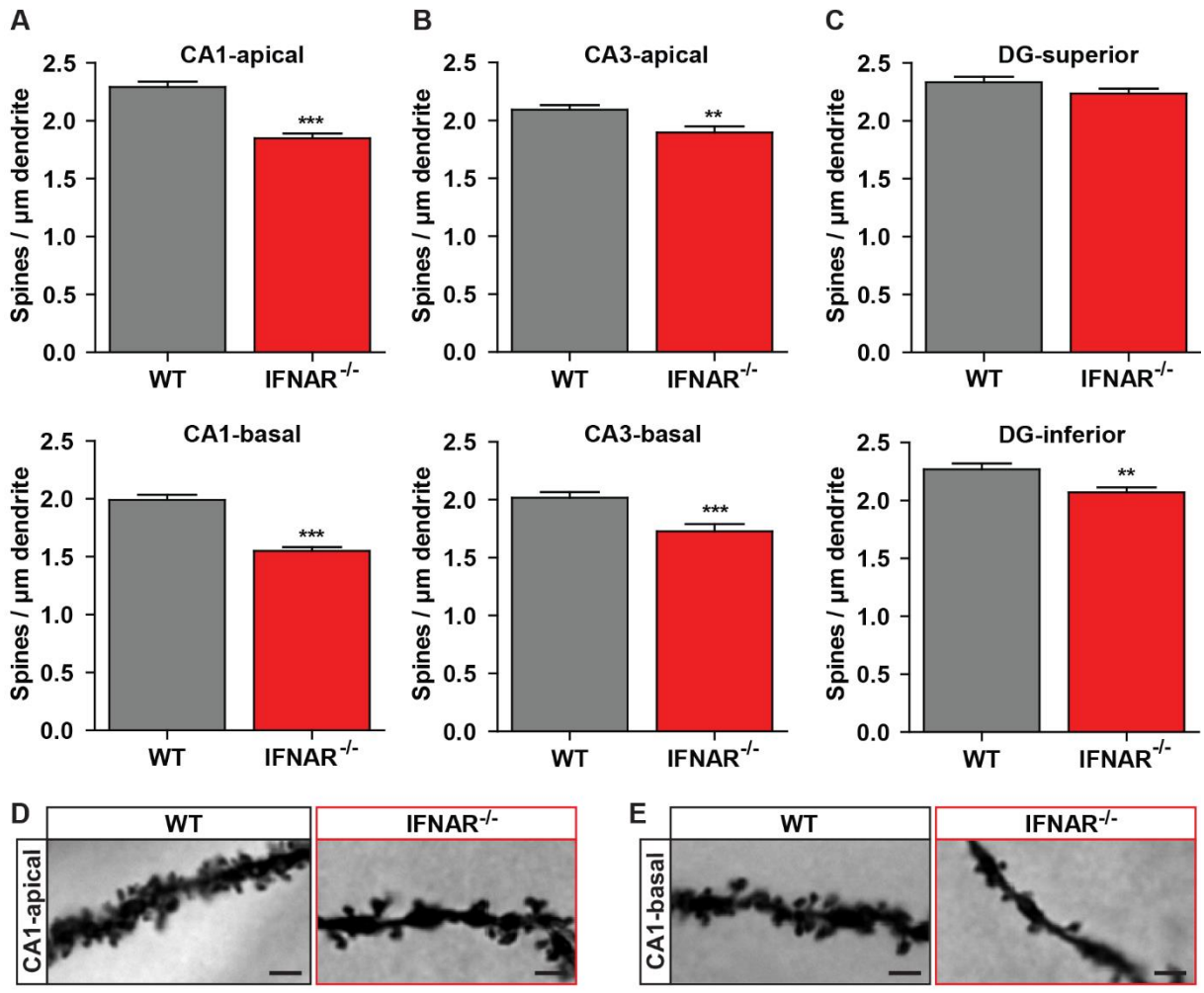

Figure 3.2.5 | Dendritic spine density assessment in hippocampal neurons of IFNAR$^{-/-}$ mice. (A), **(B)** Spine density of apical and basal dendrites of CA1 and CA3 hippocampal neurons was diminished

in IFNAR$^{-/-}$ mice compared to WT. **(C)** Dendritic spine density of dentate granule cells located in the inferior blade of the granule cell layer was reduced in IFNAR$^{-/-}$ mice in comparison to WT animals. **(D)**, **(E)** Representative images of the dendritic spine of hippocampal CA1 neurons in both tested groups (Bar=2 µm, 63X). Data are presented as mean ± SEM, (n (number of animals) in each group=4, m (number of dendrites)=40 in each group). ** $p < 0.01$ and *** $p < 0.001$ compared to WT.

3.2.1.5. IFNAR$^{-/-}$ mice do not exhibit signs of neuroinflammation

As already mentioned, microglia constitute the innate immune system of the CNS and are important cellular mediators for neuroinflammatory processes. Activation of microglia is a hallmark of inflammatory processes which are believed to play an important role for neuronal damage and synaptic plasticity impairments (Riazi et al., 2015). Previously, it was shown that IFNAR$^{-/-}$ mice are more sensitive to infections as they lack the type I IFNs signaling (Muller et al., 1994), therefore, to make sure that the observed impaired cognitive function and synaptic plasticity are not due to some subclinical levels of neuroinflammation, microglia density and activation status in the hippocampal subregions of IFNAR$^{-/-}$ mice were assessed. For this purpose, IBA-1 staining was performed and IBA-1 positive cells were counted and analyzed separately in the CA1, CA3 subregions and dentate gyrus superior and inferior blades (Figure 3.2.6). The results revealed that microglia density in all hippocampal subregions did not differ in IFNAR$^{-/-}$ mice compared to WT mice (Figure 3.2.6A). Furthermore, earlier studies indicated that a reduced number of primary processes reflects an elevated activity status of microglia cells (Papageorgiou et al., 2015). Thus, to quantify the activation status of microglia in the absence of type I IFN receptor, in each subregion of the hippocampus, 24 to 30 microglial cells of 4 to 5 regions of interest (ROIs) were selected randomly and the number of their main processes was counted (refer to 2.2.6.1) (Figure 3.2.6B). Analysis of the number of primary processes of microglial cells in all subregions of the hippocampus in IFNAR$^{-/-}$ mice revealed no differences compared to WT animals (Figure 3.2.6B). Therefore, type I IFN receptor deficiency was not associated with a general elevation of neuroinflammation in the brain of healthy animals.

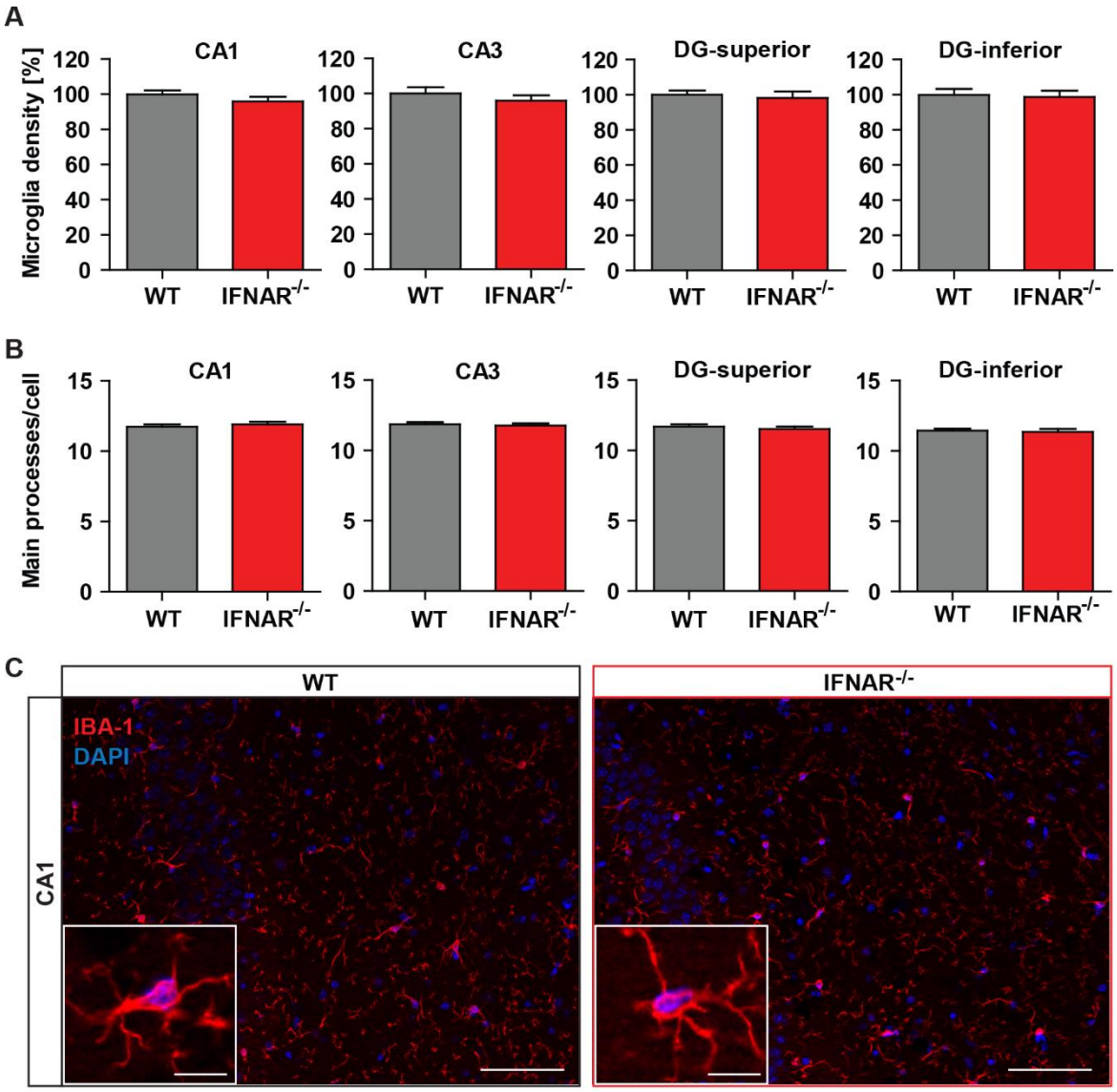

Figure 3.2.6 | Microglia density and morphology assessment in IFNAR$^{-/-}$ mice. (A) The microglia density in all hippocampal subregions of IFNAR$^{-/-}$ mice showed a phenotype equivalent to WT animals. **(B)** The activation status of microglia within all hippocampal subregions of IFNAR$^{-/-}$ mice did not show any difference compared to the WT animals. **(C)** Representative examples of IBA-1 immunostaining of CA1 hippocampal subregion in both tested groups (red is IBA-1 and blue is DAPI staining, Bar=50 µm, Inset frame Bar=10 µm, 20X). Data are presented as mean ± SEM, (Number of animals in each group=4, number of ROIs in each group=18-20, number of selected microglia in each group=108-120).

3.2.2. NesCre$^{+/-}$IFNAR$^{flox/flox}$ mice (IFNAR deletion in neurons, astrocytes and oligodendrocytes)

As indicated by the results of conventional IFNAR$^{-/-}$ mice described above interferon signaling seems to be crucial for synaptic function. However, the mechanism and especially the cell types involved in direct IFNAR signaling remain elusive. As IFNAR is present in all cell types, as a next step different conditional mouse models were used to determine where the receptor is indeed needed for interferon signaling in processes of learning and memory. First NesCre$^{+/-}$IFNAR$^{flox/flox}$ mice with type I IFN receptor deletion in neuroectodermal cells of the CNS including neurons, astrocytes and oligodendrocytes but not microglia (Detje et al., 2015) were investigated (Nestin-Cre is primarily expressed in the central and peripheral nervous system starting at embryonic day 12.5 (Tronche et al., 1999)).

3.2.2.1. Locomotor activity is unaltered in NesCre$^{+/-}$IFNAR$^{flox/flox}$ mice

NesCre$^{+/-}$IFNAR$^{flox/flox}$ mice were examined in the open field test for 5 min. Total distance traveled, average speed and time spent in the center compared to the outer edges, were recorded (Figure 3.2.7). The observed results of total distance traveled (Ctrl: 2.66 ± 0.19 m, NesCre$^{+/-}$IFNAR$^{flox/flox}$: 3.15 ± 0.14 m) (Figure 3.2.7A), average speed (Ctrl: 0.008 ± 0.0006 m/s, NesCre$^{+/-}$IFNAR$^{flox/flox}$: 0.01 ± 0.0004 m/s) (Figure 3.2.7B) and general activity in the center and periphery zones of open field arena (Periphery, Ctrl: 92.01 ± 2.79 %, NesCre$^{+/-}$IFNAR$^{flox/flox}$: 89.22 ± 2.73 % - Center, Ctrl: 7.99 ± 2.79 %, NesCre$^{+/-}$IFNAR$^{flox/flox}$: 10.78 ± 2.73 %) (Figure 3.2.7C) revealed that the phenotype of NesCre$^{+/-}$IFNAR$^{flox/flox}$ mice was indistinguishable from their respective control mice (NesCre^{negative}).

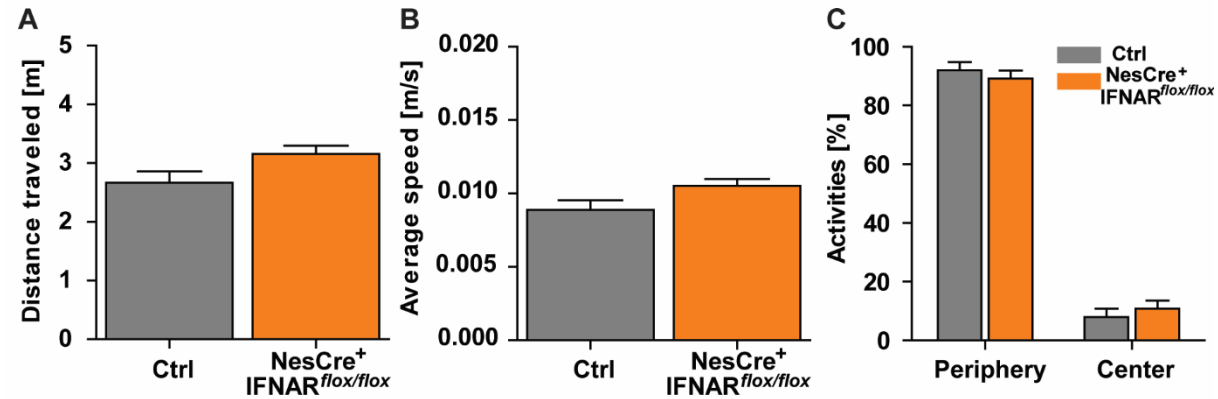

Figure 3.2.7 | General behavioral phenotype in NesCre$^{+/-}$IFNAR$^{flox/flox}$ mice. (A), **(B)** NesCre$^{+/-}$ IFNAR$^{flox/flox}$ exhibited unchanged total distance traveled and average speed in comparison with respective control mice (NesCre^{negative}). **(C)** The percentage of activity of this conditional KO and control mice in the periphery and center parts of open field arena did not indicate any significant differences. NesCre$^{+/-}$IFNAR$^{flox/flox}$ mice did not show hyperactivity and anxiety-like behavior. Data are presented as mean ± SEM, (n=7-8).

3.2.2.2. NesCre$^{+/-}$IFNAR$^{flox/flox}$ mice show impaired spatial learning and memory formation

NesCre$^{+/-}$IFNAR$^{flox/flox}$ mice were tested in the Morris water maze task like the previous groups of animals. The results of Morris water maze test indicated that the swim distance and escape latency did not reduce significantly over 8 days of acquisition training in NesCre$^{+/-}$IFNAR$^{flox/flox}$ mice unlike the respective control animals (Swim distance - repeated measure ANOVA: F_{Ctrl} (7, 48) = 8.97, $p < 0.001$ and $F_{NesCre^{+}IFNAR^{flox/flox}}$ (7, 56) = 1.012, p = 0.43, Escape latency – F_{Ctrl} (7, 48) = 5.98, $p < 0.001$ and $F_{NesCre^{+}IFNAR^{flox/flox}}$ (7, 56) = 0.4966, p = 0.8331). Furthermore, during 8 days of training, swim distance (Figure 3.2.8A) and escape latency (Figure 3.2.8B) were significantly higher in NesCre$^{+/-}$IFNAR$^{flox/flox}$ mice compared to control animals suggesting impaired learning processes in NesCre conditional KO mice (Swim distance - Two-way ANOVA: $F_{Treatment}$ (1, 104) = 26.03, $p < 0.001$, Escape latency – $F_{Treatment}$ (1, 104) = 26.67, $p < 0.001$).

The results of the reference memory tests during and after the Morris water maze test showed no differences in the amount of time spent by NesCre conditional KO mice in TQ compared to the mean value of time spent in OQs. Control mice, however, spent significantly more time in the TQ during the probe trial tests on the days 6 and 9 in comparison to the time spent in the OQs (Figure 3.2.8C). These observations suggested that NesCre conditional KO mice did not learn and remember the location of the hidden platform as efficient as respective control animals.

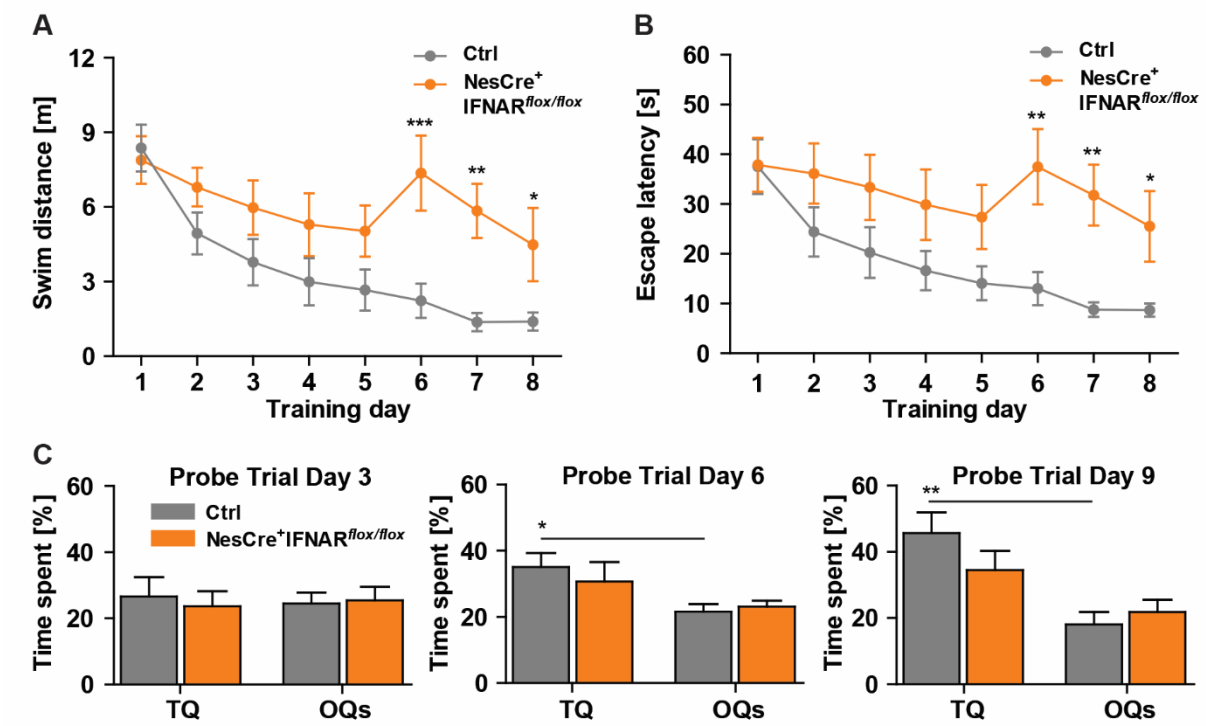

Figure 3.2.8 | Spatial learning and memory assessment in NesCre$^{+/-}$IFNAR$^{flox/flox}$ mice. NesCre conditional KO mice showed higher **(A)** swim distance and **(B)** escape latency than respective control animals. **(C)** Percent time spent in the target quadrant (TQ) in comparison to the mean time spent in the other quadrants (OQs) without the platform on days 3, 6 and 9 is presented. On days, 6 and 9 of probe trial tests only control mice spent more time in TQ significantly. Data are presented as mean ± SEM, (n=7-8). * $p < 0.05$, ** $p < 0.01$ and *** $p < 0.001$ compared to control, * $p < 0.05$ and ** $p < 0.01$ compared to OQs.

In addition, as for the conventional IFNAR KO animals, the percentage of searching strategies used were calculated and classified into four groups including directed search, chaining, scanning and random swimming (Garthe et al., 2009). The contribution of the directed search increased in the control group during the acquisition period of 8 days whereas the contribution of random swimming decreased. This was not the case in NesCre$^{+/-}$IFNAR$^{flox/flox}$ mice (Figure 3.2.9.A). Furthermore, the NesCre conditional KO mice used significantly more hippocampus-independent search strategies (Day 5: Ctrl: 35.71 ± 9.22 % and NesCre^{+}IFNAR$^{flox/flox}$: 75.00 ± 9.44, Day 6: Ctrl: 32.14 ± 14.14 % and NesCre^{+}IFNAR$^{flox/flox}$: 90.63 ± 6.57 % and Day 7: Ctrl: 25.00 ± 7.71 % and NesCre^{+}IFNAR$^{flox/flox}$: 84.38 ± 6.57 %) and less hippocampus-dependent search strategy (Day 5: Ctrl: 64.29 ± 9.22 % and NesCre^{+}IFNAR$^{flox/flox}$: 25.00 ± 9.44, Day 6: Ctrl: 67.86 ± 14.14 % and

NesCre^{+}IFNAR$^{flox/flox}$: 9.38 ± 6.57 % and Day 7: Ctrl: 75.00 ± 7.71 % and NesCre^{+}IFNAR$^{flox/flox}$: 15.63 ± 6.57 %) compared to the respective control (Figure 3.2.9B).

To summarize, the observed results revealed an impaired ability to efficiently navigate to the platform location in NesCre$^{+/-}$IFNAR$^{flox/flox}$ mice compared to the respective control which indeed points towards the fact that the expression of type I interferon receptor only on microglial cells in the CNS is not sufficient for normal spatial learning and memory function.

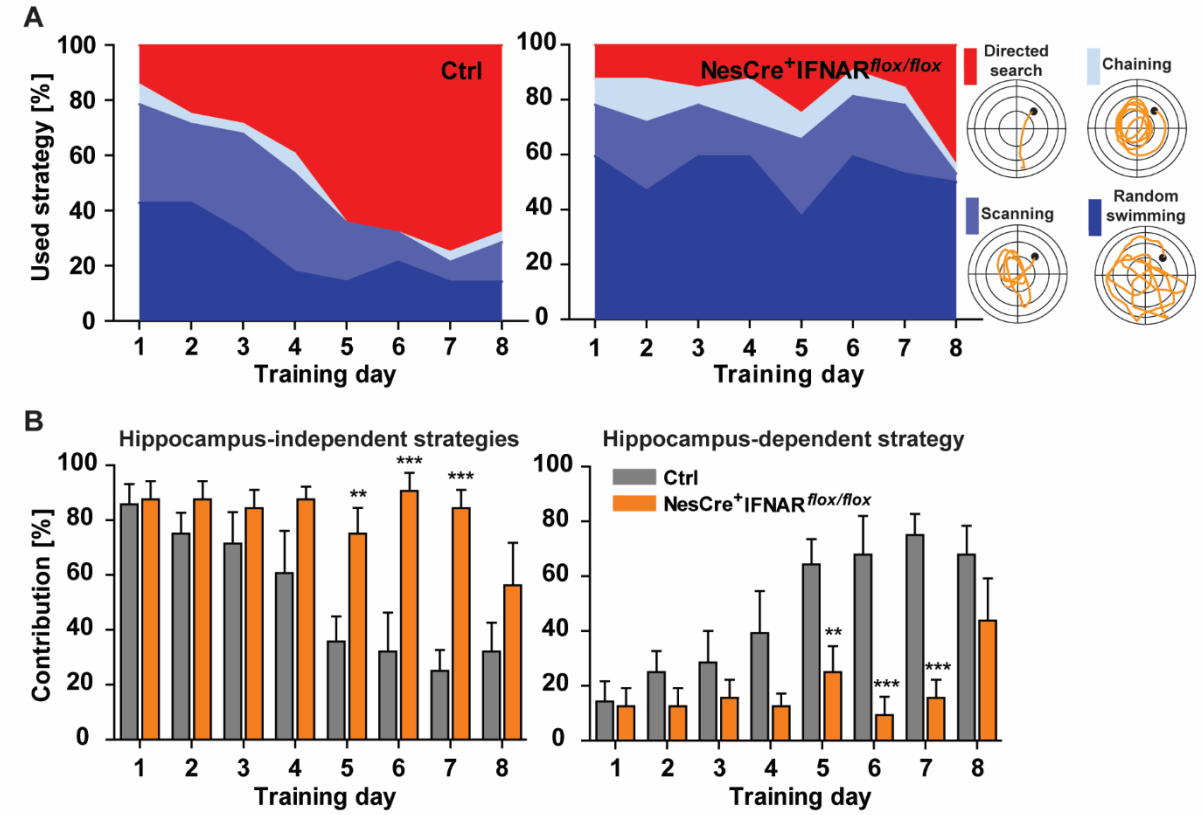

Figure 3.2.9 | Learning strategies used during the Water maze training. (A), **(B)** Hippocampus-independent search strategies were elevated and hippocampus-dependent search strategy was reduced in NesCre$^{+/-}$IFNAR$^{flox/flox}$ mice compared to the respective control animals. Data are presented as mean ± SEM, (n=7-8). ** $p < 0.01$ and *** $p < 0.001$ compared to control.

3.2.2.3. NesCre$^{+/-}$IFNAR$^{flox/flox}$ mice display defects in synaptic plasticity

As the observed results of Morris water maze test revealed a significant impairment in spatial learning ability for NesCre$^{+/-}$IFNAR$^{flox/flox}$ mice, it could be inferred that the presence of type I IFN receptor on neurons, astrocytes and oligodendrocytes is necessary for normal cognitive function but not on microglia. In the next step to evaluate the mechanism underlying these observations, synaptic plasticity was analyzed, which is important for cognitive function, by Dr. Gayane Grigoryan. The fEPSPs were recorded from hippocampal slices of 6 to 8 weeks old NesCre conditional KO and respective control mice. The input-output curve of the dependence of EPSP slope on stimulation intensity did not exhibit any significant difference between NesCre$^{+/-}$IFNAR$^{flox/flox}$ and control mice (Figure 3.2.10A). Therefore it can be concluded that basal synaptic transmission is not affected by the ablation of type I IFN receptor from neurons, astrocytes and oligodendrocytes. For a short-term synaptic plasticity, paired-pulse facilitation of fEPSP to afferent stimulation was examined in hippocampal slices. The paired-pulse facilitation of fEPSP was not affected in hippocampal slices taken from the NesCre conditional KO mice compared to the control (Figure 3.2.10B).

To study the role of type I IFN receptor on neurons, astrocytes and oligodendrocytes in synaptic plasticity, LTP was assessed. The slices taken from NesCre$^{+/-}$IFNAR$^{flox/flox}$ mice showed an impaired LTP compared to respective control as also the mean value of the maintenance phase of LTP ($T_{75\text{-}80}$ min) was significantly reduced in conditional KO mice (1.16 ± 0.01) in comparison to control group (1.47 ± 0.02) (Figure 3.2.10C).

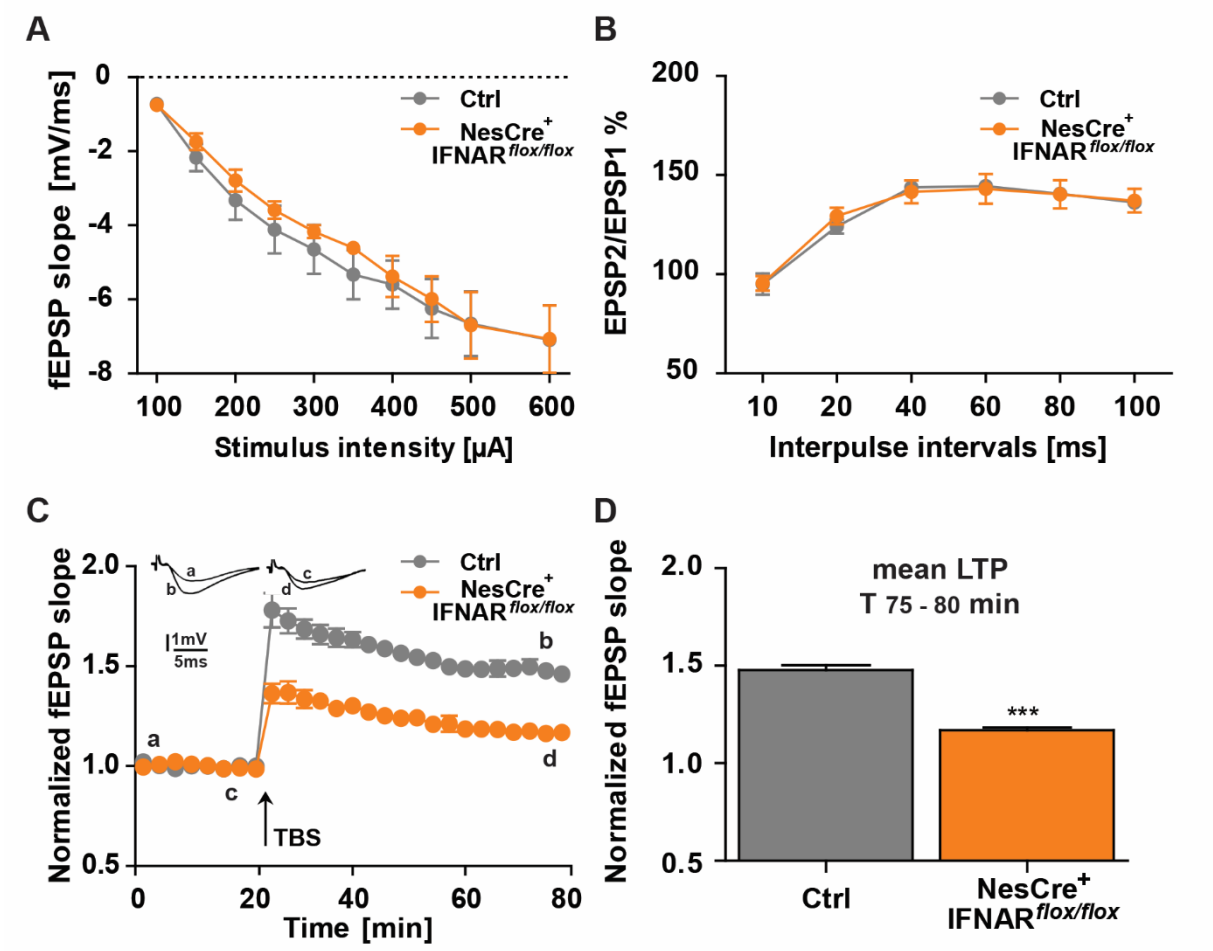

Figure 3.2.10 | Long-term potentiation (LTP) assessment in the hippocampal CA1 subregion of NesCre$^{+/-}$IFNAR$^{flox/flox}$ mice. (A) In the NesCre$^{+/-}$IFNAR$^{flox/flox}$ mice that are missing the type I IFN receptor on neurons, astrocytes and oligodendrocytes, basal synaptic transmission is not altered as can be concluded by comparison of input-output relationship. **(B)** Paired-pulse facilitation on all examined interpulse intervals is not different between NesCre$^{+/-}$IFNAR$^{flox/flox}$ and control mice. **(C)** LTP induced by theta-burst stimulation (TBS, four bursts at 100 Hz repeated 10 times in a 200 ms interval, repeated three times in a 10 seconds interval; denoted with an arrow) is significantly impaired in NesCre$^{+/-}$IFNAR$^{flox/flox}$ mice. **(D)** The difference in mean values (average of last 5 minutes of recordings) of LTP magnitude between control and NesCre$^{+/-}$IFNAR$^{flox/flox}$ mice is shown. Data are presented as mean ± SEM, (n (number of slices) = 22-24 in each group). *** $p < 0.001$ compared to respective control. Dr. Gayane Grigoryan did this experiment.

3.2.2.4. Ablation of type I IFN receptor in NesCre$^{+/-}$IFNAR$^{flox/flox}$ mice alters hippocampal neuron morphology

To reveal the possible cellular mechanism underlying the observed impairment in spatial learning and synaptic plasticity in NesCre conditional KO mice, dendritic

spines were counted separately on apical and basal dendrites of CA1 and CA3 pyramidal neurons as well as on dentate granule cells being located in the superior and inferior blades of the granular cell layer in the hippocampus of NesCre$^{+/-}$ IFNAR$^{flox/flox}$ mice compared to the respective control (Figure 3.2.11). The results of hippocampal neuron morphology assessment indicated a significant reduction in spine density of apical (Δ 13.95%) and basal (Δ 13.32%) dendrites of CA1 pyramidal neurons in NesCre$^{+/-}$IFNAR$^{flox/flox}$ mice compared to control animals (Figure 3.2.11A) whereas the spine density was not changed significantly in apical (Δ 2.92 %) and basal (Δ 1.30 %) dendrites of CA3 pyramidal neurons (Figure 3.2.11B). In addition, the dendritic spine density was reduced in neurons located in the inferior dentate gyrus blade (Δ 8.43%) while the granule cells in the superior dentate gyrus blade (Δ 3.14%) were not affected significantly (Figure 3.2.11C).

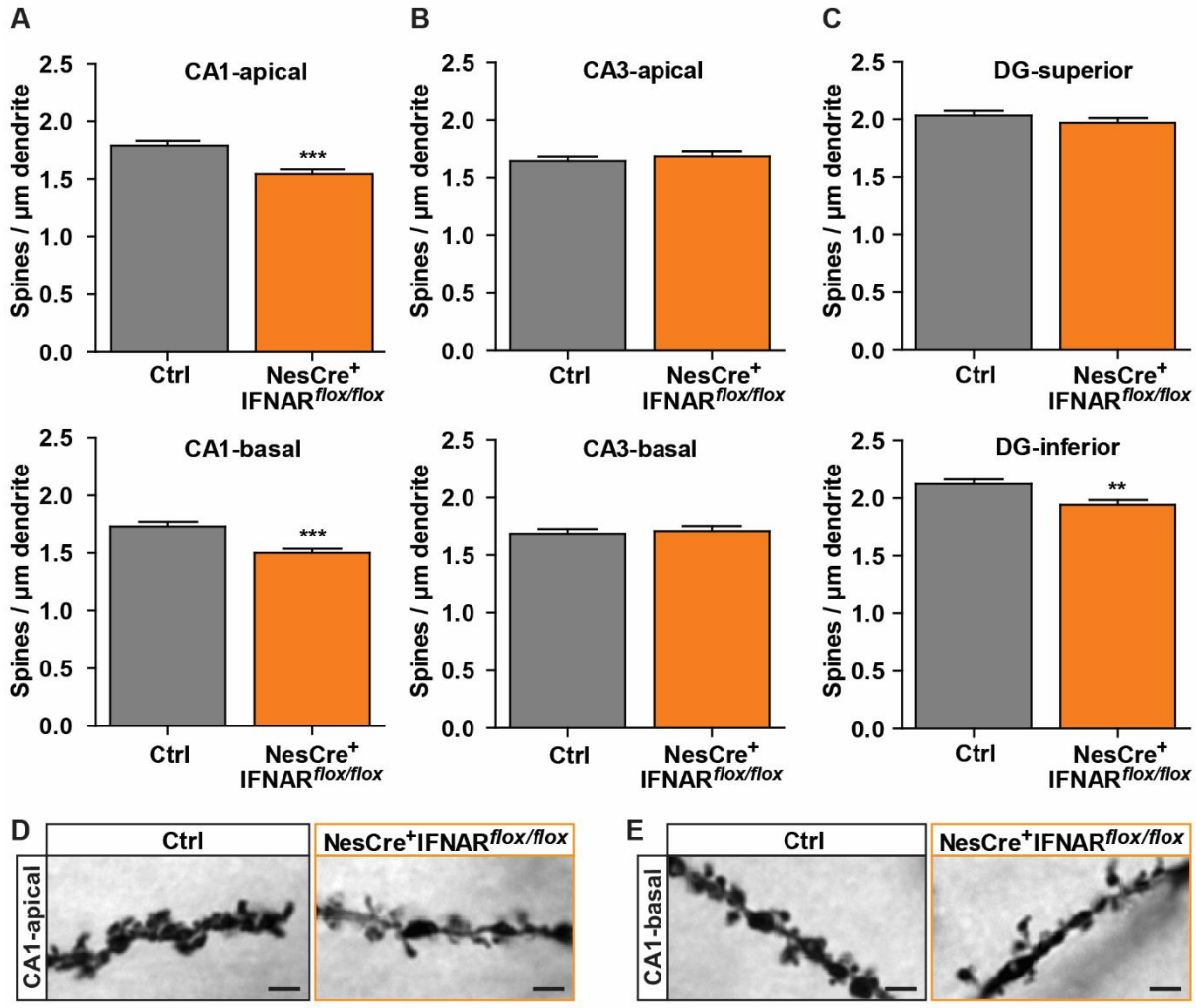

Figure 3.2.11 | Dendritic spine density assessment in hippocampal neurons of NesCre$^{+/-}$ IFNAR$^{flox/flox}$ mice. (A) The spine density of apical and basal dendrites of CA1 hippocampal neurons was decreased in NesCre conditional KO mice compared to the respective control animals. **(B)** The dendritic spine density was not changed in CA3 hippocampal neurons. **(C)** Dendritic spine density of dentate granule cells located in the inferior blade of the granule cell layer was reduced in NesCre$^{+/-}$ IFNAR$^{flox/flox}$ mice compared to control group. **(D)**, **(E)** Representative images of the dendritic spine of hippocampal CA1 neurons in both tested groups (Bar=2 µm, 63X). Data are presented as mean ± SEM (n (number of animals) in each group=4, m (number of dendrites)=40 in each group). ** $p < 0.01$ and *** $p < 0.001$ compared to control.

3.2.2.5. NesCre$^{+/-}$IFNAR$^{flox/flox}$ mice do not show signs of neuroinflammation

As previously described, the activation of microglia is a sign of inflammatory processes in the CNS leading to neuronal damage and synaptic plasticity impairment (Riazi et al., 2015). Like IFNAR$^{-/-}$ mice, NesCre conditional KO mice might be more vulnerable to inflammatory processes as they were devoid of IFNAR on brain cells with neuroectodermal origin. Therefore, microglia density and activation status in the hippocampus of NesCre$^{+/-}$IFNAR$^{flox/flox}$ mice were investigated. For this purpose, IBA-1 positive cells (10 to 15 regions of interest (ROIs) per each group) as well as number of primary processes of IBA-1 positive cells (60 to 90 IBA-1 positive cells per each group) as an activation indicator were counted and analyzed separately in the CA1, CA3 subregions and dentate gyrus at the superior and inferior blade of the granule cell layer (Figure 3.2.12). It is worth noting that a diminished number of primary processes reflects the elevated activity of microglial cells (Papageorgiou et al., 2015). The morphological analysis of microglia cells displayed an unaltered number of microglia and their main processes within all hippocampal subregions of NesCre$^{+/-}$ IFNAR$^{flox/flox}$ mice compared to the respective control group (Figure 3.2.12A,B). Therefore, the impairments in cognitive function, synaptic plasticity and neuronal morphology are not a result of neuroinflammation in NesCre conditional KO mice.

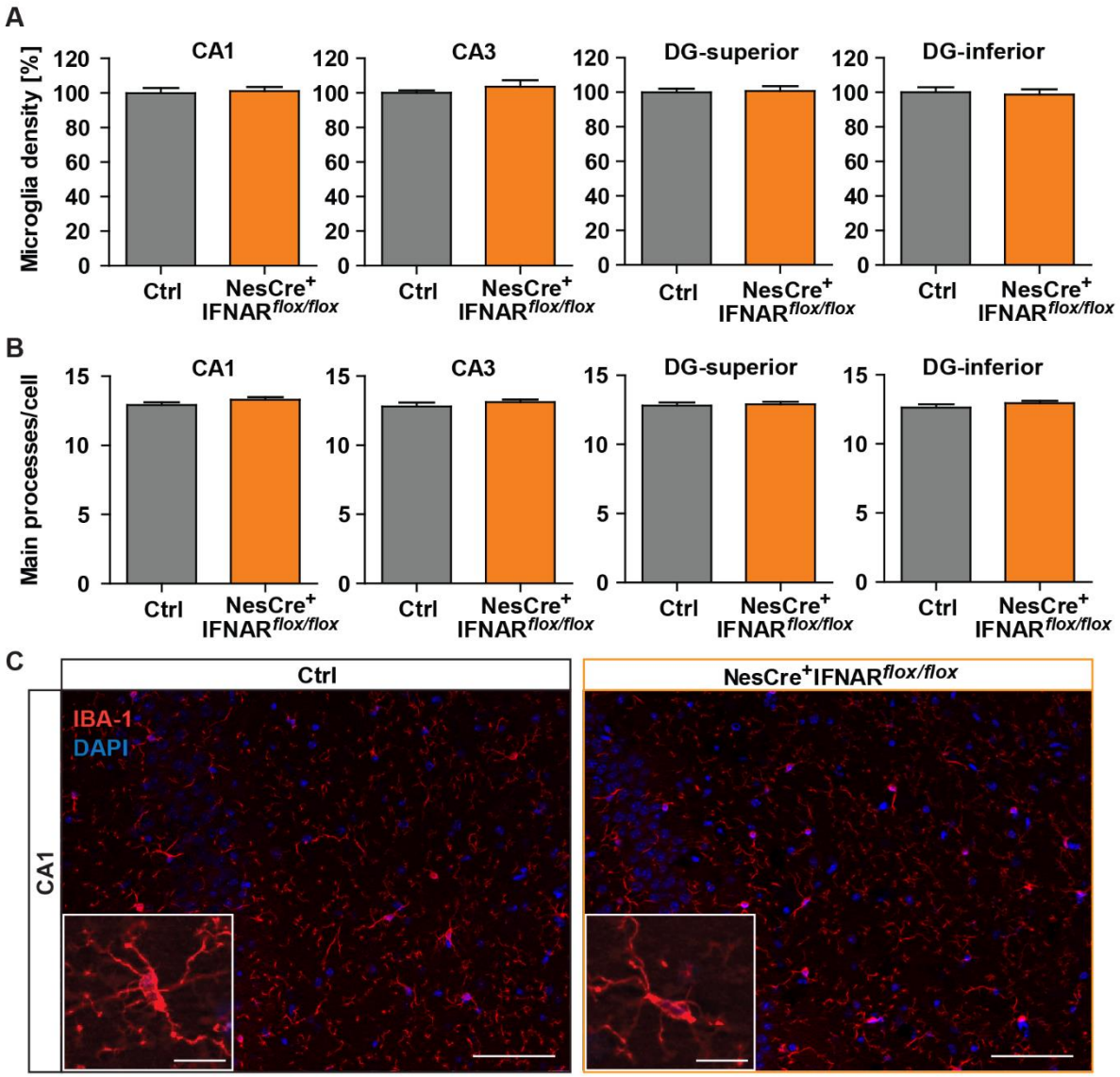

Figure 3.2.12 | Microglia density and morphology assessment in NesCre$^{+/-}$IFNAR$^{flox/flox}$ mice. (A) The microglia density and **(B)** activation status within all hippocampal subregions of NesCre conditional KO mice revealed a phenotype equivalent to the respective control animals. **(C)** Representative examples of IBA-1 immunostaining of CA1 hippocampal subregion in both control and NesCre$^{+/-}$IFNAR$^{flox/flox}$ groups (red is IBA-1 and blue is DAPI staining, Bar=50 µm, Inset frame Bar=10 µm, 20X) Data are presented as mean ± SEM, (Number of animals in each group=2-3, number of ROIs in each group=10-15, number of randomly selected microglia in each group=60-90).

3.2.3. Syn1Cre$^{+/-}$IFNAR$^{flox/flox}$ mice (IFNAR deletion in neurons)

Different types of IFNs are neuromodulators that directly affect synaptic transmission and neuronal functions. Neurons are indeed responsive to IFNs as they express interferon receptors located in both postsynaptic and presynaptic membranes (Vikman et al., 1998; Ignatowski and Spengler, 2008). Nevertheless, the neurophysiological effects of IFNs on synaptic plasticity and brain functions remain sparse. Therefore, to investigate the necessity of neuronal type I IFN signaling in cognitive functions, Syn1Cre$^{+/-}$IFNAR$^{flox/flox}$ mice with type I IFN receptor deletion in neurons were investigated. Briefly, introduction of a Synapsin I promoter driven Cre transgenic mouse strain (Zhu et al., 2001) into the conditional IFNAR background led to an ablation of the IFNAR receptor function in most differentiated neurons (Cre recombinase activity detected in neuronal cells, including brain, spinal cord and dorsal root ganglia (DRGs), as early as embryonic day 12.5, as well as in neurons in adult animals) (Detje, 2015).

3.2.3.1. Locomotor activity is unchanged in Syn1Cre$^{+/-}$IFNAR$^{flox/flox}$ mice

First, to investigate whether the loss of type I IFN receptor on neurons displayed an effect on general locomotor activity and anxiety-like behavior, the Syn1Cre$^{+/-}$IFNAR$^{flox/flox}$ mice were tested in the open field arena for 5 minutes. In this test, the activity of each mouse including the total distance traveled, average speed and time spent in the periphery and center parts of the arena were recorded. The results indicated that deficiency of type I IFN receptor on neurons did not affect exploratory and anxiety-like behaviors as the total distance traveled (Ctrl: 2.76 ± 0.29 m, Syn1Cre$^{+/-}$IFNAR$^{flox/flox}$: 2.48 ± 0.13 m) (Figure 3.2.13A), average speed (Ctrl: 0.009 ± 0.0009 m/s, Syn1Cre$^{+/-}$IFNAR$^{flox/flox}$: 0.008 ± 0.0004 m/s) (Figure 3.2.13B) and general activity in the center and periphery zones of open field arena (Periphery, Ctrl: 84.57 ± 3.27 %, Syn1Cre$^{+/-}$IFNAR$^{flox/flox}$: 75.24 ± 9.57 % - Center, Ctrl: 15.43 ± 3.27 %, Syn1Cre$^{+/-}$IFNAR$^{flox/flox}$: 24.76 ± 9.75 %) (Figure 3.2.13C) were not altered significantly compared to respective control mice (Syn1Cre^{negative}).

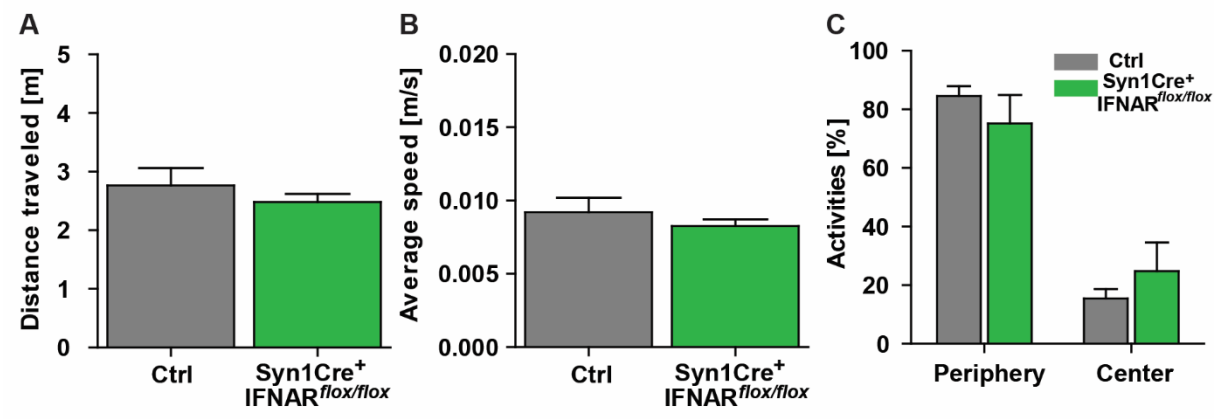

Figure 3.2.13 | General behavioral phenotype in Syn1Cre$^{+/-}$IFNAR$^{flox/flox}$ mice. (A), **(B)** Syn1Cre$^{+/-}$IFNAR$^{flox/flox}$ mice showed an equivalent phenotype of total distance traveled and average speed compared to respective control animals. **(C)** The percent time spent of Syn1Cre$^{+/-}$IFNAR$^{flox/flox}$ mice in the periphery and center part of open field arena did not show any significant differences in comparison to control group. Syn1Cre$^{+/-}$IFNAR$^{flox/flox}$ mice did not display the signs of hyperactivity and anxiety-like behavior. Data are presented as mean ± SEM, (n=6-7).

3.2.3.2. Syn1Cre$^{+/-}$IFNAR$^{flox/flox}$ mice do not exhibit impaired spatial learning and memory

As it was already mentioned, the elimination of type I IFN receptor in conventional IFNAR$^{-/-}$ and conditional NesCre$^{+/-}$IFNAR$^{flox/flox}$ mice led to spatial memory impairment. Therefore, to identify the physiologically important cell types involved in type I IFN-induced signaling under physiological conditions for cognitive function, 6 to 8 weeks old Syn1Cre$^{+/-}$IFNAR$^{flox/flox}$ mice were examined in the Morris water maze task. The analysis revealed that in both Syn1Cre$^{+/-}$IFNAR$^{flox/flox}$ and respective control mice the swim distance (Repeated measure ANOVA: F_{Ctrl} (7, 40) = 2.307, $p < 0.05$ and $F_{Syn1Cre^{+}IFNAR^{flox/flox}}$ (7, 40) = 5.828, $p < 0.01$) and escape latency (Repeated measure ANOVA: F_{Ctrl} (7, 40) = 2.880, $p < 0.05$ and $F_{Syn1Cre^{+}IFNAR^{flox/flox}}$ (7, 40) = 3.334, $p < 0.01$) decreased significantly over 8 training days. Furthermore, both Syn1Cre$^{+/-}$IFNAR$^{flox/flox}$ and respective control mice exhibited similar swim distances ($F_{Treatment}$ (1, 80) = 3.096, $p = 0.0823$) and escape latencies ($F_{Treatment}$ (1, 80) = 3.920, $p = 0.0512$) to reach the hidden platform with daily training (Figure 3.2.14A,B), suggesting no impairments in spatial learning and memory. In the probe trial tests on the day 6 and on the day 9, both tested groups spent significantly more time in the target quadrant than the other quadrants, indicating no impairment in memory retrieval. No

significant differences were observed in the time which spent in target quadrant between Syn1Cre$^{+/-}$IFNAR$^{flox/flox}$ and respective control animals (Figure 3.2.14C).

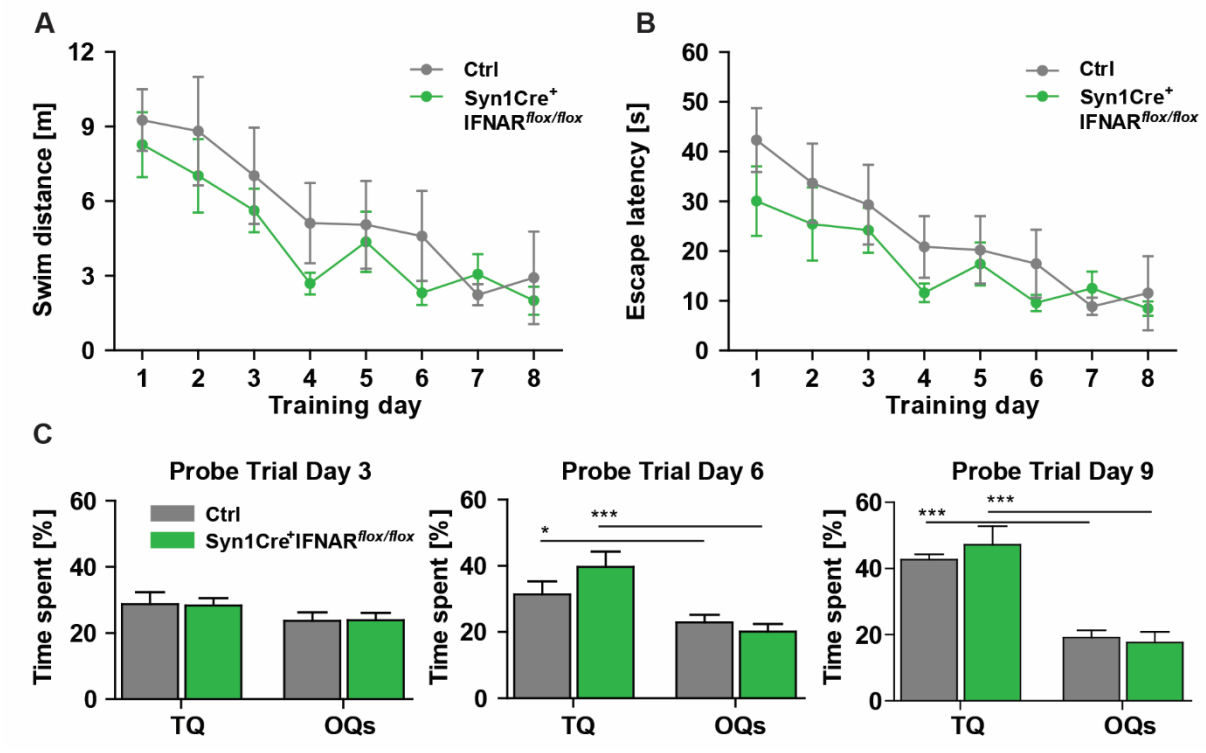

Figure 3.2.14 | Spatial learning and memory assessment in Syn1Cre$^{+/-}$IFNAR$^{flox/flox}$ mice. (A) Syn1Cre$^{+/-}$IFNAR$^{flox/flox}$ mice showed similar swim distance and **(B)** escape latency in comparison to the respective control animals. **(C)** The time spent percentage in the target quadrant (TQ) compared to the mean time spent in other quadrants (OQs) without the platform on the days 3, 6 and 9 is shown. On the day 6 and day 9 of probe trial tests, both conditional KO and respective control mice spent significantly more time in target quadrant. Data are presented as mean ± SEM (n=6). * $p < 0.05$ and *** $p < 0.001$ compared to OQs.

Subsequently, also the evaluation of the respective search strategies displayed no impairments in spatial learning for Syn1Cre$^{+/-}$IFNAR$^{flox/flox}$ and control groups (Figure 3.2.15). In both tested groups during the 8 days of acquisition training hippocampus-independent search strategies including random swimming, scanning and chaining decreased over time while directed search as a hippocampus-dependent search strategy increased (Figure 3.2.15A,B). Taken together, the ablation of type I IFN receptor from neurons was not sufficient to impair spatial learning and memory function in Syn1Cre$^{+/-}$IFNAR$^{flox/flox}$ mice compared to respective control.

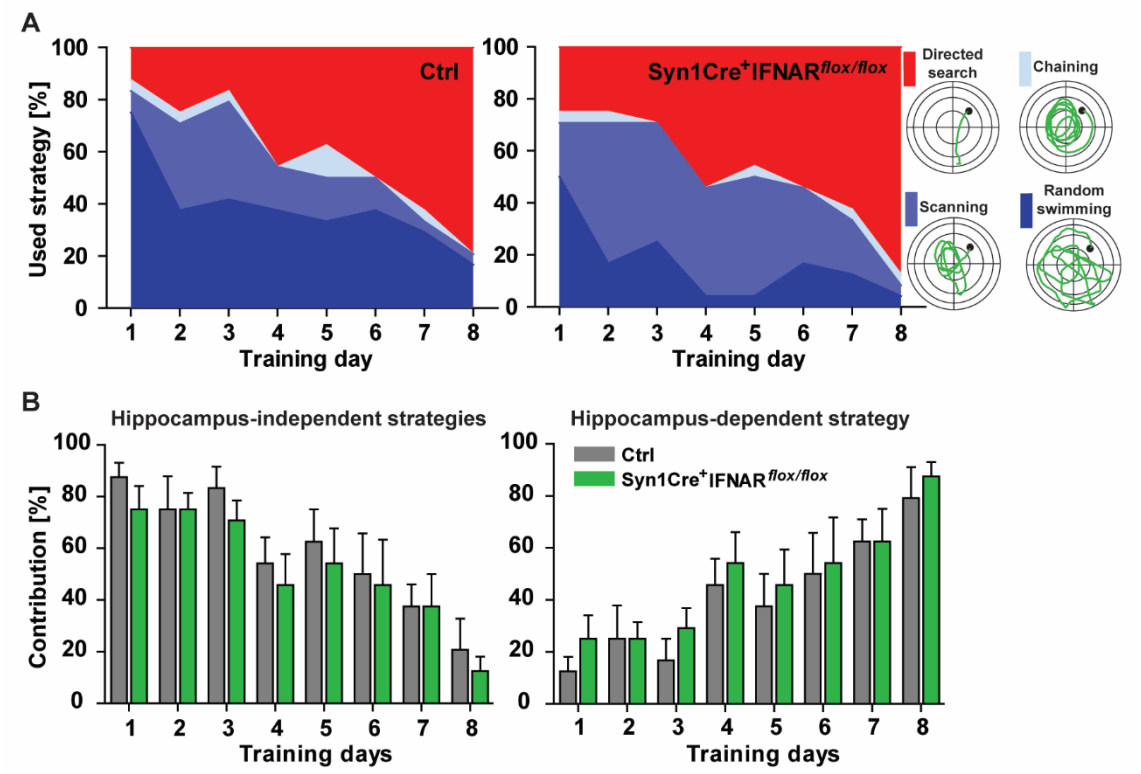

Figure 3.2.15 | Learning strategies used during the Water maze training. (A), (B) The used hippocampus-independent and dependent search strategies did not changed in Syn1Cre$^{+/-}$IFNAR$^{flox/flox}$ mice compared to respective control animals. Data are presented as mean ± SEM (n=6).

3.2.3.3. Syn1Cre$^{+/-}$IFNAR$^{flox/flox}$ mice do not show defects in synaptic plasticity

The behavioral assessments already revealed no significant differences because of the neuronal type I IFN receptor deficiency. Then in the next step, to examine the importance of neuronal type I IFN signaling in activity-dependent synaptic plasticity processes at the cellular level, the electrophysiological experiments were performed by Dr. Gayane Grigoryan. Synaptic plasticity was assessed at the CA3 - CA1 neural pathway as described above in Syn1Cre$^{+/-}$IFNAR$^{flox/flox}$ and respective control mice. First, the input-output strength at a defined stimulus intensity in both tested groups was measured. No significant difference of fEPSP slope size was detected in Syn1Cre$^{+/-}$IFNAR$^{flox/flox}$ mice compared to respective control animals (Figure 3.2.16A). In addition, the investigation of the presynaptic function by paired pulse facilitation (PPF) showed no differences between the two tested groups (Figure 3.2.16B). The slices taken from Syn1Cre$^{+/-}$IFNAR$^{flox/flox}$ mice had no detectable deficit in hippocampal LTP compared to control group. The mean value of the maintenance

phase of LTP (T $_{75\text{-}80}$ min) was comparable between both conditional SynCre KO mice (1.51 ± 0.01) and respective control animals (1.57 ± 0.01) (Figure 3.2.16C).

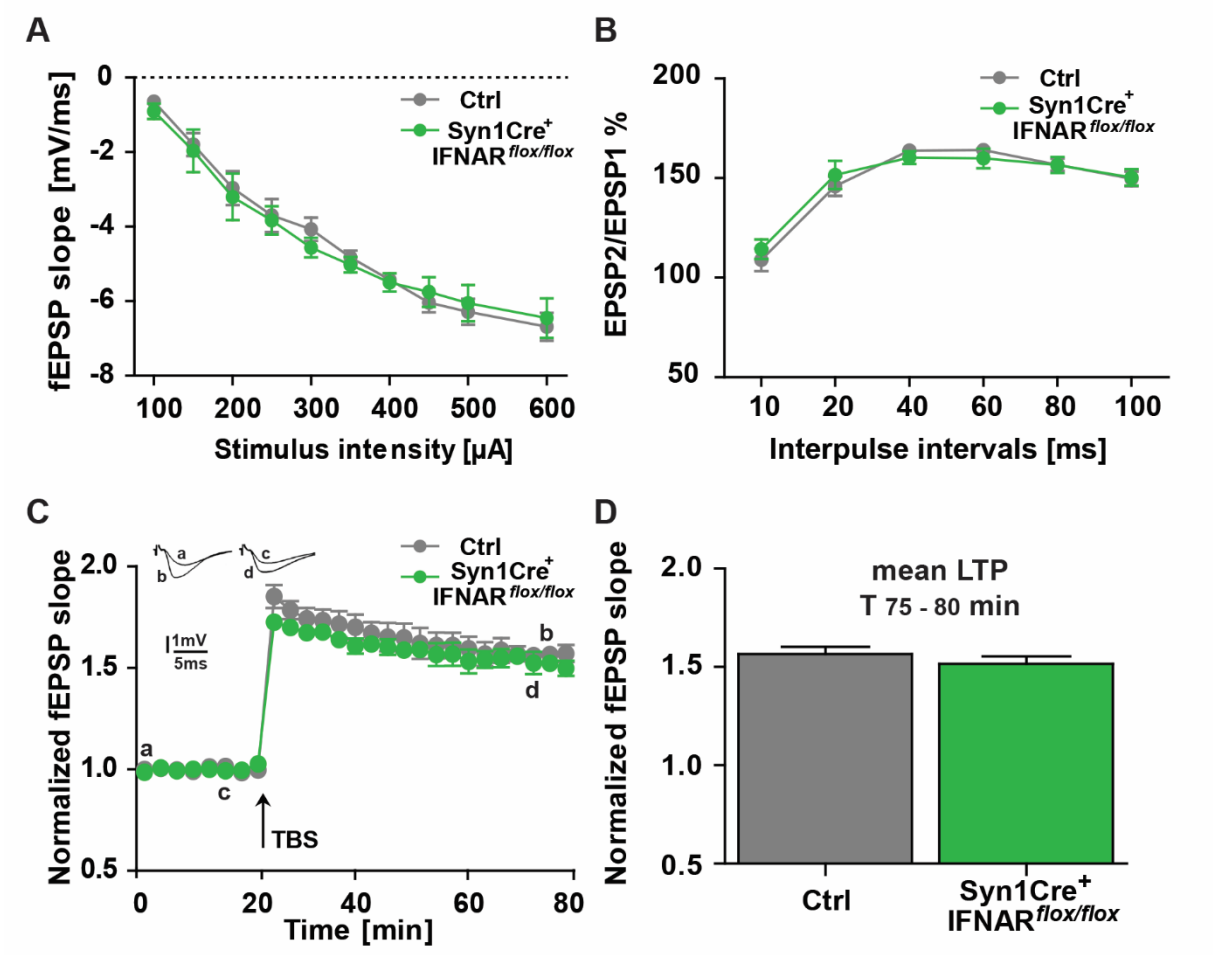

Figure 3.2.16 | Long-term potentiation (LTP) assessment in the hippocampal CA1 subregion of Syn1Cre$^{+/-}$IFNAR$^{flox/flox}$ mice. (A) Syn1Cre$^{+/-}$IFNAR$^{flox/flox}$ and respective control mice did not differ in the properties of basal synaptic transmission, and **(B)** ratios of pared-pulse facilitation **(C)**, as well as, they exhibit the same magnitude of LTP in response to strong afferent stimulation. (LTP induced by theta-burst stimulation (TBS, four bursts at 100 Hz repeated 10 times in a 200 ms interval, repeated three times in a 10 seconds interval; denoted with an arrow)). **(D)** Comparison of mean values (average of last 5 minutes of recordings) LTP magnitude in Syn1Cre$^{+/-}$IFNAR$^{flox/flox}$ and control mice summarized as bar graphs. No statistically significant difference between both tested groups was found. Data are presented as mean ± SEM (n (number of slices) = 13-15 in each group). Dr. Gayane Grigoryan did this experiment.

3.2.2.4. Ablation of type I IFN receptor in Syn1Cre$^{+/-}$IFNAR$^{flox/flox}$ mice do not alter hippocampal neuron morphology

To evaluate the physiological importance of type I IFN receptor signaling on neurons, spine density of hippocampal neurons on apical and basal dendrites of CA1 and CA3 pyramidal neurons as well as on dentate granule cells being located in the superior and inferior blades of the granular cell layer was assessed (Figure 3.2.17). No significant changes in all hippocampal subregions were detected among both tested groups (Figure 3.2.17) pointing out type I IFN receptor deficiency on neurons might not affect dendritic spine density.

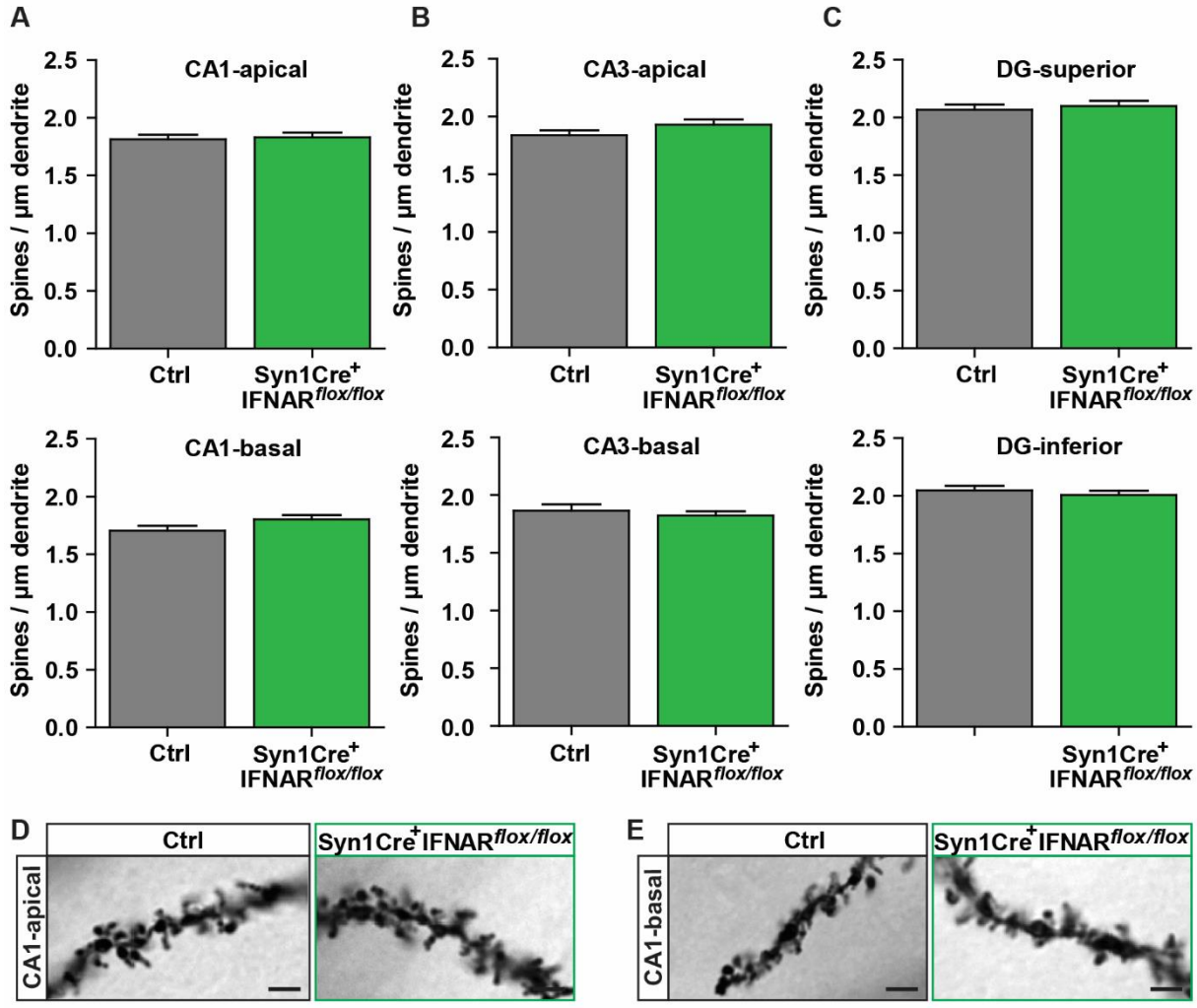

Figure 3.2.17 | Dendritic spine density assessment in hippocampal neurons of Syn1Cre$^{+/-}$ IFNAR$^{flox/flox}$ mice. (A), **(B)**, **(C)** The dendritic spine density of neurons in the different hippocampal subregions were not changed in conditional Syn1Cre$^{+/-}$IFNAR$^{flox/flox}$ KO mice compared to respective control animals. **(D)**, **(E)** Representative images of dendritic spines of hippocampal CA1 neurons in

both tested groups (Bar=2µm, 63X). Data are presented as mean ± SEM, (n (number of animals) in each group = 4, m (number of dendrites) = 40 in each group).

3.2.4. GFAPCre$^{+/-}$IFNAR$^{flox/flox}$ mice (IFNAR deletion in astrocytes)

Astrocytes are the major population of glial cells in the CNS responsible for the maintenance of CNS homeostasis. However, under pathological conditions, they can act as immune cells as well. For instance, astrocytes can produce a large amount of both IFN-α and IFN-β following viral infection (Owens et al., 2014). They express IFNAR and act as important responders to type I IFNs in the CNS (Khorooshi and Owens, 2010). On the other hand, under physiological conditions IFNs act as neuromodulators which affect synaptic transmission and function directly (Ignatowski and Spengler, 2008). The results described above obtained in different conditional IFNAR KO mouse lines revealed that ablation of type I IFN signaling in all cells but not microglia led to an impairment in cognitive function and synaptic plasticity, indicating the importance of IFNAR for the function of the adult, healthy brain. Furthermore, it became clear that IFNAR signaling directly on neurons does not play a role in these processes indicating IFNAR signaling through astrocytes might be essential for cognitive functions.

As a next step, therefore, GFAPCre$^{+/-}$IFNAR$^{flox/flox}$ mice with type I IFN receptor deletion in astrocytes were investigated (Cre recombinase activity is targeted to most astrocytes throughout the healthy brain and spinal cord as early as embryonic day 12.5) (Detje, 2015).

3.2.4.1. Locomotor activity is unaltered in GFAPCre$^{+/-}$IFNAR$^{flox/flox}$ mice

To define the effect of astrocytic type I IFN receptor deficiency on general locomotor activity and anxiety-like behavior, the GFAPCre$^{+/-}$IFNAR$^{flox/flox}$ mice were tested in the open field arena. The findings did not show any significant differences in total distance traveled (Ctrl: 2.68 ± 0.1 m, GFAPCre$^{+/-}$IFNAR$^{flox/flox}$: 2.25 ± 0.21 m) (Figure 3.2.18A), average speed (Ctrl: 0.008 ± 0.0003 m/s, GFAPCre$^{+/-}$IFNAR$^{flox/flox}$: 0.007 ± 0.0007 m/s) (Figure 3.2.18B) and general activity in the center and border of the open field arena (Periphery, Ctrl: 75.58 ± 5.9 %, GFAPCre$^{+/-}$IFNAR$^{flox/flox}$: 88.09 ± 4.12 % - Center, Ctrl: 24.41 ± 5.9 %, GFAPCre$^{+/-}$IFNAR$^{flox/flox}$: 11.90 ± 4.12 %) (Figure 3.2.18C)

between GFAPCre$^{+/-}$IFNAR$^{flox/flox}$ mice and respective control animals (GFAPCre^{negative}).

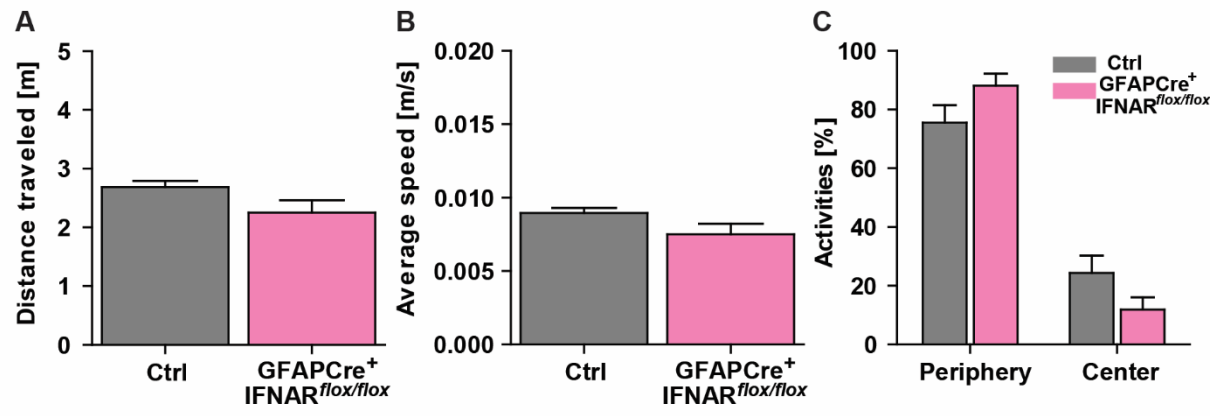

Figure 3.2.18 | General behavioral phenotype in GFAPCre$^{+/-}$IFNAR$^{flox/flox}$ mice. GFAPCre$^{+/-}$IFNAR$^{flox/flox}$ mice showed similar **(A)** total distance traveled, **(B)** average speed and **(C)** time spent in the periphery and center zones of open field arena compared to respective control mice. GFAPCre$^{+/-}$IFNAR$^{flox/flox}$ mice did not display the signs of hyperactivity and anxiety-like behavior. Data are presented as mean ± SEM, (n=6-7).

3.2.4.2. GFAPCre$^{+/-}$IFNAR$^{flox/flox}$ mice show an impairment in spatial memory formation

GFAPCre$^{+/-}$IFNAR$^{flox/flox}$ mice were tested in the Morris water maze test. The results of this test indicated that swim distance and escape latency were reduced in control group significantly throughout the daily acquisition training while this reduction could not be observed for GFAPCre$^{+/-}$IFNAR$^{flox/flox}$ mice (Repeated measure ANOVA: Swim distance - F_{Ctrl} (7, 48) = 12.47, $p < 0.001$ and $F_{GFAPCre^{+}IFNAR^{flox/flox}}$ (7, 48) = 1.24, $p = 0.29$, Escape latency - F_{Ctrl} (7, 48) = 13.15, $p < 0.001$ and $F_{GFAPCre^{+}IFNAR^{flox/flox}}$ (7, 48) = 0.44, $p = 0.86$).

In addition GFAPCre$^{+/-}$IFNAR$^{flox/flox}$ mice displayed a significantly elevated swim distance ($F_{Treatment}$ (1, 96) = 22, $p < 0.001$) and escape latency ($F_{Treatment}$ (1, 96) = 36.10, $p < 0.001$) compared to respective control animals (Figure 3.2.20A,B). In order to assess reference memory in the three probe trial tests of the Morris water maze task, the observations showed that on days 6 and 9 of probe trial tests, respective control mice spent significantly more time in the target quadrant compared to the time spent in the other quadrants (Figure 3.2.20C) while this was not the case for the conditional KO mice. Furthermore, on probe trial day 9, the time spent by control mice

in the target quadrant was nearly 48.48 ± 3.78 % whereas for conditional GFAPCre KO mice was around 31.09 ± 6.58 % which was significantly less than the control group (Figure 3.2.20C).

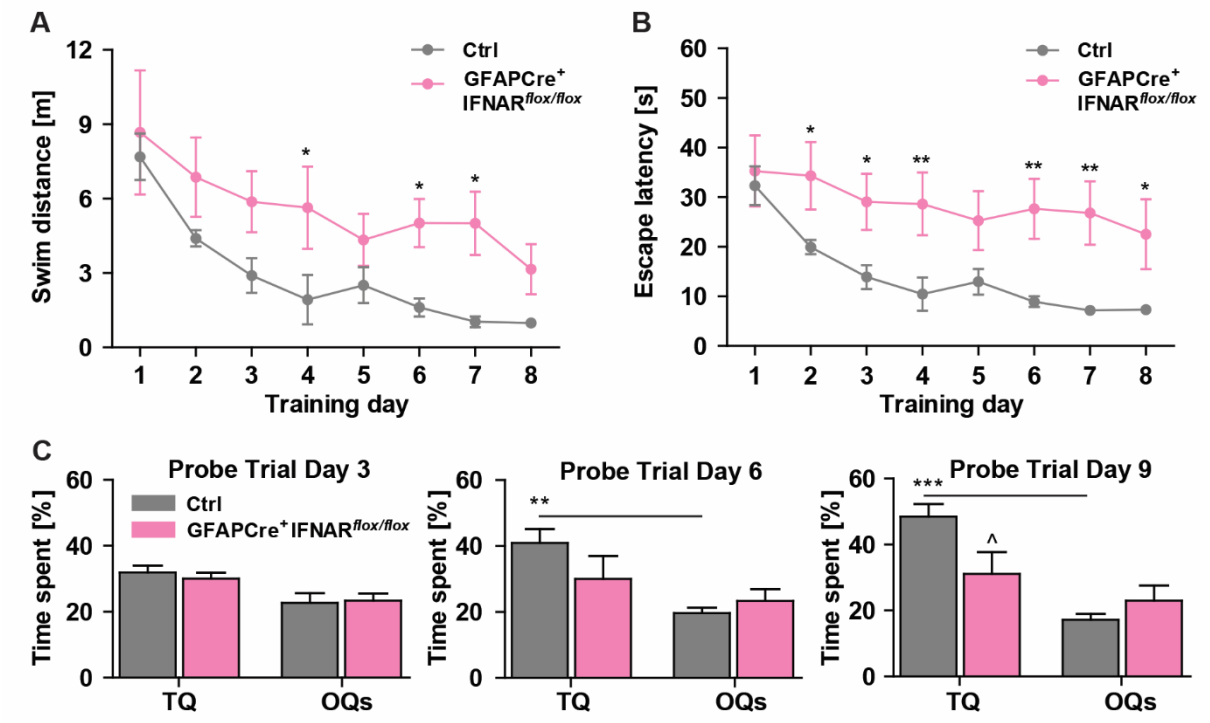

Figure 3.2.20 | Spatial learning and memory assessment in GFAPCre$^{+/-}$IFNAR$^{flox/flox}$ mice. GFAPCre$^{+/-}$IFNAR$^{flox/flox}$ mice exhibited **(A)** a significant higher swim distance and **(B)** escape latency than the respective control animals. **(C)** Percent time spent in the target quadrant (TQ) in comparison to the average time spent in the other quadrants (OQs) without the platform on days 3, 6 and 9 is presented. On days 6 and 9 of probe trial tests only control mice spent more time in target quadrant significantly. Data are presented as mean ± SEM, (n=7). * $p < 0.05$, ** $p < 0.01$ and *** $p < 0.001$ compared to control, ** $p < 0.05$ and *** $p < 0.01$ compared to OQs, ^ $p < 0.05$ compared to the time spent in TQ by respective control animals.

The analysis of the search strategies revealed an elevated contribution of directed search in the control group over the 8 days of training while the contribution of random swimming decreased. These changes did not occur in GFAPCre$^{+/-}$IFNAR$^{flox/flox}$ mice (Figure 3.2.21A). In addition, GFAPCre$^{+/-}$IFNAR$^{flox/flox}$ mice utilized significantly more hippocampus-independent search strategies (Day 4: Ctrl: 25 ± 13.36 % and GFAPCre^{+}IFNAR$^{flox/flox}$: 78.57 ± 8.50, Day 6: Ctrl: 39.29 ± 12.02 % and GFAPCre^{+}IFNAR$^{flox/flox}$: 71.43 ± 8.50 %, Day 7: Ctrl: 14.29 ± 10.71 % and

GFAPCre^{+}IFNAR$^{flox/flox}$: 67.86 ± 13.04 % and Day 8: Ctrl: 17.86 ± 7.14 % and GFAPCre^{+}IFNAR$^{flox/flox}$: 64.29 ± 14.29 %) and less hippocampus-dependent search (Day 4: Ctrl: 75 ± 13.36 % and GFAPCre^{+}IFNAR$^{flox/flox}$: 21.43 ± 8.50, Day 6: Ctrl: 60.71 ± 12.02 % and GFAPCre^{+}IFNAR$^{flox/flox}$: 28.57 ± 8.50 %, Day 7: Ctrl: 85.71 ± 10.71 % and GFAPCre^{+}IFNAR$^{flox/flox}$: 32.14 ± 13.04 % and Day 8: Ctrl: 82.14 ± 7.14 % and GFAPCre^{+}IFNAR$^{flox/flox}$: 35.71 ± 14.29 %) compared to respective control animals (Figure 3.2.21B).

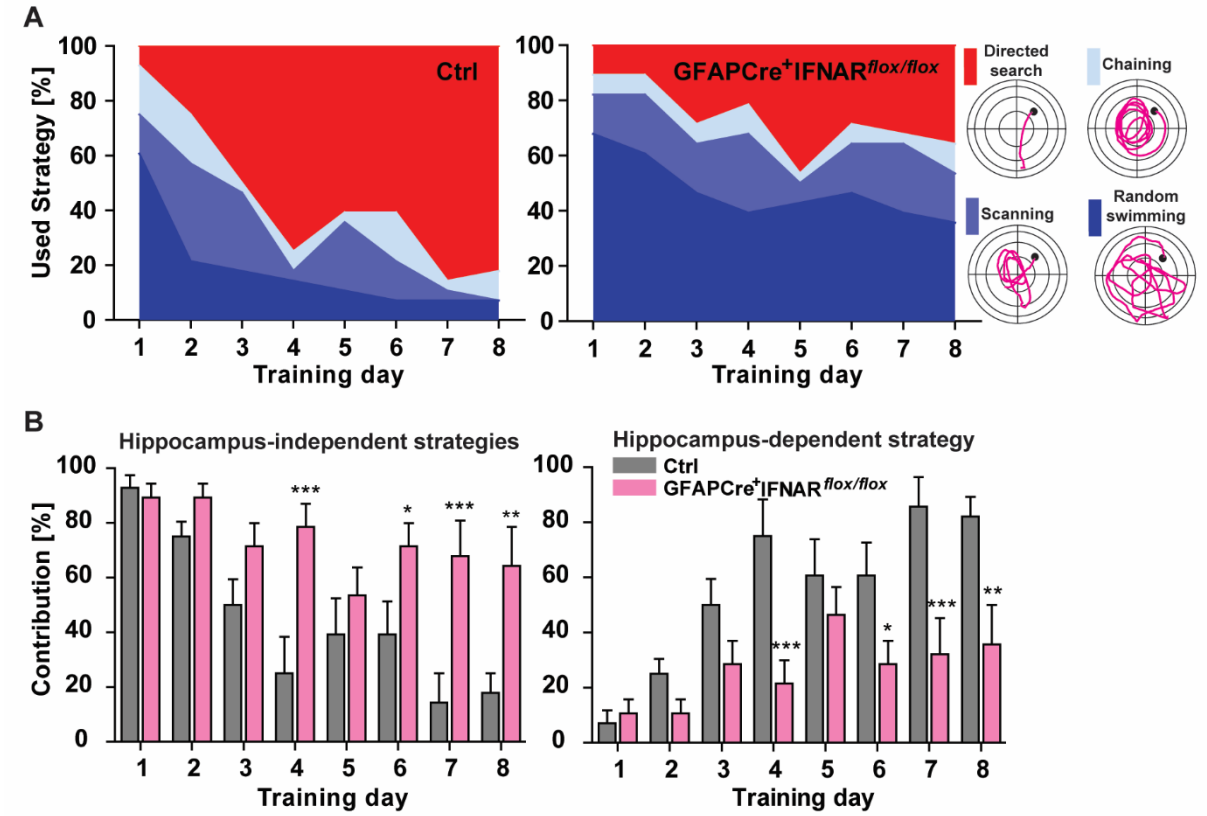

Figure 3.2.21 | Learning strategies used during the Water maze training. (A), **(B)** The used hippocampus-independent search strategies were increased and hippocampus-dependent search strategy was decreased in GFAPCre$^{+/-}$IFNAR$^{flox/flox}$ mice compared to respective control animals. Data are presented as mean ± SEM, (n=7). * $p < 0.05$, ** $p < 0.01$ and *** $p < 0.001$ compared to control.

3.2.4.3. GFAPCre$^{+/-}$IFNAR$^{flox/flox}$ mice exhibit impaired synaptic plasticity

Again, as for the other conventional and conditional KO lines, Dr. Gayane Grigoryan performed electrophysiological recordings. The fEPSPs were assessed from hippocampal slices of 6-8 weeks old obtained from GFAPCre$^{+/-}$IFNAR$^{flox/flox}$ and respective control mice. The input-output curve of the dependence of EPSP slope on stimulation intensity which is indicating the basal synaptic transmission was not

altered significantly in GFAPCre$^{+/-}$IFNAR$^{flox/flox}$ mice compared to control group (Figure 3.2.22A). The paired-pulse facilitation of fEPSP as well was not affected in conditional KO mice in comparison to control animals (Figure 3.2.22B). The slices derived from GFAPCre$^{+/-}$IFNAR$^{flox/flox}$ mice exhibited a defect in LTP compared to respective control mice as a reduced mean value of the maintenance phase of LTP ($T_{75\text{-}80}$ min) in conditional GFAPCre KO mice (1.25 ± 0.01) was observed compared to control group (1.48 ± 0.007) (Figure 3.2.22C).

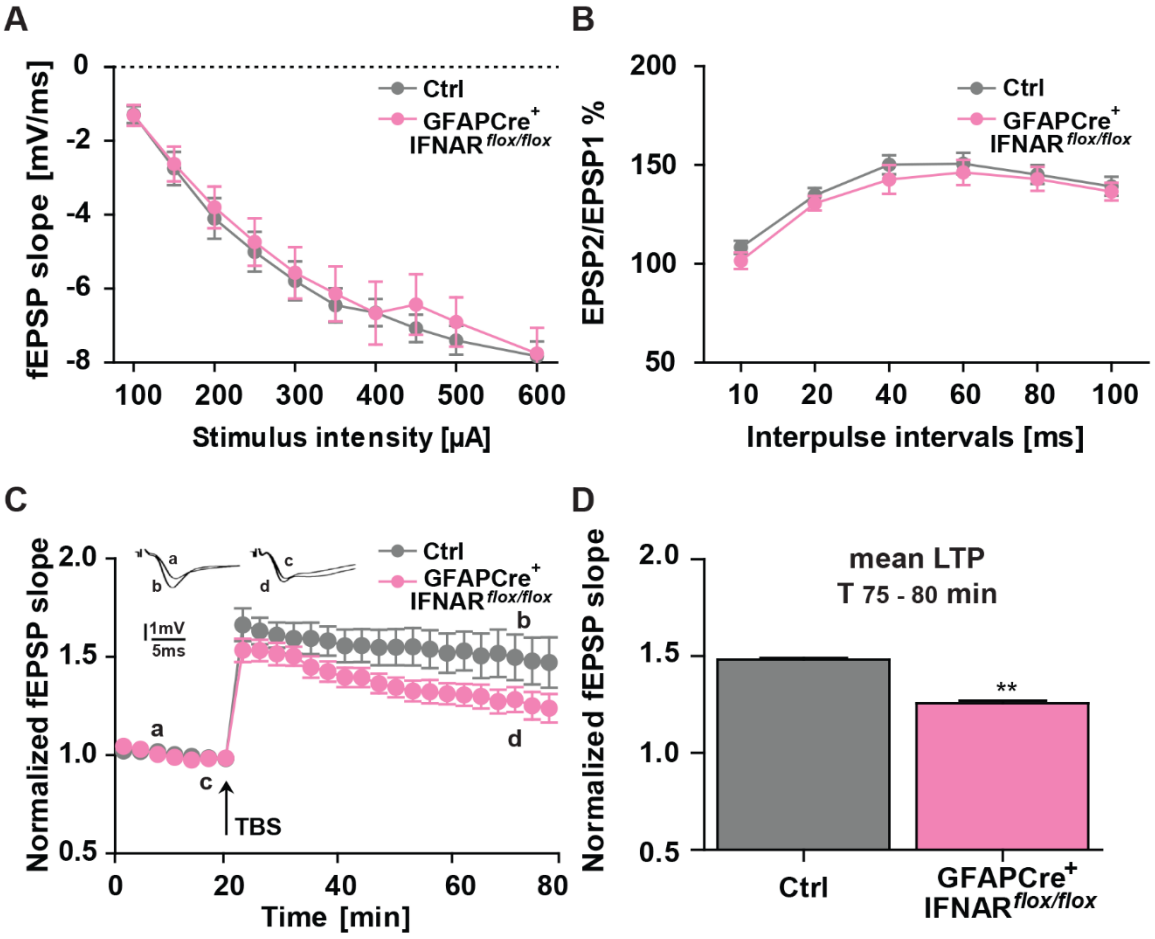

Figure 3.2.22 | Long-term potentiation (LTP) assessment in the hippocampal CA1 subregion of GAPCre$^{+/-}$IFNAR$^{flox/flox}$ mice. (A) In GFAPCre$^{+/-}$IFNAR$^{flox/flox}$ mice, the basal synaptic transmission was not altered as can be concluded by comparison of input-output relationship. **(B)** Paired-pulse facilitation on all examined interpulse intervals was not different between GFAPCre$^{+/-}$IFNAR$^{flox/flox}$ and control mice. **(C)** LTP induced by theta-burst stimulation (TBS, four bursts at 100 Hz repeated 10 times in a 200 ms interval, repeated three times in a 10 seconds interval; denoted with an arrow) was significantly impaired in GFAPCre$^{+/-}$IFNAR$^{flox/flox}$ mice. **(D)** The difference in mean values (average of last 5 minutes of recordings) of LTP magnitude between control and GFAPCre$^{+/-}$IFNAR$^{flox/flox}$ mice is shown. Data are presented as mean ± SEM, (n (number of slices) = 17 in each group). ** $p < 0.001$ compared to respective control.

3.2.4.4. Ablation of type I IFN receptor from astrocytes in GFAPCre$^{+/-}$ IFNAR$^{flox/flox}$ mice alters hippocampal neuron morphology

To investigate the possible cellular mechanism underlying the observed impaired spatial learning and synaptic plasticity function in GFAPCre$^{+/-}$IFNAR$^{flox/flox}$ mice, dendritic spines were counted separately on apical and basal dendrites of CA1 and CA3 pyramidal neurons as well as on dentate granule cells being located in the superior and inferior blade of the granule cell layer in the hippocampus of 6 to 8 weeks old GFAPCre$^{+/-}$IFNAR$^{flox/flox}$ mice compared to respective control group (Figure 3.2.23). A significant reduction in spine density of apical (CA1: Δ 14.83%, CA3: Δ 9.24%) and basal (CA1: Δ 12.61%, CA3: 12.77%) dendrites of CA1 and CA3 pyramidal neurons (Figure 3.2.23A,B) and granule cells located in the superior (Δ 6.53%) and inferior dentate gyrus blade (Δ 8.30%) (Figure 3.2.23C) in GFAPCre$^{+/-}$ IFNAR$^{flox/flox}$ mice compared to the respective control animals could be observed.

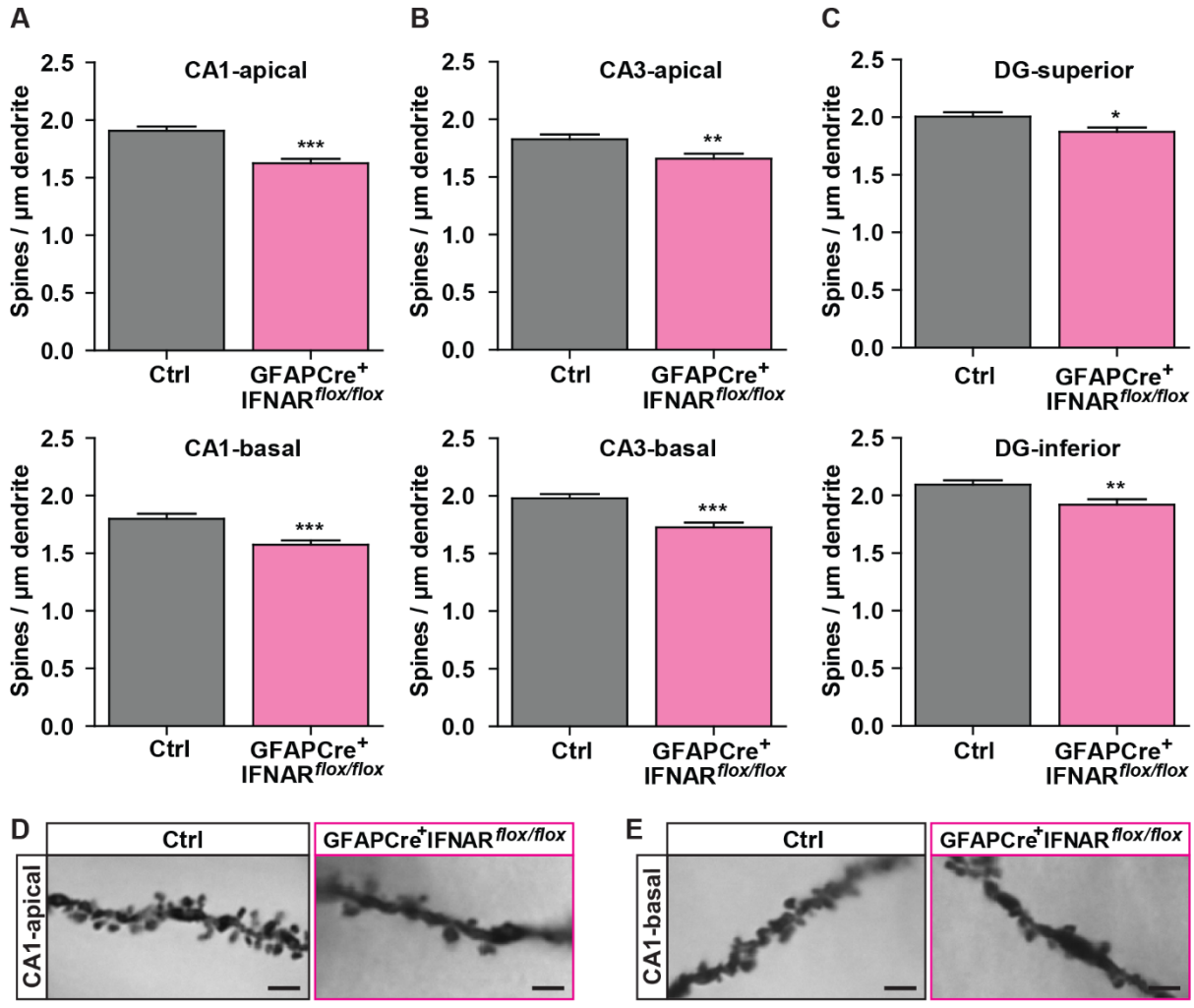

Figure 3.2.23 | Dendritic spine density assessment in hippocampal neurons of GFAPCre$^{+/-}$ IFNAR$^{flox/flox}$ mice. (A), **(B)** The spine density of apical and basal dendrites of CA1 and CA3 pyramidal hippocampal neurons were reduced in conditional KO mice compared to respective control group. **(C)** Dendritic spine density of dentate granular cells located in the superior and inferior blades of the granule cell layer was diminished in GFAPCre$^{+/-}$IFNAR$^{flox/flox}$ mice compared to respective control animals. **(D)**, **(E)** Representative images of dendritic spines of hippocampal CA1 neurons in both tested groups (Bar=2 µm, 63X). Data are presented as mean ± SEM (n (number of animals) in each group = 4, m (number of dendrites) = 40 in each group). * $p < 0.05$, ** $p < 0.01$ and *** $p < 0.001$ compared to control.

3.2.4.5. GFAPCre$^{+/-}$IFNAR$^{flox/flox}$ mice do not display signs of neuroinflammation

Again as for the other tested groups, GFAPCre conditional KO mice might be more sensitive to inflammatory processes in the CNS as they were devoid of IFNAR on astrocytes. Therefore, microglia density and activation status in the hippocampus of these mice were investigated. For this purpose, IBA-1 positive cells (in 20 regions of interest (ROIs) per each group) as well as the number of main processes of IBA-1 positive cells (120 IBA-1 positive cells per each group) were counted and analyzed separately in the CA1, CA3 region and DG superior and inferior blades of the granule cell layer of the hippocampus (Figure 3.2.24). The observations of morphological analysis of microglial cells revealed a similar number of microglia and their primary processes within all hippocampal subregions of GFAPCre$^{+/-}$IFNAR$^{flox/flox}$ in comparison to respective control mice (Figure 3.2.24A,B).

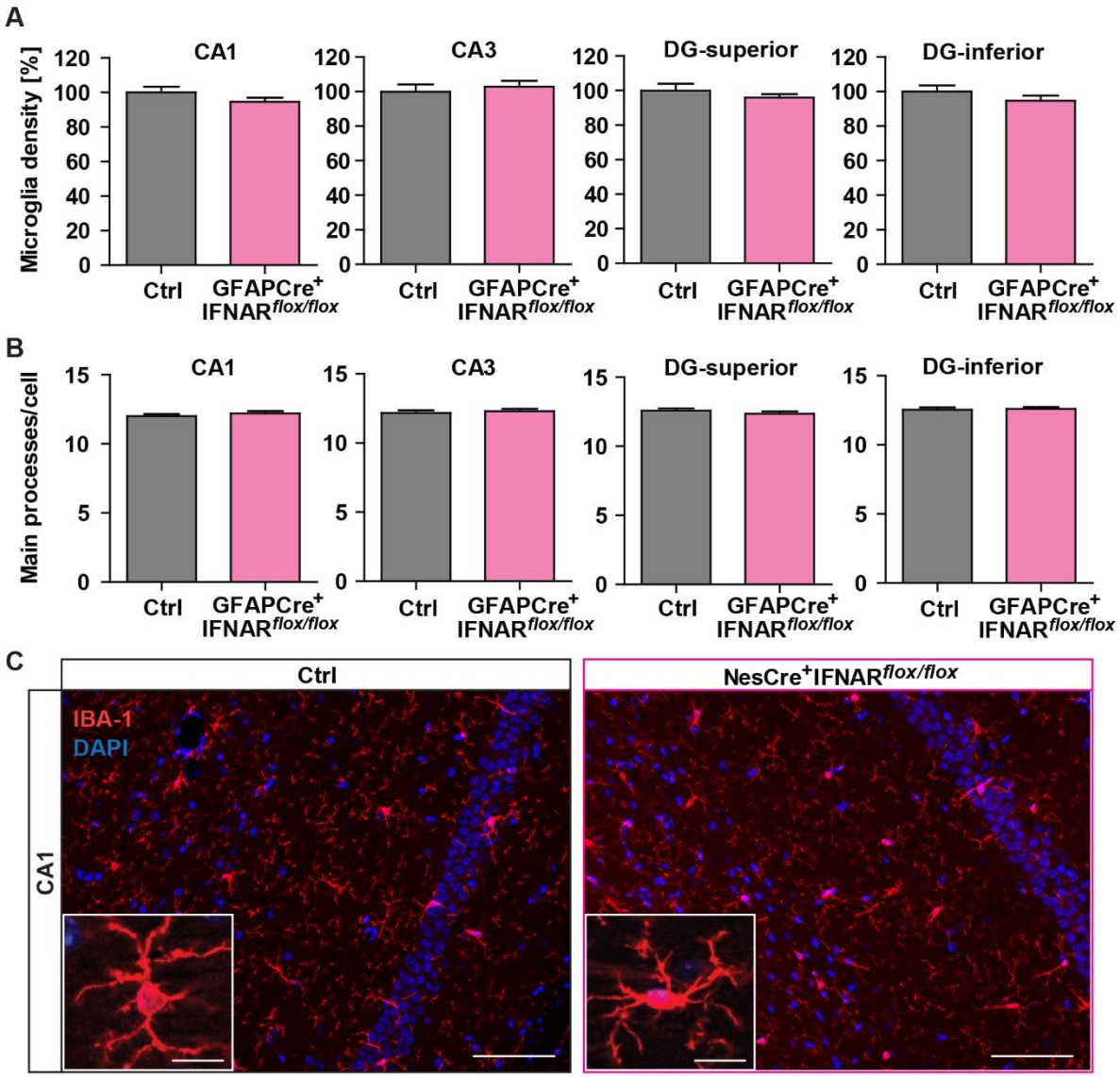

Figure 3.2.24 | Microglia density and morphology assessment in GFAPCre$^{+/-}$IFNAR$^{flox/flox}$ mice. **(A)** The microglia density and **(B)** activation status within all hippocampal subregions of GFAPCre$^{+/-}$ IFNAR$^{flox/flox}$ mice showed a similar phenotype to the respective control mice. **(C)** Representative examples of IBA-1 immunostaining of CA1 hippocampal subregion in both control and GFAPCre$^{+/-}$ IFNAR$^{flox/flox}$ groups (red is IBA-1 and blue is DAPI staining, Bar=50 µm, Inset frame Bar=10 µm, 20X). Data are presented as mean ± SEM, (Number of animals in each group = 4, number of ROIs in each group = 20, number of randomly selected microglia in each group = 120).

4. Discussion

4.1. Long-term neuroinflammation induced by influenza A virus infection and the impact on hippocampal neuron morphology and function

Influenza is primarily considered as a respiratory disease, and each year respiratory complications caused by influenza viruses lead to mortality in infected individuals. Influenza disease is common in a lot of species with species-specific virus strains although cross-species transmission can occur. Therefore, every year public health faces the seasonal epidemic, pandemic and zoonotic infections with various influenza A virus types. The well-known seasonal influenza strains responsible for yearly epidemics are H1N1 and H3N2 influenza A viruses and recent examples of zoonotic influenza A virus infections showed that H7N9 and the high pathogenic H5N1 were able to be transmitted from avian to humans. More than respiratory complications, evidence accumulates that influenza A virus infection can be associated with severe neurological complications in patients especially following different worldwide pandemics of influenza disease (Surana et al., 2011; Ekstrand, 2012; Shah et al., 2014). For example, during and after the “Spanish flu” between the year 1918 to 1920 an outbreak of encephalitis lethargica which is a disease characterized by a headache, double vision, delayed physical and mental response and lethargy was reported (McCall et al., 2008). On the other hand, investigating the impact of maternal influenza A virus infection on the offspring indicated an increased risk for schizophrenia and bipolar disorder (Brown et al., 2004; Brown and Derkits, 2010; Parboosing et al., 2013). Also, experiments in mice confirmed significant gene expression alterations in the brain of offspring after maternal influenza A virus infection (Asp et al., 2005).

Nevertheless, the pathogenesis of influenza A virus infection on the CNS still is unknown. Moreover, the knowledge about acute manifestations of neuropsychiatric syndromes and chronic effects on neurodegenerative diseases development mediated by influenza A viruses infection is still limited (Mizuguchi, 2013; Davis et al., 2014; Ludlow et al., 2016).

As influenza viruses can be either neurotropic or non-neurotropic, it is important to discriminate between alterations which are directly mediated by the actual ability of the virus to replicate in the brain and CNS disorders which are a result of the host

immune response in the periphery. However, observations and analysis of past pandemics and case reports revealed that neurological complications caused by influenza A virus infection seem to tightly depend on viral properties (Kuiken and Taubenberger, 2008; Henry et al., 2010) as well as the host-dependent factors (Mak et al., 2011; CDC, 2012; Ekstrand, 2012; van Riel et al., 2014). With respect to this, in the present study three different influenza A viruses and their effects on hippocampal features and cognitive functions were investigated.

First, the well-studied mouse-adapted human PR8 (H1N1) virus was chosen. It is known that this non-neurotropic virus can shortly (within 4 hours) after intranasal infection enter the olfactory nerves and glomerular layer of the olfactory bulb in a *Mx1*-independent (Interferon-inducible protein P78) manner without being able to further replicate in the brain or to induce neuropathology (Majde et al., 2007; Hodgson et al., 2012). It has been shown that the entry into the olfactory bulb was not prevented by immunization (Zielinski et al., 2013). This influenza A virus variant was also used previously by Jurgens et al., demonstrating altered hippocampal neuron morphology and impaired cognition during the acute phase of the infection at 7 days (Jurgens et al., 2012). Second, another mouse-adapted human non-neurotropic influenza A virus strain, the maHK68 (H3N2) (Haller et al., 1979) was used. This virus strain recently was investigated intensively using the mouse population of the Collaborative Cross which is a large panel of recombinant inbred strains and used for complex properties analysis (Leist et al., 2016). And third, to include also a neurotropic virus of avian origin rSC35M (H7N7), after being isolated from seals and adapted to mouse (Gabriel et al., 2005), was used as a model virus for high pathogenic avian derived viruses. The advantage of this virus was that a substantial amount of mice around 75% are able to survive this infection, whereas no surviving animals could be observed following infection with neurotropic H5N1 influenza A virus. Similar to H5N1, the avian H7N7 virus also caused diseases in mammals such as horse, seal and humans and represent a potential pandemic threat if species transmission occurs (Lang et al., 1981; Banks et al., 1998; Fouchier et al., 2004; Shinya et al., 2005).

In summary, in this study two human non-neurotropic influenza A variants (H1N1 and H3N2) with subsequent adaptation to the mouse and a mouse-adapted subtype of high pathogenic avian origin (H7N7) that successfully crossed the species barrier were used. Afterward, the long-term impacts on hippocampal structure and function of an infection with these influenza A virus subtypes were elucidated.

Most notably, the long-lasting consequences of an influenza infection in the brain have not been investigated before. The findings of this study provide evidence that neuroinflammation caused by non-neurotropic and neurotropic influenza viruses induces long-lasting alterations in hippocampal neuronal morphology and synaptic properties as well as cognitive function in young adult animals. However, influenza infected mice did not exhibit impairment in motor activity and anxiety-like behavior in the open field and elevated plus maze test, revealing that the cognitive impairments observed following influenza virus infection are directly due to the spatial learning deficits and not biased by anxiety-like behavior.

A comparison of the effects of H1N1 and H3N2, the non-neurotropic virus subtypes used in this study, on hippocampal structure and function revealed that infection with H1N1 did not lead to any long-term alterations in spatial memory formation and dendritic spine density 30 days post infection. In a previous study, just one week after non-neurotropic H1N1 virus infection, influenza-induced cognitive deficits were revealed only during the reversal testing in the Morris Water maze as infected mice showed an impaired ability to efficiently navigate to the new platform location (Jurgens et al., 2012). In the current study, as a memory impairment in both normal and reversal Morris water maze tasks could not be detected in the H1N1 infected mice 4 weeks after infection, therefore, the recovery from the infection with this variant seems to be fast and restricted to the acute phase of infection. However, further investigations of other time points after H1N1 infection could be interesting to reveal exactly how soon after infection the phenotype is gone. In contrast to this, 30 days post infection, non-neurotropic H3N2 influenza A virus infection caused a cognitive deficit in mice also most prominent during the reversal learning phase. The differences between the two non-neurotropic virus types might be dependent on different viral properties which are further underlined by results from the genes expression study performed here. Moreover, severe clinical features including high levels of fever, leukopenia and C-reactive protein were observed in the infected patients with H3N2 in comparison with H1N1 influenza A virus (Kaji et al., 2003).

In contrast to this, the neurotropic H7N7 influenza A virus infection caused long-lasting and robust spatial learning and memory impairment in both the initial training phase in the Morris water maze task and in the reversal testing. Therefore, this study was concentrated more on a detailed comparison between infection with non-

neurotropic H3N2 which is not able to replicate in the brain and the neurovirulent H7N7 showing replication in the CNS.

Many patients who survive from neurovirulent and non-neurovirulent infection exhibit chronic cognitive impairments. Although thousands of cases of virus-mediated memory dysfunction increase annually (Vasek et al., 2016), the mechanisms responsible for these impairments mostly are unknown until now. It has been shown that neuroinflammation during immune responses to viral infections in the brain indeed affects behavior (Rubin et al., 1999; Jurgens et al., 2012; Elmore et al., 2014; Vasek et al., 2016; Klein et al., 2017). Furthermore, previously, it has been emphasized that increased inflammatory genes expression such as IL-1ß, IL-6, TNF-α and IFN-γ in the brain can potentially cause damages resulting in spatial learning and memory deficits (Howe et al., 2012; Elmore et al., 2014; Heneka et al., 2014; Klein et al., 2017).

Yet, it is unclear whether the cognitive deficits induced by different types of viral infection are due to the presence of the virus in the brain or a peripheral infection that eventually might also affect the CNS or even both (Elmore et al., 2014). There is indeed evidence that infection with neurotropic viruses and resulting immune responses can interrupt the complex structure and function of the CNS (Ludlow et al., 2016). Neurotropic pathogens can enter the brain by different routes such as dissemination across the BBB via direct infection of endothelial cells or via infiltration of infected leukocytes across the BBB into the brain parenchyma (Ludlow et al., 2016). Non-neurotropic pathogens also can disrupt the BBB as a consequence of severe systemic inflammation (Varatharaj and Galea, 2017). The results of the present study show that the infection with both H3N2 and H7N7 virus subtypes led to a compromised BBB at 8 days post infection which was defined as the peak of infection. This is actually in line with an elevation of cytokine levels in the CNS detected here. The concentration of IFN-γ and TNF-α were increased in the case of H7N7 infection both in the blood serum and in the CNS, however, also infection with H3N2 led to elevated levels of TNF-α in the hippocampus. Moreover, the IL-1β level was increased in the CNS of both H3N2 and H7N7 influenza A virus infected mice. This inconsistency is dependent on the specific pattern of the expression of each cytokine in the different parts of the body and the time after infection (Jang et al., 2012). Indeed, several studies showed that after different types of infection in the periphery or the brain an increased inflammatory genes expression, for example, IL-

1ß, IL-6, TNF-α and IFN-γ, can be observed across multiple brain regions, including the hippocampus (Howe et al., 2012; Elmore et al., 2014; Heneka et al., 2014; Klein et al., 2017). The cytokines generated during peripheral inflammation can activate a secondary, mirror inflammatory response (indirect, immune response-mediated pathways) in the brain that is characterized by activation of microglia and production of pro-inflammatory cytokines, most importantly, TNF-α, IL-1 and IL-6 (Riazi et al., 2015). Furthermore, several findings confirmed that systemic inflammatory cytokines can alter the BBB: TNF-α via a reduction in tight junction expression, IL-1β and IL-6 through cooperation with cyclooxygenase (COX) and IFN-γ via a down-regulation of tight junction proteins. This can, in addition, lead to the entrance of more viruses into the brain parenchyma and the induction of local inflammatory responses following glial activation in the brain (Varatharaj and Galea, 2017). Indeed, in the present study, an increase in the number of microglia and astrocytes in the hippocampus of both H3N2 and H7N7 infected mice were detected which could be attributable to the leaky BBB following influenza A virus infection at least in parts. Although activated microglia are crucial for host defense against pathogens, prolonged or aberrant activation can have damaging effects on neurons and can adversely affect synaptic transmission and structure (Hanisch, 2002; Block et al., 2007; Pickering and O'Connor, 2007; Riazi et al., 2015). The findings of this study also showed the compromised BBB even 10 days after neurotropic H7N7 influenza infection which was accompanied with severe long-term cognitive dysfunction. Dissemination of pathogens and inflammatory responses elevation within the brain could potentially underlie the observed effects. It is worth noting that the increase in TNF-α and IL-1β levels 8 days post H1N1 influenza A virus infection, detected in the present study, is in line with the cognitive impairments reported during the acute infection phase with this virus one week after infection in an earlier study (Jurgens et al., 2012).

On the other hand, reductions in neuron-microglia communication markers such as CD200 (Cluster of differentiation 200), and neurotrophic factors such as NGF and BDNF were detected following virus infection induced cognitive impairments (Elmore et al., 2014). Also here a downregulation of genes encoding neurotrophic factors including *Bdnf* and *Ntf3* was observed 18 days post infection irrespective of the virus subtypes. 18 days post infection was chosen as a time point to investigate the gene expression profile, this is considered as a peak phase where gene expression alterations are strongest (Zhang et al., 2016) whereas the pathogen is already cleared

from the body (Beraki et al., 2005). It is known that neurotrophic factors such as BDNF have an essential role in synaptic plasticity and cognitive function (Minichiello et al., 2002; Lu et al., 2014). Thus, the observed long-term defects in cognitive function following H3N2 and H7N7 influenza infection could be a result of the reduction in the levels of neurotrophic factors or of the elevation of inflammatory cytokines in the brain, or a combination of both. Despite the possible differences in the mechanisms of action of different viruses in the CNS, in addition to the destructive effects of influenza A virus infection on the hippocampal function, other types of infections with herpes simplex virus, and human immunodeficiency virus (HIV) have been shown to be associated with behavioral and psychiatric disturbances in humans. Similarly, infection of mice with the LP-BM5 (murine leukemia viruses) mixture of retroviruses was shown repeatedly to cause spatial learning impairment. Vesicular stomatitis virus infection of 13 days old rats caused behavioral changes and learning deficits. Borna disease virus also can cause neurological disease in naturally infected horses and sheep, which is associated with behavioral abnormalities such as excitability, somnolence and depression (Rubin et al., 1999).

Overall, the cognitive deficits observations in this study reveal that both non-neurotropic H3N2 and neurotropic H7N7 influenza A virus infection inhibited normal hippocampal function in the young adult mice transiently. While hippocampal damage can disrupt spatial reversal learning, regions including the frontal cortex and striatum are also involved (Churchwell and Kesner, 2011) and could be additional targets of influenza infection.

Given the observed impairment in cognitive function and to provide further insights into the cellular mechanisms of influenza infection-associated functional changes in the brain, synaptic plasticity was investigated. The findings confirmed that 30 days post H3N2 and H7N7 influenza A virus infection, the maintenance phase of LTP was reduced. In line with these findings, previous electrophysiological experiments suggested that neonatal influenza infection causes weak action potential firing upon repeated strong depolarizations of hippocampal neurons (Park et al., 2015). Additionally, a reduction in the frequency of spontaneous excitatory synaptic activity and in the amplitude of the miniature excitatory postsynaptic currents and a decreased Ca^{2+} influx were recorded after exposing hippocampal neurons to influenza A viral proteins (Brask et al., 2005), which would be important to consider in the case of neurotropic influenza virus infection. It was furthermore reported that

influenza A virus infection can cause selective neurophysiological changes in hippocampal neurons which can also be persistent even after the clearance of viral antigens (Brask et al., 2001). On the other hand, several reports described that manipulations of individual cytokines can modulate learning, memory, and synaptic plasticity (Marin and Kipnis, 2013; Donzis and Tronson, 2014). The production of inflammatory mediators from brain immune cells upon infection or injury disrupts the delicate balance needed for neurophysiological actions of immune processes and can produce direct detrimental effects on memory, neural plasticity and neurogenesis (Tanaka et al., 2006; Yirmiya and Goshen, 2011). These effects are mediated by inflammation-induced neuronal dysfunction followed by reduced production of neurotrophins such as BDNF and other plasticity-related molecules, facilitating many forms of neuropathology associated with normal aging as well as neurodegenerative and neuropsychiatric diseases (Yirmiya and Goshen, 2011). Therefore, the electrophysiological findings presented here are in line with previously described inflammation-induced deficits in synaptic function and provide further physiological insights into influenza infection-associated functional changes at synapses. They might also provide an explanation for the predisposition to psychiatric and mental disorders upon infection in adult mice.

To reveal the potential cellular basis for the reduction in neuronal long-term potentiation, hippocampal neuronal morphology was assessed following influenza A virus infection. The findings revealed that H3N2 and H7N7 influenza infection led to a reduction in dendritic spine density, the postsynaptic component of excitatory synapses, 30 days post infection. It is worth noting that all three types of principal neurons in the hippocampus including pyramidal neurons in the CA1 and CA3 region as well as dentate granule cells were affected following H7N7 influenza infection while only CA1 and CA3 neurons were damaged after H3N2 infection. The present findings showed that 30 days post H1N1 influenza infection, dendritic spine density was similar to control levels, although at least at some point neuroinflammation took place as the number of microglia was increased at 18 days post infection. Furthermore, it was shown previously that 7 days post H1N1 infection both CA1 pyramidal and dentate granule neurons demonstrated retraction of distal dendrites. The architecture of granule cells was more profoundly affected (Jurgens et al., 2012). Again, the findings obtained here show that H1N1 infection seems to result only in a very brief

period of neuroinflammation which recovers much faster than the infection with H3N2 or H7N7.

It was reported that proinflammatory mediators produced during the infection can disturb neuronal morphology, synaptic structure and function (Yirmiya and Goshen, 2011; Estes and McAllister, 2015). In particular, chronic inflammation *in vivo* and exposure of cultured brain cells to LPS *in vitro* led to a loss of spines which can also be found in many neurological diseases (Chang et al., 2015). However, in the case of viral infection, it is not clear yet if alterations in dendritic morphology happen as part of a protective or pathological remodeling. Furthermore, for neurotropic virus infection, it remains to be investigated whether synapse loss takes place only at infected neurons or also healthy cells (Vasek et al., 2016), however, here it was shown that spine reduction happened following H3N2 infection there should be no infected cells as the virus is not present in the brain.

In the case of H3N2, spine numbers were reduced only in the cornu amonis (CA) region. This might indeed provide an explanation for the differentially compromised spatial learning in H3N2 and H7N7 infected individuals. Infection with the neurotropic virus led to a robust impairment in spatial map formation whereas H3N2 infection was associated with a reduced ability to update the new platform position in the reversal phase, but just with a very mild impairment in the initial formation of a spatial map in the Morris water maze task. It was indeed shown previously that the progressive nature of neurotropic virus-induced damage in the dentate gyrus such as Borna virus is associated with impaired performance in the Morris water maze (Rubin et al., 1999). In line with these findings, the reduction of dendritic spine density in DG neurons was accompanied by severe spatial learning deficits following neurotropic H7N7 influenza A virus infection could be found in the present study. In addition, the neuronal representation of behavioral flexibility for the decision between competing memories in the reversal task may reside more in the CA1 and CA3 subfield than in the DG. Therefore, the findings of this study show that the different hippocampal subregions might indeed express a different sensitivity for inflammation induced damage with the DG being more resilient. Moreover, synapse loss is very likely to provide a cellular explanation for the deficits in synaptic plasticity and also eventually the behavioral symptoms observed after influenza A virus infection in mice.

It has been defined that proper synaptic transmission in neuronal networks and maintenance of the neuronal structure in the brain relies on the functions of glial cells.

Microglia play a role in synaptic remodeling and plasticity in the healthy brain (Nimmerjahn et al., 2005; Parkhurst et al., 2013), for instance, via neuron-glia crosstalk through the *Cx3cr1* signaling axis which was found to be downregulated in the present study independent to the virus subtype. Furthermore, it was revealed that a complement system and activated microglia axis promotes synaptic loss during West-Nile virus-induced memory impairment (Vasek et al., 2016). As we detected the upregulated complement system-related genes more pronounced for H7N7 IAV infected mice. Therefore, the observed long-term alterations in spine number, synaptic plasticity and cognitive function observed in this study following influenza A virus infection might indeed result in parts from a general virus subtype-independent hyperactivation of microglia cells in the hippocampus triggered at least in part through the immune responses to the influenza virus in the periphery. Previous studies suggest that during peripheral and central inflammation, microglia play a pivotal role in cerebral functions and act as major guardians of the brain threatened by pathogens and the proinflammatory endotoxins they produce (Hughes, 2012; Kettenmann et al., 2013). Different pathogens, as well as LPS, can activate microglia (Nakamura et al., 1999), which in turn produce and release proinflammatory and inflammatory cytokines that can adversely affect synaptic structure (Hanisch, 2002). Also, the cytokines generated during peripheral inflammation can activate a secondary inflammatory responses in the brain via humoral (signaling via a leaky BBB), neural (signaling via peripheral nerves) and cellular (signaling via peripheral immune cells infiltration) pathways that is characterized by activation of microglia and production of proinflammatory cytokines, most importantly, TNF-α, IL-1β and IL-6 (D'Mello and Swain, 2014; Thomson et al., 2014). These cytokines can have profound effects on synaptic transmission and synaptic plasticity (Pickering and O'Connor, 2007; Riazi et al., 2015). Therefore, the observed activation of microglia is most likely one of the main underlying cellular explanations for the altered cognitive function that was detected following influenza A virus infection.

The number of astrocytes was increased as well following infection with neurotropic H7N7 and non-neurotropic H3N2 influenza A virus subtypes. This phenotype was associated with alterations in the expression of genes regulating glutamate and potassium clearance by astrocytes (*Slc1a2* and *Gjb6*). A downregulation of *Slc1a2* level which plays an essential role in the maintenance of normal excitatory synaptic transmission, protection of neurons from the excitotoxic action of excessive

glutamate, and regulation of glutamate mediated neuroplasticity (David et al., 2009) was observed at 18 days post infection in the present study. Previous findings indicate that astrocytes are not merely the supportive cells of the brain, rather they also play an important integral role in neural and synaptic functioning (Araque and Navarrete, 2010). Astrocyte-to-neuron communications (*Slc1a2* and *Gjb6*) also plays a critical role in synaptic plasticity processes including long-term potentiation, learning and memory (Yirmiya and Goshen, 2011). In neuropsychiatric disorders that are described by a deficiency of astrocytic function such as major depression and some neurodegenerative diseases, behavioral and neural plasticity are also severely impaired (Ben Menachem-Zidon et al., 2011). Interestingly, in both H3N2 and H7N7 infected mice elevated numbers and related-genes of astrocytes recovered faster than the number and activation status of microglia cells suggesting that an astrocyte-microglial interaction might be a key mechanism for the regulation of brain inflammation during influenza infection. In this regard, previous findings suggest that astrocytes can regulate microglial activity by stimulating their antioxidant gene expression, perhaps providing a negative feedback response to titrate the inflammatory reaction induced by proinflammatory mechanisms thus modulating microglial resting status versus activation state (Shih et al., 2006).

In parallel, in the present study, significant effects were observed while of the investigation of cell-specific genes for both astrocytes and microglia. There was an increase in the expression of *Gfap* (astrocyte-specific gene) and *Olfml3* (microglia-specific gene) in both H3N2 and H7N7 infected hippocampi. Although there were striking similarities in the phenotypes following infection with H3N2 (non-neurotropic) and H7N7 (neurotropic) influenza A virus subtypes on the level of glial cell and synapse numbers as well as the gene expression profiles which indicate the involvement of general and virus type independent mechanisms, H7N7 induced changes were much more severe. This points towards characteristic differences in the long-lasting outcome following infection with these two viruses which might be due to the neurotropic nature of the virus. In case of the H7N7 influenza A virus, a much stronger reaction which was consistent throughout all hippocampal subregions was observed. Notably, also the recovery time was slower as was the case as well for genes expression study on 30 days post infection. This indicates that the direct presence of the virus in the brain leads to even more detrimental effects (direct, virus-mediated pathways). Indeed also the gene expression profile analysis revealed that

the increase in microglia activation markers was even stronger and recovered slower in H7N7 infected individuals compared to H3N2 infected mice. Especially the levels of molecules belonging to the MHCII family were strongly increased indicating a direct contact of microglia and the influenza A virus. Members of the MHCII gene family and other phagocytosis-related genes (*Fcgr3*, *Fcgr4*, *Vav1* and *Tyrobp*) are markers of activated microglia with phagocytic activity as well increased especially following infection with H7N7.

Another possible scenario here is, that viral induced cognitive impairments are possibly mediated by inflammation-induced neuronal dysfunction followed by reduced production of neurotrophins such as BDNF (found indeed to be reduced in a virus subtype-independent manner in this study) and other plasticity-related molecules which need further investigations to confirm.

4.1.1. Conclusions and outlooks I

The current study focused in particular on the long-term impact of an influenza infection caused by non-neurotropic and neurotropic viruses on cognitive function and hippocampal structure of adult young mice. While at 30 days post infection, non-neurotropic H1N1 influenza virus did not show any detrimental effects on hippocampal morphology and function, both non-neurotropic H3N2 and neurotropic H7N7 influenza A virus Infected mice showed cognitive impairment accompanied defects in synaptic plasticity and spine loss. At the same time, an increase in both microglia and astrocyte density could be observed as well as an increase in microglia activity. This study could show that young and otherwise healthy individuals could recover from these influenza-mediated alterations 120 days post infection. The observations described here point towards influenza A virus infection induced long-term hippocampal neuroinflammation that might indeed explain the negative effects of influenza virus strains on cognitive function. Adverse effects were most pronounced for H7N7 influenza A virus.

Evidence more and more accumulates that chronic neuroinflammation may be a central mechanism contributing to the generation and progression of a number of neurodegenerative disorders including Alzheimer´s disease (Frank-Cannon et al., 2009; Heneka et al., 2014). Thus, the current findings have significant implications as an influenza infection with non-neurotropic and neurotropic viruses might initiate inflammatory cascades via microglia and astrocyte activation in the brain and therefore increase the likelihood to develop neurodegenerative disorders. Although already the indirect, purely host immune response triggered pathways were able to impair hippocampal function partially (in the case of H3N2), the direct presence of an influenza virus in the brain resulted in an even stronger and more prolonged activation of microglia with detrimental outcome for cognitive function (in the case of H7N7). While young animals used in this study were able to fully recover, future experiments will show whether this is also the case for aged individuals and how the developing brain of juveniles might be affected. As respiratory infections are common in humans, approaches to regulate glial cells activity could provide a future tool to prevent deleterious effects on the brain, especially in older individuals.

4.2. Type I interferon signaling ablation alters hippocampal synaptic plasticity and cognitive function

While the first part of this thesis was aimed at investigating the impact of influenza A virus infection on the brain and the cross-talk between the immune system and the CNS under pathological conditions, in the second part the role of cytokine signaling for the healthy CNS was investigated.

The most important cytokines involved in brain-immune interactions both under pathological and physiological conditions are interleukins (ILs), tumor necrosis factor alpha (TNF-α) and interferons (IFNs). IFN-α and -β are the predominant types of IFNs in the CNS which are mostly implicated as mediators of antiviral immune responses that are necessary for protecting the CNS during viral infection. All CNS cell types including neurons and glial cells are able to produce and respond to IFNs (Owens et al., 2014).

Earlier studies revealed that immune-deficient mice are more susceptible to mental stress, suffer from cognitive deficits and show reduced level of hippocampal neurogenesis when compared to their wild-type counterparts (Deczkowska et al., 2016). Therefore, for determining the physiologic role of type I IFN signaling for cognitive functions such as learning and memory processes also mediated by the interaction between neurons and glial cells, in this study conventional as well as different conditional knockout mouse lines for the type I IFN receptor (IFNAR) were investigated. Müller and colleagues showed that mice lacking the IFNAR1 were completely unresponsive to type I IFNs, suggesting that this receptor chain is essential for type I IFN-mediated signal transduction. Although these mice did not exhibit any overt anomalies, they were completely unable to cope with viral infections, despite normal immune responses (Muller et al., 1994).

The findings of the present study show that conventional IFNAR$^{-/-}$ mice exhibited a strong learning and memory impairment along with deficits in LTP and reduced dendritic spine density. According to these findings, it seems that IFNAR signaling is involved in brain function under physiological conditions. However, it has not yet been determined that IFN signaling is contributed in brain development and synaptogenesis, or directly involved in synaptic plasticity events or even both. Although previous studies suggested the contribution of some of the cytokines signaling in synaptogenesis and synaptic plasticity (Mehler and Kessler, 1998).

As this results were obtained in complete KO mice, in the next step, the question arises which cell types might be most involved in IFNAR signaling under physiological circumstances. Therefore, different conditional IFNAR KO mice were tested. The results indicated that NesCre$^{+/-}$IFNAR$^{fl/fl}$ mice which have a lack of IFNAR in neurons, astrocytes and oligodendrocytes (Detje et al., 2015), also exhibited an impaired cognitive function accompanied by defects in LTP and a reduced dendritic spine density which was more pronounced in CA1 pyramidal neurons. Thus, IFNAR signaling ablation from neurons and astrocytes leads to synaptic plasticity and cognitive function impairment, as it was already mentioned that these two cells in the CNS are more involved in type I IFNs release and response compared to oligodendrocytes. In addition, it can be inferred that IFNAR expression in microglia alone seems not to be sufficient to rescue impaired neuronal function.

Therefore, neurons and astrocytes were two potential candidates for mediating type I IFNs signaling in maintenance of synaptic function under physiological conditions. Previously, it has been shown that neurons respond to IFNs as they express the respective receptors in both presynaptic and postsynaptic membranes (Vikman et al., 1998; Ignatowski and Spengler, 2008). Now to determine the necessity of neuronal type I IFNs signaling for cognitive functions, Syn1Cre$^{+/-}$IFNAR$^{flox/flox}$ mice were used which are characterized by IFNAR deletion in neurons (Detje et al., 2015). Interestingly, Syn1Cre$^{+/-}$IFNAR$^{flox/flox}$ mice did not show impaired hippocampal synaptic plasticity and function, thereby indicating that IFNAR signaling directly on neurons is not be necessary for synapse number and function.

As in the conditional KO mice, Cre recombinase expression in the central and peripheral nervous system starts around embryonic day E12.5 (Liang et al., 2012). While the time point, E16 corresponds to the peak periods for which major cellular and physiological events occur during mouse hippocampal development which is involved in cognitive functions (Mody et al., 2001). Thus, the findings of this investigation suggest the possible role for type I IFN signaling pathways during developmental stages as well as during adult life via direct effects on synaptic plasticity.

Therefore, one explanation might be that IFN signaling during development is important for synapse formation for instance via the release of the synaptogenic factor by for instance astrocytes following IFNAR stimulation. If the network is not fully

developed also LTP might be indeed impaired. A different explanation for the LTP defect would be a direct involvement of IFNAR signaling in synaptic plasticity.

As the results from the SynCre conditional KO line indicated that IFNAR signaling directly in neurons is not responsible for the observed phenotypes, as a next step, GFAPCre$^{+/-}$IFNAR$^{flox/flox}$ mice with an IFNAR deletion on astrocytes (Detje et al., 2015) were investigated. Indeed, the phenotype of impaired cognitive function, as well as defects in synaptic plasticity in GFAPCre$^{+/-}$IFNAR$^{flox/flox}$ mice, was comparable to the full IFNAR KO mice. This provided further evidence for the above raised hypothesis that IFNAR signaling in astrocytes is crucial for synapse number and function.

As it was already mentioned, IFNAR KO mice are more sensitive to infections as they lack the IFNs signaling (Muller et al., 1994). However, in the present study, no changes in microglial density and activity could be observed in the groups of conventional and conditional IFNAR KO mice, indicating no increase in neuroinflammation. Therefore, it can be concluded that the observed impairments in cognitive function and synaptic plasticity deficits are indeed showing a role for IFNAR signaling under physiological conditions in the healthy central nervous system most likely involving astrocytes as a central element.

In the first scenario, the observed cognitive function deficits and synaptic plasticity impairment in the absence of IFNAR-mediated signaling particularly in astrocytes might be a developmental phenotype. It was shown previously that astrocytes release glutamate, ATP and cytokines such as TNF-α and IFNs that change the survivability and functioning of newly formed connections between the neurons (Ota et al., 2013). Furthermore, it has been shown that cytokines such as IFNs are able to control neurogenesis and brain development. Moreover, they can modulate growth, differentiation and survival of neuronal cells (Mehler and Kessler, 1998). For instance, IFNs treated fetal murine neuroblasts culture developed a differentiated neuronal population associated with the expression of the most mature neurofilament proteins (Plioplys, 1988). In addition, although type I IFN signaling enhances NGF-mediated neural differentiation, induced apoptosis by NGF in the cultured sympathetic neurons was prevented by type I and II IFNs application (Chang et al., 1990).

Also, it has been revealed that JAK-STAT signaling which is downstream of many cytokines such as type I IFNs as well as IL-2, IL-6, IL-10, and TNFα (Murray, 2007) has a critical role in various brain developmental pathways, especially in promoting astrogliogenesis (Lee et al., 2016b), as astrocytes contribute to CNS development by

controlling synaptogenesis and axon guidance factors (Chung et al., 2015b). Therefore, the presence of type I IFN signaling and subsequent JAK-STAT pathways, especially in astrocytes, might be necessary for normal hippocampal development and neurogenesis. (De Araujo et al., 2009).

On the other hand, during the development, astrocytes release and respond to other factors such as BDNF, TGF-β and thrombospondin (TSP) thereby controlling glutamatergic synapse formation (Chung et al., 2015b). It was shown that TSP-1 ablation which is the specific astrocyte-secreted protein led to synapse loss in TSP-1 KO mice (Garcia et al., 2010).

Taken together, in this scenario IFNAR signaling in astrocytes during developmental might be important for synaptogenesis possibly by releasing neurotrophic factors or thrombospondins. Impaired cognitive function and synaptic plasticity could result from the improper formation of neuronal networks. To answer the question if IFNAR signaling plays a role for synapse development inducible Cre transgenic mice under the control of the GFAP promoter could be used.

In the second scenario, the impaired memory formation and synaptic plasticity observed in IFNAR deficient animals here in this study might be due to direct effects of cytokines such as IFNs in synaptic plasticity. Previously, it has been identified that cytokines are able to exert some neuroprotective effects. Thus, elucidation of the detailed mechanisms by which immune molecules can affect neuronal function has important implications to understand both the normal brain function and the pathophysiology of a vast number of neurological disorders.

Indeed, it has been described before that immune proteins are needed for many neuronal processes and that a dysregulation of these proteins (for instance also strongly upregulation under inflammatory conditions) can lead to impairments in learning and memory functions. The roles of some cytokines including IL-1β, TNF-α and IL-6 have been studied so far in this context in the brain (Donzis and Tronson, 2014). There is evidence for the contribution of these cytokines in acquisition, consolidation, or retrieval of memory processes. For instance, several studies revealed an important role for IL-1β for hippocampus-dependent memory formation. The levels of IL-1β are reported to increase during LTP induction or following context-dependent fear conditioning suggesting a critical role for this cytokine in learning and memory processing (Schneider et al., 1998). In addition, it has been shown that low levels of IL-1β have a physiological role in the maintenance phase of LTP, whereas

high pathological concentrations of IL-1β inhibit LTP. Therefore, IL-1β depending on the concentration, can either promote or inhibit synaptic plasticity. This demonstrates a profound effect of this cytokine on neuronal function (Schneider et al., 1998).
Furthermore, it could be shown that the levels of TNF-α increase after learning, however, this cytokine was not directly required for learning and memory consolidation (Belarbi et al., 2012). It has also been shown that cytokines such as TNF-α contribute to synaptic transmission. Glutamate is the main excitatory transmitter in the CNS and transmits the signals to the postsynaptic neurons through AMPA receptors. Therefore, trafficking of these receptors into and out of the postsynaptic density is thought to be crucial for the formation of on the one hand rapid forms of synaptic plasticity and on the other hand slower homeostatic changes in synaptic transmission. The membrane insertion of AMPA receptors appears to be tightly regulated in neurons by the rapid increases or decreases in response to neurotransmitter stimulation (Stellwagen et al., 2005; Stellwagen and Malenka, 2006). There is indeed evidence that TNF-α is able to influence or regulate important neuronal functions such as synaptic transmission. Interactions between neurons and glial cells through physiological levels of this cytokine are in fact necessary to regulate the synaptic conduction between the neurons (Ignatowski and Spengler, 2008). Recent studies showed that the proinflammatory cytokine TNF-α released from astrocytes can act as a gliotransmitter by promoting membrane insertion of AMPA receptors in neurons (Theodosis et al., 2008). Therefore, the constitutive release of physiological concentrations of TNF-α contributes to the homeostatic activity-dependent regulation of synaptic connectivity (Stellwagen and Malenka, 2006).
IFNs as well can act as neuromodulators which are able to exert direct effects on synaptic transmission and function (Vikman et al., 1998). Differential signaling outcomes of IFN-α and IFN-β can determine whether type I IFNs exert pathogenic or protective roles in the CNS depending on their concentration (Owens et al., 2014). Previously behavioral and cognitive impairments, as well as neurodegeneration, were reported in *Ifnb*$^{-/-}$ mice (Ejlerskov et al., 2015). This is in line with the results shown here as learning and memory formation was severely impaired in IFNAR KO mice indicating indeed a role of type I IFNs comparable to IL-1β for hippocampus-dependent memory formation. In addition, ablation of IFNAR in particular on astrocytes led to an impaired LTP accompanied by a reduction in dendritic spine density. LTP is today considered as an important cellular correlate of learning and

memory formation. Furthermore, changes in dendritic spine density and morphology have been shown to be associated with synaptic plasticity and cognitive function deficits in general (Moser et al., 1994). Therefore, these results might indeed indicate a direct role of IFNAR signaling in astrocytes for synaptic plasticity and cognitive function. It could be shown previously that conditional astrocyte-specific IL-1 receptor KO mice displayed memory deficits (Menachem-Zidon et al., 2011).

As it was already mentioned TNF-α which is released from glial cells, can increase the surface expression of AMPA receptors in response to glutamate indicating an important involvement in synaptic plasticity (Stellwagen et al., 2005; Stellwagen and Malenka, 2006). This can be considered as another possible mechanism underlying the type I IFNs actions in synaptic plasticity. Type I IFNs signaling might exhibit a permissive for synaptic plasticity comparable to TNF-alpha. A possible mechanism might be the regulation of available glutamate in the synaptic cleft by glutamate transporters GLT-1 and GLAST which indeed has been shown to promote LTP (Swanson, 2005). Furthermore, the release of ATP from astrocytes can be used to regulate the trafficking of postsynaptic glutamate receptors, especially AMPA receptors. It has previously been shown that astrocytes by releasing and responding to different cytokines such as TNF-α, CCL2 and IL-1 are involved in different aspects of synaptic plasticity by regulating glutamate transport at the synapse as well as the insertion of AMPA receptors and inhibition of NMDA receptor activity. Moreover, astrocytes through TNF-α signaling can negatively affect the expression of gamma-aminobutyric acid ($GABA_A$) receptors (Ota et al., 2013). It has been shown under physiological conditions cytokine and chemokine receptors on astrocytes contribute to the regulation of Ca^{2+} stores as well. Also, astrocytes release and respond to chemokine (C-C motif) ligand 2 (CCL2) which regulates the activity of NMDA receptors (Gao and Ji, 2010). In conclusion, IFNAR signaling through astrocytes may modulate the glutamate concentration in the synaptic cleft and subsequently affect AMPA receptor trafficking and other related receptors in the postsynaptic compartment thereby modulating the synaptic function under physiological conditions. Another possible way of the effects of IFNAR signaling in synaptic plasticity might be through JAK/STAT pathway. It is worth noting that the important role of JAK/STAT signaling in memory and synaptic plasticity is suggested as cytokine signaling through the JAK/STAT pathway is required for long-term memory in Drosophila (Copf et al., 2011).

4.2.1. Conclusions and outlooks II

Cytokines perform a comprehensive range of overlapping functions both outside and inside the CNS (Zhang and An, 2007). Under physiological conditions, they are involved in the regulation of neuronal differentiation, survival and plasticity (Ignatowski and Spengler, 2008). IFNs are cytokines that can be released by glial and neuronal cells and not only have antiviral and immunomodulatory effects but also neuromodulatory actions. Type I IFNs and their receptor (IFNAR) are of particular interest, taking into account their role in mediating communication between cells in either absence or presence of viral infection. Indeed, it could be shown previously that a basal level of interferon signaling is necessary to maintain neuronal health and function (McGlasson and Hunt, 2017). The results presented here show that IFNAR signaling is important for hippocampal synapse number and plasticity in the healthy brain. However, the underlying mechanism of IFNAR signaling in the interaction between neurons and astrocytes in developing brain and adulthood has been remained yet to be determined in the context of learning and memory.

First, it is necessary to discriminate the developmental importance of type I IFN signaling from the role in the adult brain by inducible Cre mice. Second, it is important to show that basal levels of IFN-β as a major ligand for IFNAR are beneficial for synaptic function. in this respect, it was shown that rat IFN-α has a dose-dependent inhibitory effect on basal synaptic transmission, short- and long-term potentiation and glutamate-mediated excitatory postsynaptic functions (Mendoza-Fernandez et al., 2000). Furthermore, the detailed cellular mechanism of IFNAR signaling in astrocytes have to be determined and their role for hippocampal function. For instance, it would be important to investigate whether type I IFN signaling affects the trafficking of AMPA receptors at the synapses. It has been shown that astrocytes can modulate synaptic transmission and plasticity via glutamate transporters (GLT-1 and GLAST) and GABA uptake (GAT-1) (Chung et al., 2015a). Therefore, it will be important to determine under which conditions IFN application can regulate glutamate and GABA uptake in astrocytes and whether this plays a role for synaptic development and plasticity. In addition due to the importance of the STAT pathways for memory formation (Copf et al., 2011), it would be important to study the detailed signaling pathways involving STAT proteins. The findings of this study are also of special interest as type I interferons inhibitors are used for therapeutic reasons in people with lupus or other

severe inflammatory diseases. Inhibition of type I IFNs signaling in the brain of these patients might present a new therapeutic strategy for preventing possible CNS disorders caused by increased levels of IFNs (McGlasson and Hunt, 2017). However, the results of this thesis indicate that the therapeutic inhibition of type I IFNs signaling in the brain might not be without potential consequences, given the pivotal role of this pathway in host defense and the importance described here under physiological conditions.

5. References

Anderson CM, Swanson RA (2000) Astrocyte glutamate transport: review of properties, regulation, and physiological functions. Glia 32:1-14.

Araque A, Navarrete M (2010) Glial cells in neuronal network function. Philosophical Transactions of the Royal Society B: Biological Sciences 365:2375-2381.

Asp L, Beraki S, Kristensson K, Ogren SO, Karlsson H (2009) Neonatal infection with neurotropic influenza A virus affects working memory and expression of type III Nrg1 in adult mice. Brain, behavior, and immunity 23:733-741.

Asp L, Beraki S, Aronsson F, Rosvall L, Ogren SO, Kristensson K, Karlsson H (2005) Gene expression changes in brains of mice exposed to a maternal virus infection. Neuroreport 16:1111-1115.

Atluri VS, Hidalgo M, Samikkannu T, Kurapati KR, Nair M (2015) Synaptic Plasticity and Neurological Disorders in Neurotropic Viral Infections. Neural plasticity 2015:138979.

Bajenaru ML, Zhu Y, Hedrick NM, Donahoe J, Parada LF, Gutmann DH (2002) Astrocyte-specific inactivation of the neurofibromatosis 1 gene (NF1) is insufficient for astrocytoma formation. Molecular and cellular biology 22:5100-5113.

Banks J, Speidel E, Alexander DJ (1998) Characterisation of an avian influenza A virus isolated from a human--is an intermediate host necessary for the emergence of pandemic influenza viruses? Archives of virology 143:781-787.

Bao Y, Gao Y, Shi Y, Cui X (2017) Dynamic gene expression analysis in a H1N1 influenza virus mouse pneumonia model. Virus genes 53:357-366.

Barres BA (2008) The mystery and magic of glia: a perspective on their roles in health and disease. Neuron 60:430-440.

Barrientos RM, Sprunger DB, Campeau S, Watkins LR, Rudy JW, Maier SF (2004) BDNF mRNA expression in rat hippocampus following contextual learning is blocked by intrahippocampal IL-1β administration. Journal of neuroimmunology 155:119-126.

Belarbi K, Jopson T, Tweedie D, Arellano C, Luo W, Greig NH, Rosi S (2012) TNF-alpha protein synthesis inhibitor restores neuronal function and reverses cognitive deficits induced by chronic neuroinflammation. J Neuroinflammation 9:23.

Ben Menachem-Zidon O, Avital A, Ben-Menahem Y, Goshen I, Kreisel T, Shmueli EM, Segal M, Ben Hur T, Yirmiya R (2011) Astrocytes support hippocampal-dependent memory and long-term potentiation via interleukin-1 signaling. Brain, behavior, and immunity 25:1008-1016.

Bender C, Frik J, Gómez RM (2012) Role of astrocytes in viral infections. Astrocytes: Structure, Functions and Role in Disease:109-124.

Benes FM (2010) Amygdalocortical Circuitry in Schizophrenia: From Circuits to Molecules. Neuropsychopharmacology : official publication of the American College of Neuropsychopharmacology 35:239-257.

Benjamini Y, Hochberg Y (1995) Controlling the false discovery rate: A practical and powerful apporach to multiple testing. . J R Stat Soc 57:289-300.

Bennett ML, Bennett FC, Liddelow SA, Ajami B, Zamanian JL, Fernhoff NB, Mulinyawe SB, Bohlen CJ, Adil A, Tucker A, Weissman IL, Chang EF, Li G, Grant GA, Hayden Gephart MG, Barres BA (2016) New tools for studying microglia in the mouse and human CNS. Proceedings of the National Academy of Sciences of the United States of America 113:E1738-1746.

Beraki S, Aronsson F, Karlsson H, Ögren SO, Kristensson K (2005) Influenza A virus infection causes alterations in expression of synaptic regulatory genes combined with changes in cognitive and emotional behaviors in mice. Molecular psychiatry 10:299.

Berthoud H-R, Neuhuber WL (2000) Functional and chemical anatomy of the afferent vagal system. Autonomic Neuroscience 85:1-17.

Bi F, Huang C, Tong J, Qiu G, Huang B, Wu Q, Li F, Xu Z, Bowser R, Xia XG, Zhou H (2013) Reactive astrocytes secrete lcn2 to promote neuron death. Proceedings of the National Academy of Sciences of the United States of America 110:4069-4074.

Bialas AR, Presumey J, Das A, van der Poel CE, Lapchak PH, Mesin L, Victora G, Tsokos GC, Mawrin C, Herbst R (2017) Microglia-dependent synapse loss in type I interferon-mediated lupus. Nature.

Blazejewska P, Koscinski L, Viegas N, Anhlan D, Ludwig S, Schughart K (2011) Pathogenicity of different PR8 influenza A virus variants in mice is determined by both viral and host factors. Virology 412:36-45.

Bliss TV, Gardner-Medwin AR (1973) Long-lasting potentiation of synaptic transmission in the dentate area of the unanaestetized rabbit following stimulation of the perforant path. J Physiol 232:357-374.

Bliss TV, Lømo T (1973) Long-lasting potentiation of synaptic transmission in the dentate area of the anaesthetized rabbit following stimulation of the perforant path. The Journal of physiology 232:331-356.

Bliss TV, Collingridge GL (1993) A synaptic model of memory: long-term potentiation in the hippocampus. Nature 361:31-39.

Block ML, Zecca L, Hong JS (2007) Microglia-mediated neurotoxicity: uncovering the molecular mechanisms. Nature reviews Neuroscience 8:57-69.

Bluthe RM, Walter V, Parnet P, Laye S, Lestage J, Verrier D, Poole S, Stenning BE, Kelley KW, Dantzer R (1994) Lipopolysaccharide induces sickness behaviour in rats by a vagal mediated mechanism. Comptes rendus de l'Academie des sciences Serie III, Sciences de la vie 317:499-503.

Borden EC, Sen GC, Uze G, Silverman RH, Ransohoff RM, Foster GR, Stark GR (2007) Interferons at age 50: past, current and future impact on biomedicine. Nature reviews Drug discovery 6:975.

Bordner KA, Kitchen RR, Carlyle B, George ED, Mahajan MC, Mane SM, Taylor JR, Simen AA (2011) Parallel declines in cognition, motivation, and locomotion in aging mice: association with immune gene upregulation in the medial prefrontal cortex. Experimental gerontology 46:643-659.

Brahmachari S, Fung YK, Pahan K (2006) Induction of glial fibrillary acidic protein expression in astrocytes by nitric oxide. The Journal of neuroscience : the official journal of the Society for Neuroscience 26:4930-4939.

Brask J, Owe-Larsson B, Hill RH, Kristensson K (2001) Changes in calcium currents and GABAergic spontaneous activity in cultured rat hippocampal neurons after a neurotropic influenza A virus infection. Brain research bulletin 55:421-429.

Brask J, Chauhan A, Hill RH, Ljunggren HG, Kristensson K (2005) Effects on synaptic activity in cultured hippocampal neurons by influenza A viral proteins. J Neurovirol 11:395-402.

Brown AS, Susser ES (2002) In utero infection and adult schizophrenia. Developmental Disabilities Research Reviews 8:51-57.

Brown AS, Derkits EJ (2010) Prenatal infection and schizophrenia: a review of epidemiologic and translational studies. The American journal of psychiatry 167:261-280.

Brown AS, Begg MD, Gravenstein S, Schaefer CA, Wyatt RJ, Bresnahan M, Babulas VP, Susser ES (2004) Serologic evidence of prenatal influenza in the etiology of schizophrenia. Archives of general psychiatry 61:774-780.

Bryan KJ, Zhu X, Harris PL, Perry G, Castellani RJ, Smith MA, Casadesus G (2008) Expression of CD74 is increased in neurofibrillary tangles in Alzheimer's disease. Molecular neurodegeneration 3:13.

Bsibsi M, Ravid R, Gveric D, van Noort JM (2002) Broad expression of Toll-like receptors in the human central nervous system. Journal of neuropathology and experimental neurology 61:1013-1021.

Buccafusco JJ (2000) Methods of behavior analysis in neuroscience: Crc Press.

Cajal SRY (1894) The Croonian Lecture: La fine structure des centres nerveux. Proceedings of the Royal Society of London 55:444-468.

Calabrese F, Rossetti AC, Racagni G, Gass P, Riva MA, Molteni R (2014) Brain-derived neurotrophic factor: a bridge between inflammation and neuroplasticity. Frontiers in Cellular Neuroscience 8.

Calvet M-C, Gresser I (1979) Interferon enhances the excitability of cultured neurones. Nature 278:558-560.

Capuron L, Miller AH (2004) Cytokines and psychopathology: lessons from interferon-α. Biological psychiatry 56:819-824.

Capuron L, Miller AH (2011) Immune System to Brain Signaling: Neuropsychopharmacological Implications. Pharmacology & therapeutics 130:226-238.

Carlson M (2014) MmAgilentDesign026655.db: Agilent Chips that use Agilent design number 026655 annotation data (chip MmAgilentDesign026655).R package version 2.14.0. http://www.bioconductor.org/packages/release/data/annotation/html/MmAgilentDesign026655.db.html.

Carpentier PA, Begolka WS, Olson JK, Elhofy A, Karpus WJ, Miller SD (2005) Differential activation of astrocytes by innate and adaptive immune stimuli. Glia 49:360-374.

CDC (2012) Severe influenza among children and young adults with neurologic and neurodevelopmental conditions - Ohio, 2011. MMWR Morbidity and mortality weekly report 60:1729-1733.

Cekanaviciute E, Buckwalter MS (2016) Astrocytes: Integrative regulators of neuroinflammation in stroke and other neurological diseases. Neurotherapeutics 13:685-701.

Chang JY, Martin DP, Johnson EM (1990) Interferon suppresses sympathetic neuronal cell death caused by nerve growth factor deprivation. Journal of neurochemistry 55:436-445.

Chang PK, Khatchadourian A, McKinney RA, Maysinger D (2015) Docosahexaenoic acid (DHA): a modulator of microglia activity and dendritic spine morphology. Journal of neuroinflammation 12:34.

Chen C-J, Ou Y-C, Lin S-Y, Raung S-L, Liao S-L, Lai C-Y, Chen S-Y, Chen J-H (2010) Glial activation involvement in neuronal death by Japanese encephalitis virus infection. Journal of General Virology 91:1028-1037.

Chesnokova V, Pechnick RN, Wawrowsky K (2016) Chronic peripheral inflammation, hippocampal neurogenesis, and behavior. Brain, behavior, and immunity 58:1-8.

Cheung CY, Poon LL, Lau AS, Luk W, Lau YL, Shortridge KF, Gordon S, Guan Y, Peiris JS (2002) Induction of proinflammatory cytokines in human macrophages by influenza A (H5N1) viruses: a mechanism for the unusual severity of human disease? Lancet (London, England) 360:1831-1837.

Chiu IM, Morimoto ETA, Goodarzi H, Liao JT, O'Keeffe S, Phatnani HP, Muratet M, Carroll MC, Levy S, Tavazoie S, Myers RM, Maniatis T (2013) A neurodegeneration-specific gene expression signature and immune profile of acutely isolated microglia from an ALS mouse model. Cell reports 4:385-401.

Cho H, Proll SC, Szretter KJ, Katze MG, Gale Jr M, Diamond MS (2013) Differential innate immune response programs in neuronal subtypes determine susceptibility to infection in the brain by positive-stranded RNA viruses. Nature medicine 19:458-464.

Choleris E, Thomas A, Kavaliers M, Prato F (2001) A detailed ethological analysis of the mouse open field test: effects of diazepam, chlordiazepoxide and an extremely low frequency pulsed magnetic field. Neuroscience & Biobehavioral Reviews 25:235-260.

Chung W-S, Welsh CA, Barres BA, Stevens B (2015a) Do glia drive synaptic and cognitive impairment in disease? Nature neuroscience 18:1539.

Chung WS, Allen NJ, Eroglu C (2015b) Astrocytes Control Synapse Formation, Function, and Elimination. Cold Spring Harbor Perspectives in Biology 7.

Churchwell JC, Kesner RP (2011) Hippocampal-prefrontal dynamics in spatial working memory: interactions and independent parallel processing. Behavior Brain Research 225:389-395.

Citri A, Malenka RC (2008) Synaptic plasticity: multiple forms, functions, and mechanisms. Neuropsychopharmacology 33:18.

Collingridge GL, Isaac JT, Wang YT (2004) Receptor trafficking and synaptic plasticity. Nature Reviews Neuroscience 5:952-962.

Cooper DS, Saxena NC, Yang HS, Lee HJ, Moring AG, Lee A, Choi I (2005) Molecular and functional characterization of the electroneutral Na/HCO3 cotransporter NBCn1 in rat hippocampal neurons. The Journal of biological chemistry 280:17823-17830.

Copf T, Goguel V, Lampin-Saint-Amaux A, Scaplehorn N, Preat T (2011) Cytokine signaling through the JAK/STAT pathway is required for long-term memory in Drosophila. Proceedings of the National Academy of Sciences of the United States of America 108:8059-8064.

Costello DA, Lynch MA (2013) Toll-like receptor 3 activation modulates hippocampal network excitability, via glial production of interferon-β. Hippocampus 23:696-707.

Cox R, Brokstad K, Ogra P (2004) Influenza virus: immunity and vaccination strategies. Comparison of the immune response to inactivated and live, attenuated influenza vaccines. Scandinavian journal of immunology 59:1-15.

Crotti A, Ransohoff RM (2016) Microglial physiology and pathophysiology: insights from genome-wide transcriptional profiling. Immunity 44:505-515.

Cunningham C, Campion S, Teeling J, Felton L, Perry V (2007) The sickness behaviour and CNS inflammatory mediator profile induced by systemic challenge of mice with synthetic double-stranded RNA (poly I: C). Brain, behavior, and immunity 21:490-502.

Cuthbert PC (2007) Synapse-Associated Protein 102/dlgh3 Couples the NMDA Receptor to Specific Plasticity Pathways and Learning Strategies. 27:2673-2682.

D'Arcangelo G, Grassi F, Ragozzino D, Santoni A, Tancredi V, Eusebi F (1991) Interferon inhibits synaptic potentiation in rat hippocampus. Brain research 564:245-248.

D'Mello C, Swain MG (2014) Liver-brain interactions in inflammatory liver diseases: implications for fatigue and mood disorders. Brain, behavior, and immunity 35:9-20.

D'Mello C, Le T, Swain MG (2009) Cerebral microglia recruit monocytes into the brain in response to tumor necrosis factoralpha signaling during peripheral organ inflammation. The Journal of neuroscience : the official journal of the Society for Neuroscience 29:2089-2102.

D'Hooge R, De Deyn PP (2001) Applications of the Morris water maze in the study of learning and memory. Brain research reviews 36:60-90.

Dantzer R, Konsman JP, Bluthe RM, Kelley KW (2000) Neural and humoral pathways of communication from the immune system to the brain: parallel or convergent? Autonomic neuroscience : basic & clinical 85:60-65.

Dantzer R, O'Connor JC, Freund GG, Johnson RW, Kelley KW (2008) From inflammation to sickness and depression: when the immune system subjugates the brain. Nature reviews Neuroscience 9:46-56.

David Y, Cacheaux LP, Ivens S, Lapilover E, Heinemann U, Kaufer D, Friedman A (2009) Astrocytic dysfunction in epileptogenesis: consequence of altered potassium and glutamate homeostasis? Journal of Neuroscience 29:10588-10599.

Davis LE, Koster F, Cawthon A (2014) Neurologic aspects of influenza viruses. Handbook of clinical neurology 123:619-645.

De Araujo EG, Da Silva GM, Dos Santos AA (2009) Neuronal Cell Survival. Annals of the New York Academy of Sciences 1153:57-64.

Deczkowska A, Baruch K, Schwartz M (2016) Type I/II interferon balance in the regulation of brain physiology and pathology. Trends in immunology 37:181-192.

Demyanenko GP, Mohan V, Zhang X, Brennaman LH, Dharbal KES, Tran TS, Manis PB, Maness PF (2014) Neural Cell Adhesion Molecule NrCAM Regulates Semaphorin 3F-Induced Dendritic Spine Remodeling. The Journal of neuroscience : the official journal of the Society for Neuroscience 34:11274-11287.

Detje CN, Meyer T, Schmidt H, Kreuz D, Rose JK, Bechmann I, Prinz M, Kalinke U (2009) Local type I IFN receptor signaling protects against virus spread within the central nervous system. Journal of immunology (Baltimore, Md : 1950) 182:2297-2304.

Detje CN, Lienenklaus S, Chhatbar C, Spanier J, Prajeeth CK, Soldner C, Tovey MG, Schlüter D, Weiss S, Stangel M (2015) Upon intranasal vesicular stomatitis virus infection, astrocytes in the olfactory bulb are important interferon Beta producers that protect from lethal encephalitis. Journal of virology 89:2731-2738.

Donzis EJ, Tronson NC (2014) Modulation of learning and memory by cytokines: signaling mechanisms and long term consequences. Neurobiology of learning and memory 115:68-77.

Eccles R (2005) Understanding the symptoms of the common cold and influenza. The Lancet Infectious diseases 5:718-725.

Ejlerskov P, Hultberg J G, Wang JY, Carlsson R, Ambjørn M, Kuss M, Liu Y, Porcu G, Kolkova K, Friis Rundsten C, Ruscher K, Pakkenberg B, Goldmann T, Loreth D,

Prinz M, Rubinsztein D C, Issazadeh-Navikas S (2015) Lack of Neuronal IFN-β-IFNAR Causes Lewy Body- and Parkinson's Disease-like Dementia. Cell 163:324-339.

Ekstrand JJ (2012) Neurologic complications of influenza. Seminars in pediatric neurology 19:96-100.

Elliott R, Li F, Dragomir I, Chua MMW, Gregory BD, Weiss SR (2013) Analysis of the Host Transcriptome from Demyelinating Spinal Cord of Murine Coronavirus-Infected Mice. PloS one 8.

Elmore MR, Burton MD, Conrad MS, Rytych JL, Van Alstine WG, Johnson RW (2014) Respiratory viral infection in neonatal piglets causes marked microglia activation in the hippocampus and deficits in spatial learning. The Journal of neuroscience : the official journal of the Society for Neuroscience 34:2120-2129.

Emptage NJ, Reid CA, Fine A (2001) Calcium stores in hippocampal synaptic boutons mediate short-term plasticity, store-operated Ca 2+ entry, and spontaneous transmitter release. Neuron 29:197-208.

Estes ML, McAllister AK (2015) Immune mediators in the brain and peripheral tissues in autism spectrum disorder. Nature reviews Neuroscience 16:469-486.

Fazakerley JK, Walker R (2003) Virus demyelination. Journal of neurovirology 9:148-164.

Fouchier RA, Schneeberger PM, Rozendaal FW, Broekman JM, Kemink SA, Munster V, Kuiken T, Rimmelzwaan GF, Schutten M, Van Doornum GJ, Koch G, Bosman A, Koopmans M, Osterhaus AD (2004) Avian influenza A virus (H7N7) associated with human conjunctivitis and a fatal case of acute respiratory distress syndrome. Proceedings of the National Academy of Sciences of the United States of America 101:1356-1361.

Frank-Cannon TC, Alto LT, McAlpine FE, Tansey MG (2009) Does neuroinflammation fan the flame in neurodegenerative diseases? Molecular neurodegeneration 4:47.

Fraser K, Nairn R, McEntegart M, Chadwick C (1959) Neurotropic and non-neurotropic influenza-A infection of mouse brain studied with fluorescent antibody. The Journal of Pathology 78:423-433.

Fry M, Ferguson AV (2007) The sensory circumventricular organs: brain targets for circulating signals controlling ingestive behavior. Physiology & behavior 91:413-423.

Fu R, Shen Q, Xu P, Luo JJ, Tang Y (2014) Phagocytosis of Microglia in the Central Nervous System Diseases. Molecular Neurobiology 49:1422-1434.

Gabriel G, Dauber B, Wolff T, Planz O, Klenk HD, Stech J (2005) The viral polymerase mediates adaptation of an avian influenza virus to a mammalian host. Proceedings of the National Academy of Sciences of the United States of America 102:18590-18595.

Gao Y-J, Ji R-R (2010) Chemokines, neuronal–glial interactions, and central processing of neuropathic pain. Pharmacology & therapeutics 126:56-68.

Garcia O, Torres M, Helguera P, Coskun P, Busciglio J (2010) A Role for Thrombospondin-1 Deficits in Astrocyte-Mediated Spine and Synaptic Pathology in Down's Syndrome. PLoS One 5.

Garden GA (2002) Microglia in human immunodeficiency virus-associated neurodegeneration. Glia 40:240-251.

Garthe A, Kempermann G (2013) An old test for new neurons: refining the Morris water maze to study the functional relevance of adult hippocampal neurogenesis. Frontiers in Neuroscience 7.

Garthe A, Behr J, Kempermann G (2009) Adult-generated hippocampal neurons allow the flexible use of spatially precise learning strategies. PloS one 4:e5464.

Gentleman RC et al. (2004) Bioconductor: open software development for computational biology and bioinformatics. Genome biology 5:R80.

Geurs TL, Hill EB, Lippold DM, French AR (2012) Sex Differences in Murine Susceptibility to Systemic Viral Infections. Journal of Autoimmunity 38:J245-253.

Gimsa U, Mitchison NA, Brunner-Weinzierl MC (2013) Immune Privilege as an Intrinsic CNS Property: Astrocytes Protect the CNS against T-Cell-Mediated Neuroinflammation. Mediators of Inflammation 2013:320519.

Goffinet C (2016) Cellular Antiviral Factors that Target Particle Infectivity of HIV-1. Current HIV Research 14:211-216.

Goubert E, Mircheva Y, Lasorsa FM, Melon C, Profilo E, Sutera J, Becq H, Palmieri F, Palmieri L, Aniksztejn L, Molinari F (2017) Inhibition of the Mitochondrial Glutamate Carrier SLC25A22 in Astrocytes Leads to Intracellular Glutamate Accumulation. Frontiers in Cellular Neuroscience 11.

Griffin DE (2003) Immune responses to RNA-virus infections of the CNS. Nature reviews Immunology 3:493.

Group IMSS (1993) Interferon beta-1b is effective in relapsing-remitting multiple sclerosis I. Clinical results of a multicenter, randomized, double-blind, placebo-controlled trial. Neurology 43:655-655.

Guyon A, Massa F, Rovere C, Nahon JL (2008) How cytokines can influence the brain: a role for chemokines? J Neuroimmunol 198:46-55.

Haller O, Arnheiter H, Lindenmann J (1979) Natural, genetically determined resistance toward influenza virus in hemopoietic mouse chimeras. Role of mononuclear phagocytes. The Journal of experimental medicine 150:117-126.

Hanisch UK (2002) Microglia as a source and target of cytokines. Glia 40:140-155.

Hanke ML, Kielian T (2011) Toll-like receptors in health and disease in the brain: mechanisms and therapeutic potential. Clinical Science 121:367-387.

Haskó G, Pacher P, Vizi ES, Illes P (2005) Adenosine receptor signaling in the brain immune system. Trends in pharmacological sciences 26:511-516.

Heneka MT, Kummer MP, Latz E (2014) Innate immune activation in neurodegenerative disease. Nature reviews Immunology 14:463.

Henry J, Smeyne RJ, Jang H, Miller B, Okun MS (2010) Parkinsonism and neurological manifestations of influenza throughout the 20th and 21st centuries. Parkinsonism & related disorders 16:566-571.

Hickman SE, Kingery ND, Ohsumi T, Borowsky M, Wang L, Means TK, Khoury JE (2013) The Microglial Sensome Revealed by Direct RNA Sequencing. Nature neuroscience 16:1896-1905.

Hodgson NR, Bohnet SG, Majde JA, Krueger JM (2012) Influenza virus pathophysiology and brain invasion in mice with functional and dysfunctional Mx1 genes. Brain, behavior, and immunity 26:83-89.

Hofer MJ, Campbell IL (2013) Type I interferon in neurological disease—The devil from within. Cytokine & growth factor reviews 24:257-267.

Hogg S (1996) A review of the validity and variability of the elevated plus-maze as an animal model of anxiety. Pharmacology Biochemistry and Behavior 54:21-30.

Hosmane S, Tegenge MA, Rajbhandari L, Uapinyoying P, Kumar NG, Thakor N, Venkatesan A (2012) Toll/interleukin-1 receptor domain-containing adapter inducing interferon-β mediates microglial phagocytosis of degenerating axons. Journal of Neuroscience 32:7745-7757.

Howe CL, Lafrance-Corey RG, Sundsbak RS, Lafrance SJ (2012) Inflammatory monocytes damage the hippocampus during acute picornavirus infection of the brain. Journal of neuroinflammation 9:50.

Hoyo-Becerra C, Liu Z, Yao J, Kaltwasser B, Gerken G, Hermann DM, Schlaak JF (2015) Rapid Regulation of Depression-Associated Genes in a New Mouse Model Mimicking Interferon-alpha-Related Depression in Hepatitis C Virus Infection. Molecular Neurobiology 52:318-329.

Hristovska I, Pascual O (2015) Deciphering resting microglial morphology and process motility from a synaptic prospect. Frontiers in integrative neuroscience 9.

Huang EJ, Reichardt LF (2001) Neurotrophins: Roles in Neuronal Development and Function. Annual review of neuroscience 24:677-736.

Hughes V (2012) Microglia: The constant gardeners. Nature 485:570-572.

Ignatowski TA, Spengler RN (2008) Cytokines in synaptic function. NeuroImmune Biology 6:109-143.

Ii PAS, McGavern DB (2015) Portals of Viral Entry into the Central Nervous System. The Blood-Brain Barrier in Health and Disease, Volume Two: Pathophysiology and Pathology:23.

Irani DN, Griffin DE (2001) Regulation of T cell responses during central nervous system viral infection. Advances in virus research 56:175-197.

Jang H, Boltz D, Sturm-Ramirez K, Shepherd KR, Jiao Y, Webster R, Smeyne RJ (2009) Highly pathogenic H5N1 influenza virus can enter the central nervous system and induce neuroinflammation and neurodegeneration. Proceedings of the National Academy of Sciences 106:14063-14068.

Jang H, Boltz D, McClaren J, Pani AK, Smeyne M, Korff A, Webster R, Smeyne RJ (2012) Inflammatory effects of highly pathogenic H5N1 influenza virus infection in the CNS of mice. The Journal of neuroscience : the official journal of the Society for Neuroscience 32:1545-1559.

Jonakait GM (1996) Cytokines in neuronal development. Advances in Pharmacology 37:35-67.

Joseph-Silverstein J, Silverstein RL (1998) Cell adhesion molecules: an overview. Cancer investigation 16:176-182.

Jurgens HA, Amancherla K, Johnson RW (2012) Influenza infection induces neuroinflammation, alters hippocampal neuron morphology, and impairs cognition in adult mice. The Journal of neuroscience : the official journal of the Society for Neuroscience 32:3958-3968.

Kaji M, Watanabe A, Aizawa H (2003) Differences in clinical features between influenza A H1N1, A H3N2, and B in adult patients. Respirology (Carlton, Vic) 8:231-233.

Kamphuis E, Junt T, Waibler Z, Forster R, Kalinke U (2006) Type I interferons directly regulate lymphocyte recirculation and cause transient blood lymphopenia. Blood 108:3253-3261.

Kanehisa M, Goto S (2000) KEGG: kyoto encyclopedia of genes and genomes. Nucleic acids research 28:27-30.

Kettenmann H, Kirchhoff F, Verkhratsky A (2013) Microglia: new roles for the synaptic stripper. Neuron 77:10-18.

Khandaker GM (2016) Is there a role for immune-to-brain communication in schizophrenia? 233:1559-1573.

Khorooshi R, Owens T (2010) Injury-induced type I IFN signaling regulates inflammatory responses in the central nervous system. The Journal of Immunology 185:1258-1264.

Kim I-J, Beck HN, Lein PJ, Higgins D (2002) Interferon γ induces retrograde dendritic retraction and inhibits synapse formation. Journal of Neuroscience 22:4530-4539.

Klein MS, Conn CA, Kluger MJ (1992) Behavioral thermoregulation in mice inoculated with influenza virus. Physiology & behavior 52:1133-1139.

Klein RS, Garber C, Howard N (2017) Infectious immunity in the central nervous system and brain function. Nat Immunol 18:132-141.

Klenk H-D, Matrosovich M, Stech J (2008) Avian Influenza: Molecular Mechanisms of Pathogenesis and Host Range. Animal Viruses: Molecular Biology:253.

Korte M, Schmitz D (2016) Cellular and system biology of memory: timing, molecules, and beyond. Physiological reviews 96:647-693.

Kraft AD, Harry GJ (2011) Features of Microglia and Neuroinflammation Relevant to Environmental Exposure and Neurotoxicity. International Journal of Environmental Research and Public Health 8:2980-3018.

Kristensson K (2006) Avian influenza and the brain--comments on the occasion of resurrection of the Spanish flu virus. Brain research bulletin 68:406-413.

Kuiken T, Taubenberger JK (2008) Pathology of human influenza revisited. Vaccine 26 Suppl 4:D59-66.

Kurpius D, Wilson N, Fuller L, Hoffman A, Dailey ME (2006) Early activation, motility, and homing of neonatal microglia to injured neurons does not require protein synthesis. Glia 54:58-70.

Kyrkanides S, Miller AW, Miller JH, Tallents RH, Brouxhon SM, Olschowka ME, O'Banion MK, Olschowka JA (2008) Peripheral blood mononuclear cell infiltration and neuroinflammation in the HexB(−/−) mouse model of neurodegeneration. J Neuroimmunol 203:50-57.

Landel V, Baranger K, Virard I, Loriod B, Khrestchatisky M, Rivera S, Benech P, Féron F (2014) Temporal gene profiling of the 5XFAD transgenic mouse model highlights the importance of microglial activation in Alzheimer's disease. Molecular neurodegeneration 9:33.

Lang G, Gagnon A, Geraci JR (1981) Isolation of an influenza A virus from seals. Archives of virology 68:189-195.

Laterra J, Keep R, Betz AL, Goldstein G (1999) Blood-brain-cerebrospinal fluid barriers. Basic neurochemistry: molecular, cellular and medical aspects:671-689.

Laurent C et al. (2017) Hippocampal T cell infiltration promotes neuroinflammation and cognitive decline in a mouse model of tauopathy. Brain 140:184-200.

Lee AS, De Jesus-Cortes H, Kabir ZD, Knobbe W, Orr M, Burgdorf C, Huntington P, McDaniel L, Britt JK, Hoffmann F, Brat DJ, Rajadhyaksha AM, Pieper AA (2016a) The Neuropsychiatric Disease-Associated Gene cacna1c Mediates Survival of Young Hippocampal Neurons. eNeuro 3.

Lee H-C, Tan K-L, Cheah P-S, Ling K-H (2016b) Potential role of JAK-STAT signaling pathway in the neurogenic-to-gliogenic shift in down syndrome brain. Neural plasticity 2016.

Leist SR, Pilzner C, van den Brand JM, Dengler L, Geffers R, Kuiken T, Balling R, Kollmus H, Schughart K (2016) Influenza H3N2 infection of the collaborative cross founder strains reveals highly divergent host responses and identifies a unique phenotype in CAST/EiJ mice. BMC genomics 17:143.

Li F, Wang Y, Yu L, Cao S, Wang K, Yuan J, Wang C, Wang K, Cui M, Fu ZF (2015) Viral infection of the central nervous system and neuroinflammation precede blood-brain barrier disruption during Japanese encephalitis virus infection. Journal of virology 89:5602-5614.

Liang H, Hippenmeyer S, Ghashghaei HT (2012) A Nestin-cre transgenic mouse is insufficient for recombination in early embryonic neural progenitors. Biology open:BIO20122287.

Liddelow SA et al. (2017) Neurotoxic reactive astrocytes are induced by activated microglia. Nature 541:481-487.

Lin YS, Wang HY, Huang DF, Hsieh PF, Lin MY, Chou CH, Wu IJ, Huang GJ, Gau SS, Huang HS (2016) Neuronal Splicing Regulator RBFOX3 (NeuN) Regulates Adult Hippocampal Neurogenesis and Synaptogenesis. PloS one 11:e0164164.

Linthorst AC, Flachskamm C, Muller-Preuss P, Holsboer F, Reul JM (1995) Effect of bacterial endotoxin and interleukin-1 beta on hippocampal serotonergic neurotransmission, behavioral activity, and free corticosterone levels: an in vivo microdialysis study. Journal of Neuroscience 15:2920-2934.

Liu Y, Liu F, Iqbal K, Grundke-Iqbal I, Gong CX (2008) Decreased glucose transporters correlate to abnormal hyperphosphorylation of tau in Alzheimer disease. FEBS letters 582:359-364.

Lovell M (2009) A Potential Role for Alterations of Zinc and Zinc Transport Proteins in the Progression of Alzheimer's Disease. Journal of Alzheimer's disease : JAD 16:471-483.

Lu B, Nagappan G, Lu Y (2014) BDNF and synaptic plasticity, cognitive function, and dysfunction. Handbook of experimental pharmacology 220:223-250.

Ludlow M, Kortekaas J, Herden C, Hoffmann B, Tappe D, Trebst C, Griffin DE, Brindle HE, Solomon T, Brown AS, van Riel D, Wolthers KC, Pajkrt D, Wohlsein P, Martina BE, Baumgartner W, Verjans GM, Osterhaus AD (2016) Neurotropic virus infections as the cause of immediate and delayed neuropathology. Acta neuropathologica 131:159-184.

Lynch MA (2002) Interleukin-1β exerts a myriad of effects in the brain and in particular in the hippocampus: analysis of some of these actions. Vitamins & Hormones 64:185-219.

Maines TR, Lu XH, Erb SM, Edwards L, Guarner J, Greer PW, Nguyen DC, Szretter KJ, Chen L-M, Thawatsupha P (2005) Avian influenza (H5N1) viruses isolated from humans in Asia in 2004 exhibit increased virulence in mammals. Journal of virology 79:11788-11800.

Majde JA, Kapás L, Bohnet SG, De A, Krueger JM (2010) Attenuation of the Influenza Virus Sickness Behavior in Mice Deficient in Toll-like Receptor 3. Brain, behavior, and immunity 24:306.

Majde JA, Bohnet SG, Ellis GA, Churchill L, Leyva-Grado V, Wu M, Szentirmai E, Rehman A, Krueger JM (2007) Detection of mouse-adapted human influenza virus

in the olfactory bulbs of mice within hours after intranasal infection. Journal of neurovirology 13:399-409.

Majumdar D, Bevensee MO (2010) Na-coupled bicarbonate transporters of the Slc4 family in the nervous system: function, localization, and relevance to neurologic function. Neuroscience 171:951-972.

Mak CM, Lam CW, Fong NC, Siu WK, Lee HC, Siu TS, Lai CK, Law CY, Tong SF, Poon WT, Lam DS, Ng HL, Yuen YP, Tam S, Que TL, Kwong NS, Chan AY (2011) Fatal viral infection-associated encephalopathy in two Chinese boys: a genetically determined risk factor of thermolabile carnitine palmitoyltransferase II variants. Journal of human genetics 56:617-621.

Malenka RC, Bear MF (2004) LTP and LTD: an embarrassment of riches. Neuron 44:5-21.

Marin I, Kipnis J (2013) Learning and memory … and the immune system. Learning Memory 20:601-606.

Mastronardi CA, Paz-Filho G, Zanoni M, Molano-González N, Arcos-Burgos M, Licinio J, Wong ML (2015) Temporal gene expression in the hippocampus and peripheral organs to endoxin-induced systemic inflammatory response in caspase-1 deficient mice. Neuroimmunomodulation 22:263-273.

McCall S, Vilensky JA, Gilman S, Taubenberger JK (2008) The relationship between encephalitis lethargica and influenza: A critical analysis. Journal of Neurovirology 14:177-185.

McGlasson S, Hunt D (2017) Neuroinflammation: Synapses pruned in lupus. Nature advance online publication.

Mehler MF, Kessler JA (1998) Cytokines in Brain Development and Function. In: Advances in Protein Chemistry (Richards FM, Eisenberg DS, Kim PS, eds), pp 223-251: Academic Press.

Menachem-Zidon OB, Avital A, Ben-Menahem Y, Goshen I, Kreisel T, Shmueli EM, Segal M, Hur TB, Yirmiya R (2011) Astrocytes support hippocampal-dependent memory and long-term potentiation via interleukin-1 signaling. Brain, behavior, and immunity 25:1008-1016.

Mendoza-Fernandez V, Andrew RD, Barajas-Lopez C (2000) Interferon-α inhibits long-term potentiation and unmasks a long-term depression in the rat hippocampus. Brain research 885:14-24.

Milatovic D, Zaja-Milatovic S, Montine KS, Horner PJ, Montine TJ (2003) Pharmacologic suppression of neuronal oxidative damage and dendritic degeneration following direct activation of glial innate immunity in mouse cerebrum. Journal of neurochemistry 87:1518-1526.

Miller AH, Maletic V, Raison CL (2009) Inflammation and Its Discontents: The Role of Cytokines in the Pathophysiology of Major Depression. Biological psychiatry 65:732-741.

Minichiello L, Calella AM, Medina DL, Bonhoeffer T, Klein R, Korte M (2002) Mechanism of TrkB-mediated hippocampal long-term potentiation. Neuron 36:121-137.

Mittelbronn M, Dietz K, Schluesener HJ, Meyermann R (2001) Local distribution of microglia in the normal adult human central nervous system differs by up to one order of magnitude. Acta neuropathologica 101:249-255.

Mizuguchi M (2013) Influenza encephalopathy and related neuropsychiatric syndromes. Influenza and other respiratory viruses 7 Suppl 3:67-71.

Mody M, Cao Y, Cui Z, Tay K-Y, Shyong A, Shimizu E, Pham K, Schultz P, Welsh D, Tsien JZ (2001) Genome-wide gene expression profiles of the developing mouse hippocampus. Proceedings of the National Academy of Sciences 98:8862-8867.

Morris R (1984) Developments of a water-maze procedure for studying spatial learning in the rat. Journal of neuroscience methods 11:47-60.

Moser M-B, Trommald M, Andersen P (1994) An increase in dendritic spine density on hippocampal CA1 pyramidal cells following spatial learning in adult rats suggests the formation of new synapses. Proceedings of the National Academy of Sciences 91:12673-12675.

Mu M, Fontana A, Zbinden G, Ga BH (1993) Effects of interferons and hydrogen peroxide on CA3 pyramidal cells in rat hippocampal slice cultures. Brain research 619:157-162.

Muller U, Steinhoff U, Reis LF, Hemmi S, Pavlovic J, Zinkernagel RM, Aguet M (1994) Functional role of type I and type II interferons in antiviral defense. Science (New York, NY) 264:1918-1921.

Münch G, Gasic-Milenkovic J, Dukic-Stefanovic S, Kuhla B, Heinrich K, Riederer P, Huttunen HJ, Founds H, Sajithlal G (2003) Microglial activation induces cell death, inhibits neurite outgrowth and causes neurite retraction of differentiated neuroblastoma cells. Experimental brain research 150:1-8.

Murray PJ (2007) The JAK-STAT signaling pathway: input and output integration. Journal of immunology (Baltimore, Md : 1950) 178:2623-2629.

Nakamura Y (2002) Regulating factors for microglial activation. Biological & pharmaceutical bulletin 25:945-953.

Nakamura Y, Si QS, Kataoka K (1999) Lipopolysaccharide-induced microglial activation in culture: temporal profiles of morphological change and release of cytokines and nitric oxide. Neuroscience research 35:95-100.

Neumann H, Schmidt H, Cavalié A, Jenne D, Wekerle H (1997) Major Histocompatibility Complex (MHC) Class I Gene Expression in Single Neurons of the Central Nervous System: Differential Regulation by Interferon (IFN)-γ and Tumor Necrosis Factor (TNF)-α. The Journal of experimental medicine 185:305-316.

Neumann H, Schweigreiter R, Yamashita T, Rosenkranz K, Wekerle H, Barde Y-A (2002) Tumor necrosis factor inhibits neurite outgrowth and branching of hippocampal neurons by a rho-dependent mechanism. Journal of Neuroscience 22:854-862.

Nichol KL, Treanor JJ (2006) Vaccines for seasonal and pandemic influenza. The Journal of infectious diseases 194:S111-S118.

Nicholls JM, Chan RW, Russell RJ, Air GM, Peiris JS (2008) Evolving complexities of influenza virus and its receptors. Trends in microbiology 16:149-157.

Nicoll RA (2017) A Brief History of Long-Term Potentiation. Neuron 93:281-290.

Nimmerjahn A, Kirchhoff F, Helmchen F (2005) Resting microglial cells are highly dynamic surveillants of brain parenchyma in vivo. Science (New York, NY) 308:1314-1318.

Nuttall JR, Oteiza PI (2014) Zinc and the aging brain. Genes & Nutrition 9.

Orre M, Kamphuis W, Dooves S, Kooijman L, Chan ET, Kirk CJ, Dimayuga Smith V, Koot S, Mamber C, Jansen AH, Ovaa H, Hol EM (2013) Reactive glia show increased immunoproteasome activity in Alzheimer's disease. Brain 136:1415-1431.

Ota Y, Zanetti AT, Hallock RM (2013) The role of astrocytes in the regulation of synaptic plasticity and memory formation. Neural plasticity 2013.

Owens T, Khorooshi R, Wlodarczyk A, Asgari N (2014) Interferons in the central nervous system: a few instruments play many tunes. Glia 62:339-355.

Pannasch U, Vargova L, Reingruber J, Ezan P, Holcman D, Giaume C, Sykova E, Rouach N (2011) Astroglial networks scale synaptic activity and plasticity. Proceedings of the National Academy of Sciences of the United States of America 108:8467-8472.

Papageorgiou IE, Fetani AF, Lewen A, Heinemann U, Kann O (2015) Widespread activation of microglial cells in the hippocampus of chronic epileptic rats correlates only partially with neurodegeneration. Brain structure & function 220:2423-2439.

Parboosing R, Bao Y, Shen L, Schaefer CA, Brown AS (2013) Gestational influenza and bipolar disorder in adult offspring. JAMA psychiatry 70:677-685.

Park H, Yu JE, Kim S, Nahm SS, Chung C (2015) Decreased Na(+) influx lowers hippocampal neuronal excitability in a mouse model of neonatal influenza infection. Scientific reports 5:13440.

Parkhurst CN, Yang G, Ninan I, Savas JN, Yates JR, Lafaille JJ, Hempstead BL, Littman DR, Gan W-B (2013) Microglia promote learning-dependent synapse formation through brain-derived neurotrophic factor. Cell 155:1596-1609.

Patterson SL, Abel T, Deuel TA, Martin KC, Rose JC, Kandel ER (1996) Recombinant BDNF rescues deficits in basal synaptic transmission and hippocampal LTP in BDNF knockout mice. Neuron 16:1137-1145.

Perlmutter LS, Scott SA, Barron E, Chui HC (1992) MHC class II-positive microglia in human brain: association with Alzheimer lesions. Journal of neuroscience research 33:549-558.

Pestka S, Krause CD, Walter MR (2004) Interferons, interferon-like cytokines, and their receptors. Immunological Reviews 202:8-32.

Pickering M, O'Connor JJ (2007) Pro-inflammatory cytokines and their effects in the dentate gyrus. Progress in brain research 163:339-354.

Pivneva T (2008) Microglia in normal condition and pathology. Fiziol Zh 54:81-89.

Platanias LC (2005) Mechanisms of type-I-and type-II-interferon-mediated signalling. Nature Reviews Immunology 5:375-386.

Plioplys AV (1988) Expression of the 210 kDa neurofilament subunit in cultured central nervous system from normal and trisomy 16 mice: regulation by interferon. Journal of the Neurological Sciences 85:209-222.

Porter NM, Bohannon JH, Curran-Rauhut M, Buechel HM, Dowling AL, Brewer LD, Popovic J, Thibault V, Kraner SD, Chen KC, Blalock EM (2012) Hippocampal CA1 transcriptional profile of sleep deprivation: relation to aging and stress. PloS one 7:e40128.

Ramesh G, MacLean AG, Philipp MT (2013) Cytokines and chemokines at the crossroads of neuroinflammation, neurodegeneration, and neuropathic pain. Mediators of inflammation 2013.

Ransohoff RM (2009) Chemokines and chemokine receptors: Standing at the crossroads of immunobiology and neurobiology. Immunity 31:711-721.

Ravenholt R, Foege W (1982) 1918 influenza, encephalitis lethargica, parkinsonism. The Lancet 320:860-864.

Renegar K (1992) Influenza virus infections and immunity: a review of human and animal models. Laboratory animal science 42:222-232.

Riazi K, Galic MA, Kentner AC, Reid AY, Sharkey KA, Pittman QJ (2015) Microglia-dependent alteration of glutamatergic synaptic transmission and plasticity in the hippocampus during peripheral inflammation. Journal of Neuroscience 35:4942-4952.

Richter JD, Klann E (2009) Making synaptic plasticity and memory last: mechanisms of translational regulation. Genes & development 23:1-11.

Rock RB, Gekker G, Hu S, Sheng WS, Cheeran M, Lokensgard JR, Peterson PK (2004) Role of Microglia in Central Nervous System Infections. Clinical Microbiology Reviews 17:942-964.

Rogers TJ (2012) The Molecular Basis for Neuroimmune Receptor Signaling. Journal of neuroimmune pharmacology : the official journal of the Society on NeuroImmune Pharmacology 7:722-724.

Rubin SA, Sylves P, Vogel M, Pletnikov M, Moran TH, Schwartz GJ, Carbone KM (1999) Borna disease virus-induced hippocampal dentate gyrus damage is associated with spatial learning and memory deficits. Brain research bulletin 48:23-30.

Růžek D, Salát J, Singh SK, Kopecký J (2011) Breakdown of the Blood-Brain Barrier during Tick-Borne Encephalitis in Mice Is Not Dependent on CD8(+) T-Cells. PLoS One 6.

Scharfman HE, Binder DK (2013) Aquaporin-4 water channels and synaptic plasticity in the hippocampus. Neurochemistry international 63.

Schmitz N, Kurrer M, Bachmann MF, Kopf M (2005) Interleukin-1 is responsible for acute lung immunopathology but increases survival of respiratory influenza virus infection. Journal of virology 79:6441-6448.

Schneider H, Pitossi F, Balschun D, Wagner A, del Rey A, Besedovsky HO (1998) A neuromodulatory role of interleukin-1beta in the hippocampus. Proceedings of the National Academy of Sciences of the United States of America 95:7778-7783.

Segal M (2005) Dendritic spines and long-term plasticity. Nature reviews Neuroscience 6:277.

Shah S, Keil A, Gara K, Nagarajan L (2014) Neurologic complications of influenza. Journal of child neurology 29:Np49-53.

Shepardson KM, Larson K, Morton RV, Prigge JR, Schmidt EE, Huber VC, Rynda-Apple A (2016) Differential type I interferon signaling is a master regulator of susceptibility to postinfluenza bacterial superinfection. MBio 7:e00506-00516.

Shih AY, Fernandes HB, Choi FY, Kozoriz MG, Liu Y, Li P, Cowan CM, Klegeris A (2006) Policing the police: astrocytes modulate microglial activation. The Journal of neuroscience : the official journal of the Society for Neuroscience 26:3887-3888.

Shintani F, Kanba S, Nakaki T, Nibuya M, Kinoshita N, Suzuki E, Yagi G, Kato R, Asai M (1993) Interleukin-1 beta augments release of norepinephrine, dopamine, and serotonin in the rat anterior hypothalamus. Journal of Neuroscience 13:3574-3581.

Shinya K, Suto A, Kawakami M, Sakamoto H, Umemura T, Kawaoka Y, Kasai N, Ito T (2005) Neurovirulence of H7N7 influenza A virus: brain stem encephalitis accompanied with aspiration pneumonia in mice. Archives of virology 150:1653-1660.

Sinanan K, Hillary I (1981) Post-influenzal depression. The British journal of psychiatry : the journal of mental science 138:131-133.

Singh A, Abraham WC (2017) Astrocytes and synaptic plasticity in health and disease. Experimental Brain Research:1-11.

Smyth GK (2004) Linear models and empirical bayes methods for assessing differential expression in microarray experiments. Statistical applications in genetics and molecular biology 3:Article3.

Sofroniew MV (2009) Molecular dissection of reactive astrogliosis and glial scar formation. Trends in neurosciences 32:638-647.

Sofroniew MV, Vinters HV (2010) Astrocytes: biology and pathology. Acta neuropathologica 119:7-35.

Soulet D, Rivest S (2008) Microglia. Current Biology 18:R506-R508.

Spadaro PA, Flavell CR, Widagdo J, Ratnu VS, Troup M, Ragan C, Mattick JS, Bredy TW (2015) Long Noncoding RNA-Directed Epigenetic Regulation of Gene Expression Is Associated With Anxiety-like Behavior in Mice. Biological psychiatry 78:848-859.

Sroga JM, Jones T, Kigerl KA, McGaughy VM, Popovich PG (2003) Rats and mice exhibit distinct inflammatory reactions after spinal cord injury. Journal of Comparative Neurology 462:223-240.

Stellwagen D, Malenka RC (2006) Synaptic scaling mediated by glial TNF-[alpha]. Nature 440:1054.

Stellwagen D, Beattie EC, Seo JY, Malenka RC (2005) Differential regulation of AMPA receptor and GABA receptor trafficking by tumor necrosis factor-alpha. The Journal of neuroscience : the official journal of the Society for Neuroscience 25:3219-3228.

Stevens B, Allen NJ, Vazquez LE, Howell GR, Christopherson KS, Nouri N, Micheva KD, Mehalow AK, Huberman AD, Stafford B, Sher A, Litke AM, Lambris JD, Smith SJ, John SW, Barres BA (2007) The classical complement cascade mediates CNS synapse elimination. Cell 131:1164-1178.

Stevens CF, Wesseling JF (1999) Augmentation is a potentiation of the exocytotic process. Neuron 22:139-146.

Streit WJ, Mrak RE, Griffin WST (2004) Microglia and neuroinflammation: a pathological perspective. Journal of neuroinflammation 1:14.

Surana P, Tang S, McDougall M, Tong CY, Menson E, Lim M (2011) Neurological complications of pandemic influenza A H1N1 2009 infection: European case series and review. European journal of pediatrics 170:1007-1015.

Suzuki Y (2005) Sialobiology of influenza: molecular mechanism of host range variation of influenza viruses. Biological and Pharmaceutical Bulletin 28:399-408.

Swanson RA (2005) Astrocyte neurotransmitter uptake. Neuroglia Oxford University Press, Oxford:346-354.

Sweatt JD (1999) Toward a molecular explanation for long-term potentiation. Learning & Memory 6:399-416.

Takeshita Y, Ransohoff RM (2012) Inflammatory cell trafficking across the blood-brain barrier (BBB): Chemokine regulation and in vitro models. Immunological Reviews 248:228-239.

Tanaka S, Nishimura M, Ihara F, Yamagishi J, Suzuki Y, Nishikawa Y (2013) Transcriptome Analysis of Mouse Brain Infected with Toxoplasma gondii. Infection and Immunity 81:3609-3619.

Tanaka S, Ide M, Shibutani T, Ohtaki H, Numazawa S, Shioda S, Yoshida T (2006) Lipopolysaccharide-induced microglial activation induces learning and memory deficits without neuronal cell death in rats. Journal of neuroscience research 83:557-566.

Team RC (2013) R foundation for statistical computing. Vienna, Austria 3.

Teijaro JR (2014) The role of cytokine responses during influenza virus pathogenesis and potential therapeutic options. In: Influenza Pathogenesis and Control-Volume II, pp 3-22: Springer.

Theodosis DT, Poulain DA, Oliet SHR (2008) Activity-dependent structural and functional plasticity of astrocyte-neuron interactions. Physiological reviews 88:983-1008.

Thomas C, Moraga I, Levin D, Krutzik PO, Podoplelova Y, Trejo A, Lee C, Yarden G, Vleck SE, Glenn JS (2011) Structural linkage between ligand discrimination and receptor activation by type I interferons. Cell 146:621-632.

Thomson CA, McColl A, Cavanagh J, Graham GJ (2014) Peripheral inflammation is associated with remote global gene expression changes in the brain. Journal of neuroinflammation 11:73.

Tomonaga K (2004) Virus-induced neurobehavioral disorders: mechanisms and implications. Trends in molecular medicine 10:71-77.

Tong L, Balazs R, Soiampornkul R, Thangnipon W, Cotman CW (2008) Interleukin-1β impairs brain derived neurotrophic factor-induced signal transduction. Neurobiology of aging 29:1380-1393.

Tong L, Prieto GA, Kramár EA, Smith ED, Cribbs DH, Lynch G, Cotman CW (2012) Brain-derived neurotrophic factor-dependent synaptic plasticity is suppressed by interleukin-1β via p38 mitogen-activated protein kinase. Journal of Neuroscience 32:17714-17724.

Tong S et al. (2013) New World Bats Harbor Diverse Influenza A Viruses. PLoS Pathogens 9.

Toulmond S, Vige X, Fage D, Benavides J (1992) Local infusion of interleukin-6 attenuates the neurotoxic effects of NMDA on rat striatal cholinergic neurons. Neuroscience letters 144:49-52.

Tronche F, Kellendonk C, Kretz O, Gass P, Anlag K, Orban PC, Bock R, Klein R, Schütz G (1999) Disruption of the glucocorticoid receptor gene in the nervous system results in reduced anxiety. Nature genetics 23:99-103.

Uddin M, Koenen KC, Aiello AE, Wildman DE, de los Santos R, Galea S (2011) Epigenetic and inflammatory marker profiles associated with depression in a community-based epidemiologic sample. Psychological Medicine 41:997-1007.

van Heeckeren AM, Tscheikuna J, Walenga RW, Konstan MW, Davis PB, Erokwu B, Haxhiu MA, Ferkol TW (2000) Effect of Pseudomonas infection on weight loss, lung mechanics, and cytokines in mice. American journal of respiratory and critical care medicine 161:271-279.

Van Heteren JT, Rozenberg F, Aronica E, Troost D, Lebon P, Kuijpers TW (2008) Astrocytes produce interferon-alpha and CXCL10, but not IL-6 or CXCL8, in aicardi-Goutières syndrome. Glia 56:568-578.

van Riel D, Munster VJ, de Wit E, Rimmelzwaan GF, Fouchier RA, Osterhaus AD, Kuiken T (2006) H5N1 Virus Attachment to Lower Respiratory Tract. Science (New **York, NY) 312:399.**

van Riel D, Leijten LM, Verdijk RM, GeurtsvanKessel C, van der Vries E, van Rossum AM, Osterhaus AD, Kuiken T (2014) Evidence for influenza virus CNS invasion along the olfactory route in an immunocompromised infant. J Infect Dis 210:419-423.

Varatharaj A, Galea I (2017) The blood-brain barrier in systemic inflammation. Brain, behavior, and immunity 60:1-12.

Vasek MJ et al. (2016) A complement-microglial axis drives synapse loss during virus-induced memory impairment. Nature 534:538-543.

Veckman V, Österlund P, Fagerlund R, Melén K, Matikainen S, Julkunen I (2006) TNF-α and IFN-α enhance influenza-A-virus-induced chemokine gene expression in human A549 lung epithelial cells. Virology 345:96-104.

Verkhratsky A, Butt AM (2013) Glial physiology and pathophysiology: John Wiley & Sons.

Vesce S, Rossi D, Brambilla L, Volterra A (2007) Glutamate release from astrocytes in physiological conditions and in neurodegenerative disorders characterized by neuroinflammation. International review of neurobiology 82:57-71.

Vikman K, Robertson B, Grant G, Liljeborg A, Kristensson K (1998) Interferon-γ receptors are expressed at synapses in the rat superficial dorsal horn and lateral spinal nucleus. Journal of neurocytology 27:749-760.

Vikman KS, Owe-Larsson B, Brask J, Kristensson KS, Hill RH (2001) Interferon-γ-induced changes in synaptic activity and AMPA receptor clustering in hippocampal cultures. Brain research 896:18-29.

Vitkovic L, Bockaert J, Jacque C (2000a) “Inflammatory” cytokines. Journal of neurochemistry 74:457-471.

Vitkovic L, Konsman JP, Bockaert J, Dantzer R, Homburger V, Jacque C (2000b) Cytokine signals propagate through the brain. Molecular psychiatry 5:604-615.

Vorhees CV, Williams MT (2006) Morris water maze: procedures for assessing spatial and related forms of learning and memory. Nature protocols 1:848-858.

Wake H, Moorhouse AJ, Jinno S, Kohsaka S, Nabekura J (2009) Resting microglia directly monitor the functional state of synapses in vivo and determine the fate of ischemic terminals. Journal of Neuroscience 29:3974-3980.

Walsh RN, Cummins RA (1976) The Open-Field Test: a critical review. Psychological bulletin 83:482-504.

Wang G, Li R, Jiang Z, Gu L, Chen Y, Dai J, Li K (2016) Influenza Virus Induces Inflammatory Response in Mouse Primary Cortical Neurons with Limited Viral Replication. BioMed research international 2016.

Wang H-Y, Hsieh P-F, Huang D-F, Chin P-S, Chou C-H, Tung C-C, Chen S-Y, Lee L-J, Gau SS-F, Huang H-S (2015) RBFOX3/neuN is required for hippocampal circuit balance and function. Scientific reports 5:17383.

Weed MR, Gold LH (2001) Paradigms for behavioral assessment of viral pathogenesis. Adv Virus Res 56:583-626.

Whishaw IQ (2004) Posterior neocortical (visual cortex) lesions in the rat impair matching-to-place navigation in a swimming pool: a reevaluation of cortical contributions to spatial behavior using a new assessment of spatial versus nonspatial behavior. Behavioural brain research 155:109-116.

Wilk E, Schughart K (2012) The Mouse as Model System to Study Host-Pathogen Interactions in Influenza A Infections. Current protocols in mouse biology 2:177-205.

Wilson CJ, Finch CE, Cohen HJ (2002) Cytokines and cognition—the case for a head-to-toe inflammatory paradigm. Journal of the American Geriatrics Society 50:2041-2056.

Winther B, Gwaltney JM, Jr., Mygind N, Hendley JO (1998) Viral-induced rhinitis. American journal of rhinology 12:17-20.

Wolf Y, Yona S, Kim KW, Jung S (2013) Microglia, seen from the CX(3)CR1 angle. Frontiers in Cellular Neuroscience 7.

Xiao M, Hu G (2014) Involvement of aquaporin 4 in astrocyte function and neuropsychiatric disorders. CNS neuroscience & therapeutics 20:385-390.

Yamada T, Horisberger MA, Kawaguchi N, Moroo I, Toyoda T (1994) Immunohistochemistry using antibodies to alpha-interferon and its induced protein, MxA, in Alzheimer's and Parkinson's disease brain tissues. Neurosci Lett 181:61-64.

Yamashita N (2016) Neurotropic Influenza Virus Infections. In: Neurotropic Viral Infections, pp 295-314: Springer.

Yirmiya R, Goshen I (2011) Immune modulation of learning, memory, neural plasticity and neurogenesis. Brain, behavior, and immunity 25:181-213.

Yong VW (1996) Cytokines, astrogliosis, and neurotrophism following CNS trauma. Cytokines and the CNS: Development, Defense and Disease:309-324.

Yu JE, Kim M, Lee J-H, Chang B-J, Song C-S, Nahm S-S (2014) Neonatal influenza infection causes pathological changes in the mouse brain. Veterinary Research 45:63.

Zeng X-N, Sun X-L, Gao L, Fan Y, Ding J-H, Hu G (2007) Aquaporin-4 deficiency down-regulates glutamate uptake and GLT-1 expression in astrocytes. Molecular and Cellular Neuroscience 34:34-39.

Zhang D, He F, Bi S, Guo H, Zhang B, Wu F, Liang J, Yang Y, Tian Q, Ju C (2016) Genome-wide transcriptional profiling reveals two distinct outcomes in central nervous system infections of rabies virus. Frontiers in microbiology 7.

Zhang JM, An J (2007) Cytokines, Inflammation and Pain. International anesthesiology clinics 45:27-37.

Zhao B, Schwartz JP (1998) Involvement of cytokines in normal CNS development and neurological diseases: recent progress and perspectives. Journal of neuroscience research 52:7-16.

Zhong L, Chen XF, Wang T, Wang Z, Liao C, Wang Z, Huang R, Wang D, Li X, Wu L, Jia L, Zheng H, Painter M, Atagi Y, Liu CC, Zhang YW, Fryer JD, Xu H, Bu G (2017) Soluble TREM2 induces inflammatory responses and enhances microglial survival. The Journal of experimental medicine 214:597-607.

Zhu Y, Romero MI, Ghosh P, Ye Z, Charnay P, Rushing EJ, Marth JD, Parada LF (2001) Ablation of NF1 function in neurons induces abnormal development of cerebral cortex and reactive gliosis in the brain. Genes & development 15:859-876.

Zielinski MR, Souza G, Taishi P, Bohnet SG, Krueger JM (2013) Olfactory bulb and hypothalamic acute-phase responses to influenza virus: effects of immunization. Neuroimmunomodulation 20:323-333.

Zucker RS, Regehr WG (2002) Short-term synaptic plasticity. Annual review of physiology 64:355-405.

6. List of Abbreviations

ACSF	Artificial cerebrospinal fluid
AGS	Aicardi-Goutieres syndrome
AMPA	α-amino-3-hydroxy-5-methyl-4-isoxazolepropionic acid
AQP4	Aquaporin-4
BBB	Blood brain-barrier
BCSFB	Blood-cerebrospinal fluid barriers
BDNF	Brain-derived neurotrophic factor
BSA	Bovine serum albumin
C1, C5a	Complement component
CA	Cornu ammonis
CCL2	Chemokine (C-C motif) ligand 2
CCR	CC chemokine receptors
CD (14, 22, 45, 47, 200)	Cluster of differentiation
CD200R	Cell surface glycoprotein CD200 receptor 1
CNS	Central nervous system
CVOs	Circumventricular organs
CX3CL1	Chemokine (C-X3-C motif) ligand 1
CX3CR1	CX3C chemokine receptor 1
CXCR	CXC chemokine receptors
DAPI	4',6-diamidino-2-phenylindole
DEPs	Differentially expressed probesets
DG	Dentate gyrus
ELISA	Enzyme-linked immunosorbent assay
fEPSP	Field excitatory postsynaptic potential
FFA	Focus forming assay
FFU	Focus forming unit
$GABA_A$	Gamma-aminobutyric acid
GAT-1	GABA transporter 1
GFAP	Glial fibrillary acidic protein
GLAST	Glutamate aspartate transporter
GLT-1	Glutamate transporter 1
GLUT-1	Glucose transporter 1

HA	Hemagglutinin
HPA	Hypothalamic–pituitary–adrenal axis
IBA-1	Ionized calcium-binding adapter molecule 1
ICAM-1	Intercellular Adhesion Molecule 1
IFN (IFN-α, -β, -γ)	Interferon
IFNAR	Type I interferon receptor
IL (IL-1, -1β, -6, -10)	Interleukin
IPI	Interpulse interval
IRF7	Interferon regulatory factor 7
IRF9	Interferon regulatory factor 9
ISG3	Interferon-stimulated gene factor-3
ISREs	Interferon-stimulated response elements
JAK1	Janus kinase 1
LPS	Lipopolysaccharide
LTP	Long term potentiation
MCP-1	Monocyte chemoattractant protein 1
M-CSF	Macrophage colony-stimulating factor
MHC class II	Major histocompatibility complex class II
MilliQ	Millipore 'ultrapure' water
MS	Multiple sclerosis
MWM	Morris water maze
NA	Neuraminidase
Nes	Nestin
NGF	Nerve growth factor
NMDA	N-methyl-D-aspartate
NO	Nitric oxide
NTS	Nucleus tractus solitarius
OD	Optical density
PAMP	Pathogen-associated molecular pattern
PB	Phosphate buffer
PBS	Phosphate-buffered saline
PFA	Paraformaldehyde
PGE2	Prostaglandin E2

PPF	Paired pulse facilitation
ROI	Region of interest
SOCS	Suppressor of Cytokine Signaling
ssRNA	Single-stranded ribonucleic acid
STAT	Signal transducer and activator of transcription
Syn1	Synapsin 1
TBS	Theta burst stimulation
TCA	Trichloroacetic acid
TGF-β	Transforming growth factor beta
Th1	T helper cells
TLR	Toll-like receptor
TNF-α	Tumor necrosis factor alpha
TSP	Thrombospondin
Tyk2	Tyrosine kinase 2
WT	Wild-type
NP	Nucleoprotein
dpi	Day post infection
pi	Post infection
BDV	Borna disease virus
HSV	Herpes simplex virus
SIV	Simian immunodeficiency virus
IAV	Influenza A virus
LCMV	Lymphocytic choriomeningitis
MLV	Murine leukemia virus
DEGs	Differentially expressed genes
TQ	Target quadrant
NT	Non-target quadrant
OQ	Other quadrant

7. Acknowledgement

It was the middle of November 2013, I can remember it very well, despite the low internet speed and its connection problems in Iran, I could talk with Prof. Martin and Dr. Kristin. It was the day for me that my life was changed. Then I was waiting for a long time to acquire a German visa but finally, I got it around April 2014. Now I am very happy because now, at these last steps of my PhD studying, I have a huge treasure all around me and in my heart, you lovely people, all are my treasure. It is the time that I can only say, I am appreciating you so much.
First I would like to really appreciate Prof. Dr. Martin Korte and Dr. Kristin Michaelsen-Preusse, my dear supervisors, without your great knowledge, advice, support, great help, patience, kindness, optimism and encouragement, definitely I was unable to do anything. Many many thanks for all your goodness. Thank you so so much for this great opportunity that you gave me. I am proud to be your student forever.

I would like to thank Prof. Dr. Reinhard Köster and Prof. Dr. Robert Hänsch for giving me this valuable opportunity to have their great scientific opinions to improve myself in my disputation. Many thanks for your great time.

I would like to appreciate our collaborator in Influenza project, Prof. Dr. Klaus Schughart (HZI) and Dr. Esther Wilk for establishing the Influenza mouse model and genome microarray study and also because of their valuable help and suggestions in progress of this project. I also thank his team member Christin Kurch, Karin Lammert, Rebecka Wünsche and Dr. Heike Kollmus because of their always warm welcoming me in their lab.
I also appreciate Prof. Dr. Ulrich Kalinke (Twincore) our collaborator in interferon project because of his great suggestions and help for progress the project. Thanks to his Ph.D. student Chintan Chhatbar because of accompanying in the project and providing the mice.

I very appreciate Dr. Marta Zagrebelsky and Dr. Andreas Holz for their great suggestions and support during my PhD studying. Always your points helped me to improve.
I would like to appreciate Dr. Martin Rothkegel for his always great and valuable help to me and his kindness. Also, I very appreciate Tania Meßerschmidt for her always great help and smiley and very kind face. Thank you so much Tania for everything.
I appreciate Dr. Gayane Grigoryan providing the electrophysiology data for interferon project. Many thanks Gayane for your help.
I really appreciate Diane Mundil, Carmen Wucherpfennig and Heike Kessler because of their help and kindness to me. I would like to thank Sybille Bläsche and Ilona Demesvary for their help and glamorous behavior. Also, I very appreciate Dr. Doris Pester because of her great help and suggestions.
Then I really appreciate Reinhard Huwe because of the great time that we had and have together. I really enjoy talking with you Reinhard. Many thanks for your Kindness. I very appreciate Eva and Alwin Saxinger, I am very very fortunate girl that I met you in my life. I really love you and thanks for your kindness.
Now also it is the time to appreciate my very nice and lovely colleagues, those who are not here at the moment including Dr. Mariana Bayer (Bevil), Dr. Franziska Scharkowski (Dr. F), Susann Ludwig, Dr. Nina Gödecke and Jan Kleveman, thank you very much for all of your kindness and very nice time that we had together. Special thanks to my friend Dr. Cristina Iobbi and her husband Dr. Andrea Pasquali, they know how much that I love them. I never forget their kindness and great help to me.
I would like to appreciate from my very nice current colleagues: Jonas (my IT (U) son), Nikki (my bright son), Abi (my very nice friend, you are memorial of Sanjay Dutt for me, thanks for taking care of me in the dark), Charlotte (my lovely daughter), Claudia (lovely globi), lovely Kristin, lovely Leonie, Max (my very nice neighbor son) and Steffen (my very nice son), Thanks a lot to all of you for everything.

Also, I would like to appreciate my lovely father in law Mr. Javad Fereidoni because of his encouragement and his kindness. He is one of the persons who is really waiting for Influenza paper to get publish ☺
At the end, I want to say it very very loud because I want all the world to hear this that I very very very appreciate my treasure in life Prof. Dr. Masoud Fereidoni. You know you are not only my professor and my husband but you are the spring of my life, you are my self-confidence, you are my knowledge, you are the sun in my life. Without you, I am nothing, nothing. Without you, I couldn't do anything. Without you, I don't know anything. How can I appreciate you? This PhD is belonged to you, not me. All of my life belongs to you. With you, I can do everything… I love you.